THIRD NATIONAL CONFERENCE ON

RAPID PROTOTYPING, TOOLING, AND MANUFACTURING

Edited by
A E W RENNIE
D M JACOBSON
C E BOCKING

Rapid Prototyping, Tooling, and Manufacturing

Acknowledgements

Organizing Committee

Dr A E W Rennie	Buckinghamshire Chilterns University College
Dr D M Jacobson	Buckinghamshire Chilterns University College
Dr C E Bocking	Buckinghamshire Chilterns University College

Technical Review Committee

Mr G R Bennett	Buckinghamshire Chilterns University College
Dr C E Bocking	Buckinghamshire Chilterns University College
Dr I T Chang	University of Birmingham
Prof. T H C Childs	University of Leeds
Dr T J Coole	Buckinghamshire Chilterns University College
Dr S S Dimov	Cardiff University
Dr P Fox	University of Liverpool
Mr P M Hackney	University of Northumbria at Newcastle
Dr D M Jacobson	Buckinghamshire Chilterns University College
Dr A D Linney	University College London
Dr W O'Neill	University of Liverpool
Mr R Pocock	Buckinghamshire Chilterns University College
Dr A E W Rennie	Buckinghamshire Chilterns University College
Prof. D Wimpenny	De Montfort University

Third National Conference on

Rapid Prototyping, Tooling, and Manufacturing

20–21 June 2002
Centre for Rapid Design and Manufacture
Buckinghamshire Chilterns University College,
High Wycombe, UK

Edited by

Dr A E W Rennie
Dr C E Bocking
Dr D M Jacobson

Professional Engineering Publishing Limited,
Bury St Edmunds and London, UK

First Published 2002

This publication is copyright under the Berne Convention and the International Copyright Convention. All rights reserved. Apart from any fair dealing for the purpose of private study, research, criticism or review, as permitted under the Copyright, Designs and Patents Act, 1988, no part may be reproduced, stored in a retrieval system, or transmitted in any form or by any means, electronic, electrical, chemical, mechanical, photocopying, recording or otherwise, without the prior permission of the copyright owners. *Unlicensed multiple copying of the contents of this publication is illegal.* Inquiries should be addressed to: The Publishing Editor, Professional Engineering Publishing Limited, Northgate Avenue, Bury St. Edmunds, Suffolk, IP32 6BW, UK. Fax: +44 (0) 1284 705271

© 2002 with Professional Engineering Publishing Limited, publishers to the Institution of Mechanical Engineers, unless otherwise stated.

ISBN 1 86058 374 1

A CIP catalogue record for this book is available from the British Library.

Printed by The Cromwell Press, Trowbridge, Wiltshire, UK

The Publishers are not responsible for any statement made in this publication. Data, discussion, and conclusions developed by authors are for information only and are not intended for use without independent substantiating investigation on the part of potential users. Opinions expressed are those of the Authors and are not necessarily those of the Institution of Mechanical Engineers or its Publishers.

About the Editors

Dr Allan E W Rennie

Allan Rennie obtained a Bachelors in Computer-aided Engineering from Glasgow Caledonian University in 1995 which spurred his interest in rapid prototyping. This led to a move to the Centre for Rapid Design and Manufacture where he has conducted his research in various areas of rapid prototyping technologies, finally leading to the award of a PhD from Brunel University in 2001. His current role, which he has fulfilled for the last two and a half years, is as a research and development engineer with CRDM, mainly conducting research into the downstream processes of rapid prototyping and implementing these as rapid tooling techniques.

Dr Chris E Bocking

Chris Bocking obtained a Graduateship of the Institute of Metal Finishing from the South Bank Polytechnic in 1981 and a PhD on applied electrochemistry from Loughborough University in 1994. He has worked in surface engineering for 30 years, of which 19 were spent at the GEC Hirst Research Centre in the Electrochemistry Group, as both Project Leader and Group Manger working on the development of new electroplating processes and their applications for the electronics industry. He is currently employed on a part-time basis as Research Co-ordinator at the Centre for Rapid Design and Manufacture, working on the development and use of new materials for rapid tooling and the application of electroforming to toolmaking and advanced manufacturing processes. He is also a Vice-President of the Institute of Metal Finishing, and also runs a surface engineering consultancy business – Surface Technology Support.

Dr David M Jacobson

David Jacobson obtained a doctorate in Materials Science from the University of Sussex. He has established a career in industrial research, with specialist expertise in metal joining and electronics packaging. After managing the Materials Fabrication Division of GEC-Marconi in north London from 1985 to 1997, he now works as a freelance consultant. His connection with the Centre for Rapid Design and Manufacture was a two-year appointment (2000–2002) as a research fellow, helping to set up collaborative research projects on rapid manufacturing. While at GEC-Marconi, he co-authored a textbook on *The Principles of Soldering and Brazing*, published by the American Society of Materials, which is now entering its second edition. David is the author of over 70 publications in the scientific and technical literature, and was a recipient of the Robert R Peaslee Award of the American Welding Society for 1997 and the Cook Prize of the Institute of Materials for 1996/1997.

Related Titles of Interest

Title	Editor/Author	ISBN
IMechE Engineers' Data Book – Second Edition	C Matthews	1 86058 248 6
Advances in Manufacturing Technology XV	D T Pham, S S Dimov and V O'Hagan	1 86058 325 3
Rapid Prototyping Casebook	J A McDonald, C J Ryall and D I Wimpenny	1 86058 076 9
Software Solutions for Rapid Prototyping	I Gibson	1 86058 360 1
Computer-aided Production Engineering CAPE 2001	H Bin	1 86058 367 9
Developments in Rapid Prototyping and Tooling	G Bennett	1 86058 048 3
Rapid Prototyping and Tooling Research	G Bennett	0 85298 982 2
Quality, Reliability and Maintenance QRM 2002	G J McNulty	1 86058 369 5
Computer-aided Production Engineering CAPE 2000	IMechE Conference	1 86058 263 X

For the full range of titles published by Professional Engineering Publishing contact:

Marketing Department
Professional Engineering Publishing Limited
Northgate Avenue
Bury St Edmunds
Suffolk
IP32 6BW
UK

Tel: +44 (0)1284 724384
Fax: +44 (0)1284 718692
Website: www.pepublishing.com

Contents

Foreword
A E W Rennie *ix*

RPBloX – a novel approach towards rapid prototyping
T Lim, J R Corney, J M Ritchie, and J B C Davies 1

Development of saddle components using CAD, rapid prototyping, rapid tooling, and reverse engineering
S G Dhande and A Chatterjee 9

Laser engineered net shaping™ – technology and applications
M Hedges and D Kiecher 17

The microstructure of laser-fabricated Ti6A14V
J Liang, J Mei, M H Loretto, and X Wu 25

Rapid manufacture of burn-resistant Ti components using direct laser fabrication (DLF)
R Sharman, S Wu, M H Loretto, and W Voice 31

Preliminary investigation of surface roughness and dimensional accuracy of ThermoJet and SLA parts
I H Mulyadi, N G Bennett, and S O Onuh 39

Optimizing tapping operations on hardened steels in a prototyping environment
J F A Simões, E Matos da Rocha, and R M Oliveiera Baptista 47

Multi-axis machining using a six-axis anthropomorphic robot
J F A Simões, A R Pires, T J Coole, and D G Cheshire 55

Fabrication of customized bioceramic implants using selective laser sintering
F Cruz, J F A Simões, T J Coole, and C Bocking 63

A review of the manufacture of below-knee prosthetic sockets using rapid prototyping technologies
N S Herbert 71

Lean rapid production concept realization in the compact manufacturing system
D N Svirsky 79

Reducing the uncertainty of the prototyping decision
K A M Steele, G J Ryder, W J Ion, and A I Thomson 89

Benchmarking the rapid design and manufacture process
G J Ryder, D K Harrison, G Green, W J Ion, and B M Wood 97

The development of three-dimensional printing techniques for 'concept modellers' to competitive rapid prototyping systems
P M Hackney 105

Fabrication of functional metal parts using laser sintering – a case study
D E Dimla, H Singh, and M Day 115

Influence of the heat treatment cycles on the properties of selective laser sintered (SLS) Rapidsteel$^{2.0}$
D Uzunsoy and I T H Chang 123

Ceramic microcomponents by rapid prototyping process chains
R Knitter, W Bauer, D Göhring, and P Risthaus 131

Experimental investigation of the direct metal laser re-melting of dissimilar metals
S Pogson, P Fox, and W O'Neill 139

Rapid manufacturing of complex shapes by electrochemical machining
R Temur 149

Tool electrode design for electrochemical machining
R Temur and C Bocking 157

Authors' Index 165

Foreword

It is with pleasure that I introduce in this volume, the proceedings of the Third National Conference on *Rapid Prototyping, Rapid Tooling, and Rapid Manufacturing*, held at the Chalfont campus of Buckinghamshire Chilterns University College, UK.

There has been a significant gap since the Second National Conference, however, the number of papers submitted has ensured that there is significant interest in the UK in having a national event for the dissemination of research conducted in the areas of RP, RT, RM, and advanced manufacturing. The papers selected for presentation here are those that passed through a stringent reviewing process – in total, nine papers have been rejected. Therefore, I am certain that the success of this latest event will ensure that the conference will continue for many years to come.

The spread of papers in this volume represents many developments, particularly in the advancement of processes such as LENS and sintering technologies and the materials used within these techniques. New to this series of conferences is the use of RP in the medical industry, an area of development that has come to the fore over the last few years. This is a good indicator that RP is not only used for the traditional 'engineering' and 'manufacturing' functions that it has been associated with.

I trust that you will find these proceedings to be an excellent record of some of the research carried out over the last couple of years which will be of benefit to both established and young practitioners of rapid prototyping, tooling, and manufacturing technologies.

I would like to give my thanks to the reviewing panel who have performed their duties diligently – without their assistance, the refereeing of the papers would have been an insurmountable task. Thanks are also extended to them for their assistance, chairing the individual sessions for the duration of the conference. Finally, the editors would like to thank the authors for their interest in the conference and for making it a success.

Dr Allan E W Rennie
Centre for Rapid Design and Manufacture
Buckinghamshire Chilterns University College
High Wycombe, UK

This page intentionally left blank

RPBloX – a novel approach towards rapid prototyping

T LIM, J R CORNEY, J M RITCHIE, and **J B C DAVIES**
Department of Mechanical and Chemical Engineering, Heriot-Watt University, UK

ABSTRACT

Various forms of Rapid Prototyping and Manufacturing (RP&M) technologies are being employed extensively in many engineering fields such as Aerospace, Automotive and Medical Engineering. Despite their diversity existing RP technologies are often slow and limited in the types of material which can be employed to build components.

This paper describes the early stages of the RPBloX project, which aims to demonstrate the feasibility of a novel technique with the potential to not only supplement current RP techniques but also act as a standalone method capable of shortening the design-manufacture cycle time. The RPBloX methodology involves a cellular approach to building up a part. Rather than slicing up the CAD model into numerous thin sheets, RPBloX segments the model into 3D cells (or BloXs) of varying sizes, which are then manufactured and assembled using conventional CNC machine tools and robotics. Potentially, production costs could be significantly reduced without the forfeiting accuracy and timeliness.

KEYWORDS: Rapid prototyping, Graph Theory, Manufacturing and Assembly planning.

1. INTRODUCTION

The building of pre-production models is important as it allows a product to be tested for flaws during various stages of its design. Speed and flexibility means that new products and/or variations within the product family can be developed and produced in shorter times [1]. To this end, various rapid prototyping (RP) techniques have been developed to produce physical prototypes in an effort to reduce the time to market [2][3]. Table 1 provides a brief overview of some current RP techniques and their application.

Technique	Application Range	Advantages	Disadvantages
SLA	• Functional parts for assembly tests. • Pre-series production tools. • Medical models. • Electro-forms for EDM.	✓ Manufacturing parts that are impossible to produce conventionally in a single process. ✓ High resolution. ✓ Virtually no limitation of geometrical shape. ✓ Continuous unattended operation.	× Sophisticated sequence of processes required. × Support structures necessary. × Accuracy not in the range of mechanical part manufacturing. × Needs post processing/cleaning.
SLS	• Visual representation models. • Functional tough prototypes. • Cast metal parts (lost wax). • Short run and soft tooling.	✓ Virtually any material that has decreased viscosity upon heating can be used. ✓ No post curing except for ceramics. ✓ No support structures required for overhanging geometry. ✓ Advanced software allows concurrent slicing of part geometry while process is in place.	× Raw surface appearance due to borderline additional powder hardening during solidification. × Requires special chamber with continuous supply of nitrogen for safe sintering. × Emission of toxic gases. × Sloping and high curvature parts exhibit surface roughness due to staircase effect.
LOM	• Typically used in conceptual designs of large bulky components (e.g. sand casting patterns)	✓ Variety of organic (e.g. paper) and inorganic (e.g. composite) materials can be used. ✓ Relatively low cost. ✓ Process produces virtually no internal stress and undesirable deformation. ✓ Ability to handle imperfect STL files. ✓ Best suited for large parts.	× Stability of objects limited by the bond strength between layers. × Not suitable for thin-walled parts or parts complex geometry. × Hollow parts like bottles cannot be built.
BPM	• Enables metal parts/tools to be created directly from thermoplastic prototyped models.	✓ Low cost and good performance. ✓ True desktop system. ✓ Non-toxic.	× Very slow process. × Little literature and knowledge available as it is a relatively recent technique.
FDM	• Mainly conceptual modelling. • Functional models for further *manufacturing procedures*. • Investment casting and injection moulding.	✓ Quick and cheap generation of models. ✓ Easy and convenient date building. ✓ *No toxic chemicals, lasers or liquid polymer bath.* ✓ No material wastage and clean up required.	× Restricted accuracy due to size and shape of the material used (wire of 1.27mm diameter).
RLM	• Mainly for bulky components and rapid prototype tooling (RPT).	✓ Shaped plates are easily modified if designs need changes. ✓ Different material can be combined in one tool. ✓ Plate thickness from 10 – 100mm.	× Removal of large amounts of material may be necessary. × Plates must be joined. × Loss of stiffness and danger of staggered joints.

SLA – StereoLitography, SLS – Selective laser sintering, LOM – Laminated object manufacturing, BPM – Ballistic particle manufacturing, FDM- Fused material deposition
RLM – Rapid layer milling

Table 1: *Overview of some current RP techniques*

All RP techniques work on broadly the same principle. The CAD model is sectioned into a series of thin horizontal slices and built up layer upon layer. How thin these slices are depends on the technology applied and the resolution required. Throughout the RP industry, the StereoLithography (or SLA) technique and its data file format STL has dominated [4]. However, loss of information is inevitable in STL and this greatly influences surface quality, form error, build-time and contributes significantly to post processing time [5][7].

The need to eliminate layering errors is consequently a widely researched topic within RP communities [5]-[10]. Many alternatives have been suggested from set-up and build orientation [7],[12]-[14] to geometric optimisation and the use of features [12] and perhaps the most widely researched issue – adaptive slicing [5],[6],[8]-[15]. Material cost and cycle time is always an issue with any manufacturing process. StereoLithography, the most commonly employed RP&M process, is not cheap [2][10]. As new RP technologies emerge along with increasing demands of niche markets it is only a matter of time before other prototyping techniques gain widespread acceptance [10][11]. However, regardless of the technique applied the key issue remains: **rapidity** and **flexibility** [17].

The research project described in this paper aims to develop a new idea that will augment and/or improve the efficacy of RP&M. It is envisaged that the RP&M system proposed will not only complement existing RP techniques but will also be viable as a stand-alone system. The research has several objectives but the primary ones are:

a) The development of an adaptive subdivision algorithm that can produce both 2.5D slices and/or 3D blocks.
b) The creation and assembly of the subdivided parts using well-established technologies of CNC part-programming, CNC machining and industrial robots.

The main application area of this research is in the prototyping of thick walled and/or large complex components as opposed to current RP method that are typically orientated towards components with thin walls or shells.

2. THE RPBLOX APPROACH

Tse and Chen [18] report that there are two approaches to minimise prototyping time: a) develop new prototyping technology and b) improve upon traditional methods. This paper reports preliminary research work that aims to exploit conventional machine tools, such as CNC machines and robots, to manufacture prototype models. The research has been motivated by several observations about existing RP techniques and systems:

- All current commercial RP systems build 3D shapes from layers of 2D profiles and the final prototype always require some form of post-processing. Algorithms that partition the CAD model to obtain the layers (whether 2D, 2.5D or ruled) even with adaptive slicing have to analyse the tessellated CAD model and/or its surfaces to ensure that the user specified maximum layer thickness is not exceeded [6][9].

  Although adaptive slicing has improved fabrication efficiency, it suffers two major drawbacks:

  a) Layer thickness is generally determined by calculating the thickness over a set of sample points along a sliced level and then selecting the minimum value for the actual layer thickness. This is inefficient since a large amount of data has to be calculated when only a small amount is useful [5][15].
  b) All algorithms rely on cusp height to measure the error between the CAD model and the part. However, when the surface normal vector is perpendicular to the sliced level, the error measured by the cusp height becomes questionable [5][9][15].

- Current systems generally accelerate a product's time to market. However, this is largely dependent on the complexity of the product's design, scale and associated machinery / apparatus [19].
- Cost of raw materials (e.g. photocurable resins) and dedicated machinery (i.e. up to £250K for a state-of-the-art SLA machine) are relatively expensive.
- Current commercial RP systems generally work at a limited number of resolutions (i.e. there is no option to generate a 'rough' model in much less time than a precise one).

Aware of these issues the authors have proposed a new approach which has the potential to create prototypes within a short design-manufacture cycle time, i.e. the RPBLoX methodology. The RPBLoX system essentially involves a

cellular approach to building prototypes. It segments the model into 3D cells (or BloXs) of various sizes. Conventional equipment such as CNC machines and robots are then used to manufacture and assemble them.

3. RPBLOX FUNCTIONAL OVERVIEW

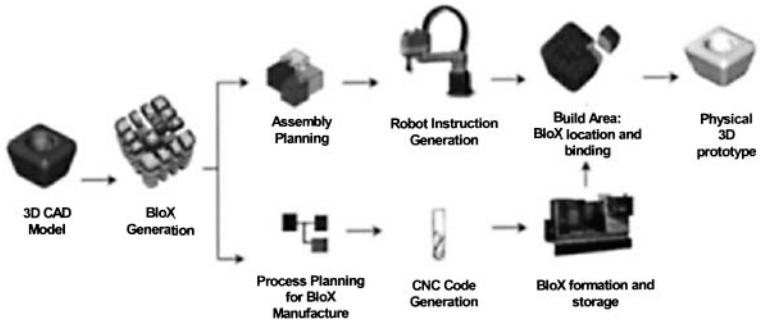

Figure 1: Functional overview of the RPBloX methodology

RPBloX advances the concept of creating 3D "blocked" shaped objects (BloXs) in preference to working with 2D (Figure 1). Solid models are used to provide an unambiguous and complete mathematical representation of the shape of each BloX. The main advantage of subdividing the CAD models directly as opposed to an intermediate faceted model, are greater model accuracy and reduced RP post-processing time. Furthermore, it provides a natural interface to well-established technologies of CNC part programming, machining and robotics [2][20].

In order to generate the BloX set, RPBloX will interrogate the 3D model and apply an adaptive subdivision algorithm. The shape of each individual BloX must allow the automatic generation of a part-program, i.e. CNC code, for its manufacture from bar stock. Since speed and accuracy is essential, each BloX generated by the system should contain simple features (e.g. planar faces, axis aligned holes) as far as possible such that any features can be machined at one pass on the CNC machine. To help eliminate the "staircase" effects on conventional RP systems, C-axis machines can be used to generate the required free-formed surfaces on a BloX.

3.1 Adaptive subdivision

The subdivided model is represented using the Cellular Topology Component of ACIS® [21], which allows the modelling of sub-regions in a solid. These cells can be either 2D sheets or 3D solids. The benefit of this is that unique information can be associated with each cell. Currently, a uniform subdivision strategy has been implemented (Figure 2b) but the aim is to develop an algorithm that automatically subdivides the solid model into a number of geometrically simple regions for the purpose of simplifying calculations and interrogation (Figure 2c and d). It is anticipated that each BloX generated by the adaptive subdivision algorithm will contain information defining its spatial adjacency, geometry and topology. Attributes can be added to each BloX such as datum location, pick up positions and gripping surfaces.

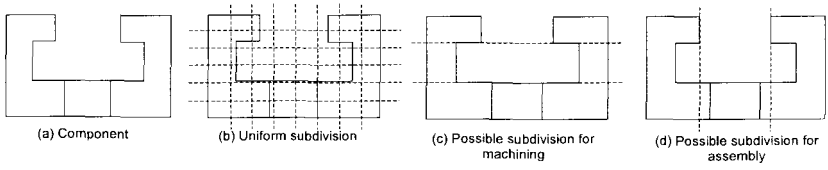

Figure 2: Adaptive subdivision strategies. Note: In c and d, the dashed lines represent possible slicing planes

Importantly, the adjacency data of the BloXs allow the use of graph theory to assist in the generation of process and assembly plans. A graph is a mathematical abstraction of relationships [22]. This graphical representation will help understand connectivity between the BloXs. As solid-model data structures are usually graph structures, it lends itself naturally to the use of graph-based approaches [23]. For example, in applications such as graph-based feature recognition, a class of generic features is represented in terms of their geometric and/or topological characteristics (i.e. the graph structure). The most common graph used is the *face-edge* graph (FEG) [24], which is frequently *attributed* or *augmented* [26]. Search algorithms and other geometric reasoning techniques are then devised to determine if characteristic patterns are present.

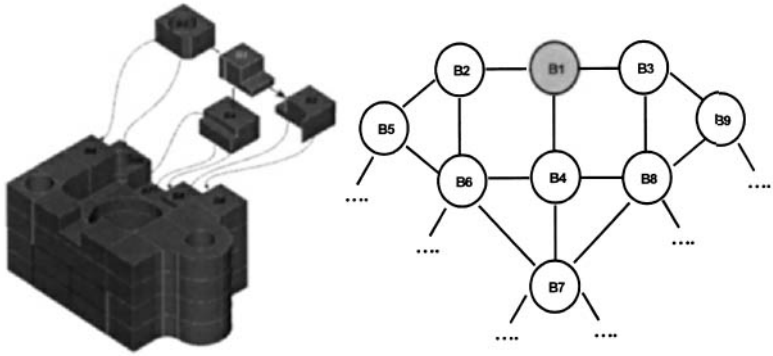

Figure 3: A fragment of the adjacency graph associated with the illustrated cellular structure. BloX adjacencies are shown via the arrows on the left and represented by the graph structure shown on the right. The selected BloX is B1.

In graph theory, a *cycle* is a sequence of vertices $v_0, v_1, v_2, ..., v_n$ such that $v_0 = v_n$ and $v_0, v_1, ..., v_{n-1}$ is a path. A graph is called a *cycle* if it is connected and non-empty and if every vertex is of degree two. A vertex v is called a *cycle vertex* of the graph G if v belongs to a cycle in the graph G. The *degree* of a vertex is the number of adjacent edges to the vertex. The *distance* between two vertices in a graph is the length of the shortest path in the graph from one vertex to the other. A *path* is a distinct sequence of vertices $v_0, v_1, ..., v_n$ such that for all $i<n$, v_i is adjacent to v_{i+1}. The integer n is the length of the path. Sometimes the graph defined by the sequence of vertices together with the edges that connect them is also called a *path* [22].

The graph structure employed by the RPBloX system (known as a BloX Adjacency Graph, BAG) is similar in many ways to the FEG. Here BloXs represent vertex nodes while the adjacent faces of each BloX represent the connectivity edges in the graph. Figure 3 illustrates a fragment of the BAG associated with the example part (BloX B1 has been chosen at random simply for illustration purposes). The *degree* of B1 is 3, while the shortest *cycle* (i.e. spatial distance) of B1 includes BloXs B2, B6, and B4.

It is anticipated that by parsing the RPBloX adjacency graph an assembly sequence of the final prototype can be generated. With this scheme there are many opportunities for optimisation. For example, BloXs with geometry conforming to cuboids can be merged to form a larger BloX thereby reducing machining and assembly time. Building of the prototype will be done with a SCARA robot [27] fitted with an automatic adhesive dispenser and a manipulator for picking up the BloXs.

4. IMPLEMENTATION AND EXAMPLE

In order to manually explore possible subdivision and assembly strategies a graphical user interface (GUI) for the BAG has been developed using Visual C++ and the ACIS geometric modelling kernel from Spatial Technology.

Figure 4 shows the current GUI referred to as 'The HWUTestBed', which will be the user interface for the RPBloX manufacturing system.

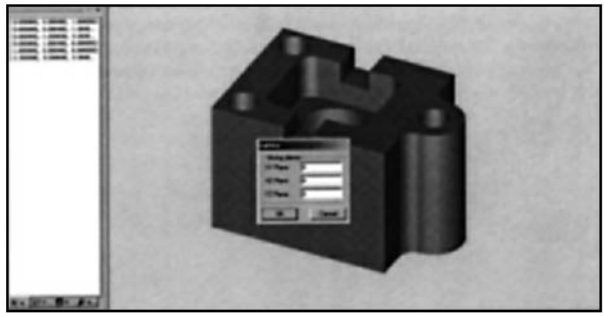

Figure 4: Setting a slicing lattice. Here, 4 slices have been selected for the XY, XZ and YZ plane

To create an initial subdivision, the user has to manually input the number of slicing planes as seen in Figure 4. The set of slicing planes generated is referred to as a slicing lattice. The users therefore has a choice of generating lamina slices similar to current RP&M techniques or using a uniform slicing lattice to subdivide the 3D model into unit BloXs. Note the first tabbed-view in the docking window on the left of the GUI contains several vectors. The vectors are called *Aspect vectors* and are found by interrogating the surface normal of the faces on the model [24]. Aspect vectors represent default build direction for the prototype and in future will provide information to support the automated adaptive subdivision algorithm by defining possible tool approach directions for the CNC machine.

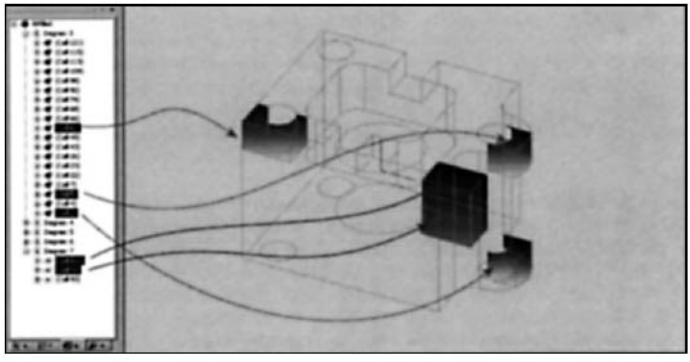

Figure 5: BAG representation displayed in a tree control for selected External and Internal BloXs

Figure 5 shows a tree-control, which displays the BAG resulting from a uniform RPBloX subdivision operation. Using the graph-based approach together with cellular topology, the tree structure of the set of BloXs generated by the slicing lattice is ordered with a precedence based on the *degree of connectivity* between the cells (shown in the partially expanded tree). Each BloX has a name and also contains some other information such as its *level* and a classification *type*. Level represents the positive distance of the BloX from the datum (in this case the base of the model) while its *type* indicates whether the BloX is *external* or *internal* (Figure 5). An internal BloX will typically have the highest *degree* value indicating that it has many other adjacent BloXs around it. In the example, the degree of the set of BloXs shown range between 3 and 7.

Optimisation of BloXs is fundamental to enhancing the efficiency and lowering the costs of operations needed to build a prototype. Several algorithms are in development; amongst them is one that looks to reduce the overall set size by merging simple BloXs that correspond to primitive shapes such as a cuboid.

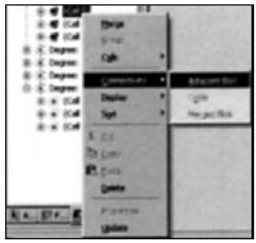

Figure 6: Interactive menu for visualisation and exploration of BloXs

To support development of the algorithms several interactive functions are provided for data visualisation and manipulation. Figure 6 illustrates how the user can manually parse the tree structure and ask each BloX for its immediate neighbours. Our example shows that BloX (Cell 5) has a three adjacent BloXs that are of type *external* (Figure 7). Although the menu also provides manual merging of BloXs, an algorithm is being developed that will scan through the BloX set to provide intelligent automatic merging. This merging algorithm is currently based on determining cut vertices and shortest cycles within the graph structure. Geometric reasoning and heuristics derived from automatic feature recognition research will also be applied to verify the machinability of merged BloXs [25].

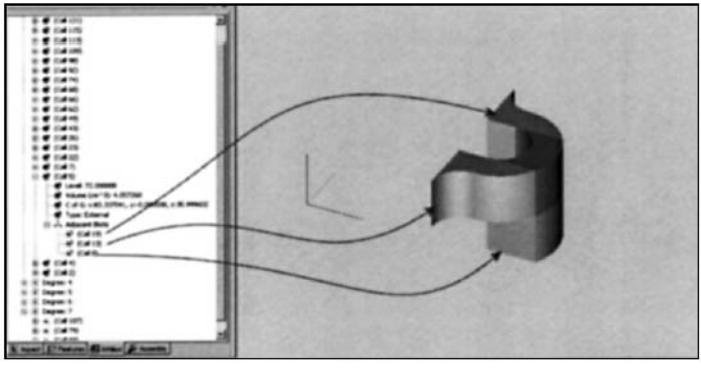

Figure 7: Connectivity of adjacent BloXs for the selected BloX

5. DISCUSSION

This section aims to look at the potential advantages of the RPBloX method.

- **Low Cost**: The value of the RPBloX approach is most clear when the raw material costs are considered.
- **High Speed**: Although each BloX could be manufactured and positioned in a matter of seconds the overall build time will be determined by the adhesive cure rate. A rough estimate performance measure can be made determined by the time required to machine and assemble the component shown in Figure 8 (approximately

130x70x180mm and subdivided into approximately 800 BloXs). Machining time: Assume an average CNC machining (including loading/unloading) time of 8 sec./BloX, implies a total machining time of approximately 107 minutes. Assembly time: Assuming a working volume $0.5m^3$, an average robot traversal speed of 1.26m/s, an average return distance travelled to locate a block of 0.75m, an average cure time of 5 seconds/block (for ABS plastic) and a time for block pick-up and adhesive application of 1.5 seconds. This implies that, once manufactured, 800 blocks could be positioned in around 100 minutes. Therefore the total production time is approximately 207 minutes (~3½ hours), potentially much faster than traditional methods on components of a similar size (~15 hours).

- **Variable Resolution**: Assembly based systems would be able to trade accuracy against speed. For example if an approximate model is needed quickly, the system could use larger cuboids.
- **Variable Material**: Blocks can be created out of different materials and bonded together. For example certain types of cyanoacrylate adhesives can bond plastic to metal.
- **Variable Strength**: There are trade-offs available between curing time and adhesive strength that assembly based systems should be able to exploit. For example a slow build time may be acceptable if the resulting solid has superior strength and controlled anisotropy.

6. CONCLUSION

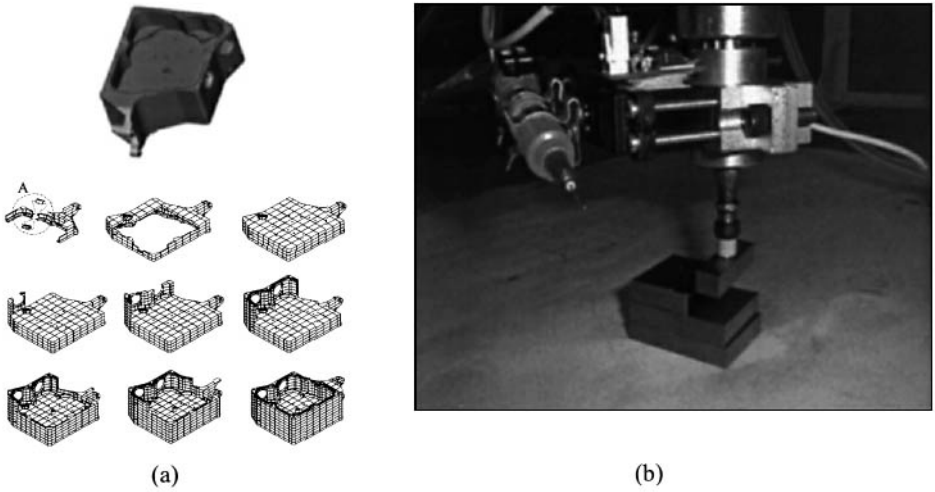

Figure 8: RPBloX building process

The feasibility of the individual elements of the process described is not in doubt, since the technologies already exist as commercial products. The challenges presented by generation of CNC code and robot instructions for the manufacture and assembly of the blocks are essentially similar to many problems found in Computer Aided Process Planning (CAPP) research and as Figure 8a illustrates, the solution will not be trivial. Although the systems' accuracy should be superior to other RP methods this hypothesis can only be verified experimentally. Figure 8b presents some initial work to establish performance parameters (e.g. assembly, gripping and positioning).

The 3-year RPBloX project started in late September 2001. However, the concepts and the methodology proposed here appears to be viable ones. Potential economic gains can be achieved through the use of bar stock materials such

as plastic, metal, MDF, etc. that are already mass-produced. BloXs of dissimilar materials can also be bonded together. Although there are still many hurdles, the results achieved so far are very encouraging.

ACKNOWLEDGEMENTS

This work is supported by the EPSRC grant GR/R35285/01. The authors also gratefully acknowledge the support of the following industrial partners: BAE Systems, Bridgeport Machines, C.A Models, Pathtrace and Renishaw.

REFERENCES

[1] R. Glardon and A.Stagno, *Proc. Of the Conf. Of CAD/CAM* 1999, pp.308-314.
[2] X. Yan and P. Gu, *CAD* 1996, 28(4), pp.307-318.
[3] S. Ashley, *Mech. Eng. Conf. on Rapid Prototyping* 1995, pp. 63-68.
[4] P. Jacobs, *Rapid Prototyping & Manufacturing: Fundamentals of StereoLithography* (McGraw-Hill, 1992).
[5] K. Tata, G. Fadel, A. Bagchi and A. Aziz, *Rapid Prototyping Journal* 1998, 4(4), pp.151-167.
[6] F. Lin, W. Sun, Y. Yan, *Rapid Prototyping Journal* 2001, 7(2), pp.73-81.
[7] P. Alexander, S. Allen and D. Dutta, *CAD* 1996, 30(5) pp.343-356.
[8] D.A. Maekelae, *CAD* 1994, 26(5) pp.119-126.
[9] P.J. de Jager, J.J. Broek and J.S.M. Vegeest, *Assembly Automation* 1997, 17(3), pp.233-238.
[10] A. Kochan, *Assembly Automation* 1997, 17(3), pp.222-225.
[11] A. Kochan, *Assembly Automation* 1997, 17(3), pp.218-221.
[12] D. Frank and G. Fadel, *J. of Intelligent Manufacturing* 1995, 6, pp.339-345.
[13] S.H. Choi and S. Samavedam, *Computers in Industry* 2002, 47(1), pp.39-53.
[14] P. Kulkarni and D. Dutta, *CAD* 1996, 28(9), pp.683-697.
[15] R.C. Luo, Y.C. Cheng and J.H. Tzou, *Proc. 2001 IEEE Int'l Conf. on Robotics & Automation*, pp. 1334-1339.
[16] B. Koc, Y.S. Lee, Y. Ma, *Proc. 6th ACM Symp. On Solid Modeling and Applications* 2001, pp.225-233, 2001.
[17] H.A. Elmaraghy, J.B. Davies, W.H. Elmaraghy, W. Eversheim, D.G. Halevi, I. Ham, H.B. Jasperse, F. Jovane, H.J.J. Kals, A.Y.C. Nee, G. Solenius, V.A. Tipnis, H.K. Tonshoff, C.A. van Luttervelt, R. Weill and H.P. Wiendahl, *Annals of the CIRP* 1993, 42(2), pp.739-749.
[18] W.C. Tse and Y.H. Chen, *Proc. Of the 1997 IEEE Int'l Conf. On Robotics & Automation* 1997, pp.1815-1820.
[19] CA Models Ltd., http://www.camodels.co.uk.
[20] Q. Ji and M.M. Marefat, *ACM Computing Surveys* 1997, 24(3), pp264-311.
[21] Spatial Technology, 2425 55th Street Building A, Boulder, CO 80301-5740. ACIS® Geometric Modeler, V7.0.
[22] Frank Harry, *Graph Theory* (Addison-Wesley Reading, MA, 1969).
[23] A.A.G. Requicha, *ACM Computing Surveys* 1980, 12(4), pp437-464.
[24] T.Lim, J. Corney and D.E.R Clark, *IEEE Trans. PAMI* 2001, 23(9), pp.1043-1048.
[25] T.Lim, J. Corney, and D.E.R Clark, *Int. J. Adv. Manuf. Technol.* 2000, 16, pp.791-802.
[26] S. Joshi and T.C. Chang, *CAD* 1988, 20(2), pp58-66.
[27] EPSON Robots, http://www.epson.co.jp

Development of saddle components using CAD, rapid prototyping, rapid tooling, and reverse engineering

S G DHANDE and **A CHATTERJEE**
CAD Laboratory, Indian Institute of Technology, Kanpur, India

ABSTRACT

At IIT, Kanpur, a central facility of rapid prototyping, rapid tooling, reverse engineering, computer aided design and simulation has been established. Based on the work carried out in this facility, this paper outlines the product development process that has been adopted successfully for leather, footwear and saddlery industry.

It is true that rapid prototyping and tooling technologies complement successfully the computer aided design technique but it is necessary to refine these technologies for successful product development especially in the case of freeform objects for which no readymade mathematical definitions are available.

The components like shoe last, soles, saddle-tree has free form, complex shapes and they generally have a lot of freedom to modify according to user requirement. The prototypes of these components are conventionally manufactured by hand carving, clay modeling etc. Now, using rapid prototyping and tooling as well as reverse engineering, these prototypes can be made in a far more effective manner.

Furthermore, the prototype can be evaluated using a rigorous first article inspection procedure. Based on the approach developed at IIT, Kanpur, it has now become possible to design and develop not only the prototype but the mould also. These moulds can be used for large scale manufacturing of the components.

A clay model can be digitalized with a robotic scanner to generate point cloud definition on the outer bounding surface of the model. After data acquisition the next step entails "registration" and point processing, defining of curve and surface definition in the point cloud. A solid model with watertight geometry is the final output of the process. The next step is to test the CAD model using computer aided engineering analysis in which the model is analyzed using Finite Element method. The CAD model is then realized using rapid prototyping. This RP model can be used to check the fit and form and for functional evaluation using the techniques of experimental stress analysis such as photo-elasticity. Then g-code (data concerning the location of the movement of the cutter) is generated to make the mould in CNC (Computer Numerically Controlled) machine. After the mould is manufactured and checked, shots are taken using the Injection molding process.

KEYWORDS: Saddle, Point Clouds, Free form shape, First article inspection, Registration

1. INTRODUCTION

A large number of universities worldwide are performing research in rapid prototyping, rapid tooling and reverse engineering. CAD laboratory in Indian Institute of Technology at Kanpur in India is one of the institutes doing research and trying to bring the results into manufacturing industry. Rapid prototyping decreases development time by allowing corrections to a product to be made early in the process. By giving engineering, manufacturing, and purchasing a look at the product early in the design process, mistakes can be corrected and changes can be made while they are still inexpensive. Rapid prototyping improves product development by enabling better communication in a concurrent engineering environment.

In CAD laboratory of Indian Institute of Technology, Kanpur, India, the development of saddle and saddletree began in early 2000 by using the techniques of rapid prototyping, rapid tooling and reverse engineering.

Equestrians have been using saddle from ancient times. A saddle is a rigid structure that connects the dynamic structures of the horses with the rider. The fit and position affect the movement of the horses and the ability of the rider to communicate his wishes to the horse. Saddletree is the basic skeleton structure of the saddle. It is designed in such a way to fit both the rider and back of the horses. It can be divided into three basic parts: the cantle, pommel and the neck or twist portion. The cantle is the backside of the saddle, which is wider to centrally locate the rider. The pommel is the front portion that fits on the shoulder blades of the horse and the neck or twist portion is generally narrow to accommodate the legs of the rider. There are various categories and sizes of the saddle. The basic features of the saddle are shown in figure1.

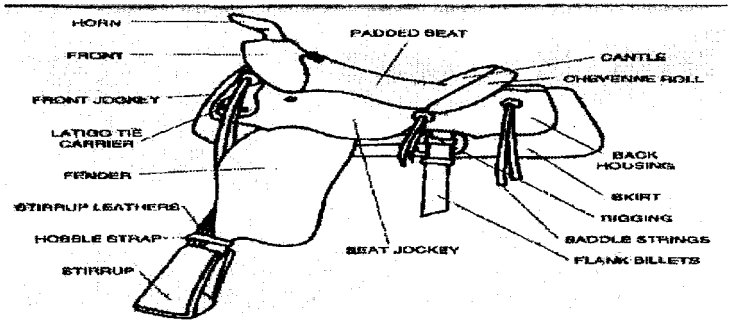

Figure 1: Schematic diagram of a saddletree

The shape and geometry of the saddletrees are extremely important from the point of view of saddle fitting. The saddle fit is neither static nor stable due to motion and due to the fact that the horses change their shape through gain or loss of weight or muscle. Improper saddle fit causes problems and gives rise to pressure points.

2. OBJECTIVE

The present work is related to the complete product development of plastic saddletree with total mass manufacturing solution integrating the advantages of all the high-end technologies namely CAD, CAM, rapid prototyping and rapid tooling. The methodology of the work is divided into following tasks:

2.1 Issues about saddletree design;
2.2 Reverse Engineering to develop a solid model of the saddle and test the design using Computer Aided Engineering Analysis tools;
2.3 Visualize the product with Rapid Prototyping;
2.4 Design the mold using Rapid Tooling and Product Manufacturing.

2.1. Some important issues about saddletree design

The major concern of designing a saddletree is the proper fit. The following factors needs to be considered while designing:

- The structure of the saddletree;
- The position of the saddle on the back;
- The contact of the panels against the horse's back;
- The panel shape for good support;
- A wide gullet to clear the spine completely;

- The levelness of the seat.

The question is how to take care of above-mentioned factors, since our paper does allow us to describe each single point in details, we describe here in brief, how one can achieve a good design. The first issue is **Placement of saddle on the horse's back**, though placement may vary according to the size and design of the saddle but most of the saddles are designed to fit behind the shoulder blade. The flexible flaps of the jumping saddle may extend over the shoulder blades as long as the actual points of the tree are behind the shoulder blades. The points of the saddletree are usually made of steel and rigid. If the tree point rests on the shoulder blades, the horse can not extend his front legs forward easily.

The next point is **Tree Width**. The tree size and the shape of the metal head plate in the tree must conform to the horse's shape being neither narrow nor too wide. If the tree doesn't fit well it will cause pressure points, which can be extremely painful. Figure 2 shows the basic shape to which saddle must conform:
The section 1 represents the shape at the withers where the spine is prominent. The section 2 is at lower side and section 3 again produces outwards. The two parts namely A and B divides the saddle shape into two sections.
The other important points are balance, stability, shape of twist portion, shape of the withers, weight distribution and saddle padding.

Conventional saddletrees are wooden, fiberglass and plastic. Since the present work deals with the plastic saddletree design and development, we would like to describe some advantages of plastic saddletree. Plastics are light in weight, flexible and can have high fatigue strength. They can be easily injection molded to produce in large numbers. Thermoplastic Polypropylene co polymer is used as basic material.

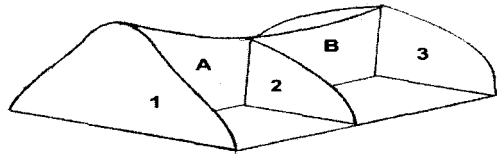

Figure 2: Shape of the horses back at cross-section

The other advantage of plastic saddletree is that metal reinforcement is not necessary except the gullet plate, which fits in the gullet recesses for connecting stirrup bars.

2.3.1 Paper review

We would like to review some papers concerning product development. Product design process involves various stages, which evolve from initial concept to the final product.

Grotenhius and Van den Broek [1] have put forward a basic conceptual model of the design with various assumptions. This model is over simplified by various assumptions.

Nijssens [2] has extended the basic model.

A more practical model is developed by taking into various considerations by J. Encarnacao and E.G. Schlechtendhl [3] which reviews the design concept and deals with the design process and environment and their extended theory to the CAD.

The main aspect of our work is Reverse Engineering and in reverse engineering the generation of CAD model from the digitized data is an inferential process. Mrs J.Kanchan [4] has described certain aspects.

Tamas Varday, Ralph R Martin and Jordan Coxt [5] have taken an overall view of the reverse engineering process starting from data capturing technique to final solid model creation. They have discussed the problem with data acquisition, data segmentation techniques and computational aspects of surface fitting.

2.4 Reverse engineering

Reverse Engineering is useful in many areas. It replaces the first phase of Product design in CAD when we already have a prototype with no geometrical definitions. For instances, it may be necessary to produce a spare part when no original drawings or specifications of a component are available. Further, it may be necessary to modify design of such a component. In these cases a geometric module is required to support processes such as finite element analysis. Reverse Engineering also helps in manufacture of prototypes by Rapid Prototyping. The scanned model is transferred directly through a CAD interface (STL file for layer manufacturing, in our case in FDM process). Reverse Engineering enables CAD to be Master by automatically updating the computer model to reflect changes in a physical tool or prototype. The basic procedures of Reverse Engineering followed in our work are:
a) Data Acquisition b) Data Segmentation c) Surface fitting d) CAD model generation. Now in the following sections these procedures are discussed in brief.

2.2.1 Digitization of saddle with FARO arm

A clay model of saddle is scanned using 6 degree of freedom, multiple axes articulated robotic arm type contact scanner (Faro Arm) and point clouds are obtained in different segments. To obtain the complete digital representation of the model, it is often necessary to digitize it with several relative orientations between the sensor and the model. Before digitizing, the model, fixtures are prepared keeping in view of the geometry, so as to protect positional accuracy and prevention from vibrations. After calibrating the tip the next step is scanning. It was necessary to scan the model in multiple views. There are many practical problems in acquiring usable data, like Calibration, Accuracy, Accessibility, Occlusion, Fixturing, Multiple views, Noises and incomplete data, Statistical distribution of model and Surface finish.

2.2.2 Point cloud processing and data segmentation

A point cloud is in fact an assembly of independent points, each of one of these points being known by it's Cartesian co-ordinates in three dimensional space. The model of the complete saddletree can be composed starting from the regrouping of several point clouds. Point cloud analysis is very important from the point of view of accurate surface fitting. The first phase in point processing is to identify the characteristics of data. In brief we describe these characteristics below:
Density of points: We should obtain reasonably uniformly distributed points and more points in the areas of high change i.e. fillets, edges, corners etc.
Coverage: The data collected should cover the complete object that is to be surfaced, there should be ideally no holes or gaps in between the data sets.
Noise level: Every sensor has some level of noise, and noise level must be kept in mind while fitting the surface.
Outliers: These are incorrect points, which are present in the point cloud due to operator's error. These should be removed.
Number of Points: The number of points obviously affects the performance of the system. It is dependent on the surface accuracy and the way in which the point cloud is used.
After capturing the data we get the dense set of points sampled from the surface of the component (saddle) where each point is modeled by its three dimensional co-ordinates. Now considering all the above characteristics and following those steps to remove unwanted data, all point clouds must be readjusted to create the digital image of the complete saddle in one co-ordinate system. This is called 'Registration'. The quantity of information generally makes it impossible the exploitation of the rough data in the form. Segmentation means to logically divide the original point set into subset, one for each natural surface, so that each subset contains just those points samples from a particular natural surface as shown in figure 3.

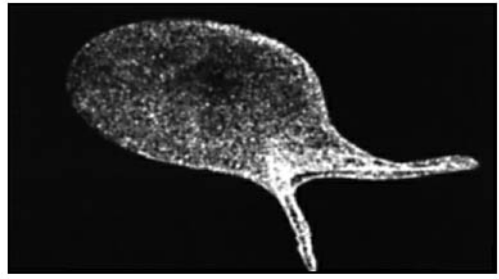

Figure 3: Processed point cloud of saddletree

2.2.3 Curve creation using Imageware Surfacer

After point cloud processing the curves are created. Before surface fitting it is important to visualize and build curve network since the correct surface building depends on the quality of the curve and curve network. There are basically two types of curves, Curves on surface and 3D curves. Also three types of curve fitting procedure is possible while creating curves with point cloud and these are Interpolated curve, Fit free form curve, Fit to tolerance curve. In our case, saddle component is an example of free form geometry. In free form curve generation, it creates the 3D B-spline by approximating the selected points. The curve produced will pass through the average data points. It has control over the number of data points and is uniformly parameterized. Curves are created, interrogated, modified and edited using the technique discussed above and a network of curve is built area by area. The curve network of saddletree is divided into three main parts namely the front, the back and the portion in the leg side. Then curves are then checked again and edited if necessary so that they fit correctly. The curves are then joined (called 'stitching' also) together and continuity again checked between the surfaces as shown in figure 4.

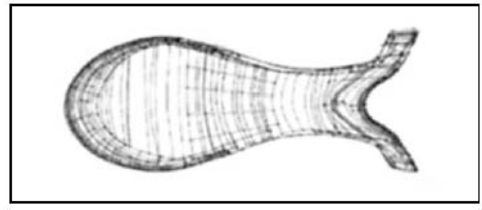

Figure 4: Curve-model of the saddletree

2.2.4 Surface fitting and solid model generation

There are many methods through one can fit the surfaces either using curves or point cloud directly. The basic option is the Free Form surface which fits a uniformly parameterized B-spline surface to the selected cloud with maximum accuracy. The main purpose of Reverse Engineering is to convert discrete data sets into a continuous smooth model. The smoothness and continuity of the model depend upon the creation of a watertight geometry of the surface of the model where both the adjacency relationship between the constituent elements and mathematical equations of underlying edges, curves and surfaces are explicitly maintained. There are various surfacing strategies to fit a surface. The decision depends on many factors like downstream process (manufacturing, rapid prototyping, FEA etc.) requirements and any specific restrictions that are imposed and the limitations of the downstream process.

After the generation of surface model, it is necessary to transfer the data to another system for further process like Mold design, FEM analysis, Machining etc. There are four types of modeling data, Shape data, Non-shape data,

Design data, and Manufacturing data. There are two basic types of data translators: Direct Translators and Indirect Translators.

Direct data transfer involves translating the modeling data stored in a product database directly from one CAD system to another. The data conversion is done in one step. These are dedicated translator program for data base conversion.

Indirect transfer of data adopts the philosophy of creating a neutral database structure, which is independent of any further CAD/CAM system and acts as an intermediary focal point of communication between dissimilar database structure of CAD/CAM systems. There are various data interfaces like IGES, VDA/FS, DIN TAP, STEP etc. Surface model of the saddletree is shown in figure 5.

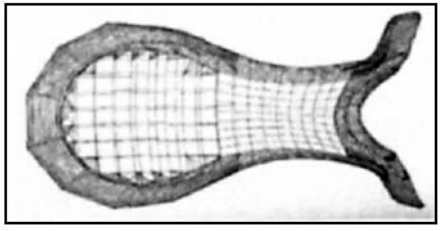

Figure 5: Surface model of the saddletree

2.3 Visualize the product with rapid prototyping

A prototype is necessary for the conceptualization of the design. It is usually required for start of the full production of the component. After the solid model is prepared, it is checked for fit and form of design and if any changes is needed that can be accommodated at this stage. Rapid prototyping is a new class of manufacturing process to make a prototype fast and parts with increased complexity are prepared with a short period of time. The basic procedures followed in these approaches are:

A component like a saddletree is modeled on a CAD/CAM system is made, then the model which represents the physical component, must be represented as closed surfaces, which unambiguously defined an enclosed volume.

This requirement ensures that all horizontal cross sections are closed curves to create the component. The solid or surface model to be built is next covered into a format called the .STL file format.

The .STL formats approximates the surfaces of the model by polygons. It is a triangulated file containing the information about vertices of the triangles and the normal vector direction.

A computer analyses the .STL file and slices the model into cross sections. The cross sections are symmetrically created through the solidification of layer deposition (built layer by layer) process to form a 3D model.

The final task is post processing in which some manual operation like cleaning, finishing are involved.

We have used a FDM-1650 machine to make the prototype, here modeling material is ABS plastic and is in spools. The filament in the spools is fed to the extrusion head and heated to a semi liquid stage. The semi liquid material is extruded through the head and deposited in ultra thin layers, one layer at a time. Since the air surrounding the head is maintained at a temperature below the melting point, the exiting material quickly solidifies. Moving on X-Y plane the head follows the path generated by slicing software and next layer is built. The horizontal width of the extruded material can vary between 0.254 to 2.54 mm. This feature is called 'road width'. Two materials, one for modeling and the other for support, are dispensed through a dual tip mechanism of FDM-1650 machine. The support material

forms a bond with the modeling material and with some minimum force, the support structure could be removed and then the model can be finished to a have a smooth surface.

2.4 *Design the mold using rapid tooling*

A mold is one in a series of devices that act to shape a plastic material to form the product. Manual design of plastic injection molding machine depends primarily on the experience of mold designers. Drawings are used as the main communication medium. They are interactively redesigned using trial error method making it a slow and costly process. Mold design consists of following:
Cavity design, Runner design, Gate design, Design of cooling system and determination of clamping, ejection, and mold-opening forces.
The following steps were followed in designing the mold for saddle component using mold design and Ideas version 7 software.

1) Preparation of design part: The solid model of the saddletree is imported in SDRC Ideas through IGES. It is necessary that the part is a complete solid with no free edges. All the diagnostics and modification are done prior to the start of the mold design.
2) Preparation of the mold part: The mold part is first oriented to the position at which it will be molded in the final mold. Then it is compensated for shrinkage allowances if any accounting for the materials properties of the part.
3) Parting line determination: The surfaces of the mold plates that meet to form a seal when mold closes creates a boundary line that is called a Parting line. Selection of parting line is very important as a combination of several mechanical, metallurgical and process parameters influences the parting line location and also to achieve dimensional stability, minimize the numbers of cores, and removal of undercuts. The command *Silhouette* curve creates parting edges automatically in Ideas software based on view direction.
4) Creating the mold base: The mold base can be created manually or directly chosen from the VGA Mold Base Catalogue. It can be oriented with suitable coordinate system to locate the mold. Inserts are created separately and added to the mold base.
5) Creating the parting surface: In this step, parting surface are created and added to the mold part, which creates a partitioning tool. The Capping surfaces are created to cap the openings in the part. It cam be created using various surface creation operations.
6) Partitioning the Mold: After creating the parting surface, the mold block is partitioned with the partition tool. It creates three parts namely part A, part B and the cavity. The next phase is to extract the partition volume to create the separate entities.
7) Adding mold component: This includes creating the ejector pins, support pillars, modifying any part if required and creating the bill of materials. The Gate and Runner systems are designed accordingly and assembled in the mold.

Figure 6: Saddletree mold

Mold Analysis: Mold analysis and simulation was done in C-MOLD. It provides the necessary information about injection pressure, clamping force and tonnage required to mold the part as well as suggestion for correcting or improving design. It includes the MFR, machine clamp force, short size required for the part, machine set up information including filling and cooling time, required injection pressure, melt and mold temperature, part information using part weight, projected area of a single cavity, average part thickness and standard deviation of the part thickness.
Mold Manufacturing: To validate the design, the components are manufactured on Injection Molding machine. The injection machine molds are manufactured on CNC machine and the required G-code is generated using DELCAM software.

3. CONCLUSION

The CAD/CAM in product design and development enables to integrate different activities through seamless data transfer. It also compresses the design cycle time, which is an important factor in competitive market. Besides that Reverse Engineering and Rapid Prototyping as a newer technology have a greater role to play than conventional manufacturing which is all about this paper. Although we know that rapid prototyping is "rapid" but how rapid is it and how it's rapidity helps today's manufacturing? The product development process in this paper answers those questions and also it proves that in this particular case following benefits are obtained over conventional manufacturing.

1) Present Polymer saddle are injection molded compared to traditional hand crafted wooden saddle (in our country) and hence there is no material waste or scrap
2) As the present saddletree is made with the help of CAD/CAM techniques, the number of prototypes requires to just one, compared to certain finite number depending on the skill set of the craftsmen.
3) There is absolutely no rework required, as the standardization is very high in this case.
4) Traditional saddletree manufacturing took around 6 months but with this technology, it takes less than a month.
5) The present methodology leads to a product, which conforms to international quality standard.

References

[1] G. Grotenhuis, J. Van Den Brock, " A Conceptual Model for Information Processing", in Modeling Data base Management Systems pp 149 – 183, North Holand Publication Co., 1976

[2] G.M. Nijseen, " A Gross Architecture for the Next Generation Database Management", in Modeling in Database Management Systems. Pp 1-30, North Holand Publication Co. 1976

[3] J.Encarnacao, E.G. Schlechtendahl, "Computer Aided Design: Fundamentals and System Architecture", Springer – Varlag, Berlin 1983

[4] J Kanchana, "Reverse Engineering", 4th SERC School on Advanced Manufacturing Technology, May 18-30, No6, pp 30-40, 1998

[5] Tamas Varaday, Ralph R. Martin and Jordan Coxt, " Reverse Engineering of Geometric Models – An Introduction", Computer-Aided Design, Vol 29, No4, pp 251-273, 1997

Laser engineered net shaping™ – technology and applications

M HEDGES
Neotech Services MTP, Nuremberg, Germany
D KIECHER
Optomec Inc. Alberquerque, USA

ABSTRACT

Laser Engineered Net Shaping ™ (LENS) is a commercially emerging additive manufacturing technique which is being used in an increasing array of RP and RM operations. This paper will introduce the technology, examine its benefits, introduce current applications and outline recent and future planned developments.

The LENS™ process allows the design engineer to rapidly create fully functional prototypes and finished parts, using a wide array of engineering materials including Titanium, Nickel, Cobalt, Steel and Aluminium alloys. In addition it can also produce parts from novel materials such as Metal Matrix Composites and functionally gradient materials (FGMs). Mechanical properties are comparable to standard manufacturing techniques and the produced components can be used directly on critical engineering applications. Significant effort is underway to develop this technique to improve performance and capitalise on the ability to create unique components of complex geometry and functional gradients.

KEYWORDS: LENS™, Rapid Manufacture, Rapid Prototyping, Functionally Graded Materials, Near Net Shape.

1. INTRODUCTION

Laser Engineered Net Shaping ™ (LENS) is a commercially emerging Rapid Manufacturing technique developed over a period of 10 years. Originally conceived at Sandia National Laboratories; it has been commercialised since 1997 in the USA. From the beginning of 2002 this technology will be available to industrial and research users in Europe for the first time. This paper will introduce this technology and will be split into three parts examining:

- The fundamentals of the technology;
- The technical and commercial benefits of the technology in relation to Rapid Manufacture; and
- Outline the recent and future developments of this technology.

The aim is to provide users with an overview of the current status of the technology and direction of future development.

2. FUNDAMENTALS OF LENS™ TECHNOLOGY

Optomec's LENS™ process is functionally similar to many of the Rapid Prototyping (RP) technologies in that it is able to use a three-dimensional CAD solid model to produce a part directly without intermediate steps. Unlike the existing RP methods, the LENS™ technology uses a wide variety of metal powders to create 100% dense, *fully functional* parts that can be used critical applications. Metallic materials processed include: Titanium Alloys, Steels, Aluminium, Nickel Based Alloys and Metal Matrix Composites. Table 1 shows a representative list of the types of materials successfully processed.

Alloy Class	Alloy
Steels	1018
	H13
	A2
	S7
	17-4 PH
	15-5 PH
	PH 13-8 Mo
	304
	309
	316
	410
	416
	420
	MM 10
	CPM 10V
	Aermet 100
Al-alloys	CP Al
	6061
	4047
	2024

Alloy Class	Alloy
Ti alloys	CP Ti
	Ti-6-4
	Ti-6-4 + B
	Ti-6-4 + C
	Ti-6-2-4-2
	Ti-6-2-4-6
	Ti-8Al-1Er
	Ti-48-2-2
	Ti-22Al-23Nb
	Ti-10Cr
	Ti-10Nb
Ni alloys	CP Ni
	IN600
	IN625
	IN690
	IN713
	IN718
	Haynes 188
	Haynes 230
	MarM247
	Rene 142
	Rene N5

Alloy Class	Alloy
Cu alloys	CP Cu
	Cu-10%Sn
	Cu-Ni
Coated Powders	Ni on Cu
	Ni on Cu on B-60C
	Ni on BN
	Ni on YSZ
	Ni on W on Cu
	Ni on TiB2
Miscellaneous	CP W
	CP V
	CP Mo
	CP Ta
	CP Re
	CP Nb
	Mo-Si-B
	Nb-Si
	C103
	Norem
	Metglass

Table 1: Materials successfully deposited by LENS™

A schematic representation of the LENS™ process is depicted in figure 1. The process, uses a high power (>300W) Nd:YAG laser focused onto a metal substrate to create a molten weld pool. Powder is then injected into the weld pool to increase the material volume by additive manufacture. The substrate is then scanned relative to the deposition apparatus to write lines of the metal with a finite width and thickness. Rastering of the part back and forth creates a pattern and fill to complete the layer of material to be deposited. Finally, this procedure is repeated many times until the entire object represented in the three-dimensional CAD model is produced on the machine. In this fashion, a part is essentially built up from powders to form a solid object. The finished part is Near Net Shape and requires only final light finishing. Figure 1b shows an actual component being fabricated on a LENS™ system.

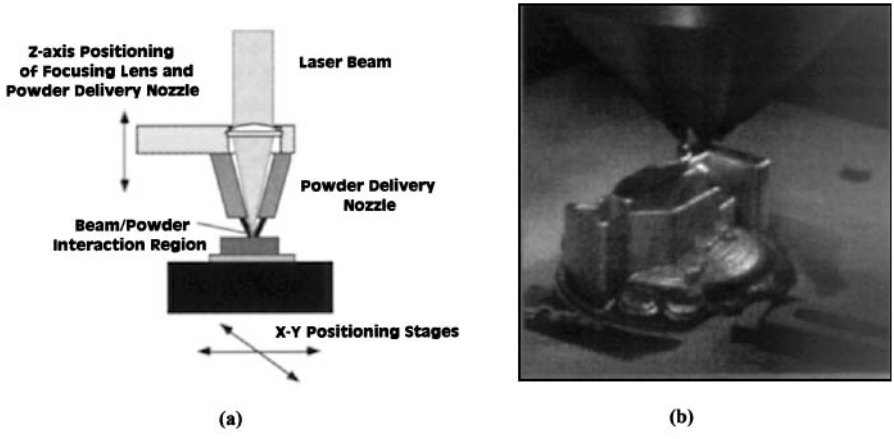

Figure 1: Depiction of the LENS™ process, (a) schematic representation; (b) photograph of thin walled structure being fabricated using the LENS™ process

3. TECHNICAL & COMMERCIAL ADVANTAGES

This additive manufacturing technique has several fundamental features, which offer wide ranging technical and commercial benefits:

Feature	Benefit
Single Step Build	Time Compression
Additive Process	Reduced Material Waste
Improved Microstructures	Superior Materials Properties
Novel 3D Shapes	Increased Design Flexibility
Functional Gradients	Optimised Component Properties

3.1 Time Compression

LENS^{TM} allows significant reduction in time to market by removing the need for standard tooling. A newly designed component can be produced, finished and in service in a matter of days. Costly tooling is eliminated and a greater flexibility in implementing design changes is offered which reduces the financial risk associated with the development process.

Studies in the aerospace industry have identified that this route can offer significant time compression benefits and impact positively upon the customers competitive advantage (1). The greatest benefit can be obtained in structures with fine detail or thin walls which are costly and time consuming to produce by standard subtractive methods.

One application currently under development is an electrical system housing used in defence applications as shown in figure 2. This is a demanding program for the designer as the number of production parts required is low (a few tens of parts per year) and the designs often change. Typical lead times for this component by traditional casting are around 52 weeks. Using LENS^{TM} the part can be scheduled into production and built in around 10 hours. For a reference the domed substrate shown in figure 2 is manufactured from 316 stainless steel, is approximately 20 cm in diameter and the vertical walls were approximately 10 cm tall with a thickness of 2.3mm. In casting such a part, a great deal of care must be taken to insure that the high aspect ratio provided by the vertical walls does not cause defects to occur. In addition, the casting houses would prefer to offer a medium or high volume manufacturing service, which seriously affects development costs.

Figure 2: Rapid Manufactured Electrical Housing

As shown in figure 2, the substrate that was used to build the electrical system housing was machined prior to fabricating the vertical walls to provide a domed substrate. Thus, LENS™ can also be incorporated in to existing manufacturing routes (Hybrid Manufacture) adding detail or special features on components produced by casting, machining, PM or forging. During this parts development the customer requested a design change during prototype manufacture. This request was accommodated by simply adding the new details to a semi finished part.

For the 316 the material properties which can be achieved directly from the LENS™ process are superior to cast properties. In addition, it is not uncommon for large inclusions to occur within a casting. Since the properties are superior and inclusions do not occur within a LENS™ fabricated structure, the designers are moving to a thinner wall design to help reduce the weight of the final housing.

LENS™ is also finding use in Rapid Manufacture in the Medical Implant Market. The implant designer working closely with a team of surgeons has developed a new type of modular revision prostheses for hip replacement. Parts have been produced from Ti 6-4 by LENS™ which are then tested during a normal replacement procedure. The prototype part is put into the patient to check for form & fit and then removed for redesign. Standard RP parts cannot be used as they do not stand up to the high temperatures and pressures used in sterilisation. Therefore, the designer is required to use metallic parts. LENS™ can quickly produce these prototypes in the desired Ti 6-4 alloy.

3.2 Reduced Material Waste

The additive nature of LENS™ allows manufacturers to more effectively utilise raw material inputs. LENS™ is typically 50% efficient with respect to material usage. Standard aerospace forging and machining routes are typically 5-20% efficient and require long post machining on €2m CNC machining centres. This process is costly, time consuming and wasteful. In addition LENS™ requires only one raw material feedstock for each alloy. Thus materials stock levels can be significantly reduced and quality assurance operations simplified.

3.3 Materials Properties

During the LENS™ process, the localized heating provided by the laser allows the deposited material to solidify extremely rapidly (10^4 C°/second) leading to improved material properties in the deposited structures.

Table 1 shows measured tensile properties for LENS™ compared to standard wrought materials. Fatigue properties have also been measured for Ti 6-4 and exhibit properties similar to cast materials in the as deposited state (2,3). With the addition of a post deposition HIP treatment the fatigue properties equal or exceed those of wrought materials. Full fatigue crack testing is currently underway for Ti 6-4. As this technology matures it is expected that the materials properties can be further optimised.

Material Type	**Yield Strength** (MPa)	**Ultimate Tensile Strength** (MPa)	**Elongation** (%)
LENS Processed 316 Stainless Steel	276	661	67
316 Wrought Annealed Bar	*289*	*578*	*50*
LENS Processed Inconel 625	579	930	38
625 Annealed Bar	*400*	*834*	*30*
LENS Processed Ti-6Al-4V	973	1077	11
Ti-6Al-4V Annealed Bar	*834*	*975*	*10*

Table 2: Measured tensile values for LENS fabricated specimens as compared to conventionally processed materials.

It is believed that the materials properties obtained are a direct result of the fast cooling rates and resultant fine grain size. Metallographic analysis of several materials processed using the LENS™ technology have shown substantial reductions in grain size are achieved as compared to like compositions in wrought forms. Although very preliminary, results showed a significant difference in microstructure between the LENS™ fabricated material and the heat-treated wrought material. Measurements of these structures in H-13 tool steel have shown that the grain size within the LENS™ deposited material has an average size of approximately 3 μm as compared to a grain size of approximately 26 μm in the wrought structure. Similarly, the grain size in a LENS™ deposited 316 stainless steel structure was measured to be approximately 6 μm as compared to 60 μm for the like composition wrought material. The 316 stainless steel specimens showing grain size refinement are shown in figure 3. This feature of the LENS™ process holds long term promise for developing materials and components with novel properties.

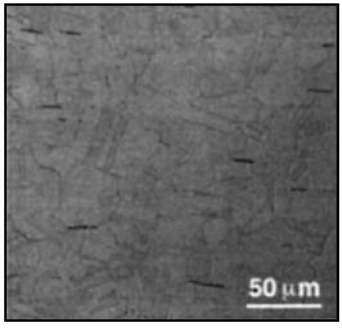

Conventional Process

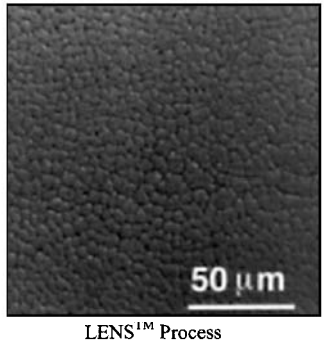

LENS™ Process

Figure 3: Photomicrographs contrasting differences between (a) wrought 316 stainless steel grain structure; and (b) LENS™ deposited 316 stainless steel grain structure.

3.4 Improved Design Flexibility

The additive nature of the LENS process allows the user to fabricate the part with features that cannot be readily produced by other methods, thus increasing design flexibility. A few of these novel features include:

- Hollow passages that can conform to a surface – applications being developed include internal cooling channels in casting dies.
- Internal structures to help reduce weight or tailor mechanical properties – for example the use of internal structures to reduce the stiffness of hip prostheses stems.
- Deposition and encapsulation of other materials within a normally homogeneous structure – for example for building in sensors or magnets into parts.

Figure 4. shows a photograph of a lattice structure that was fabricated using the LENS™ process. The structure shown is fabricated from an H-13 tool steel; however, this structure could as easily have been processed using any of the materials in table 1.

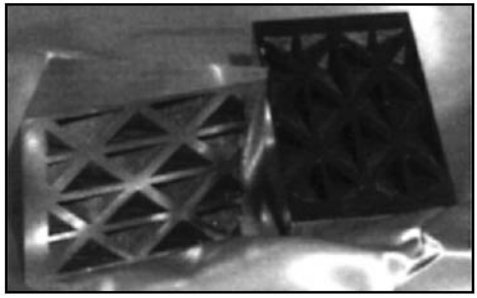

Figure 4: Photograph showing lattice structures fabricated using the LENS™ process

3.5 Optimised Component Properties

The current state of the LENS™ technology allows for binary transitions between the different materials; however, ongoing research efforts are focused on developing a fully integrated multiple-material capability that allows graded material structures to be created directly from CAD information. This opens up an entirely new range of potential applications and products. This area is practically untouched in reality and a significant amount of materials research is needed before its possibilities can be properly exploited. However, actual working applications already exist. One example of using FGMs is the exhaust valves for racing motorbikes, figure 5. For this application, a Ti-6Al-4V shaft is to be used with different titanium alloy being attached to the head region to create the actual valve body. The titanium alloy to be used for the valve body has better high temperature properties that Ti-6Al-4V and so it is expected that these valves will be able to have improved life over conventionally produced valves. In addition, using unique processing conditions to achieve a deposition rate in excess of 25cm^3/hr, it is anticipated that these valves will be sold at 2/3 the cost of the standard machined valves.

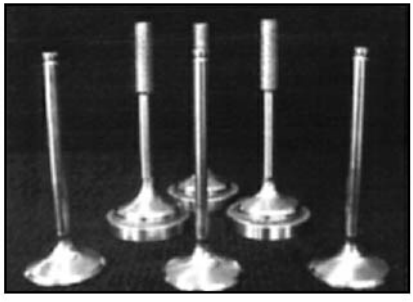

Figure 5: Motorbike Racing Valves composed from FGMs

4. RECENT & FUTURE DEVELOPMENTS

LENS™ is an emerging technology and therefore significant development effort is underway to improve system performance. Several new advances have been made recently including:

1. The ability to deposit materials using five axes of control. This development is largely driven by the desire to provide increased ability to fabricate complex components directly from a CAD solid model. A series of photographs of a simple sample component being fabricated using the five axis control is shown in Fig. 6. As can be seen this part being built is a jack like those used in a child's toy set to demonstrate the capability to produce 90° overhangs. For this build, the center post is first fabricated and then the head is oriented such that each of the arms can then be added to the structure.

2. Online Control System. For functional prototyping where repeatable engineering material properties are expected for all of the parts produced on the LENS system, a melt pool monitor and control system has been developed. This allows the material properties to be controlled throughout the entire build. The melt pool system images the melted puddle size in real time and then controls the laser power to maintain a predetermined pool size throughout the entire build sequence. This increases the ability to produce reliable, repeatable results.

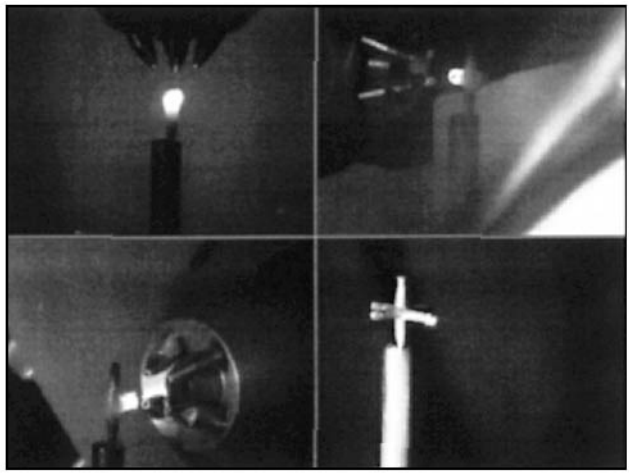

Figure 6: Multiple build axes of complex shapes

3. Increased deposit Rate. One of the factors currently limiting the wider industrial usage of LENS™ is the relatively low deposit rate of ca. 10-15cm^3/hr for most material systems. Recent developments include increased deposition rates in Titanium to ca. 25cm^3/hr. System improvements are now being studied which will allow deposition at over 100cm^3/hr.

System developments are ongoing with the aim of continually improving quality, reliability and meeting a wider range of customers' requirements.

5. CONCLUSIONS

The LENS™ system is an emerging RP and RM tool with a wide range of potential applications. Ongoing developments are aimed at continually improving the system. It is predicted that long term LENS™ will challenge not only existing RP/RM techniques but also establish itself as a volume manufacturing method.

References

1. N. J. Calder, "Rapid Manufacturing for Airframe Production", TCT 99, Nottingham UK. 12-13 10th 1999

2. P.A. Kobryn and S.L. Semiatin , "Mechanical Properties of Laser-Deposited Ti-6Al-4V", *12th Solid Freeform Fabrication Symposium*, Aug. 2001.

3.Donachie, M. J. Jr., ed., *Titanium: A Technical Guide*, ASM International, 1988.

This page intentionally left blank

The microstructure of laser-fabricated Ti6A14V

J LIANG, J MEI, M H LORETTO, and **X WU**
IRC in Materials, The University of Birmingham, UK

ABSTRACT

Direct Laser Fabrication (DLF) or Laser Engineered Net Shaping (LENS) is a manufacturing process for fabricating metal parts directly from metal powder and from CAD solid models by using a laser. In this study Direct Laser Fabrication has been used to produce Ti6Al4V samples for microstructural and mechanical property studies. It has been found that nearly fully dense Ti64 samples can be produced using this technique. The density of Ti64 samples varies, for a range of processing conditions, between 94 to 99%; the density depending upon laser processing parameters, such as powder feed rate, scan speed and z-increment. A much lower density highly porous structure can be obtained when the ratio of the powder feed rate/scan speed is low. The macrostructure and microstructure of a build are influenced by processing conditions and heat extraction rate along x,y,z directions. Long columnar grains are commonly obtained along the length of samples (the z-direction) at low scanning speeds (<800 mm/min). A fine basket-weave microstructure is obtained in most of the samples and alpha and beta laths become even finer with increase of the scan speed. The correlation between the microstructure of DLFed samples and the input energy density has been assessed. The effects of laser processing conditions on microstructure and density are discussed.

KEYWORDS: Direct Laser Fabrication, Ti6Al4V.

1. INTRODUCTION

DLF or LENS is a free form metal deposition process first developed in 1980s that transforms a computer model of a desired part into a fully dense near net-shape metal part in a single step without dies or moulds and without forming, pressing or forging equipment [1]. Some research has been done on DLF which showed important features of the process like build height and width, residual stress, microstructure are strongly dependent on DLF processing parameters including laser power, laser scanning velocity, powder feed rate etc. [2][3][4]. Many metals have been processed including stainless steel, aluminium, titanium, nickel, iron alloy, tungsten and rhenium [5][6][7]. Although there have been a significant number of investigations on DLF, much of the previous work was focused on equipment and software development [8][9], with limited research having been reported on high performance materials such as Ti64 [10,11] to define the relationship between the process parameter and the structure of the deposited parts. Layer banding has been observed and theories to explain this effect were put forward by Kelly etc [10], and Griffith et al [11] have used visible radiation and thermocouple techniques to determine the micro (molten pool) and macro (part) thermal history to gain an understanding of DLF.

DLF is particularly attractive for the manufacture of titanium aerospace components because of the great reduction of the product time, and a major effort is underway in the IRC, the University of Birmingham, to develop titanium alloy laser powder deposition. The present paper reports progress on our study of DLF of Ti64.

2. EXPERIMENTAL MATERIAL AND PROCEDURES

Ti64 powder with particle size about 100-250 μm supplied by Crucible Research was used in the present work. Specimens of dimensions 20×20mm were produced on the substrate of Ti64 rolled plate. A 1.75kW CO_2 laser operating in continuous wave (CW) mode was used in the experiments with power between 180W and 817W and laser scanning speed from 150mm/min to 1000mm/min. Focused and defocused laser beam with diameters between 1.1-3.2mm were used. A CAD and CNC control system was used to control the x-, y-axis movement and z-axis increment. Z-axis increment from 0.2 to 0.4mm was used. Four-nozzle powder feed system controlled the powder feed rate between 2 and 21 g/min. An atmosphere control unit was used to ensure that the O_2 content was less than 5ppm to prevent oxygen pick-up by the titanium alloy. Densities of specimens under different

processing parameters were measured using a balance with an accuracy of 0.001g simply by measuring the weight in air and in water. Specimens were polished to remove the rough surface, which is usually formed during DLF processing by the fine Ti64 powder, which becomes attached to the free surface of the sample. Optical microscopy and scanning electron microscopy (SEM) were carried out to examine the microstructure of the specimens built using different process parameters.

3. RESULTS AND DISCUSSIONS

A porous structure, which is illustrated in Figure 1a, is obtained when a laser power of 180W is used because the laser power is too low to melt all the powder particles. If the laser power is increased to 264W, fully dense specimens with little porosity are obtained as shown in fig1b, which suggests that the laser power should be above the value that provides enough energy to melt the powder which is fed into the laser beam.

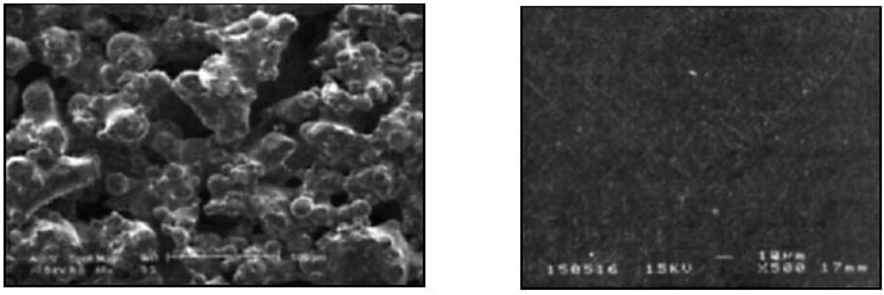

(a) (b)

Figure 1: Secondary electron scanning electron micrographs, which show the influence of the laser power on the microstructure. Scanning velocity: 200mm/min, powder feed rate: 6g/min, z-increment: 0.3mm. (a) Laser power 180W, (b) Laser power 264W.

The bulk densities of all the specimens are over 94% of the bulk density 4.43g/cm^3. Figure 2 shows the influence of the powder feed rate over the scanning speed on the bulk density (%) of DLF specimens at a constant laser power of 264W and with z (built-up direction) increment 0.3mm. The density increased slightly with increase of the parameter of the powder feed rate divided by the scanning speed.

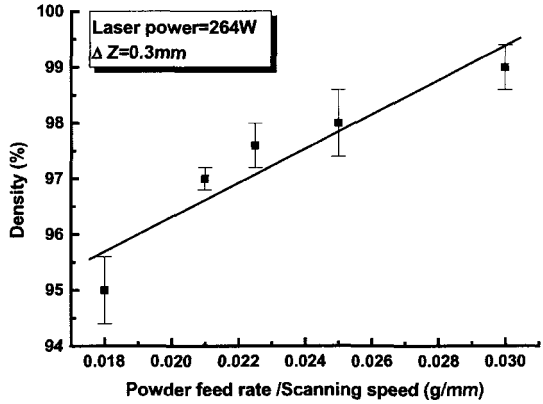

Figure 2: Influence of the powder feed rate over the scanning speed on the bulk density of DLF samples relative to the density of bulk Ti64.

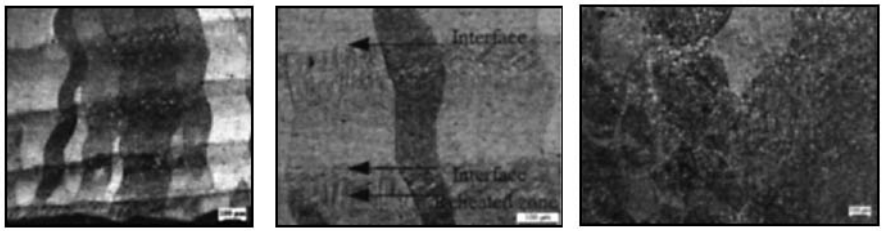

Figure 3: Optical micrograph showing a typical example of columnar grains at the bottom of a specimen of Ti64, Laser power: 264W, powder feed rate: 6g/min, z-increment: 0.3mm scanning velocity: (a) 300mm/min, (b)(c) 200mm/min.

Figure 3a shows columnar grains of 1-20mm. Layer bands, which are associated with each laser traverse, appear as a thin strip of darker material running across the width of the part. The arrangement of the columnar grains forms a zig-zag pattern as the molten pool follows the laser scanning direction in each layer. The axes of the columnar grains are approximately parallel to the build direction of the deposit because the growing grains align themselves along the steepest temperature gradients. Solidification of the columnar grains occurs from the previously deposited layers allowing the columnar grains to continue growing across successively deposited layers, because it is easier for grains to grow from the pre existing grains rather than to nucleate new grains.

The optical micrograph (Figure 3b) of the darker interface regions visible in figure 3(a) taken at a higher magnification shows that a coarser microstructure is observed at each layer. These bands are formed because of the reheating of the previous layer when the new layer was built upon the pre-existing layer. The microstructure of the layer band consists of large colonies of acicular α outlined in partially transformed β while adjacent, the uncoarsened microstructure consists of smaller colonies with the same kind of structure. This is in general agreement with the report by Kelly [10]. Essentially, a new HAZ had been formed locally in the deposit each time a laser pass is made which results in the observed coarsening of the microstructure. However, as would be expected on that basis the thickness of these coarsened layers is reduced and they eventually disappear at the very top of the specimens. In fact the very top region of these samples consists of equiaxed grains because the cooling via the substrate becomes more and more difficult with the increase of sample height and the cooling rates gradually become similar at all directions, the growth of columnar grains is then replaced by the formation of large equiaxed grains.

The relationship between the microstructure and the laser scanning speed is shown in Figure 4 obtained at a constant laser power of 264W and z increment of 0.3mm.

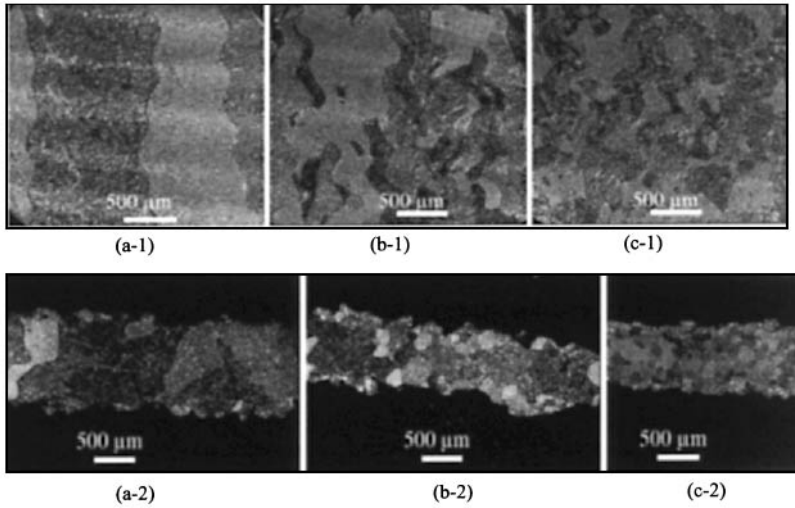

Figure 4: Optical micrographs showing that the grain size is reduced with increase of laser scanning speed (side surface). Laser power: 264W, z-increment: 0.3mm,Laser scanning speed (mm/min): (a-1, a-2)200, (b-1,b-2)500, (c-1,c-2)800; with powder feed rate (g/min): (a-1,a-2) 6,(b-1,b-2)15,(c-1,c-2) 18.

Figure 4a-1 shows that when the laser scanning speed is 200 mm/min with a powder feed rate of 6 g/min, the columnar grains grow up to 4-10mm long and almost 1 mm wide. When the laser scanning speed is increased to 500 mm/min with the powder feed rate 15 g/min, the grain size decreases to 2-7mm long and 0.5-1mm wide (Fig.4b-1). The grain size becomes even smaller when the scanning speed is above 800 mm/min, the thickness of layer band is reduced and eventually disappears at the speed 800mm/min as shown in Fig 4c-1. The microstructure of the cross section of each specimen shows more clearly that the grain size is reduced with increase of laser scanning speed. It is interesting that there is only one grain across the cross section of the specimen when the laser scanning speed is low at 200mm/min (Fig.4a-2), and the grain size reduces to one half at the scanning speed of 500mm/min (Fig. 4b-2), while one third or one fourth the size at the scanning speed of 800mm/min though the powder feed rate increase from 6 to 15 and to 21 g/min.

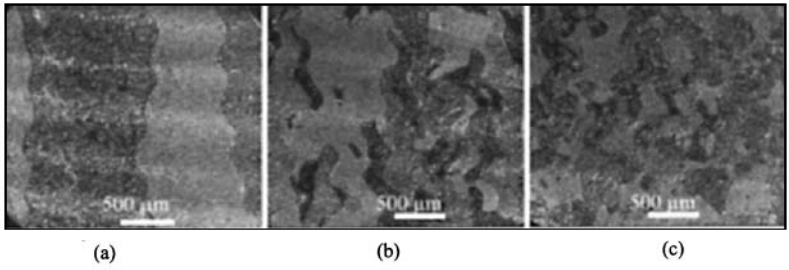

Figure 5: Secondary electron scanning electron micrographs, which show the influence of laser scanning velocity on the microstructure (at the bottom of the specimen). Laser power: 432W, powder feed rate: 18g/min, z-increment: 0.3mmScanning velocity (a) 300mm/min, (b) 600mm/min, (c) 900mm/min.

The scan velocity has a significant influence on the microstructure of the DLF samples and this is illustrated in figure 5. It can be seen in figure 5 that a fine basket-weave microstructure is obtained in most of the samples with the alpha and retained beta becoming even finer with increase of the scan velocity under constant laser power, which means with the decrease of the line energy (the energy absorbed in a unit length within an unit time).

The mechanical properties are currently being measured in DLF samples prepared using a range of conditions, both before and after Hipping in order to define the optimum processing conditions.

4. CONCLUSIONS

Laser fabrication of Ti-6Al-4V is a freeform fabrication process, which produces high temperature gradients and high cooling rate. These give rise to a columnar macrostructure growing from the substrate to a height which is influenced by the DLF conditions and for the conditions used here these grains can be 1-20mm in height. The very top of some specimens consists of equiaxed grains. A very fine transformed microstructure is found throughout samples although this is coarsened to some extent where re-heating occurs as successive layers are deposited. The grain size decreases with increase of the lasers scanning speed. The transformed β laths become finer and longer with increase of laser scanning velocity or decrease of line energy. Near fully dense Ti64 can be obtained with the density over 94% and up to 99% of bulk density.

Acknowledgements

The support of the IRC, Dept of Metallurgy and Materials, the University of Birmingham and ORS scholarship scheme and Rolls-Royce UTC are gratefully acknowledged.

References

[1] Richard Mah, Directed light fabrication, Advanced Materials and Processes 3 (1997) 31-33.
[2] E. W. Kreutz, G. Backes, A. Grsser etc. Rapid prototyping with CO_2 laser radiation. Applied Surface Science 86 (1995) 310-316.
[3] P. A. Kobryn, E. H. Moore and S. L. Semiatin. The effect of laser power and traverse speed on microstructure, porosity and built height in laser deposited Ti-6Al-4V.Scripta Mater. 43 (2000) 299-305.
[4] D. Srivastava, I. T. H. Chang, and M.H. Loretto. The optimisation of processing parameters and characterisation of microstructure of direct laser fabricated TiAl alloy components. Materials & Design, Volume 21, Issue 4, 1 August 2000, 425-433.
[5] N. F. Anoshkin, G. G. Demchenkov, Material science and technological aspects of rapid solidified titanium alloy production. Materials Science and Engineering A 243 (1998) 263-268.
[6] J. O. Milewski, G. K. Lewis, J. C. Fonseca, R. B. Nemec, Laser power deposition of a near net shape injection mold core—a case study, Materials and Manufacturing Processes, Vol. 15, No. 2, (2000) 247-258.
[7] J. E. Smugeresky, Laser engineered net shaping process-optimization of surface and microstructures, Metal Powder Report, Volume 53, Issue 9, September 1998, 57.
[8] G. K. Lewis, E. Schlienger, Practical consideration and capabilities for laser assisted direct metal deposition, Material Design 21 (2000) 417-423.
[9] J. O. Milewski, G. Dickerson, R. B. Nemec, G. K. Lewis, J. C. Fonseca, Application of a manufacturing model for the optimisation of additive processing of Inconel alloy 690, Journal of Materials Processing Technology 91 (1999) 18-28.
[10] S. M. Kelly, S. L. Kampe, C. R. Crowe, Microstructural study of laser formed Ti-6Al-4V, Solid Freeform and Additive Fabrication-2000. Editors: Stephen C. Danforth, Diane Dimis, Frinz, MRS.
[11] M. L. Griffith, M. T. Ensz, J. D. Puskar, C. V. Robino, J. A. Philiber, J. E. Smugeresky, W. H. Hofmeister, Understanding the microstructure and properties of components fabricated by laser engineered net shape (LENS). Solid Freeform and Additive Fabrication-2000. Editors: Stephen C. Danforth, Diane Dimis, Frinz, MRS.

This page intentionally left blank

Rapid manufacture of burn-resistant Ti components using direct laser fabrication (DLF)

R SHARMAN, S WU, and **M H LORETTO**
IRC in Materials, The University of Birmngham, UK
W VOICE
Rolls-Royce plc, Derby, UK

ABSTRACT

The technique of direct laser fabrication (DLF) has been used to manufacture 3-dimensional shapes from a burn-resistant Ti alloy, Ti25V15Cr2Al0.2C (wt%). The effects of laser processing parameters, such as laser power, scanning speed and powder feed rate, on the microstructure and mechanical properties have been assessed using optical microscopy, SEM and TEM. Some of the observations are reported here.

These observations have been used to define the optimum process parameters for building samples and for generating strong interfaces since the aim of this work is to use DLF to repair and to join other Ti alloys.

KEYWORDS: Direct Laser Fabrication, Titanium alloys, Processing parameters, Carbides, Microstructure.

1. INTRODUCTION

It is well known when Ti alloys rub against each other in the conditions within a gas turbine they can catch fire. The IRC has developed a new low cost, burn-resistant beta Ti alloy with a composition of Ti-25V-15Cr-2Al-0.2C (wt%) [1] It has been found that the C forms a fine distribution of TiC precipitates (composition corresponding to Ti_2C), which pin grain boundaries and thus limit grain growth. In addition the Ti_2C particles act as getters and remove oxygen from the matrix by forming Ti(CO). This removal of oxygen not only improves the ductility of the forged and heat treated alloy, but also reduces the tendency for precipitation of alpha phase during high temperature exposure, again leading to an increase in ductility over that found in exposed non carbon-containing alloy.

Direct Laser Fabrication (DLF) processing has been developed in the USA, for example at Sandia Labs and Los Alamos National Laboratory, New Mexico, over the last ten or so years [2-4] to provide a single-step, waste-free process to fabricate near net shape components using metal powders. In this method of component production powder is fed at a controlled rate into the focal point of a laser where the individual particles are melted. The component is produced using a CAD file to move the sample in the XY plane and the laser in the Z-direction to add successive layers, thus directly generating a 3D shape without the necessity of any tooling. Clearly this method of producing solid material from powder can be used in the same way as can conventional welding to build up material or to repair damaged components. This method eliminates all the steps for the production of welding rods.

The many processing parameters such as scan speed and laser power need to be optimised in order to achieve successful production of a component and to obtain the desired microstructure and mechanical properties.

The objective of the present work is to investigate the effects that these processing parameters have on the development of the microstructure of the Ti-25V-15Cr-2Al-0.2C (wt%) and to understand the relationship between the microstructure and the mechanical properties of the laser fabricated material.

2. EXPERIMENTAL PROCEDURE

An ingot of the burn-resistant alloy Ti-25V-15Cr-2Al-0.2C (wt.%) was produced in the plasma melter in the IRC, and was gas atomised by Crucible, Pittsburgh, USA. The oxygen content in the atomised powder was ~1900 ppm (0.19 wt%). The laser-built specimens were produced using a 1.75kW CO_2 laser in an argon atmosphere with O_2< 5ppm. The laser fabrication parameters used in this study are shown in Table 1.

In this work, 20x20x1.3mm rectangular samples were generally produced using a single pass of the laser in the X-Y plane to deposit successive layers on Ti6Al4V substrates. A Philips XL30 Scanning Electron Microscope (SEM), fitted with Electron Diffracted X-ray (EDX) and Electron Backscattered Diffraction (EBSD) systems was used to examine the microstructure and grain orientations. An optical microscope was also used to assess the morphology of the microstructure of the entire build.

Processing parameters	
Laser power(W)	222 to 516
Powder size(μm)	100-250
Powder feed rate(g/min)	8-27
Laser scanning rate(mm/min)	150-1050
Z-increment(mm)	0.25-0.35

Table1: Showing the parameters used for deposition of Ti25V15Cr2Al0.2C(wt.%)

3. RESULTS AND DISCUSSION

The morphology of the laser-fabricated samples varies over the sample from the bottom to top. The burn resistant alloy generally forms equiaxed grains but columnar grains can occasionally form at the bottom of the sample with some processing conditions. This tendency to form columnar grains is clearly associated with the directional heat flow during the early stages of the build of the sample. Thus in the lower regions and at the initial stages of the build the substrate has a major effect in extracting heat it as the fabricated material cools and it is therefore possible to form columnar grains under these conditions. During the later stages of build the influence of the conduction of heat to the substrate via the thin wall is evidently comparable to that of the heat loss from the sides of the sample since equiaxed grains are formed. In the results presented below 3 regions within DLFed samples (bottom, middle and upper) and their relative sizes will be discussed in relation to the processing parameters.

3.1 Effect of laser power

Changes in power over a wide range have little effect on the overall morphology of the burn resistant alloy (figure 1) but have a significant effect on the precipitation of carbides. At low power (222W) carbides are small (~2μm) and they are uniformly distributed. As the power of the laser is increased the precipitates become both longer and thicker. At a laser power of 516W the precipitates can be as large as 10μm in length (Figure 2). Although in general the precipitates are smaller in size and higher in density at the bottom of samples, the effect of power on the carbide size is evident at all levels within the samples. The reasons for this are currently under investigation as discussed below.

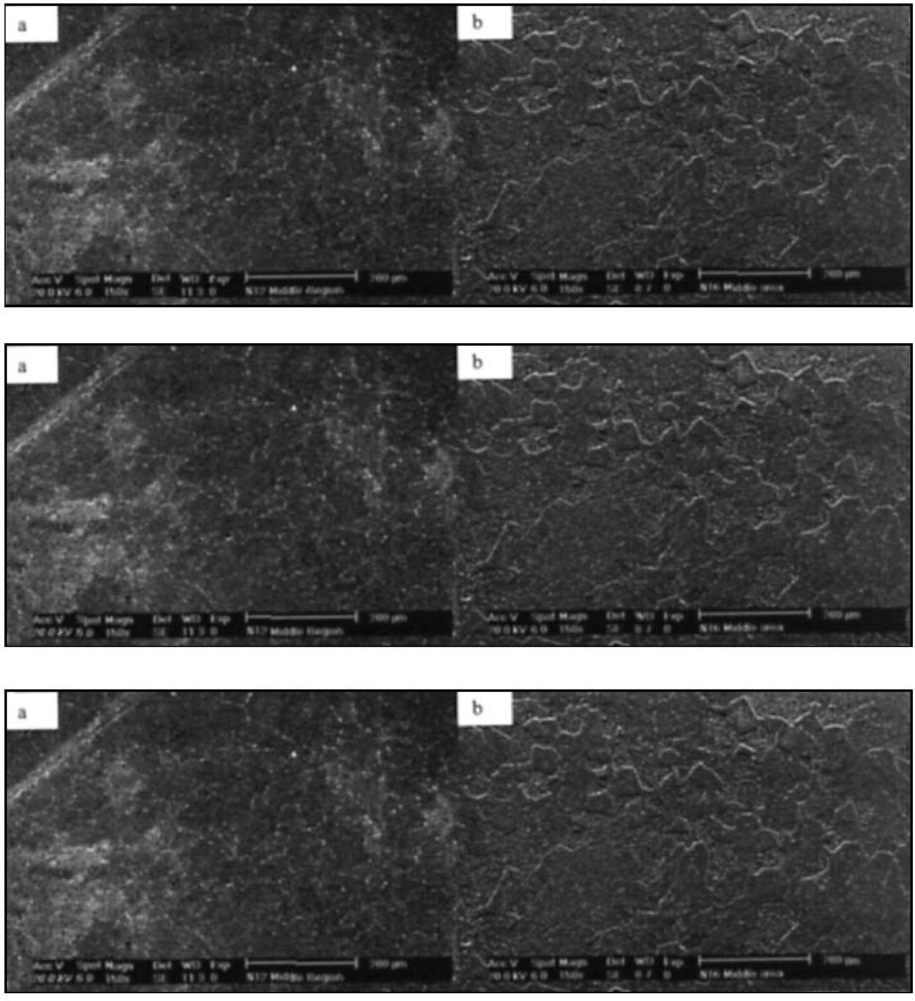

Figure 1: SEM Secondary Electron micrographs showing laser power has little effect on the morphology of DLFed samples, but a marked effect on the size and density of carbides. (a) 222W; (b) 264W; (c) 306W; (d) 348W; (e) 390W; (f) 516W. All samples have the same scan speed of 200mm/min and powder feed rate of 9g/min

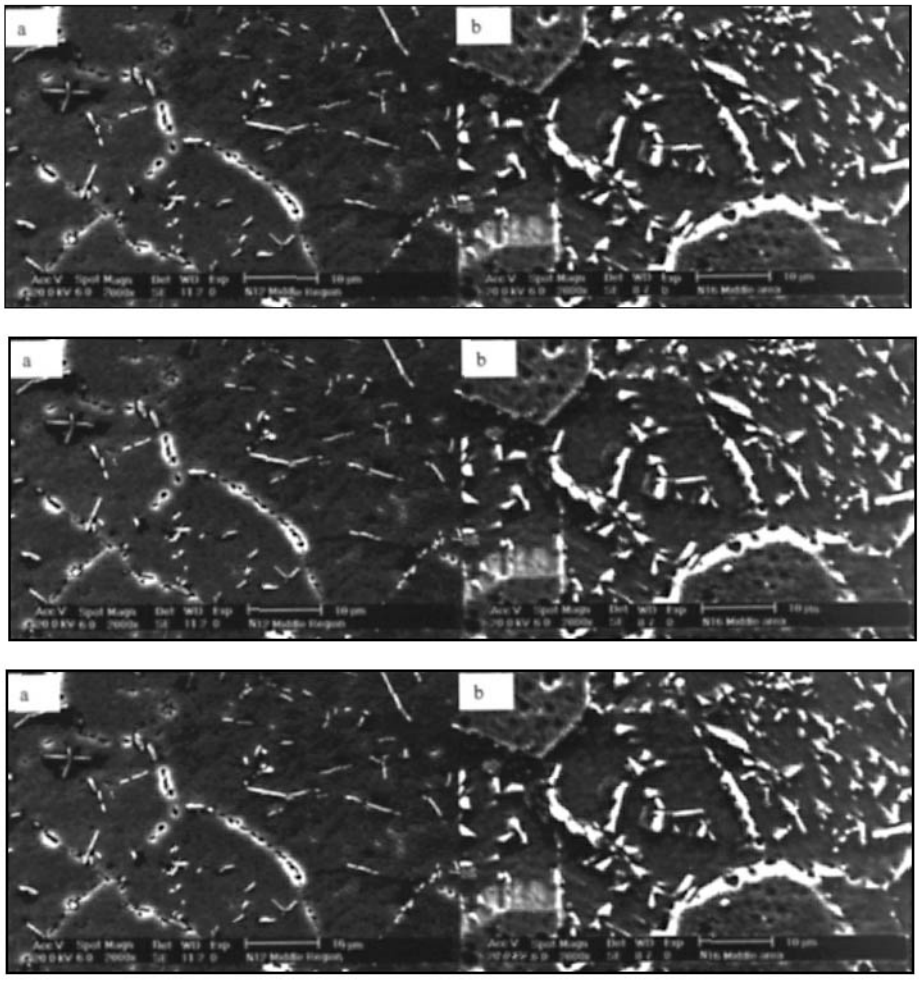

Figure 2: SEM Secondary Electron micrographs showing the influence of laser power on carbide size and density. (a) 222W; (b) 264W; (c) 306W; (d) 348W; (e) 390W; (f) 516W. All samples have the same scan speed of 200mm/min and powder feed rate of 9g/min

3.2 Effect of scan speed

Scan speed has an effect on the morphology of a build. This is particularly noticeable at the base of the samples near the substrate. As the scan speed is increased the morphology becomes more directional in the lower regions of the sample. At high scan speeds and high laser powers the microstructure at the base of the sample can be columnar (Figure 3). The columnar grains are 5-10 mm in length, which is 15-30 times longer than the Z-increment (0.35 mm) used. The colour in Fig. 3-shows the orientation of grains (taken using Electron Back Scatter Diffraction Pattern information). It is evident the columnar grains have the same orientation throughout their entire length.

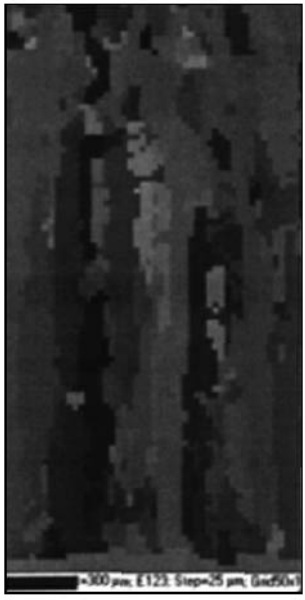

Figure 3: EBSD pattern showing the orientation of the epitaxial columnar growth region with the grain size many times the Z increment

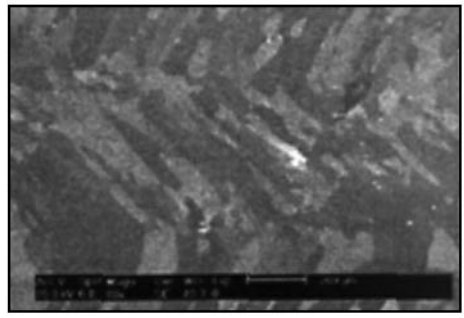

Figure 4: SEM micrograph showing the zig-zag microstructure obtained at low and medium scan speeds near the bottom of the sample

When the scan speed is decreased it can be seen that columnar grains are still present, but now with a length of the Z-increment (0.25 or 0.3 mm), (Figure. 4). In some cases the columnar grains incline to right or left following the motion of the laser beam or molten pool in each layer. Figure 5 shows the orientation image of this morphology and it can be seen that individual grains in consecutive layers have random orientations. The height of this region with elongated grains is in the order of mm. Above this region grains normally are equiaxed.

3.3 Mechanical properties

Some DLFed samples have been HIPped (Hot Isostatically Pressed) and tested under tensile load and in creep. Figure 6 shows the yield stress of these samples is ~ 1100 MPa and the elongation is 2-3% at room temperature. At a temperature of 450°C the yield stress is ~ 800 MPa and the elongation is about 4%. These properties are comparable with those obtained from the material from conventional process route of forging at a similar oxygen level.

Figure 6 also shows that there are some samples that have failed at low stresses prior to any plastic deformation. Those samples (which were made using multi passes) were fabricated with inadequate over-lapping distance between the multi laser passes and large pores are present in these samples.

The creep resistance of the DLFed burn resistant alloy has also been assessed at a range of stresses and temperatures. Figure 7 shows the creep property of the material at 650 MPa at 450°C. It can be seen that the creep resistance is considerably higher than that of equivalent extruded microstructure of the same alloy, with the extruded condition failing after 200hs at 650MPa at 450°C. As for the DLFed condition the creep test was interrupted after nearly 400hrs. The improved creep property might be attributed to high volume fraction of precipitates obtained in DLFed samples (see section 4.4).

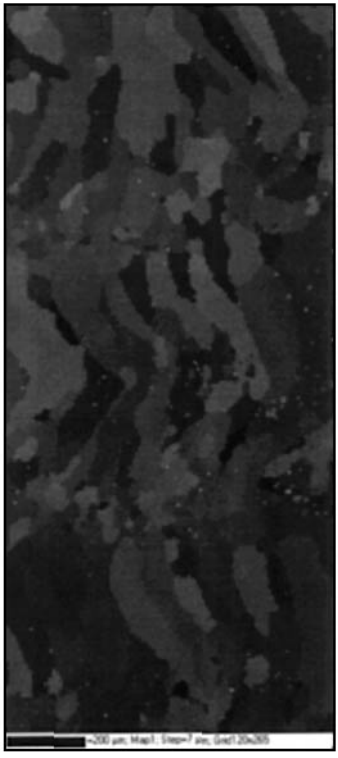

Figure 5: EBSD pattern showing random orientations of the elongated grains with a height of the Z increment obtained near the bottom of the sample at low and medium scan speeds

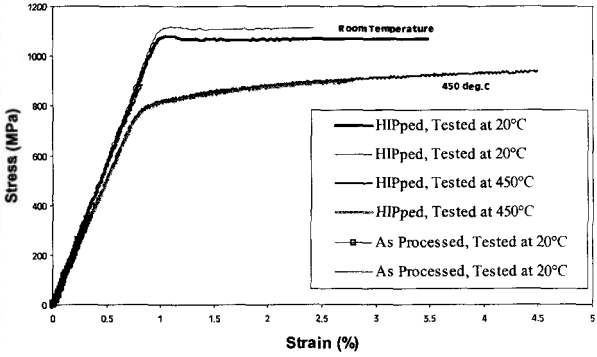

Figure 6: Stress-strain curves of burn resistant titanium showing elongation of ~2% for HIPped at room temperature and ~3.5% for hipped at 450°C. The high levels of porosity in the multi pass samples (labelled as processed) explain their poor tensile performance

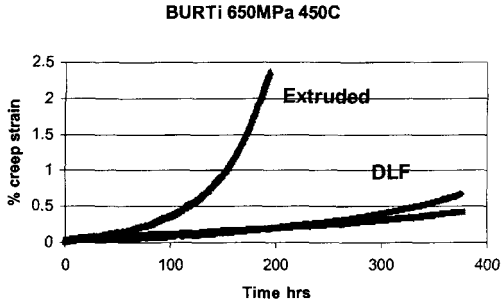

Figure 7: Creep curve of DLFed burn resistant alloy obtained at 650MPa and at 450°C

3.4 Comparison of microstructures between the forged and laser fabricated conditions

Figure 8 and figure 9 show the microstructures obtained after forging and after laser fabrication, respectively. The volume fraction of carbides in the forged microstructure is about 3-4%, which corresponds to the expected volume fraction of Ti(CO) as calculated from the content of the C in the material. However it has been observed that the volume fraction of carbides in the laser fabricated microstructure appears to vary under different processing conditions and it can be more than 15% as can be seen in Figure 2. Figure 10 shows the microstructure that was obtained after laser fabrication, followed by HIPping at 1000°C at 100 MPa. It is evident that the volume fraction of carbides has been reduced to approximately 3%. This perhaps suggests that they have transformed into equilibrium Ti(CO). It thus appears that these precipitates, are a non-equilibrium phases, rather than Ti(CO) but further detailed Transmission Electron Microscopy (TEM) is required in order to understand these observations. TEM examination has in fact found the particles in the as DLFed microstructure contain carbon and oxygen but quantitative analysis and diffraction analyses have not yet been carried out.

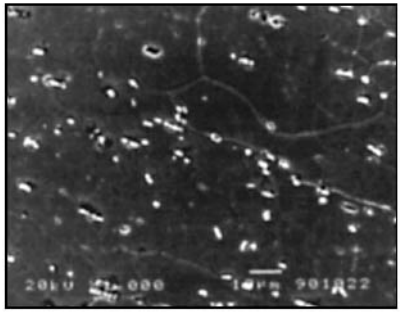

Figure 8: SEM micrograph of forged burn-resistant alloy Ti-25V-15Cr-2Al-0.2C (wt.%) showing precipitate density 3-4%

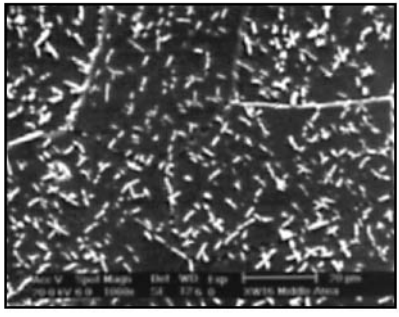

Figure 9: SEM micrograph of laser fabricated burn-resistant alloy Ti-25V-15Cr-2Al-0.2C (wt.%) showing a higher density of precipitates. (>15%)

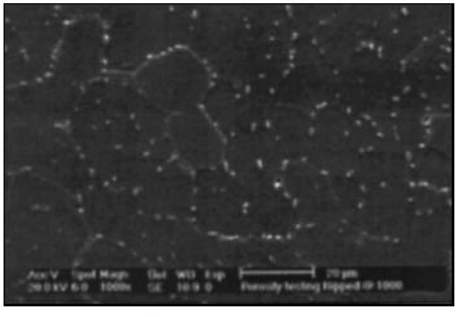

Figure 10: SEM micrograph showing the microstructure and reduced density of precipitates which has transformed from that seen in Figure 9 after HIPping at 1000°C at 100Mpa. The density of carbides is 3-4%

4. CONCLUSIONS

1. Scan speed affects the morphology of the build. The microstructure at the base of the sample can be directional at high scan speed and high laser power. In general this alloy tends to form equiaxed grains.

2. The tensile properties of the laser fabricated burn resistant alloy are comparable to those of conventionally processed condition at the same oxygen content.

3. The creep properties of the laser fabricated burn resistant alloy are considerably better than those of conventionally processed condition.

4. Laser power affects the volume fraction of precipitates with a greater density at the higher laser power used, but the nature of these precipitates appear to be different from those found in extruded samples and in DLFed samples which have been HIPped at 1000C.

References

1. Li Y.G., Blenkinsop P.A., Loretto M.H., Rugg D., Voice W. (1999) "Effect of Carbon and Oxygen on Microstructure and Mechanical Properties of Ti-25V-15Cr-2Al (wt%) Alloys", Acta Materialia Vol.47, No.10, pp2889-2905.
2. Lewis G.K. and Schlienger E. (2000) "Practical Considerations and Capabilities for Laser Assisted Direct Metal Deposition", Materials & Design Vol.21, pp.417-423.
3. Milewski J.O., Lewis G.K., Fonseca J., Nemec R.B. (2000). "Laser Powder Deposition of a Near Net Shape Injection Mold Core - A Case Study." Materials and Manufacturing Processes, Vol. 15, issue 2, pages 247-258.
4. Milewski J.O., Lewis G.K., Thoma D.J., Keel G.I., Nemec R.B., Reinert R.A. (1998) "Directed Light Fabrication of a Solid Metal Hemisphere Using 5-Axis Powder Deposition." Journal of Materials Processing Technology, Vol. 75, pages 165-172.

Acknowledgements

This work was funded through the Rolls-Royce Ti-UTC by Rolls-Royce plc, the Ministry of Defence, The Department of Trade and Industry CARAD program, Timet UK Ltd. and EPSRC.

Preliminary investigation of surface roughness and dimensional accuracy of ThermoJet and SLA parts

I H MULYADI, N G BENNETT, and **S O ONUH**
Regional Centre for Manufacturing Industries (RCMI), University of Portsmouth, UK

ABSTRACT

Rapid Prototyping (RP) technology has introduced new generation of tool-making techniques commonly referred to as Rapid Tooling (RT) processes. These processes have been and continue to be developed with the aim of producing technical prototypes, i.e. prototypes made using the same material and by the same process as the intended production part. However, RP techniques are far from meeting the requirement for high part qualities, which are necessary for manufacturing the tool. Fortunately, the development of new material and new research results has led to the successful application of RP technique in RT. Stereolithography (SLA) technique has been shown to produce prototypes of higher quality especially surface finish. However, the build time and investment cost are the key weaknesses of SLA. The production of tool is a costly process; hence, by using 3DP (Thermojet) technique, these weaknesses relating to build time could be overcome. Unfortunately, the information about part qualities of this technique (3DP) has not been publishing widely yet. In RP systems such as SLA and 3DP, the orientation of the part during fabrication is critical as it can affect surface finish, reduce the production time, and minimize the requirement for supports and, thus, the cost of building the model. This present investigation is intended to provide preliminary information about 3DP technique especially as it relates to part qualities (i.e. surface roughness) by considering part orientation. Preliminary results show that surface roughness of 3DP technique is better than SLA technique in some given build conditions. These results have not been used to decide the best technique yet, however it is sufficient to mention that 3DP technique has ability to produce good part qualities similar to what could be provide by SLA. This is a preliminary report as further works are being done to advance the knowledge in 3DP technique.

KEYWORDS: Rapid Prototyping, Rapid Tooling, Part Orientation, Dimensional accuracy, Surface roughness.

1. INTRODUCTION

For many years, research for improving Rapid Prototyping (RP) techniques has been a significant issue across the technology. During this period, new rapid prototyping techniques have also been developed to provide RP users with different options. However, each system still has its advantages and disadvantages, which are reflected in downstream applications. This is caused by several reasons such as cost, product quality and material as well as builds time. One of the downstream application areas is Rapid Tooling (RT). In RT materials are important parameters due to their influence on the mechanical and functional properties of the models. In addition, materials also affect the choice of the most suitable RT techniques, which is appropriate for each application, i.e. indirect tooling or direct tooling.

It has been suggested that soft materials are not suitable for RT if used as a build medium. Recently, there were a number of successful applications [1] such as Resin Tools, Metal Powder Tools, Ceramic Powder Tools, Microcast Tools and Laminated Metal Sheets. RP techniques such as stereolithography (SLA), Selective Laser Sintering (SLS), Three-dimensional Printing (3DP), Direct Shell Production Casting (DSPC), Selective Deposition Fabrication (SDF) and Laminated Object Manufacturing (LOM), are used to develop these application areas. However, most of the studies seem to focus on the use of SLA for RT applications, which to date provides the prototype with highest surface finish and dimensional accuracy amongst current RP techniques.

Research results and experience show that the part quality that can be achieved by using 3DP machine is not as good as SLA machine however; 3DP has excellent speed in building a prototype. Unfortunately, research relating to 3DP have not been widely published in literature. However, the importance of RP application in RT has been a major issue both in academia and industry.

Prototyping is an essential part of product development and has been used for many years to visualize the final product design. The advantage of this method is its ability to make the initial prototype directly from the actual final product material so it is easy to assess all requirements needed for final product. However, this method certainly has several limitations in efforts to reduce time-to-market, obtain high complexity of the models, and reduce the use of very labour intensive work [2].

Along with increasing customer demand for high-quality products delivered on time in today's globally competitive manufacturing arena, the product design must have short life-cycle. In other words, product design will be changed and updated more frequently than ever before. This concept is called Rapid Response Manufacturing (RRM) [3]. This method has been pursued by many companies to shorten time-to-market, improve quality-to-cost and enhance product reliability. In addition, this method also has prompted research and development in order to find the suitable and sufficient new technique in prototype production process for the implementation of RRM. The implementation of RRM methods makes product realization cycles shorter and in turn, will lead to rapid product entry into market. A 20% reduction in product realization cycles time translates to roughly 20% reduction of the product as the operating costs of product development [4].

The emergence of Desktop Manufacturing technique provides design engineers with easy and economic tools to build a prototype or even a functional part in order to considerably reduce the process time [3]. Principally, this technology includes desktop Numerical Machining (NC) and Solid Freeform Fabrication (SFF). Desktop numerical machining is based on traditional machining process, which could provide products with high surface finish and high dimensional accuracy. However, this technology still has weakness especially in producing complex hollow parts. SFF could overcome the weakness of desktop numerical machining because of its ability to build any complex shape from the designed electronic data.

Among the rapid prototyping processes, research tends to focus on exploration of improvement of prototype quality, prototype cost and reduction in build time. The research is concentrated on the processes, which have machine available commercially such as SLA, Fused Deposition Modelling (FDM), SLS, 3DP and LOM. The primary benefit of utilizing RP technologies is its ability to produce high quality and complex pattern such as used in investment casting, lower cost and shorter lead-time. This technology is very suitable for low volume production such as building a tool directly or indirectly from rapid prototyping models. The current desire of the manufacturing industry is the need for complete elimination of tooling, as this would reduce lead times, investment costs and provide complete manufacturing flexibility which is scalable. The evolutionary trend in RP is split into Flexible Tooling (FT), High Performance Tooling (HPT) and Rapid Manufacturing (RM) [5, 6]. The goal should be in such a way that a prototype tool should be the production tool as well.

Currently, tooling is one of the slowest and most expensive steps in manufacturing because of its requirement for extreme high quality. In some extent, tools have complex geometries, yet must be dimensionally accurate. Moreover, tools also must be hard, wear resistant and have very low surface roughness. Traditionally, tools are made using CNC machining, Electro Discharge Machining or by hand, which are obviously expensive and time consuming. Peter Hilton, President of Technology Strategy Consulting in Concorde, MA, believes that tooling costs and development time could be reduced by 75% or more by implementing rapid tooling and related technologies [7].

At present there are different processes, which are referred to as RT but may not meet the necessary conditions to be classified as such. In a study [1], a Rapid Tooling technology has been classified into three main methods as shown in figure 1. The ultimate challenge in RT is the creation of tools directly from rapid prototyping machine. Therefore, most research in improving rapid prototyping technologies being done and probably for future development tend to concentrate on improving quality such as surface finish, dimensional accuracy and part strength and stability.

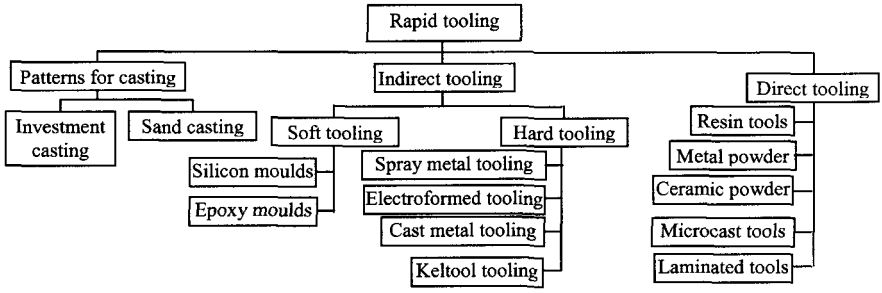

Figure 1: Classification of Rapid Tooling

2. RESEARCH OBJECTIVES

The aim of this study is to carry out preliminary theoretical and experimental investigations of the quality and surface finish of parts built in SLA and 3DP machines. This is to assist in determining the suitability of parts built by these machines in RT applications. It is also expected that empirical models developed in this study will help in assessment of part quality and surface finish. The main objectives of this study are:

1. Comparison of the effect of build parameters on dimensional accuracy and surface roughness.
2. Investigation of the characteristics of both dimensional accuracy and surface roughness of prototypes built by either stereolithography machine or thermo jet machine due to variation of part orientation.
3. To make appropriate recommendations related to part qualities of prototype built by the 3DP technique.

3. EXPERIMENTAL METHODS

In this present investigation, SLA- 250/50 machine and 3DP ThermoJet machine were used to build the experimental models with different part orientation. Experimental prototypes were measured by Mitutoyo surface roughness testing machine and Mitutoyo BN 706 Coordinate Measuring Machine. The experimental model was designed in Pro-Engineering Software (Pro-E) and converted into stl format. This file was created with 0.02 mm chord height to avoid problems (such as large file size) in its transfer to SLA and 3DP ThermoJet machines. The dimensions and features of experimental prototype, as shown in figure 2, were designed by considering part cost; build time; standard engineering features, which normally appeared on common engineering product; and machine constraints.

The surface measurement was taken in the directions as shown in figure 3. The distance between each point is assigned in order to obtain the measurement data close to actual characteristic of the surface. In this research surface roughness measurements were taken to comply with the British Standard (BS 1134).

The dimensional accuracy measurement was carried out using the CMM. The following dimensional measurements were carried out: The X and Y dimensions, flatness and straightness. Every type of measurement was taken a number of times and the average values recorded. To minimize the occurrence of error, as suggested in a study [8], randomisation method was used in obtaining the data from measurement process. This is to reduce residual factor caused by uncontrolled factors, which occur during the experiment.

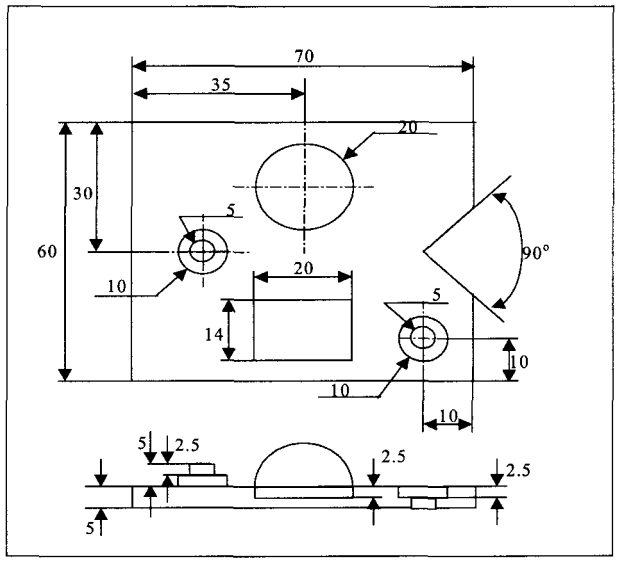

Figure 2: Experimental drawing model (All measurement in mm)

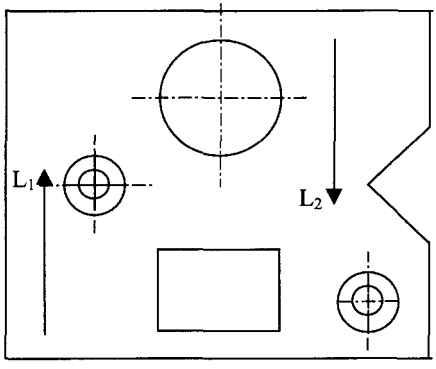

Figure 3: Surface roughness measurement method

4. RESULTS AND DISCUSSIONS

4.1 Surface finish

By assuming that the spreading of the data follows normal distribution and by using one-way ANOVA analysis methods with F-test, the result gives a 99% confidence level. The characteristics of surface roughness of both techniques due to the variation of orientation can be seen in figure 4.

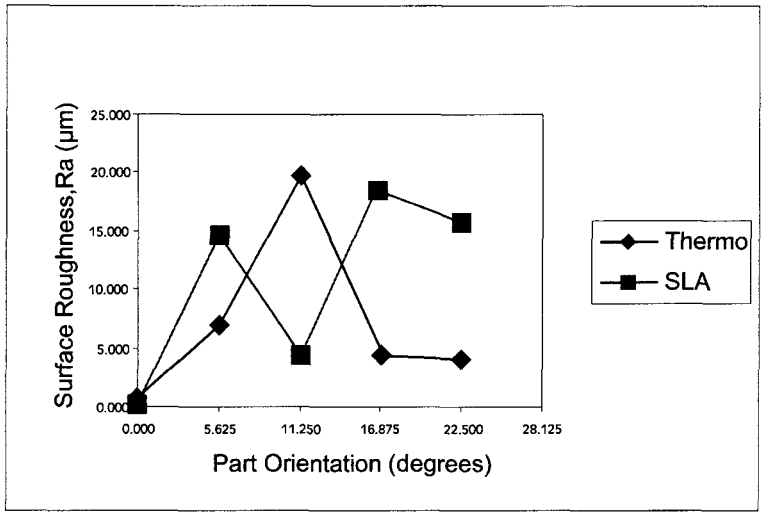

Figure 4: Surface roughness comparison between SLA's model and 3DP Thermojet's model

From figure 4, by varying the part orientation, surface roughness of SLA models tend to fluctuate. The lowest roughness value is obtained at 0° and the highest value is at 19μm. Meanwhile, characteristics of surface roughness of 3DP's models follow parabolic pattern, where the highest roughness is when the model is orientated at 11.25° and the lowest occurred at 0° orientation. From 16.875° to 22.5°, the surface roughness tends to be flat. Since the process on either SLA machine or 3DP machine was carried out at the default setting for the other parameters, the only explanation why this occurred may be due to staircase effect created by varying the part orientation. Stair case effect generates the cusp-height (δ), which is one of the factors influencing the surface roughness.

However, if the characteristics of surface roughness of both 3DP Thermojet's models and SLA's models are compared, it is clear that on the orientation of 0°, the surface roughness of SLA's models is slightly lower than 3DP models (Table 1.). This result is in line with our assumption that the roughness of 3DP models on this angle (0°), will considerably be higher than SLA's model because of the influence of the material used in 3DP technique (droplets), which will influence the surface roughness. In addition, from figure 4, the results give a surprising phenomenon. It can be seen that between 0° and 22.5°, 3DP Thermojet's models have surface roughness lower than SLA's model at 5.625°, 16.875°, and 22.5°. In addition, if it is examined closely, at 11.25°, while SLA's models surface roughness is minimal, 3DP models surface roughness values are maximal. Further investigation is being carried out to enable us to find out the reason(s) for this behavior at 11.25°. Subsequently, from 16.875° both display linearity and at highest part orientation, surface roughness for 3DP Thermojet's models are lower but higher for SLA.

Part Orientations	Surface Roughness (in μm)	
	SLA	3DP-ThermoJet
0°	0.247	0.645
5.625°	14.530	6.910
11.25°	4.289	19.682
16.875°	18.430	4.302
22.5°	15.747	4.023

Table 1: Comparison table for surface roughness between SLA and 3DP Thermojet

Furthermore, by taking the average surface roughness value for all experimental orientations, 3DP model gives significantly lower surface roughness, which is 7.1124μm (10.6486 μm for SLA model). This may be due to the problem of support structure in SLA. If the support structure is not designed sufficiently, it could affect the part stability. However, in this present study, the support structure design was neglected (as the default was used), therefore the frame only supports the model on several contact points. This means that the support structures, which are located at higher elevation from platform, would have the longest height. This makes the rigidity of the support structure on this part lower than other areas near the platform (smaller value of angle of orientation). Beside that, since this is a liquid environment, the gravity effect would also influence the surface roughness.

4.2 Dimensional Accuracy

The dimensional accuracy of an RP model determines to a large extent its application in Rapid Tooling (RT). In this study, data for different features were obtained on dimensional accuracy by using a CMM. However, to achieve the project objectives, the analysis is only carried out on several features as can be seen in figure 2 such as straightness of outside edges of the model, flatness of up-facing surface and parallelism of two sides facing each other in rectangular hole. Other features will be considered as the investigation progresses.

ANOVA one-way method was used to analyze the data as it was acquired for the surface finish. From ANOVA table for dimensional accuracy and by using Upper Percentage Points of the F-Distribution Table [8], it can be stated that the result is significant at 1% level, which means 99% of confidence level of the result has been achieved. Besides, from F-ratio, the residual value also shows that data error is not too significant. In other words, the result is quite accurate and out of bias. The result, which already satisfied 99% confidence levels are then plotted on charts. These graphics are provided with nominal value and tolerance values (±0.025).

4.2.1 Straightness

It has been shown that the straightness of a part is a reflection of its dimensional accuracy, distortion and flatness [9, 10]. To measure the straightness of the experimental model, some assumptions have to be made as shown in figure 5. The lines or the edges can be said to be straight if they meet the criteria for which A2 angle must be 90° or A1 angle must be 45°. This is because the distance of the line does not necessarily give the straightness.

Figure 6 is the chart showing the straightness of the model. From this figure, it can be stated that both SLA technique and 3DP technique do not give good results for straightness for this part. It shows along y-side, which is used to assess straightness, that there are some deviations. These deviation will be seen clearly if the points along y-axis are examined.

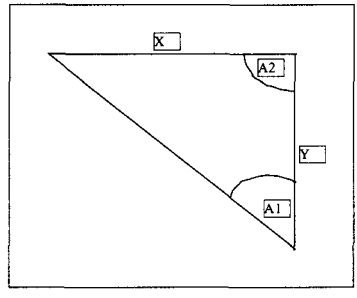

Figure 5: Straightness assumption

From figure 6, although the values of angle A1 are far from nominal value (45°), the variations in 3DP technique as a result of increasing the part orientation are not so significant. This may be due to the fact that the droplet compensation in 3DP technique is adequate to give the needed stability. Meanwhile, for SLA's models, the angle of A1 increases slightly from 0° to 11.25° and between 11.25° and 22.5° reach the plateau. These tendencies were probably occurred because of several reasons such as:

a. The support structure is not sufficient enough to support the model and also to eliminate the gravity effect.
b. Shrinkage is not uniform between each layers.

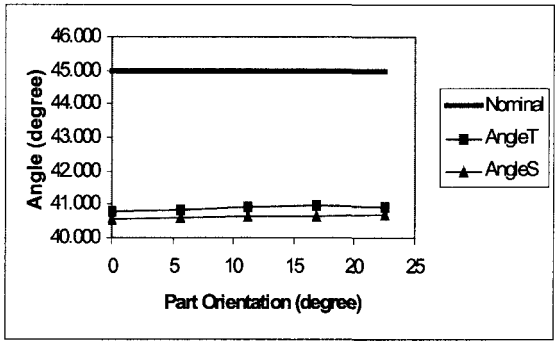

Figure 6: Straightness comparison between models built by SLA and 3DP Thermojet

4.2.2 Flatness

From figure 7, it is shown that both SLA (FlatS) and 3DP (FlatT) techniques do not provide good flatness. By varying the orientation angles, the flatness tends to be varied as well. For SLA, this may be caused by shrinkage effect and overcure effect, which causes distortion. For 3DP, Thermojet might be caused by non-uniform printing process that creates low-density model.

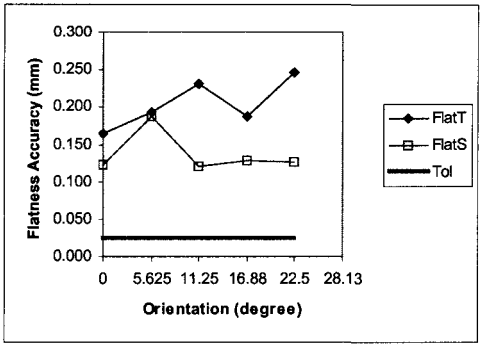

Figure 7: Flatness comparison between models built by SLA and 3DP Thermojet

5. CONCLUSIONS

The aim of this present study is to compare the part qualities (especially surface roughness) of models built by SLA technique and 3DP technique as to improve the model for use in Rapid Tooling applications. The main findings are:

By varying the orientation of the models, 3DP Thermojet gives a better overall result than SLA. This is achieved when models are orientated at 5.625°, 16.875°, and 22.5°. However, for models built parallel to platform, SLA provides slightly good surface roughness.

Moreover, the characteristics of both techniques by increasing part orientation angles are totally different. 3DP Thermojet shows the parabolic pattern while SLA tends to fluctuate. In addition, it can also be concluded that surface roughness of 3DP Thermojet's models from 0° to 22.5° part orientation lies in the range between ± 0.65μm and ± 19.7μm. While for SLA's model the surface roughness lies between ± 0.25μm and ± 18.4μm. This results compare favorably with earlier study [11].

An interesting phenomenon was observed for both the SLA and 3DP machines at 11.50° whereby the experimental value is either maximum or minimum. This is an area we intend to study further as the result may be of significant value to the RP process improvement. In addition, other features like the roundness and the accuracy of the square cut and the prisms will be studied further. Building the part in Selective Laser Sintering (SLS) machine may also be carried out as to give a better understanding of the effect of varying the part angle of orientation in the different systems (powder environment). It is also expected that the study will develop empirical relationships between these parameters and build time prediction.

References

1. A Rosochowski and A Matuszak, (2000) Rapid tooling. The state of art. *Journal of Materials Processing Technology*, Vol. 106 pp. 191-198.
2. K Y Root, What is Rapid Prototyping: a beginner's guide to Rapid Prototyping [Online]. Available from: http://www.eng.uah.edu/~rootk/Engineering/RP2.htm#geo [Accessed : 9 May 2001].
3. J Dong (1998) Introduction to rapid response manufacturing. In: J.Dong eds. *Rapid Response manufacturing*: Contemporary methodologies, tools and technologies. London. Chapman and Hall, 1-7.
4. J Ajay (2001) An introduction to Rapid Prototyping [Online]. Available from: http://iesu5.ust.hk/dfaculty/ajay/courses/ieem513/RP/RPlec.html [Accessed: 10 July 2001].
5. S.O. Onuh, K.K.B. Hon, (1998) Application of taguchi method and new hatch styles for quality improvement in Stereolithography product. Journal of Engineering Manufacture. Proc. of IMECHE Part B. Vol. 212 pp461-472.
6. D.T. Pham, R S. Gault (1996), Rapid Prototyping: Solid Ideas, Manufacturing Engineer, 75(5), 239-243.
7. J S Lamancusa. (2000) Rapid prototyping primer: what is Rapid Prototyping [Online]. Available from: http://www.me.psu.edu/lamancusa/rapidpro/primer/chapter2.htm. [Accessed: 9 May 2001].
8. C Chatfield (1983) Statistics for technology: A course in applied statistics. London. Chapman and Hall.
9. S.O Onuh and K.K.B. Hon, (2001) Improving stereolithography part accuracy for industrial applications. *International Journal Advanced Manufacturing Technology*, 17:61-68.
10. C Lynn-Charney and D.W. Rosen, (2000). Usage accuracy models in stereolithography process planning. *Rapid Prototyping Journal*, 6(2), 77-86.
11. M Shellabear (1998). Model Manufacturing processes-state of the art in rapid prototyping (First report of literature research. Feb.1998). Available from: http://129.69.86.144/raptec/Reports/deliverables/Deli2_t42_all.PDF. [Accessed: 12 July 2001.

Optimizing tapping operations on hardened steels in a prototyping environment

J F A SIMÕES and **E MATOS DA ROCHA**
Escola Superior de Tecnologia, Instituto Politécnico de Setúbal, Portugal
R M OLIVEIERA BAPTISTA
Universidade Técnica de Lisboa, Portugal

ABSTRACT

The Tool & Die companies are always looking for new production processes, to reduce the cost and the lead-time in order to achieve improved competitiveness. In general these companies work in a prototyping environment since the work specifications change significantly from job to job.

Nevertheless, all the research made in the Advanced Machining Technologies (AMT), regarding mainly finishing operations, metal machining operations remain most of the time out off the technical literature interest. Included in that case is the tapping (internal thread cutting) operation in hardened steels. In industry this operation assumes a relevant importance, since the traditional production process is very slow.

This paper relates a case study developed for the MP S.A. Company (Tool & Die industry for the automotive sector). This work investigates a new production approach tapping holes in the hardened steels used in the Tool & Die industry. The work presents a description of the traditional approach used in the industry as well as a new production methodology. A comparison between the two methods is also shown, for the M6 tapped hole, using real production data from the MP S.A. Company. Finally, the actual limitations of the new methodology are highlighted, and new technical solutions are identified.

KEYWORDS: CNC tapping, Hardened steels, Tool and Die manufacture

1. INTRODUCTION

Presently, the automotive production is strongly depended from the part fabrication generated by the tool and die industry. These tools are mainly produced in high strength steels and hardened using heat treatments. Different kinds of parts, from metal to plastic components are transformed using this type of tool.

During the last decade, research was made in the development of the production process like, for example in the AMT (5-axis and high-speed machining) and in rapid manufacturing [1, 2]. In the future this research, on tapping on hardened steels, can lead to important savings in the tool and die industry and will have a tremendous impact on the cost of the automotive components.

In the manufacturing of Tool & Dies is necessary good quality steels with the following requirements:

- ✓ Good machinability
- ✓ Minimal bending with heat treatment
- ✓ Good polishing capability
- ✓ Good wear resistance
- ✓ Good corrosion resistance

References			Chemical Composition					
Thyssen	DIN	AISI/SAE	C	S	Mn	Cr	Mo	Ni
1.2738	40crMnNiMo864	P20 + Ni	0.40	≤0.005	1.5	1.9	0.2	1.0

Table 1: Steel Composition (material used in the tests) [3]

Table 1 presents the material composition of a steel reference (1.27.38) used in the Tool & Die industry. Because of its hardness these materials are difficult to machine, causing some problems to the production department if any machining operation is left to be done after the material receive the heat treatment. The mechanical characteristics of this steel reference, after the heat treatment, are shown in Table 2.

Hardness *(HRC)*	Yield Stress *(N/mm^2)*
58	1,730

Table 2: Material Mechanical Characteristics (material used in the tests) [3]

Figure 1 shows a picture of a Tool & Die to generate metal components, using a progressive cut and stamping operations

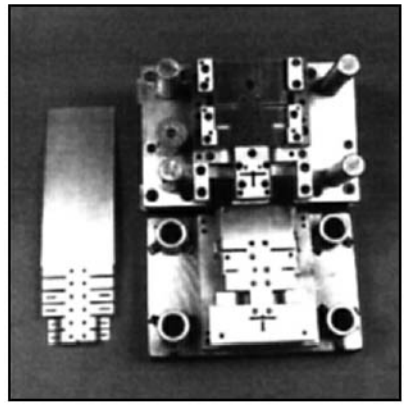

Figure 1: A Tool & Die picture (Progression Sheet Metal Punching Die)

2. NEW TAPPING APPROACH

This work explores a particular area, in the complex field of the Tool & Die production. The tapping operation was analysed. This operation creates specific problems in the production, if the work is done after the material receives the heat treatment.

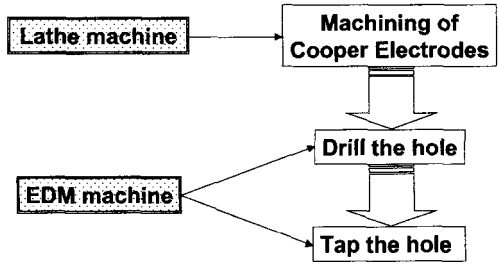

Figure 2: Steps to Machine a Thread Hole – Traditional Approach

Usually, the tapping operation involves the machining of an electrode and a slow EDM machining operation (see Figure 3). All that work consumes time and contributes significantly to increase the final cost of the Tool & Die product. Figure 2 shows the typical steps necessary to machine a thread hole, using the traditional method.

Figure 3: EDM CNC Machine - ONA Didatic2030
(EDM – Electrical Discharge Machine; CNC – Computer Numerical Control)

In order to investigate new solutions to the tapping operation, a research in the market for new tools was made. From this work, a new tap-cutting tool that can work with hardened steels was selected. Using this solution, the work involved in the tapping operation can be tremendously simplified. Figure 4 presents the production steps in the new machining approach. Basically, the tapping operation is executed in two phases: a) drilling of the hole; b) tapping of the hole.

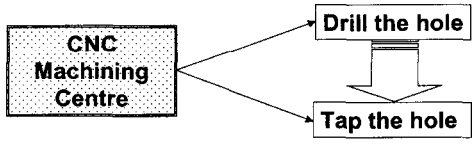

Figure 4: Steps to Machine a Thread Hole – New Approach

All the work is made in a CNC machining centre, reducing the total lead-time for this operation. The CNC programming is made with predefined machine cycles, for tapping. Figure 5 shows a CNC Machining Centre.

Figure 5: CNC Machining Centre - Cincinnati Arrow 750

3. EXPERIMENTAL WORK

Table 3 shows a comparison between the new and the traditional tapping process, in terms of machining time, costs and operation lead-time [4]. The data corresponding to the "traditional production approach" was collected from the production management records of the MPSA Company (Magneti Marelli Group). The tests ran with three replications, this data represents an average of the normal values involved in a M6 tapping operation. The company works in the tool and mould industry, supplying the automotive sector.

Characteristics	Traditional Approach	New Approach
1. Machining Time		
CNC Lathe	30 *min*	-
CNC Machining	-	20 *min*
EDM Machine	1.5 *hours*	-
2. Costs		
Machines	69 EURO	10 EURO
Tools	1 EURO	30 EURO
Total	70 EURO	40 EURO
3. Lead-time	2 *hours*	20 *min*

Table 3: Comparison Between the Traditional and the New Tapping Approach

The values indicated in Table 3 correspond to a single M6 tapping operation. The tool cost indicated in the table is the tool total cost divided by the tool life. The same methodology was applied in regard to the electrode tools, used in the EDM machine by the traditional approach.

In order to evaluate the life of the tapping tool an experimental investigation was undertaken. The experimental work was carried out in a CINCINATI CNC machining centre (ARROW 750) with the ACRAMATIC controller (version A2100). The CNC code G84.1 was used to programme the tapping operation.

In order to simulate the industrial conditions, a set of tests was run with hardened steel. The tests were made in a hardened steel block – 58 HRC (supplied by MPSA Company - tool and mould makers), with the dimensions of 250 by 200 millimetres, in which several blind tapped holes were machined. The cutting tools used in the tests were made in solid carbide material. The drill tools were coated with TiAlN (Titanium Aluminium Nitride) and the tap tools were coated with TiCN (Titanium Carbon Nitride). Titex-Plus Company (Sandvik Group) supplied both tools. The tests were carried out in M6 threaded holes with a depth of 12 millimetres (see Figures 6 and 7).

Figure 6: Cutting drill tool used in the experiments [5]
(*5.1 millimetres diameter*)

Figure 7: Threading tap tool used in the experiments [5]
(*6 millimetres diameter – M6*)

Table 4 presents the tool references and the machining parameters used in the tests. The oil used in the tests was applied automatically during the drilling operations, and manually, inside the holes, before the tapping operations.

	Drill	Tap
Reference Catalogue	A3269TFL	B1278TCN
Diameter	5.1 *mm*	M6
Cutting Speed	20 *m/min*	1 *m/min*
Coolant	Oil (soluble)	Oil

Table 4: Tools and Machining Parameters

Figure 8 shows the tap experiments carried out in the CNC machining centre. The tests were made in a block of hardened steel, where several blind holes where drilled initially and tapped in a second operation.

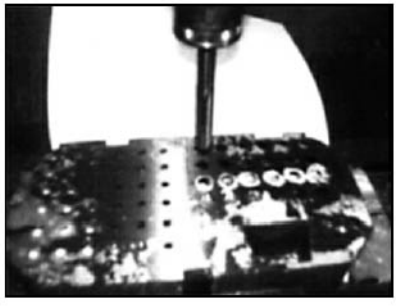

Figure 8: Hole being tapped in the experiment work piece

Figure 9 shows the range of tap tool life values obtained in the tests. A high variance in the results regarding the tap tool life was verified. The tap tool life was accessed through the number of tapped holes made by the tool before tool failures occur.

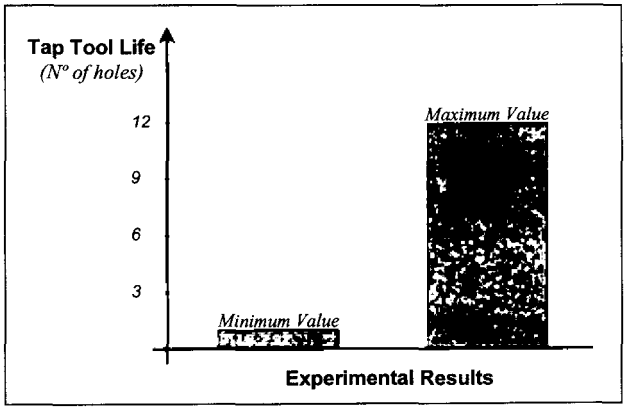

Figure 9: Tapping tool life results

Several catastrophic tap tool failures occurred during the tests at different cutting speeds, causing this high range of tool life values for the same machining parameters. Figure 10 shows pictures of some tap tools crashed during the experimental work.

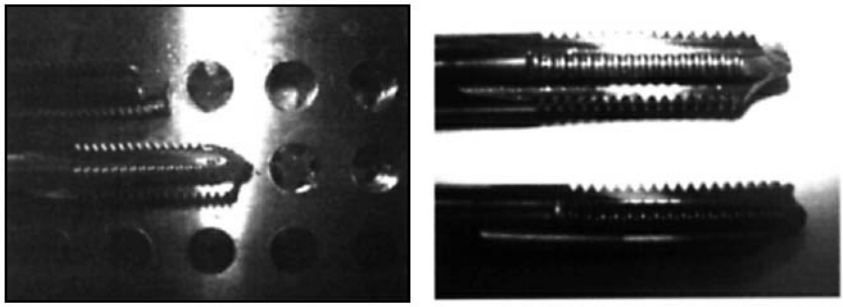

Figure 10: Tap tools crashed during the experimental work

4. CONCLUSIONS AND FUTURE DEVELOPMENTS

This work, developed for the MPSA Company, presents a new production approach to tap hardened steels. The new method saves time reducing substantially the lead-time in the production of the Tool & Die components. The production costs involved in the new methodology are also reduced. This methodology can be applied in others companies working for the enormous automotive sector.

Nevertheless all the benefits referred before, the new methodology also has some limitations. The depth of the thread hole is limited to a value equal to the double of the tap tool diameter. In the market the maximum available tap diameter is the M12. Following the toolmaker technical recommendations the cutting speed in this specific tapping tool is limited to 5 metres per minute.

Presently, in the cutting tool market new tap tools are emerging. Two of the alternatives with higher potential to improve the performance of the thread milling cutters are:

i) Thread milling cutter with tip (see Figure 11).

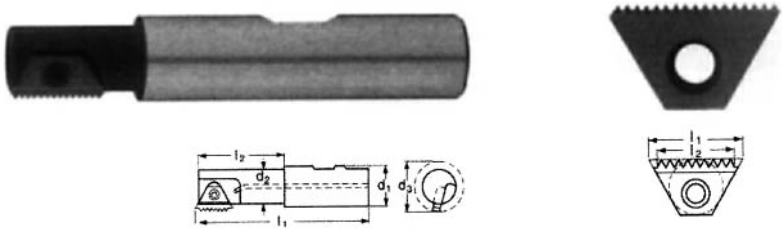

Figure 11: Thread milling cutter with tip [6]

This solution has the advantage of generating a cost reduction of the cutting tool through the use of inserts / tips. If the insert fails the cutting tool core cost is always saved.

ii) Solid carbide milling cutter to work by orbiting cycles (see Figure 12).

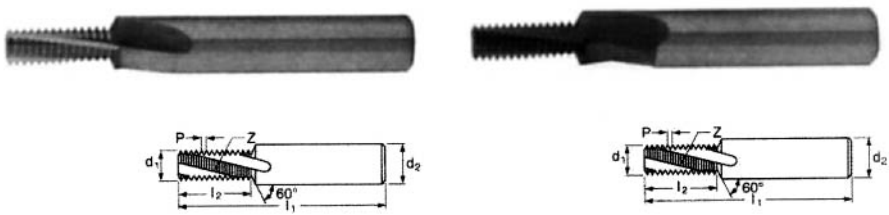

Figure 12: Solid carbide milling cutter to work by orbiting cycles [6]

These solid carbide milling cutter will tap the holes through orbiting milling cycles. The CNC programs with the cutter path, to generate the thread holes, as well as the correct value for drill are supplied by the toolmaker. The tools can be coated with TiAlN.

The advantage of these new tools is based in a reduction of the cutting forces due to the orbiting cutting strategy. The lower values of the cutting forces potentate better resistance conditions for the milling cutter leading to a higher tool live.

In order to optimise the tapping operation an analysis of the machining parameters of these new tools, using the factorial design of experiments, will form part of future developments in this research.

Acknowledgements

The authors wish to acknowledge "Escola Superior de Tecnologia de Setúbal" and "Instituto Superior Técnico" as well as Sandvik Portuguesa and MPSA Companies for the use of equipment and resources, during the period of this work.

References

1. Baptista, Rui M. S. O.; Antunes S., José Filipe C. P., "*3 and 5 Axis Milling of Sculpured Surfaces*", Journal of Materials Processing Technology, Volume 103 (3), July 2000, ISSN 0924-0136.

2. Baptista, Rui M. S. O.; Antunes S., José Filipe C. P., "*The Implementation and Analysis of a 5-axis Milling Operation*", Fourth International Symposium on Product Development in Engineering Education, PDEE98, Cologne/Germany, 1998, ISBN 3-00-003754-3.

3. Thyroplast 2738, "Thyssen Catalogue", 3rd Edition, pp. 113-114, Thyssen Portugal, Lda.

4. Antunes S., José Filipe C. P.; Baptista, Rui M. S. O.; Matos da Rocha, E.; "Tapping On Hardened Steels - A Case Study", 3rd International Conference on Metal Cutting and High Speed Machining, Metz/France, 2001.

5. "*Solid Carbide Tools for Hard Machining*", Titex Plus – Precision Cutting Tools (Sandvik Group) catalogue, 2000.

6. "*Thread Milling Cutters*", Titex Plus – Precision Cutting Tools (Sandvik Group) catalogue, 2001.

This page intentionally left blank

Multi-axis machining using a six-axis anthropomorphic robot

J F A SIMÕES and **A R PIRES**
Instituto Politécnico de Setúbal, Portugal
T J COOLE
Buckinghamshire Chilterns University College, UK
D G CHESHIRE
Staffordshire University, UK

ABSTRACT

Currently, the concept of Advanced Machining Technologies (AMT) includes different processes such as high-speed machining, multi-axis machining, etc. The common characteristic between these technologies is that they aim to improve the cutting process. Research done in the past has mainly concentrated on metal machining. In this research efforts are made to apply these techniques to the ceramic industry. This work forms part of the ongoing research at Staffordshire University on the application of CNC machining techniques in the production of models and moulds, with regards to the tableware and sanitary ware industries.

This paper focuses on the analysis of multi-axis milling using an anthropomorphic robot to produce near net shape plaster parts. The milling tests were carried out on plaster using conventional cutting tools (slot-mills).

The Design of Experiments (DoE) was implemented using factorial techniques. Surface quality and geometric accuracy of the plaster parts were the response variables used to characterise the part quality and to test the levels of acceptability of feed-rate and robot arm extension. A mathematical equation based on the geometric accuracy was developed and used to plot flatness contours. Through these plots it is easy to define other possible combinations of feed-rate and robot arm extension that can be used.

KEYWORDS: Plaster machining, Robot milling, Factorial design, Mathematical modulation

1. INTRODUCTION

The plaster machining operation executed with a robot was a relatively unknown process before this research. The technical knowledge available before this work, regarding this process, was reduced to a few experiments and the initial studies conducted during the CRAFT project BE-S5-2523. Also, with the new aspect of the use of the robotic system, the machining of plaster was also a process not very well studied, including the tool wear occurring during plaster machining [1, 2].

All characteristics presented before illustrate the "lack of knowledge" conditions in the initial phase of this research, and indicate the necessity to initialise research predicting all the possible important process variables. In order to identify the more important variables involved with this machining operation the factorial DoE methodology was used. With this factorial design and analysis approach it was possible to optimise the use of the experimental resources, during the study of the effect of the main variables.

The work was divided into several phases, including the choice of variables and respective levels, selection of response variables, choice of experimental design, experimental work, and finally the statistical analysis of data. As a fundamental aspect of the factorial DoE methodology, the capability of the plaster machining operation executed by a robot was identified, as the problem to be analysed through this study. This process capability was considered on three basics aspects: the tool wear occurring on the cutting tools; the quality of the machined surface; and the geometric accuracy of the parts. This specific paper presents the study made on the:

- *Quality of the machined surface* – The evaluation of the quality in the surface machined with this process, will define the process capabilities to produce the industrial products, in terms of surface roughness;

and

- *Geometric accuracy of the parts* – Through the evaluation of the geometric accuracy achieved with this process, it will be defined by the capabilities of the process to produce the necessary parts within the required tolerances.

In the following section, the independent variables (factors) and respective levels will be identified, and the characterisation of the response (dependent) variables will be carried out.

2. EXPERIMENTAL SCREENING

In the factorial DoE methodology the process variables are named "factors". For the screening design and analysis procedure fifteen different factors were identified as being important in the plaster machining process using a robotic system [3, 4]. In the identification of factors all the possible variables that could influence the surface quality and the geometric accuracy of the end product were considered.

For the purposes of this screening methodology, each factor was evaluated at two different levels. The two levels correspond to two different values/characteristics of the factor. The minimum and the maximum values are within the range of values in which the factor can work [5].

In Table 1 the factors considered in this screening analysis procedure and their respective levels are listed.

	Levels	
Factors	*Low*	*High*
Step-over *(mm)*	2	6
Step-down *(mm)*	2	5
Tool flute angle *(degrees)*	30	40
Feed-rate *(m/min)*	2	12
Spindle-speed *(rpm)*	5,000	10,000
Lead/lag angle *(degrees)*	0	10
Cutting strategy	Conventional	Climb
Tool material	High-Speed-Steel	Solid carbide
Tool length *(mm)*	20	50
Machining table	Horizontal	Vertical
Machining direction	Horizontal	Vertical
Block dimensions *(mm)*	100	800
Machining time *(minutes)*	50	150
Arm extension *(mm)*	800 *(Retracted)*	2,000 *(Extended)*
Plaster material	Molda 6	Newcast 71

Table 1: Factors and Levels in the Screening Process

The work was carried out on a 6-axis ABB anthropomorphic robot using an S3 controller. The technical characteristics of this robotic system are: Reach / Envelope (2.8 m); Repeatability (0.1 mm); Spindle Speed (10,000 rpm). The tests were run on parallelepiped plaster blocks. The surface of these raw blocks was machined using toolpaths with a "one-way" strategy (see Figure 1). These plaster blocks were bolt fixed on the vertical and on the horizontal machining tables available in the robotic system.

The *Step-over* (radial depth) factor corresponds to a linear increase perpendicularly to the tool direction. The objective of step-over is the establishment of the cut width in each toolpath. This value is measured in millimetres. The *Step-down* factor corresponds to a linear increase perpendicularly to the machining plane. The objective of step-down is to define the depth of the cut in each toolpath. This value is measured in millimetres.

The *Tool flute angle* is one of the geometric characteristics of the cutting tools (slot- mills). Usually, this value is dependent on the materials to be machined and affect the extraction of the chips generated during the machining. The factor value is measured in degrees. Using the *Feed-rate* factor it can be controlled the linear speed of the cutting tool. This value is obtained by multiplying the feed per tooth by the number of tool teeth. The factor value is measured in metres per minute. The *Spindle-speed* factor corresponds to the rotation of the cutting tool. This value is calculated using the cutting speed defined in the tool catalogues with regard the material to be cut. Since the tool catalogues define the value of feed per tooth per rotation, the calculation of the feed-rate should be affected by the value of the spindle-speed. The factor value is measured in rotation per minute.

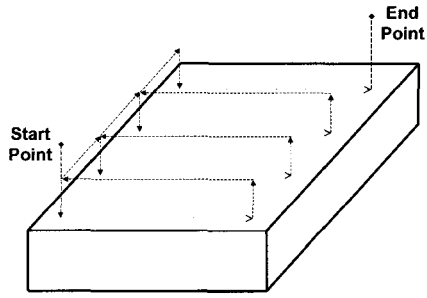

Figure 1: Raw Block

The *Lead/Lag angle* factor corresponds to an inclination of the cutting tool axis in the direction of the tool movement. This angle is measured between the tool axis and the vector defined, in each point of the toolpath, by the normal direction on the machined surface. The factor value is measured in degrees. By the *Cutting strategy* factor it is specified if the chip cutting is generated using the conventional strategy or the climb strategy. The *Tool material* factor was studied in just two different materials, high-speed-steel and solid carbide tools. Both tool types were tested without coating materials. The *Tool length* factor specifies the length of the cutting tool measured from the holding system in the spindle head of the robot. This value is usually related with the depth of the surface profile, and with the amount of tool vibration. Usually the tool length is specified with the lowest possible value in order to reduce the amount of vibration in the cutting tool. This value is measured in millimetres.

The *Machining table* factor specifies the orientation of the machining table. In this robotic system there were two machining tables installed. There is one table where the raw material is fixed in the horizontal position (horizontal table) and another one where the raw material is fixed in the vertical position (vertical table). As a way to verify the influence of the robot movements in the response variables the *Machining direction* factor was considered. This analysis tested two different machining strategies, one considering toolpath through the horizontal position and another with toolpath in the vertical position. The *Block dimensions* factor was considered as a variable to test the influence of the continuous toolpath length, during machining. This factor measures the dimension of the material block that is been machined in the direction of the toolpath. The value is measured in millimetres.

The *Machining time* factor quantifies the amount of time taken in the machining operation. The value is measured in minutes. Through the *Arm extension* factor the effect of the robot arm position in the response variables is studied. This factor considers the linear distance, measured in the horizontal plane, from the robot centre axis to the top of the spindle-speed head. The arm is considered retracted if the value is lower than 1,000 mm, and extended if it is equal or bigger than this value. The product references used on the *Plaster material* factor correspond to two different plaster material suppliers. Both references are very common in the ceramic industry, regarding the plaster mould making production process. Both materials are prepared using the same manufacturing conditions.

Response Variables	Scales
Surface Quality	Roughness Analysis
Geometric Accuracy	Flatness Analysis

Table 2: Response Variables

Table 2 identifies the response variables used in the screening procedure, and shows the scale used in the evaluation of each one. Because of the low surface resistance of the plaster material the analysing surface equipment available, using traditional contact probes, could not be used. The evaluation of the surface roughness generated during the machining was made visually using the scale presented in Table 3. The evaluation of the surface flatness was made using the same scale presented in Table 3.

Scale					
1	*2*	*3*	*4*	*5*	*6*
Poor	Not acceptable	Acceptable with rework	Acceptable	Good	Excellent

Table 3: Scale for Surface Quality and Geometric Accuracy Analysis

The surface roughness was evaluated through the visual analysis of the maximum roughness ($R_{Z\,max}$). The flatness was evaluated through the measurement of the distance between two parallel planes that limited the top and the bottom levels of the machined surface. Through this concept the best surface flatness corresponds to the smallest distance between those planes.

2.1. Screening design

Screening designs are specifically constructed to allow testing of the largest number of main effects with the least number of tests. The experimental design was carried out using a fractional factorial design. A resolution III design, referred to in the literature as Plackett-Burman design was applied. The advantages of these III resolution designs were discussed by Montgomery [6]. All the calculations were supported by the software "Statistica, version 5.1".

The sixteen experiments were established and a randomise sequence order was generated, as a way to minimise the possibility that some systematic changes in the dependent (response) variables over the consecutive runs could bias the estimates. Table 4 shows the design generated by the software for this screening procedure.

In each experiment the two levels of the 15 different factors through a *-1* or a *1* value are identified. The *-1* corresponds to the lower level of the factor and the *1* to the higher level. The results obtained in the 16 experiments are also presented in Table 4. Two experienced mould makers assessed the experimental results.

	Experiment Number															
Factors	*1*	*2*	*3*	*4*	*5*	*6*	*7*	*8*	*9*	*10*	*11*	*12*	*13*	*14*	*15*	*16*
(1) Lead/lag Angle	1	1	1	1	1	1	1	1	-1	-1	-1	-1	-1	-1	-1	-1
(2) *Step-down*	1	1	1	1	-1	-1	-1	-1	1	1	1	1	-1	-1	-1	-1
(3) *Flute Angle*	1	1	-1	-1	1	1	-1	-1	1	1	-1	-1	1	1	-1	-1
(4) *Feed-rate*	1	-1	1	-1	1	-1	1	-1	1	-1	1	-1	1	-1	1	-1
(5) *Cutting Strategy*	1	1	1	1	-1	-1	-1	-1	-1	-1	-1	-1	1	1	1	1
(6) *Arm Extension*	1	1	-1	-1	1	1	-1	-1	-1	-1	1	1	-1	-1	1	1
(7) *Block Size*	1	-1	1	-1	1	-1	1	-1	-1	1	-1	1	-1	1	-1	1
(8) *Tool Material*	1	1	-1	-1	-1	-1	1	1	1	1	-1	-1	-1	-1	1	1
(9) *Tool Length*	1	-1	1	-1	-1	1	-1	1	1	-1	1	-1	-1	1	-1	1
(10) *Machining Table*	1	-1	-1	1	1	-1	-1	1	1	-1	-1	1	1	-1	-1	1
(11) *Machine Direction*	1	1	-1	-1	-1	-1	1	1	-1	-1	1	1	1	1	-1	-1
(12) *Spindle-Speed*	1	-1	1	-1	-1	1	-1	1	-1	1	-1	1	1	-1	1	-1
(13) *Machining Time*	1	-1	-1	1	1	-1	-1	1	-1	1	1	-1	-1	1	1	-1
(14) *Step-over*	1	-1	-1	1	-1	1	1	-1	1	-1	-1	1	-1	1	1	-1
(15) *Plaster Material*	1	-1	-1	1	-1	1	1	-1	-1	1	1	-1	1	-1	-1	1
Surface Roughness *[1 6]*	1	1	1	1	1	1	1	1	2	6	2	3	2	4	2	3
Surface Flatness *[1 6]*	1	3	1	3	1	2	1	4	2	5	1	3	2	4	1	2

Table 4: Experimental Design / Results

2.2. Screening analysis

The screening analysis was made in order to evaluate the statistical "significance" of the selected 15 (independent variables) factors, in each of the 2 dependent (response) variables. The following two sections will present the analysis of the surface quality and geometric accuracy, respectively. The analysis was made initially through a

Pareto chart of effects. The analysis was complemented using the ANOVA table in order to access the statistical validity of the analysis. The graphical representation of the normal probability distribution of residuals was also carried out in order to verify that the ANOVA requirements were met.

2.2.1. Surface quality analysis

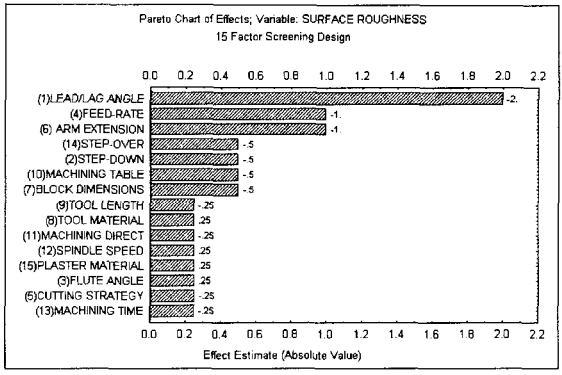

Figure 2: Pareto Chart (Surface Roughness)

The Pareto chart for the surface roughness (see Figure 2) shows that the more significant factors are Lead/lag angle, Feed-rate and the Arm-extension. As it was expected Lead/lag angle has the largest effect on surface quality. As it can be seen in Figure 2 the parameter value (effect) of the Lead/lag angle factor is negative, thus the higher lead/lag angle values corresponds the higher surface roughness, and consequently the worst surface quality.

Table 5 presents the ANOVA table for the 3 factors selected previously through the analysis of the Pareto chart. As it is indicate by the asterisks (using F "*Fisher*" test as the test statistic) that all three factors are statistically significant with a confidence interval of 95 percent.

Experimental Design	**ANOVA – Surface Roughness** *[1 6]*			
Factors	SS	df	MS	F
(1) Lead/lag angle	16.000	1	16.000	32.000 *
(14) Feed-rate	4.000	1	4.000	8.000 *
(6) Arm extension	4.000	1	4.000	8.000 *
Error	6.000	12	0.500	
Total SS	30.000	15		

$F_{0.05,\,1,\,12} = 4.75$ *(Fisher distribution)*

Table 5: ANOVA Table (Surface Roughness)

2.2.2. Geometric accuracy analysis

The Pareto chart for the surface roughness (see Figure 3) shows that the more significant factors are Feed-rate and the Arm-extension. Feed-rate showed the largest effect in the surface flatness. The effect of the Feed-rate factor is negative, thus the lower surface flatness, and consequently a worst geometric accuracy, corresponds to the higher Feed-rate values.

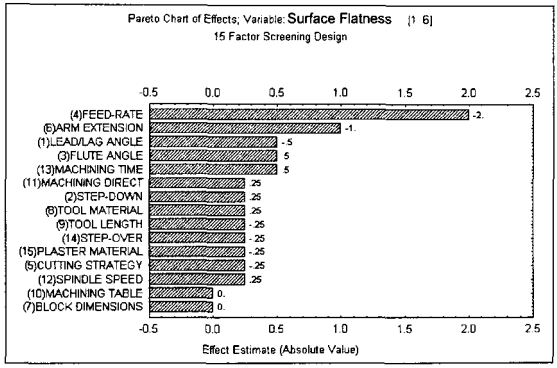

Figure 3: Pareto Chart (Surface Flatness)

Table 6 presents the ANOVA table for the 2 factors selected previously through the Pareto chart analysis. As the asterisks indicate it, both factors are statistically significant with a confidence interval of 95 percent.

Experimental Design	**ANOVA – Surface Flatness** *[1 6]*			
Factors	SS	df	MS	F
(4) Feed-rate	16.00000	1	16.00000	55.46667 *
(6) Arm Extension	4.00000	1	4.00000	10.40000 *
Error	5.00000	13	0.38462	
Total SS	25.00000	15		

$F_{0.05,\,1,\,13} = 4.67$ *(Fisher distribution)*

Table 6: ANOVA Table (Surface Flatness)

3. SURFACE QUALITY AND GEOMETRIC ACCURACY MODULATION

3.1. Mathematical modulation

The analysis of the geometric accuracy of the plaster parts was based on two factors, the feed-rate and the arm-extension, respectively. These two factors were identified in the previous screening analysis as two of the most significant factors in regard to the geometric accuracy response variable. The Lead/lag angle was kept constant, reducing the study to 3-axis milling operations, because the surface quality became unacceptable for angles different from 0 degrees.

The final objective with this work is the specification of a mathematical equation to express the effects of feed-rate (F) and arm-extension (L) on the surface flatness (P) of a plaster block. The proposed relationship between the machining response (surface flatness) and the independent variables can be represented by the following function:

$$P = f(F, L) \tag{1}$$

The first order equation can be written by:

$$y = \beta_0.x_0 + \beta_1.x_1 + \beta_2.x_2 + \beta_{12}.x_1x_2 + \varepsilon \tag{2}$$

where: *y is the measured surface flatness (measured with the scale defined in Table 2.3);*
$x_0 = 1$ (dummy variable);
x_1, x_2 represent respectively the feed-rate (m/min.) and the arm-extension (mm), x_1x_2 represents the interaction between x_1 and x_2;
ε is assumed to be a normally-distributed uncorrelated random error with zero mean and constant variance;
β_0, β_1, β_2, β_{12} are the model parameters.

To develop the mathematical equation, a factorial design consisting of 8 experiments was conducted. Four experiments constitute a 2^2 factorial design, with an added centre point repeated four times. The added centre points were used to estimate pure error.

The milling operations were performed on the vertical table of the robotic system, through horizontal toolpaths. During the tests the constants were (Step-over = 2 millimetres, Step-down = 3 millimetres, Lead/lag angle = 0 degrees). In the experiments 10 millimetres diameter slot-mill cutting tools in uncoated solid carbide material were used. Table 7 shows the experimental cutting conditions together with the obtained surface flatness values.

Trial Number	Feed-rate F *(m/min.)*	Arm-extension L *(mm)*	Surface Flatness *[1 6]*
1	2	800	5
2	12	800	2
3	2	2,000	3
4	12	2,000	1
5	7	1,400	2
6	7	1,400	2
7	7	1,400	2
8	7	1,400	2

Table 7: Experimental Conditions and Results

The ANOVA table for the 2 factors, feed-rate and arm extension indicated that both factors (Feed-rate and Arm extension) were statistically significant. This table also indicated that the effect of the two factors interaction is not statistically significant. The mathematical equation representing the first-order model for the surface flatness, based on the eight experiments, is shown in Equation 3.

$$\hat{y} = 5.8750 - 0.2500x_1 - 0.00125x_2 \qquad (3)$$

$\hat{y}$ *is the estimate response for the surface flatness*

Equation 3 shows that the surface flatness decreases with the increase of feed-rate and arm-extension. This equation also shows that the feed-rate has the most dominant effect on the geometric accuracy. It was verified that using this equation the predicted values give a good estimation of the experimental results and the deviation between the experimental and the predicted values can be accepted for the purpose of the surface flatness prediction. Equation 3 was used to develop surface flatness contours in the feed-rate and arm-extension (see Figure 4). These contours help to predict the geometric accuracy at any zone of the experimental domain.

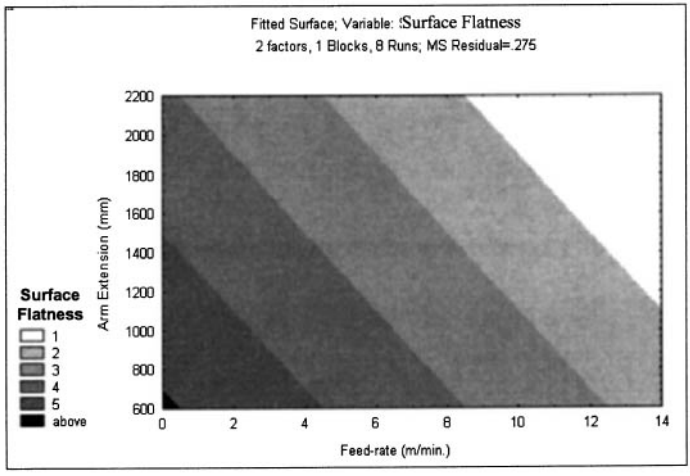

Figure 4: Surface Flatness Contours

4. CONCLUSIONS

The work presented in this paper characterises the capabilities of the robotic system to produce the plaster moulds and models by milling operations. The experimental designs and the mathematical calculations were carried out with the software "Statistica, version 5.1".

In the second section of this paper the screening method for the selection of the major important factors are presented. The experimental design was made according to the *Plackett-Burman* designs. It was verified in this study that:

- Surface Roughness - the most statistically significant factors to this response variable are Lead/lag angle, Feed-rate and Arm extension, respectively;

- Surface Flatness - the most statistically significant factors identified to this response variable were the Feed-rate and the Arm-extension, respectively.

The surface quality and the geometric accuracy modulation on plaster parts was investigated. This work was carried out using the factorial "Design and Analysis of Experiments" methodology. The results showed, in regard to the Lead/lag angle, that the surface quality became unacceptable for angles different from 0 degrees. This problem can be justified by the specific movements in the robot displacement, generated by rotations in the robot joints, instead of the typical linear movements of the machining centres. It will be important to develop a further study to compare the results achieved in the machining of sculptured surfaces using slot-mill and the typical ball nose cutting tools.

The mathematical modulation of the geometric accuracy of the plaster parts was carried out in terms of feed-rate and arm extension. The mathematical equation generated during this study was used to develop flatness contours in the feed-rate and arm extension, which can help to predict the geometric accuracy at any zone of the experimental domain.

Acknowledgements
The authors wish to acknowledge the Staffordshire University, the Sandvik Portuguesa and Ceramic Product Development (CPD) companies for the use of equipment and resources during the period of this work.

References

[1] Coole, T. J.; Cheshire, D. G.; Newman, D. J., "Excessive Tool Wear and Moisture Content of Plaster in Ceramic Plaster Machining", British Ceramic Transactions Magazine, 1999, Vol. 98, N°3, pp 151- 155, ISSN 0967-9782

[2] Antunes Simões, J. F. C. P.; Coole, T. J.; Cheshire, D. G.; Mesquita, R. M. D., "The Analysis of Tool Wear in the Machining of Plaster Material Prototypes", ISATA 2000 - International Symposium on Automotive Technology & Automation, Dublin/Ireland, 2000, Vol. Advanced Manufacturing – modular *manufacturing, supplier integration, production planning*, pp. 149-156, ISBN 1-902856-16-3

[3] Coole, T. J.; Cheshire, D. G.; Mesquita, R. M. D.; Antunes Simões, J. F. C. P.; "Analysis of robot system capabilities in machining of full scale prototypes for sanitary ware industry", British Ceramic Transactions – International Journal, 2000, 99, (4), pp. 175-178, ISSN 0967-9782

[4] Antunes Simões, J. F. C. P.; Coole, T. J.; Cheshire, D. G.; Mesquita, R. M. D., "Analysis of a Robot System Capabilities in the Machining of Full-Scale Prototypes", International Symposium on Automotive Technology & Automation, Vienna/Austria, 1999, Vol. Advanced Manufacturing in the Automotive Industry, pp. 93-100, ISBN 1-902856-02-3

[5] Antunes Simões, J. F. C. P.; "Advanced Machining Technologies in the Ceramics Industry", Ph.D. Thesis, Staffordshire University, July 2001

[6] Montgomery, Douglas C.; "Design and Analysis of Experiments", 4th Edition, John Wiley & Sons, 1997, ISBN 0-471-15746-5

Fabrication of customized bioceramic implants using selective laser sintering

F CRUZ and **J F A SIMÕES**
Escola Superior de Tecnologia de Setúbal, Instituto Politécnico de Setúbal, Portugal
T J COOLE
Faculty of Technology, Buckinghamshire Chilterns University College, UK
C BOCKING
CRDM, Buckinghamshire Chilterns University College, UK

ABSTRACT

Rapid Prototyping (RP) is an excellent manufacturing process to produce medical models. These models are designed and optimised using anatomical scan information obtained from internal structures of the patient's body (e.g. Computed Tomography (CT), Magnetic Resonance Imaging (MRI) and Ultrasound) and the 3D shape is manufactured straight from 3D medical image data, from an appropriate material exhibiting desired proprieties. This route is a reverse engineering (RE) process.

Several of the existing RP processes are able to produce medical models in different materials and are being used for different applications. However, those models cannot be used directly as implants due to its non-biocompatibility.

Present research work investigates the industrial production of biocompatible ceramic medical models to be used directly as implants in the human body, using the hydroxyapatite (HA) ceramic material. This osseous-inductive calcium phosphate bioceramic has a structure similar to human bones and is classed as a biological active material, which encourages bone growth on its surface. It is the material of choice for implants due to its safety and efficiency as biocompatible implantable material. HA has been used in medicine and dentistry for nearly twenty years. Currently it is manually formed to the required shape or machined.

The objective is to produce implants using the SLS (Selective Laser Sintering) process, from poly (L – lactide) / hydroxyapatite composites (PLLA / HA).

The expected benefits include a considerable time and cost reduction to produce the implants, as well as its long-term biocompatibility.

KEYWORDS: Rapid Prototyping of Medical Models, Bioceramics, Biopolymers, PLLA/HA Composites, Selective Laser Sintering

1. INTRODUCTION

In recent years several research institutions, medical industries and commercial organizations have integrated Computer Aided Design (CAD) and Rapid Prototyping (RP) to fabricate 3D physical medical models. These models are being used for several applications: visualization, diagnosis, operation planning, design of implants, external prosthesis, surgical templates, production of artificial organs, communication (between the medical team and/or medical doctors and patients), and teaching, or didactic aids. Another application field is the production of medical surgical instrumentation tooling. Concerning the implants, medical models obtained by RP are normally used indirectly, as masters, to produce prosthesis in biocompatible conventional materials (e.g. titanium, cobalt-chrome alloys, medical-grade alumina, medical-grade silicone elastomer, apatite, etc.), namely by casting and spray metal moulding [1-3].

RP has the ability to fabricate models with complex geometric forms, and so is very suitable to reproduce the intricate forms of the human body. With the aid of a RP model, visualization of intricate and hidden details of traumas by surgeons is enhanced [4].

The majority of the references founded in literature on this subject concerns to the production of medical models via Stereolithography (SL), mainly in the scope of the EARP (European Action on Rapid Prototyping) and PHIDIAS Projects, sponsored by the EU. However, SL medical models cannot be used inside the human body,

as direct implants, due to the resin toxicity, which create concerns about the long-term biocompatibility of SL models. Nevertheless, the range of applications of those models is very large [5-9, 13].
Other RP processes that were already used to produce medical models, in different materials, are Fused Deposition Modelling [10], Selective Laser Sintering [11], Sanders Prototyping Technology and Z Corporation System [12], Laminated Object Manufacturing and Solid Ground Curing [13].

The use of RP in medical applications is a relatively young field, and the main limitations of this manufacturing route, so far, are: Non-biocompatibility of the existing materials used in the RP machines; Model production costs still high; Time needed for model production and Model quality (surface finish, anatomical accuracy).

The next steps to improve the use of RP in the production of medical models are: To produce customised implants; To produce implants to be used directly, in biocompatible materials (e.g. hydroxyapatite); To assure long-term compatibility of the implants.

2. BACKGROUND

2.1-Rapid prototyping technologies

Rapid Prototyping (RP), or Solid Freeform Fabrication (SFF), or Layer Manufacturing (LM), or Desktop Manufacturing (DM), is one of the fastest developing manufacturing technologies in the world today. It is different to the conventional fabrication processes (i.e. *subtractive* type as milling or *compressive* type like casting and moulding). RP processes are of *additive* type, because parts are built on a layer-by-layer basis [14-15].

The prototypes can be made from plastic, paper, wax, ceramics and metals, and, in general, RP systems can be classified into *three different categories* based on the initial form of materials used: Liquid-based (e.g. SL); Solid-based (e.g. LOM) and Powder-based (e.g. SLS).

A distinct advantage of creating a part layer-by-layer is that the geometric complexity of the part has significantly less impact on the fabrication process than in the case of traditional manufacturing processes. Other advantages are: no need of tools, short time to produce the parts, very little human intervention and set-up time, and lower fabrication costs.

Some of the more popular RP processes are: Stereolithography (SL); Fused Deposition Modeling (FDM); Selective Laser Sintering (SLS); Laminated Object Manufacturing (LOM); 3Dimensional Printing (3DP) and Solid Ground Curing (SGC). The characterisation of these RPT can be found elsewhere [14-15].

After the part is built, and depending on the system, post-processing will normally be necessary (i.e. cleaning, removal of supports, sanding, painting, post-curing, infiltration, etc).

2.2-RP of medical models

The manufacturing of medical models using RP techniques starting with the acquisition of three dimensional shape data of both internal and external human body structures, allow the production of 3D physical objects, via a CAD/CAM system, in a RP apparatus. This is a Reverse Engineering (RE) process [12, 16-17].

In the medicine area, the common systems used in medical imaging to obtain anatomical information are: Computed Tomography (CT); Magnetic Resonance Imaging (MRI); Ultrasound System (US); Mammography; Radiography (plain X-ray) and Laser Digitiser [12, 18-20]. Most medical models are produced via CT for bone structures and MRI for soft tissues [20].

2.3-Requirements of RP in surgery

An RP medical model to be useful in medical applications must simplify and help an otherwise complicated procedure, to reduce the risk to the patient owing to the shortened time of surgical procedures, and to be less expansive than the alternatives. Thus, an RP medical model should deliver: Efficiency in surgery, with reduced

operating theatre costs; Procedures with fewer complications; Increased surgical precision to reduce possible damage to healthy tissue; Improved patient outcome (i.e. faster rehabilitation at lower cost); An opportunity to perform new, or previously impossible, minimal invasive procedures [13].

3. BIOMATERIALS

Biomaterials are materials that can be safely used within the human body. Among this group of materials, certain high-purity ceramics offer long-term biocompatibility and therefore have a large potential to be used in medical applications [21-22].

3.1-Biocompatibility

No one material is suitable for all biomaterial applications. As a class of biomaterials, ceramics, glasses, and glass-ceramics are generally used for repair or replacement of musculoskeletal hard connective tissues. Nevertheless, no material implanted in living tissues is inert; in fact, all materials elicit a response from living tissue [21].

The environment inside the body is both hostile and extremely sensitive. To select materials for use in this environment requires attention be paid to both the physical function and the biocompability of the candidate substance. *Biocompability* is defined as the ability of a material to perform with an appropriate host response in a specific application [21]. It is thus distinct from *inertness*, which would imply no response from the host. Moreover, it is not a single phenomenon, but rather is a collection of processes involving different but interdependent mechanisms of interaction between a material and the tissue. It is also specific to a particular application and location in the body. Four types of response from living tissues against foreign materials are possible, as can be seen in Table1.

Implant material characteristics	Tissue response
Toxic	Surrounding tissue dies
Nontoxic, biologically inactive	Fibrous tissue of variable thickness forms
Nontoxic, bioactive	Interfacial bond forms
Nontoxic, dissolves	Surrounding tissue replaces material

Table 1: Possible tissue responses to biomedical implants [21]

3.2-Calcium phosphate ceramics (hydroxyapatite)

Calcium phosphate based bioceramics have been used in medicine and dentistry for the last twenty years, in several applications: dental implants, periodontal treatment, alveolar ridge augmentation, orthopedics, maxillofacial surgery, and otolaryngology. Different phases of calcium phosphate ceramics are used depending upon whether a resorbable or bioactive material is desired [21-22].

Hydroxyapatite (HA or HAp) is a complex phosphate of calcium ($Ca(PO_4)_3OH$) that occurs as a mineral and is the chief structural element of vertebrate bone. It is a very important material for bioceramics. In present work we are using HA powder, supplied by Plasma Biotal Ltd (UK), the characteristics of which are shown in Table2.

Trivial Name	Synthetic Bone Mineral	
Trade Name	Captal 90	
Physical Form	Powder, Granules	120 +/- 20 microns
Toxicity	Non-Toxic	
Chemical Reactivity	Acids Alkalis Organic Solvents	Dissolves Below pH 5.5 Insoluble Non-Reactive
Crystal Structure System	Hexagonal	
Ca O / P_2O_5 Ratio	1.33	
Ca / P Ratio	1.68	
Bulk Density (g/cm^3)	1.45 +/- 0.2	
Green Density (%)	52-58	
Sintered Density at 1250°C (%)	86-97	

Table 2: Hydroxyapatite characterisation (Plasma Biotal Ltd)

One of the important research issues concerning HA is its mechanical behaviour limitation. In fact, brittleness, poor fatigue resistance, low tensile strength, and low fracture toughness value, precludes HA from use in load bearing situations.

The mechanical behaviour of calcium phosphate ceramics strongly influences their applications as implants. Therefore, in clinical practice calcium phosphate bioceramics should be used as: powders; small, unloaded implants such as in the middle ear; with reinforcing metal posts, as in dental implants; as coatings, (for example in metal or ceramic composite implants); as low-loaded porous implants where bone growth acts as a reinforcing phase, providing long-term fixation; as bone grafting; drug delivery (as a carrier of bone morphogenetic proteins, antibiotics or materials that stop inflammation); as bone cement [23-24].

In recent years, bioceramics research published work shows that dense, porous, or particulate forms of HA have been prepared. However, porous HA as an implant is preferred. The pores (100-300μm) allow bone to grow into implant, promoting mechanical fixation with the natural bone. Nevertheless, porosity and pore size can reduce the mechanical properties of HA ceramic. The minimum pore size of approximately 100-150μm has been established as necessary for the continued health of bony ingrowth [33].

Several references of research work exist in literature related with HA and calcium phosphate ceramics applications in medicine, thus showing the importance of these bioceramics in the medical field.

3.3-Biodegradable polymers – poly (L-lactide)

PLLA [poly (L-lactide)] is a biodegradable semi-crystalline polymer derived from lactic acid ($C_3H_6O_3$). Lactic acid can be produced naturally (by fermentation of sugar and water) or synthetically by chemical process.

Applications of this polymer in medicine and pharmacy include wound closure products, drug delivery systems and surgical implant devices. The main advantages of these polymers are their mechanical strength, combined with biodegradability and biocompatibility. The biodegradation of PLLA takes place by random hydrolysis, being the final degradation products eliminated in a natural way.

The physical properties of the PLLA used in present work, supplied by PURAC (Netherlands), are given in Table3.

Young's Modulus (GPa)	Elongation (%)	Tensile Strength (MPa)	Density (g/cm^3)	Melting Temperature (°C)	Glass Transition Temperature (°C)	Degradation Time (months)
3-5	3-6	50-60	1.25-1.30	170-200	55-65	> 24

Table 3: PLLA physical properties (Purac Biochem bv)

3.4-HA/PLLA composites

Because metals are too stiff to prevent stress protection, polymers tend to be too flexible and too weak to meet the mechanical demands for an internal fixation device, and bioceramics (e. g. HA) are to brittle and have unfavourable mechanical properties where weight bearing is concerned, composite materials should be considered for this purpose. Recently attention has been paid to the application of HA in combination with a polymeric substance. The use is still confined to the field of the filling of bony defects and as drug carrier. Polyethylene, polybyturate and PLLA are the most frequently used polymers in such composite materials. Composites of HA / PLLA combines bioresorption (PLLA) with bone bonding potentials (HA) resulting in a potentially bioactive and bioresorbable composite with higher strengths and stiffness than the unfilled polymer [34]. Figure1 below shows SEM images of HA/PLLA composites - "green bodies" - with different ratios (wt %).

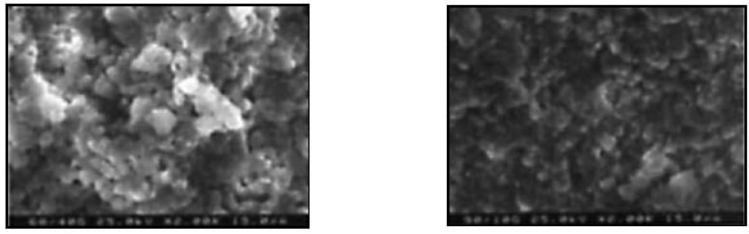

Figure 1: HA / PLLA *composite ratios – 60/40 (left hand image), 90/10 (right hand image)*

Figure2 shows new bone formation surrounding an implant of HA/PLLA after 32 weeks.

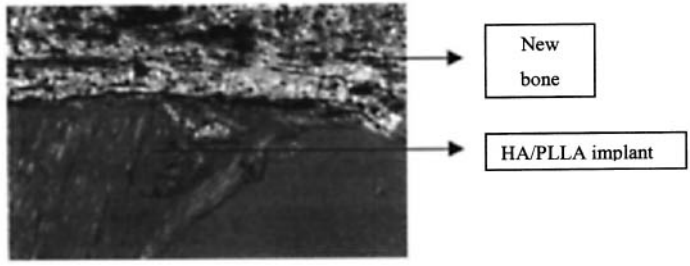

Figure 2: HA/PLLA implant [Biocomposites]

4. RP OF HA MEDICAL MODELS – STATE OF THE ART

Little information is available in literature on the applications of HA medical models produced by RP. This material has a structure similar to the human bone, is obtained by sintering, and currently manually formed to the required shape, or machined by milling [25]. Other used processes of manufacturing are the slip-casting technology, and hot isostatic pressing (HIP). The main applications of HA models are in dentistry, bone repair

(in bone grafting implants), and as coatings for internal implants. The cost of this material is a major concern in these cases and an alternative method of shape development is required to produce the models.

The following references of HA's RP models for biocompatible applications can be found:

- Using the CerLOM (LOM of ceramics) technology, at Lone Peak Engineering, Inc. (USA) [26] and University of Dayton (USA) [32];
- Using the FDC (FDM of ceramics) technology, at Rutgers University (USA) [27];
- Using the SLS technology, at Wilford Hall Medical Centre (UK) [28] and at University of Texas (USA) [29];
- Using SL technology, with Ceramic Resins, at University of Nancy (FRANCE) [30], and University of Michigan (USA) [31].

5. RAPID PROTOTYPING OF HA/PLLA IMPLANTS

At CRDM (Centre for Rapid Design and Manufacture), based in the Buckinghamshire Chilterns University College / High Wycombe, Selective Laser Sintering of HA/PLLA composites is currently under investigation to produce sintered customised implants for lower load bearing applications.

Although a large number of materials can be used in the SLS process (polycarbonate, nylon, nylon / glass composite, wax, ceramics, elastomeric and metal – polymer powders), only plastic and metals materials are, so far, commercially available.

Therefore, a modified SLS Sinterstation 2000 (from DTM) is being used to perform experiments using HA powders coated with a PLLA binder, to produce, layer – by – layer, implants in a new biocompatible / biodegradable composite. The selective laser sintering process creates three – dimensional objects from powdered materials with the heat generated by a CO_2 laser of 50W.

The procedure to build the models with the DTM Sinterstation System comprises the following steps:
1 – *Processing requirements*: Reading the medical data from scanning systems; Selecting the appropriate region of interest; Interpolating the data; Produce 3D CAD data; Converting it to the industry standard .STL format.
2 – *The process*: A thin layer of powder is deposited into the part build chamber; An initial cross-section of the model under fabrication is selectively drawn on the layer of powder by a heat- generating CO_2 laser; The interaction of the laser beam with the powder elevates the temperature to the point of melting the polymeric binder, forming a solid mass with the ceramic; An additional layer of powder is deposited via a roller mechanism on the top of the previously scanned layer; The process continues, with each layer fusing to the layer below it; The process is repeated until the part is complete; No support systems are needed.
3 – *After processing*: The part is removed from the build chamber and the loose powder falls away; Parts may then require some post-processing, depending upon the intended application.

6. DISCUSSION

The aim of the procedure is to improve the mechanical properties of macroporous HA models, using a composite of poly (L – lactide) / hydroxyapatite powders to produced sintered implants of composite biomaterials with optimized strength and resorption characteristics allowing the manufacture of medical models capable of functional low load bearing applications.

Aspects to be followed up: To overcome some actual limitations of the SLS process, as the surface finish, tolerance and detail of replication; To follow up possible situations of inflammation, absence of resorption and only partial biocompatibility of "in vivo" implants; To operate in accordance with the existing international standards on the biological evaluation of medical materials and devices.

7. SUMMARY

The production of HA medical models using RP technologies is still at an embryonic stage, mainly at laboratory research level and, therefore, far from the industrial production stage.

Although there is little information published in this field, some RP technologies commercially available show the potential for the production of HA medical models (e.g. SL of ceramic suspensions, CerLOM, SLS, 3DP, and FDC), using modified apparatus.

Present work is directed to the application of the SLS process to produce medical implants to be used directly in the human body, from a composite of hydroxyapatite and poly (L – lactide) biomaterials.

For this purpose the laser technology, as well as the hardware and software to be used, must be researched to permit the industrial production of the HA / PLLA implants, as desired.

The RP system has to combine operating simplicity and geometric, dimensional and finish accuracy of the models, in order to become competitive in terms of costs, time and quality relating to other manufacturing processes already in use.

Future work includes a benchmarking study of RP processes for use in biomedical applications, using the above mentioned biomaterials, for comparison in terms of surface finish, geometric accuracy, processing speed and production costs of the implants.

References

1. Jacobs, P.F., *Medical Models Using RP&M Technologies*, In *Stereolithography and Other RP&M Technologies*, Society of Manufacturing Engineers, ISBN 0-87263–467-1, Ch. 9, pp. 339-347,1996.
2. Kay, C.C.; Fai, L.K., *Biomedical Industry*, In *Rapid Prototyping: Principles & Applications in Manufacturing*, John Wiley & Sons, Inc., ISBN 0-471-19004-7, Ch. 7, pp. 221-224, 1997.
3. Popat, A. H., "Rapid Prototyping and Medical Modelling", *Phidias Newsletter – Rapid Prototyping in Medicine*, BRITE/EURAM 3-BRRT985051, No 1, pp.10-12, December 1998.
4. Jensen, K. L., "Instant Medico Models", *EARP (European Action on Rapid Prototyping) Newsletter*, Danish Technological Institute, Denmark, No 2, pp. 1-2, August 1993.
5. Haex, J. K. Th. [et al.], "The Use of Stereolithographic Models in Patients with Large Cranial Defects", *Phidias Newsletter*, No 1, pp. 4-5, December 1998.
6. Kermer, C., "Preoperative stereolithography model planning in craniomaxillofacial surgery", *Phidias Newsletter*, No 2, pp. 1-3, June 1999.
7. Haex, J. K. Th. [et al.], "Preoperative planning with the use of stereolithographic model", *Ibidem*, No 3, pp. 1-2, December 1999.
8. "Human skull reproduced by computed tomography scanning and stereolithography", *Rapid Prototyping Report*, CAD/CAM Publishing, Inc., USA, Volume 2, No 1, p. 1, January 1992.
9. McAloon, K., "New Directions in Stereolithography in Medicine, *EARP Newsletter*, No 4, p. 9, August 1994.
10. "Fused deposition modelling creates custom orthopedic implant", *Rapid Prototyping Report*, Volume 2, No 5, p. 1, May 1992.
11. "Selective laser sintering used to manufacture artificial leg", *Ibidem*, Volume 2, No 10, p. 1, October 1992.
12. Chelule, K. L. [et al.], "Fabrication of Medical Models from Scan Data via Rapid Prototyping Techniques", *Paper presented at TCT (Time-Compression Technologies) 2000 Conference & Exhibition*, Cardiff, UK, October 2000.
13. Kai, C. C. [et al.], "Rapid Prototyping Assisted Surgery Planning", *The International Journal of Advanced Manufacturing Technology*, Springer-Verlag London Limited, ISSN 0286-3768, Volume14, 9, pp. 624-630, 1998.
14. Kulkarni, P. [et al.], "A review of process planning techniques in layered manufacturing", *Rapid Prototyping Journal*, MCB University Press, ISSN 1355-2546, Volume 6, No 1, pp. 18-35, 2000.
15. Chua, C. K. [et al.], "A Study of the State-of-the-Art Rapid Prototyping Technologies", *The International Journal of Advanced Manufacturing Technology*, ISSN 0286-3768, Volume 14, No. 2, pp. 146-152, 1998.
16. Brown, J.M., "What is Rapid Prototyping", *EARP Newsletter*, Special Medical Edition, No 5, pp. 1-3, February 1995.
17. Swaelens, B.; Kruth, J. P., "Medical Applications of Rapid Prototyping Techniques", *Proceedings of the Fourth International Conference on Rapid Prototyping - 1993*, The University of Dayton, Dayton, Ohio, pp. 107-120, June 1993.
18. Cleynenbreugel, J. V.; Suetens, P., "CT/MRI Medical Data Processing", *EARP Newsletter*, Special Medical Edition, No 5, pp. 8-9, February 1995.

19. Swann, S.,"Integration of MRI and stereolithography to build medical models: a case study", *Rapid Prototyping Journal*, ISSN 1355-2546, Volume 2, No 4, pp. 41-46, 1996.
20. Kalender, W. A., *Computed Tomography*, Publicis MCD Verlag, ISBN 3-89578-081-2, Munich, Germany, 2000.
21. Hench, L. L., *Medical and Scientific Products*, In *Ceramics and Glasses*, Section 13-Volume 4 of *Engineered Materials Handbook*, ASM International, ISBN 0-87170-282-7, pp. 1007-1013, 1991.
22. Ravaglioli, A; Krajewsky, A., *Bioceramics: Materials, Properties, Applications*, Chapman & Hall, ISBN 0-412-34960-4, London, England, 1992.
23. Willmann, G., "Bioceramics", *Ceramic Industry*, Business News Publishing Co., ISSN 0009-0220, pp. 27-28, December 1999.
24. "2000 Materials Handbook", *Ibidem*, January 2000.
25. Chelule, K. L. [et al.], "An Investigation Into The Machinability of Hydroxyapatite for Bone Restoration Implants", *Paper presented at the Research and Development in Net Shape Manufacturing Conference*, Birmingham, UK, 9-11 April 2001.
26. Klosterman, D.A. [et al.], "Development of a curved layer LOM process for monolithic ceramics and ceramic matrix composites", *Rapid Prototyping Journal*, ISSN 1355-2546, Volume 5, No 2, pp. 61-71, 1999.
27. Venkataraman, N. [et al.], "Feedstock material property – relationships in fused deposition of ceramics (FDC)", *Ibidem*, Volume 6, No 4, pp. 244-252, 2000.
28. Schmitt, S. M. [et al.], "An Integrated Approach for Utilization of Emerging Technologies in Medicine and Dentistry", *Proceedings of the Sixth International Conference on Rapid Prototyping - 1995*, The University of Dayton, Dayton, Ohio, pp. 51-55, 1995.
29. Lee, G.; Barlow, J.W., "Selective Laser Sintering of Calcium Phosphate Powders", *Solid Freeform Fabrication Symposium Proceedings – 1994,* The University of Texas, Austin, ISSN 1053-2153, pp. 17-24, pp. 191-197, September 1994.
30. Taha, F.; Wouters, K., " First French Workshop on Medical Applications of Rapid Prototyping Techniques", *Phidias Newsletter*, No 1, pp. 2-3, December 1998.
31. Griffith, M. L. [et al.], "Ceramic Stereolithography for Investment Casting and Biomedical Applications", *Solid Freeform Fabrication Symposium Proceedings – 1995,* ISSN 1053-2153, The University of Texas, Austin, pp. 31-38, September 1995.
32. Steidle, C. [et al.], "Automated Fabrication of Custom Bone Implants Using Rapid Prototyping", *Paper presented at the 44th International SAMPE Symposium and Exhibition,* Long Beach, CA, USA, May 1999.
33. Hing, K. A. [et al.], "Characterization of porous hydroxyapatite", *Journal of Materials Science: Materials in Medicine, European Society of Biomaterials*, Kluwer Academic Publishers, ISSN 0957-4530, Volume 10, 3, pp. 135-145, March 1999.
34. Bronzino, J. D. [et al.], "*The Biomedical Engineering Handbook*", CRC Press Inc., ISBN 0-8493-8346-3, Boca Raton, USA, 1995.
35. Braybrook, J. B., *Biocompatibility Assessment of Medical Devices and Materials,* John Wiley & Sons, ISBN 0-471-96597-9, Chichester, England, 1997.

A review of the manufacture of below-knee prosthetic sockets using rapid prototyping technologies

N S HERBERT
Rapid Design and Manufacture Centre, Glasgow, UK

ABSTRACT

This paper presents a comprehensive review of the attempts to date to use Rapid Prototyping (RP) technologies for the manufacture of below-knee (BK) prosthetic sockets. Several groups worldwide are currently investigating the feasibility of using these technologies in order to remove the labour intensive fabrication that is required using both traditional and current CAD/CAM methods. This research has shown that the fabrication of functional BK sockets using RP is indeed possible. However, several problem areas have been identified including the high cost of RP machines and materials, the availability of custom developed systems and the need for a simple methodology that can be easily adopted by prosthetic centres.

1. INTRODUCTION

Between 1998 and 1999 there were 5665 new referrals to prosthetic centres in the United Kingdom [1]. Of this total the most common level of amputation was at the trans-tibial level (below-knee, BK), accounting for 2721 patients, 48% of the total. For the vast majority of these patients a significant degree of mobility and quality of life can be regained through the fitting of a prosthetic limb.

Traditionally the design and manufacture of a below-knee prosthesis has been a manual process and this remains the dominant technique used by the National Health Service in the UK. This process relies heavily on the use of plaster casts, moulds and manual fabrication techniques. Advances in computer-aided design and manufacture (CAD/CAM) technologies have helped to automate several aspects of the process, but despite these advances the final manufacture of the prosthetic socket, the most critical component of a prosthesis, is still performed manually. This process has several drawbacks, as we shall see.

Rapid Prototyping, a relatively new class of manufacturing technologies, has the potential to replace manual socket fabrication with a direct, automated process. Several research groups worldwide are currently researching the use of these promising new technologies for the manufacture of BK prosthetic sockets.

2. CONSTRUCTION OF A BK PROSTHESIS

The design of a typical BK prosthesis features a prosthetic foot that is connected via a pylon (usually a length of metal tubing) to the socket. In most cases the prosthesis is fitted with a cosmetic cover to provide a more realistic appearance.

Of critical importance is the design of the socket - the interface between the patient and the prosthesis. Each socket is a tailor-made device, designed to exactly fit the geometry of the patient's stump. The socket must be carefully designed so that the patient is supported correctly and so that pressure is not exerted on sensitive tissues. It is the socket that determines the comfort and performance of the prosthesis and ultimately whether or not the device will be accepted and worn regularly.

3. TRADITIONAL METHODS OF SOCKET MANUFACTURE

3.1 Process description

There are several variations on the traditional method for prosthetic socket manufacture, but most methodologies follow the same basic steps. The process description that follows is based upon that currently used by staff at

both the Bioengineering Unit and The National Centre for Training and Education in Prosthetics and Orthotics at The University of Strathclyde, Glasgow, UK.

1. Marking-up the residual limb
The process begins with the application of a thin stocking to the patient's stump. The prosthetist then uses an indelible pencil to mark key landmarks of the stump onto the surface of this stocking. In particular areas of hard and soft tissue are highlighted. The indelible nature of the pencil means that these marks are subsequently transferred to the plaster-wrap cast and then the positive mould.

2. Plaster wrap casting of the residual limb
A plaster wrap cast is taken of the stump to capture its geometry. Plaster impregnated bandages are soaked in water and then wound around the patient's stump. The prosthetist uses his judgement to apply pressure to key areas of the stump in order to produce a better fitting socket and reduce the need for modifications later in the process. The plaster bandages typically set in 5-10 minutes after which the cast is carefully removed by placing a small incision in its upper edge.

3. Production of the positive mould
The wrap cast is filled with a plaster slurry. Once this slurry has set the wrap cast is removed, leaving a positive mould of the patient's stump. It is important to note that the original wrap cast is destroyed in this process. Should a new positive mould be required then the plaster wrap cast must be performed again. This may require further consultations with the patient and delay the rehabilitation process.

4. Rectification of the positive mould
Before socket fabrication the positive mould may require modification by the prosthetist in order to produce a comfortable and correctly fitting socket. This process is known as rectification. Guided by the marks made in stage 1 the prosthetist uses his skill and judgement to selectively add and remove material on the mould. This takes into account the location of bone, muscle and sensitive tissues to ensure that the socket supports the patient's stump correctly.

5. Socket fabrication
Finally the socket is fabricated over the top of the positive mould. Layers of felt, nylon, glass-fibre and carbon-fibre are draped over the mould and then acrylic or polyester resin is applied under vacuum conditions. The vacuum ensures that the resin soaks completely through the fibres and that the socket closely conforms to the geometry of the positive mould. Once the resin has cured the positive mould is removed leaving the finished socket. In most cases the positive mould requires to be destroyed in order to remove it from the socket.

An alternative method of manufacture is thermoforming in which a sheet of thermoplastic material (typically polypropylene) is heated until soft and then formed over the positive mould.

3.2 Discussion of traditional method

The traditional method of design and fabrication is able to produce well performing, comfortable devices in reasonably short timescales. However the process has several drawbacks:

- The wrap casting process can be messy.
- There is no permanent record of the patient's stump geometry.
- Both the wrap cast and the positive mould are destroyed during the process. Duplicate sockets require the entire process to be repeated from the beginning.
- Although relatively quick, the fabrication of the socket is a labour intensive and often messy procedure.

4. COMPUTER AIDED METHODS OF SOCKET MANUFACTURE

4.1 Typical CAD/CAM process description

In recent years computer aided design and manufacture (CAD/CAM) tools have begun to be adopted by the prosthetics sector. There are numerous systems on the market, each of which has its own pros and cons.

However these will not be discussed in this paper. Although there is a great deal of variation between systems, most follow the same basic stages:

1. Data Acquisition – The process begins with the digital acquisition of 3D geometric data from the patient's residual limb. This is achieved using a touch probe, laser or photographic based 3D scanning system. The 3D data is usually collected in the form of a point-cloud - a database of points with known coordinates in 3D space. This data can easily be converted into an accurate 3D representation of the patient's stump.

2. Data Manipulation – Once captured, the 3D stump data requires to be manipulated using specialist CAD software. In this manner the prosthetist can carry out rectification as he would during the traditional method. Since the data is digitally stored then such rectification does not destroy the original data. The design can be modified time and time again until the prosthetist is happy with the result.

3. Manufacture of the Positive Mould – The modified 3D data is sent to a CNC carving machine in order to manufacture a positive mould of the stump. The carver machines the positive mould from a block of plaster (or a polymer material) known as a blank.

4. Socket Fabrication
Socket fabrication is performed manually in the traditional manner and as before the positive mould is usually destroyed during the process.

4.2 Discussion of CAD/CAM methods

The use of CAD/CAM technology has helped to overcome some of the shortcomings of the traditional process of socket design and manufacture. It removes the mess associated with plaster casting and it creates a permanent digital record of the patient's limb that can be repeatedly modified without destroying the original data. However as *Rolock & Tucker* point out, despite the use of automated machinery CAD/CAM processes are actually only semi-automated [2]. There are several drawbacks to CAD/CAM:

- The fabrication of the socket is still performed manually and remains a labour intensive process.
- The positive mould is destroyed during fabrication and so the production of each socket requires a new mould to be manufactured using a CNC carver. This wastes time, material and money.
- Blanks for the CNC carver must either be purchased from a supplier - leading to possible inventory problems, or they must be fabricated in-house - resulting in extra labour for staff.
- CAD/CAM equipment (the 3D scanner, software and CNC carver) is expensive. This is especially problematic for publicly funded health services such as the NHS in the UK who have limited budgets.
- Staff must be retrained with new skills at further expense.

5. THE POTENTIAL OF RAPID PROTOTYPING TECHNOLOGIES

5.1 Introduction to Rapid Prototyping (RP)

Rapid Prototyping (RP) is a generic term that refers to a relatively new class of manufacturing technologies that build models directly from 3D CAD data.

Although there are many different RP technologies, all RP processes are based upon the common principal of building parts in a layer-by-layer manner. Unlike traditional manufacturing technologies that remove material, RP adds material to create the finished component.

Computer software is used to split the 3D CAD data into a series of thin horizontal cross-sections (slices). These slices are then sent sequentially, starting with the bottom slice, to the RP machine. Each slice is fabricated on top of the previous one and the slices are bonded together. Depending upon the technology used it may also be necessary to build a scaffolding structure around the model in order to support overhanging features. This support structure is removed once the build is complete.

Traditionally RP has been viewed as a quick and cost-effective method of making non-functional prototypes with limited mechanical properties. However advances in both process capabilities and RP materials have led to the possibility of Rapid Manufacture – the manufacture of finished components directly from 3D CAD data.

5.2 The potential of RP for socket manufacture

Rapid Prototyping would appear to be an ideal process for the fabrication of prosthetic sockets because it is especially suited to creating one-off custom designs, regardless of geometric complexity. The advantages of RP include:

- Socket fabrication is automated, greatly reducing the amount of manual labour required.
- Sockets can be built directly without the need for a positive mould or other intermediate stages.
- Wall thickness can be accurately controlled.
- Duplicate sockets can be easily manufactured without the need for new positive moulds.

6. STEREOLITHOGRAPHY (SLA)

6.1 Introduction

Stereolithography (SLA) was the first rapid prototyping process to be developed. It was introduced in 1987 by the 3D Systems Corporation of California, USA [16]. Today SLA remains the most widely used RP technology despite increased competition from other technologies.

6.2 The SLA process

The process uses a liquid, photosensitive polymer that hardens when exposed to UV light. The SLA machine consists of a vat of this resin containing a vertically moving platform upon which the model is built. This platform is submerged in the resin leaving a thin layer covering its surface. A UV laser then scans a cross section from the CAD model onto the surface of the resin, causing it to solidify and form a layer of the model. The platform then moves down by a layer thickness and the next cross section is scanned onto the surface of the resin. This process repeats until the model is completed. Finally the finished model is removed from the machine and placed in an UV 'oven' where it is fully cured.

6.3 Research into SLA socket manufacture

The use of Stereolithography for the manufacture of prosthetic sockets began in 1990 by a research group based at Northwestern University Medical School, Chicago, USA in collaboration with Baxter Healthcare Corp [3]. The SLA process was successfully used to directly manufacture a socket from 3D CAD data. However, the process was slow, taking over 48 hours, and the resulting socket had limited functionality and was only suitable for demonstrating the potential of the process.

In 1998 Freeman & Wontorcik carried out a cost/benefit analysis between traditionally manufactured sockets and those made using the SLA process [4]. Two sockets were manufactured, the most successful taking 26 hours to build at a cost of $1,560. The finished socket had a similar fit and comfort to a traditionally manufactured socket, but the material was found to be very brittle and not suitable for the stress levels generated in a socket when worn. The SLA sockets were able to be used as test sockets to check form and fit. This was aided by the translucent nature of the material, allowing the prosthetist to view the liner worn on the patient's stump.

Freeman & Wontorcik concluded that production times and costs must be reduced significantly to make SLA practical. Although SLA technology and materials have improved since this research was carried out the process remains relatively slow and expensive with high capital and running costs. Currently materials are not strong enough to be used in final production sockets and although new materials have been developed they tend to become brittle over time due to continued exposure to UV light. The combination of these factors has led to little research into SLA manufactured sockets being carried out in recent years.

7. SELECTIVE LASER SINTERING (SLS)

7.1 Introduction

The Selective Laser Sintering (SLS) process was commercialised in 1992 by the DTM Corporation of Texas, USA [16]. In 2001 the DTM Corporation was acquired by the 3D Systems Corporation. The technology was originally developed at The University of Texas at Austin, USA and this institution remains at the forefront of SLS research and its applications.

7.2 The SLS Process

SLS uses a CO2 laser to selectively fuse a layer of powdered material. Materials currently available include nylons, polycarbonates and specially prepared metals, allowing a wide range of components to be manufactured. The process begins with a thin layer of powder being spread over the build platform. A laser is then scanned onto the surface, sintering the powder to form a cross-section of the CAD model. Once the layer is complete the build platform is lowered by a layer thickness, a new layer of powder is spread on top and the next cross-section is sintered. Once the build is complete the loose, unused powder is removed leaving the finished part.

7.3 Research into SLS socket manufacture

SLS has proved to be one of the most successful RP technologies for prosthetic socket manufacture. Researchers at The University of Texas at Austin and The University of Texas Health Centre at San Antonio have been investigating the SLS manufacture of sockets since 1991.

Initial research by *Rogers et al* developed custom software to manipulate the data generated by a laser scanning system and transform it into a socket design ready for manufacture using SLS technology [5]. A significant addition to the socket design was the integration of a pylon fixture. This integrated fixture allowed a standard 30mm pylon to be fitted without additional devices, thus simplifying the prosthesis design. This new software and SLS technology were later successfully used to build both scaled and full-size sockets, proving the viability of the process [6]. No clinical trials of the SLS sockets were conducted at this time.

SLS research was developed further by *Stephens et al,* who investigated ways of controlling the rigidity of the socket in selected areas in order to improve patient comfort [7]. A double-wall design was selected featuring a thin, flexible inner wall and a thicker, more rigid outer wall. Struts were strategically placed between the two walls to control the degree of compliance in key areas.

Once again custom software was developed to manipulate the scan data, create the double-walled socket design, and export the final data ready for fabrication. Manufacture was carried out using a DTM Sinterstation 2500 and Duraform material. Duraform is a nylon derivative developed by the DTM Corporation. Its robust mechanical properties make it an ideal choice for socket fabrication. It took approximately 10.5 hours to build the socket.

The SLS socket was then fitted with a pylon and prosthetic foot and this assembly was clinically tested on a patient. Although the trials were limited, the patient reported a high level of comfort and performance of the device was found to be comparable to traditionally manufactured prostheses.

The double-wall design has several shortcomings as highlighted by *Rogers et al* [8]. The design is complicated, significantly heavier than a traditional socket and requires the use of several software packages in a time-consuming and labour intensive design process. As a result recent research has focused upon a single wall design that features a variable wall thickness in an attempt to control rigidity in key areas [8] [9]. New software has been developed to help simplify the design process. This software takes the scan data and gives the socket a nominal thickness of 6mm. The prosthetist can then easily alter this wall thickness where required, add the integrated pylon fixture, and choose how the socket is trimmed at its upper edge.

Clinical trials of this single-wall socket have been carried out on 4 patients, comparing SLS sockets to those manufactured using standard CAD/CAM techniques. The results of these trials show that SLS sockets are clinically acceptable and can be manufactured in a competitive timescale. However it was found that there was little flexibility in the socket despite the variations in wall thickness. A minimum thickness of 1.3mm is required

in order to maintain structural integrity and at this thickness there is little flex in the Duraform material. Another problem that has been identified is the use of the non-standard pylon adapter that is integrated into the socket design. In order to be clinically acceptable the prosthesis will require the more widely used pyramid design.

8. FUSED DEPOSITION MODELLING (FDM)

8.1 Introduction

FDM is currently the second most popular RP system worldwide. The first commercial system was introduced in 1991 by Stratasys Inc., USA [16].

8.2 The FDM process

A typical FDM machine consists of a vertically moving build-platform that is housed inside a heated oven chamber. Located above the build-platform is an extrusion head that is capable of moving in the x and y directions. Polymer material (usually ABS or polycarbonate) is fed into the head where it is heated and extruded in semi-molten form through a nozzle. The head is moved over the build-platform and polymer is deposited where needed to create the current cross-section of the model. The polymer material solidifies immediately after it is deposited and bonds to the layer below. Once the current layer has been completed the build platform is lowered by a layer thickness and the next cross-section is fabricated on top of the previous one. A support structure is also built simultaneously. This structure can be removed by hand once the model has been completed, or if the system uses soluble support material it can be dissolved away.

8.3 Research into FDM socket manufacture: Rapid Manufacturing Machine (RMM)

Collaborative research between the Institute of Materials Research and Engineering Singapore, Temasek Polytechnic Singapore and The National University of Singapore has investigated the use of FDM technology for the manufacture of BK sockets.

Initial work proved the technical feasibility of the process by building two BK sockets [9]. Scan data was acquired from two BK amputee volunteers – a male adult and a female child. FDM sockets were then fabricated with a commercial Stratasys FDM machine a polyamide material. In order to increase the rigidity of each socket the wall thickness was tapered from 3mm at the base to 7mm at the upper rim. The sockets took 29 and 39 hours to build for the adult and child respectively.

Subsequent research has verified the biomechanical performance of these FDM sockets [10]. Gait analyses were performed on the two volunteer patients wearing both FDM and traditionally manufactured sockets. The tests were filmed using a 5-camera motion analysis system and force platforms were used to measure loading. The results show that the biomechanical characteristics of the FDM sockets are very similar to those of traditionally manufactured sockets.

During refinement of this FDM fabrication process, concerns were raised about the long fabrication times and potentially high costs of the process [11], [12]. The authors concluded that the slow build times were due to the fact that commercial Stratasys systems are tailored to precision engineering work, laying down thin filaments of material to create highly accurate parts. BK sockets are not geometrically complicated and do not require a high level of dimensional accuracy. As a result the research group have built a custom machine to fabricate BK sockets. It is known as the Rapid Manufacturing Machine (RMM) [13]. The machine is very much based on the FDM process, but it features a wider extrusion nozzle and higher working temperatures that allow for greatly increased material mass flow. Air blowers have also been used to ensure solidification of each layer before the next is fabricated on top. The benefits of these modifications are clearly evident - the fabrication time for one particular socket was reduced from 29 hours to just 4 hours. Also, due to improved inter-laminar bonding, the need for a tapering wall thickness has been removed. This simplifies the creation of the 3D CAD file and its subsequent fabrication, helping to further reduce timescales.

At the time of writing sockets made using the RMM system are undergoing clinical and biomechanical testing.

8.4 Research into FDM socket manufacture: Squirt Shape

Squirt Shape is a customised RP process developed specifically for the manufacture of prosthetic sockets that has been developed at Northwestern University, Chicago, USA [2]. The process is heavily based upon FDM technology.

The socket is built upon a rotating platform that is also capable of moving in the x, y and z directions. A bead of semi-molten polypropylene material is extruded onto this platform in a continuous helix, following the contours of the socket design. In this manner the socket is created layer by layer. As the polymer cools it solidifies and bonds the layers together. Initially Squirt Shape technology was successfully used to create a 9-inch tall BK socket in 1.5 hours.

Subsequent research has raised concerns over the layered nature of the socket and the anisotropic nature of the material [14]. Static and cyclical tensile tests have been carried out that show that the material properties of the polypropylene are comparable to traditional socket materials and are of an acceptable level for clinical applications. It has been found that failure typically occurs across several layers rather than between individual layers, indicating the integrity of inter-laminar bonding within the socket.

BK sockets manufactured using Squirt Shape technology have successfully been fitted to three patients in long-term clinical trials. In the most successful case the socket has been used exclusively by an active patient for over 34 months. When the socket was inspected after 20 months of use there was no sign of mechanical failure.

9. DISCUSSION

It has been shown that both SLS and adaptations of FDM technology are capable of successfully fabricating prosthetic sockets directly from 3D CAD data. These sockets are comparable in terms of comfort, strength and biometric performance to those manufactured using traditional or CAD/CAM techniques.

What has yet to be addressed is the practicality of installing and using a RP system, and the economic viability of a RP based process.

SLS is an expensive technology, both in terms of capital investment and running costs. The system is also large and requires to be housed in special facilities. It is unlikely that a prosthetic centre or hospital could justify such an investment. The alternative is to make use of a central fabrication centre or a bureau service. However, this could prove to be more expensive in the long run and also lengthen the time taken to deliver the finished socket to the patient. A full cost/benefit analysis of the SLS process is required before it can be seriously considered as an alternative to existing techniques of socket fabrication.

The FDM based technologies, Squirt Shape and the Rapid Manufacture Machine, are currently lab-based research projects and are not available as commercial systems that can be purchased by prosthetic centres. It remains to be seen if these technologies can be developed into economically competitive systems.

If RP technologies are to be adopted by the prosthetics sector then an optimised process in which all the components (3D scanner, CAD software, RP machine) are designed to compliment each other is required. Such a process must be easy to install and require minimal staff retraining. If this can be achieved and if the benefits of RP socket manufacture can be clearly demonstrated then it may well prove to be a valid alternative to current techniques.

References

1. Information and Statistics Division, The National Health Service in Scotland, *Amputee Statistical Database for the United Kingdom: 1998/99 Report*, (Crown Copyright, 2000).

2. J. Rolock and K. Tucker, *Development, Evaluation, and Use of a Computer Aided Manufacturing Technique Based on "Rapid Prototyping" Principles,* Capabilities, January 1998, Northwestern University Prosthetics Research Laboratory and Rehabilitation Engineering Research Program.

3. J.S. Rovick, R.B. Chan, R.L. Van Vorhis and D.S. Childress, *Computer-Aided Manufacturing in Prosthetics: Various Possibilities Using Industrial Equipment,* Proceedings of the Seventh World Congress of the International Society for Prosthetics and Orthotics 1992, Chicago, pp. 22.

4. D. Freeman and L. Wontorcik, *Stereolithography and Prosthetic Test Socket Manufacture: A Cost/Benefit Analysis,* Journal of Prosthetics and Orthotics 1998, Vol. 10, No. 1, pp. 17-20.

5. W.E. Rogers, R.H. Crawford, J.J. Beaman and N.E. Walsh, *Fabrication of Prosthetic Sockets by Selective Laser Sintering,* Solid Freeform Fabrication Proceedings 1991, pp. 158-163.

6. W.E. Rogers, R.H. Crawford, V.F. Faulkner and J.J. Beaman, *Fabrication of an Integrated Prosthetic Socket Using Solid Freeform Fabrication,* Proceedings of the Seventh World Congress of the International Society for Prosthetics and Orthotics 1992, Chicago, pp. 23.

7. S. Stephens, R. Crawford, W. Rogers, A. Gitter and G. Bosker, *Manufacture of Compliant Prosthesis Sockets Using Selective Laser Sintering,* Solid Freeform Fabrication Proceedings 2000, pp. 565-577.

8. B. Rogers, A. Gitter, G. Bosker, M. Faustini, M. Lokhande and R. Crawford, *Clinical Evaluation of Prosthetic Sockets Manufactured By Selective Laser Sintering,* Solid Freeform Fabrication Proceedings 2001, pp. 505-512.

9. M. Lokhande and R. H. Crawford, *Testing of Compliance in a Prosthetic Socket Fabricated Using Selective Laser Sintering,* Solid Freeform Fabrication Proceedings 2001, pp. 513-526.

10. K.C. Tan, V.S.P. Lee, K.F. Tam and S.L. Lye, *Automation of Prosthetic Socket Design and Fabrication Using Computer-Aided-Design / Computer-Aided-Engineering and Rapid Prototyping Techniques*, The First National Symposium of Prosthetics and Orthotics 1998, Singapore.

11. V.S.P. Lee, K.C. Tan, K.F. Tam and S.L. Lye, *Biomechanical Evaluation of Prosthetic Sockets Fabricated using Fused Depository Method,* The First National Symposium of Prosthetics and Orthotics 1998, Singapore.

12. K.C. Tan, V.S.P. Lee, K.F. Tam and S.L. Lye , *Development of Artificial Limbs Using Digitizer, CAD and RPT – A Case Study,* Proceedings of the CAD/CAE/CAM for Internet and Intranet Conference and Exhibition 1998, Singapore.

13. E.H. Tay, L. Liu, V.S.P Lee, K.C. Tan, P. Ng and J. Goh, *Refinement of Prosthetic Socket Fabrication Process with the FDM Technology*, Proceedings of the 9th International Manufacturing Conference 2000, China, 11, pp. 97-100.

14. P. Ng, L. Lui, V.S.P. Lee, K.C. Tan, E.H. Tay and J. Goh, *Rapid Manufacturing Machine (RMM) for Prosthetic Socket Fabrication*, Proceedings of the 10th International Conference on Biomedical Engineering 2000, Singapore, pp 417-481.

15. J.S. Rovick, *An additive Fabrication Technique for the Computer-Aided Manufacturing of Sockets,* Proceedings of the Seventh World Congress of the International Society for Prosthetics and Orthotics 1992, Chicago, pp. 24.

16. T. Wholers, *Wholers Report 2000 – Rapid Prototyping & Tooling State of the Industry Annual Worldwide Progress Report,* (Wholers Associates Inc, 2000).

Lean rapid production concept realization in the compact manufacturing system

D N SVIRSKY
CAD Centre, Vitebsk State Technological University, Republic of Belarus

ABSTRACT

In the paper the author's methodology and experience of lean production realisation in the Time-Compression Technologies area are considered. Compact Manufacturing Systems (CMS) for the Rapid Production on the laser machining base, which consists of low-cost equipment of the Reverse Engineering, CAD, Rapid Prototyping, Rapid Tooling and Manufacturing type is offered. It is a human-machine complex combining a curtailing in space and time with a minimum level of structural and resource redundancy, supported by highly intellectual tools of concurrent engineering [1]. Designing of such complex technical systems as CMS requires both simultaneous collective work and wide use of modern information technologies and computer network systems. A similar methodological approach was applied in the computer aided design research Centre at Vitebsk State Technological University. The offered lean production concept was realised by a number of CMS for small-to-media enterprises.

KEYWORDS: Time-compression technologies, rapid production, lean production, compact manufacturing system, concurrent engineering.

1. INTRODUCTION

The quick response to change of a market situation and achievement of competitive advantages requires a strategy of maximum increase of production variety within existing limitations of resources in the manufacturing framework. The known structural, morphological and space-temporary redundancy of traditional manufacturing systems causes not only quick response to change of the orders stream but also (in some more greater degree) high cost of creation and operation of manufacturing systems. The attempts of essential lowering expenses of the equipment of the manufacturing system have resulted in the "Lean Production" concept.

The determination of productivity as a ratio of the price of the realised production and its manufacturing cost should be a basic criterion of an estimation of production efficiency (and technological process in particular). The disappearance of a parameter of the time from a parameter of productivity is apparent, as it is estimated through a parameter of a rate of turnover of the reduction means at a production sale of under the settlement prices. The major principle of creation of effective technical systems – sub-optimisation is important too. In our case it means that best productivity should be achieved not by manufacture of one type of the product (or in general, one product absolutely), but of all products which are included in the release program.

The industrial system can be presented as " a black box " with output variable **Y** (production); an entry variable **X** (resources) and uncontrolled effects or disturbance **f** (changes of the orders stream). Examining thus CMS as the object of a control it is possible to apply a known method of control with disturbance compensation. It requires that in a control system the special disturbance compensating function - the equalizer is added (Figure 1).

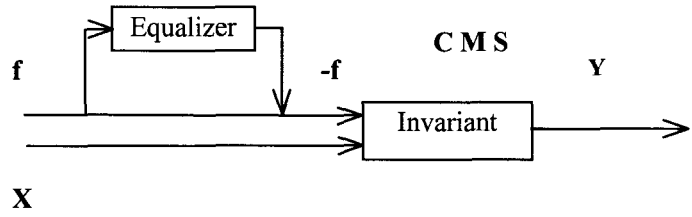

Figure 1: The CMS cybernetic model

The modern theory of invariance allows the determination of the conditions of independence (invariance) of the output variable **Y** from the disrupting effects **f**, by the addition to the industrial system of the equalizer, in which the disturbance **f** will be transformed in **-f** and effects on CMS. So the compensation turns out [2], since $\mathbf{f} - \mathbf{f} = \mathbf{0}$. In result, despite the constant order stream change, the main (invariant) CMS part functions in a stable (given) mode of greatest efficiency. So the CMS structure consists only of two functional, structural and space isolated units: an invariant and an adapter (equalizer). The second of these consists of compensating (adapting) functions-technologies. The existence in the system organization of the invariant and adapting components is characteristic of all levels of CMS hierarchical structure. At an organizational level the inverse form of market research adapts an existing configuration of the industrial system (as invariant) for the usual conjuncture of the market. At a functional and technological level quasi-optimal technological processes adapt an available CMS equipment complex (invariant) for production, from which manufacture is theoretically profitable. At a structural and arrangement CMS level, for example, with operation of an automatic line for moulding or punching, the system of the changeable manufacturing equipment adapts the high-efficiency specialized equipment (invariant) to change in a configuration of products. In technological complexes (Rapid prototyping systems etc.) the function of the adapter is executed by a computer in relation to a universal program to control process equipment (invariant) realizing high technologies.

During the design of technological process for a given nomenclature of production (with careful preliminary selection of products for manufacture on economic preferences) it is necessary first of all to determine both the most effective method of form creation and physical technical effect allowing this production. The tentative estimation of methods for form creation shows that all of them can be divided to be made into two essentially different groups. The first group consists of methods ensuring manufacturing of details with the help of "level-by-level synthesis". In this case the formation of surfaces of the detail is carried out consistently from section to section. In particular cinematic or layering methods of traditional machining just concern to this group. The "level-by-level synthesis" methods are rather universal but have the lowest temporary and price productivity. The second group includes "shell-cover" methods of the simultaneous creation of all detail surfaces (and detail "body" if it is necessary). The punching and moulding processes fit in just this group. Manufacture of detail by such methods has highest temporary and lowest price productivity under small-lot manufacture conditions. Then it is necessary to establish the most suitable (by the degree of scope of a given product spectrum) invariant of the process equipment for a technological process. Also, it is necessary, to achieve "non-redundancy" to make or to get a set of the adapters allowing the whole production nomenclature to be made.

2. PRINCIPLES OF COMPACT MANUFACTURE

The creation of such efficient manufacture is based on maintenance of various aspects of its **compactness**. The basic parameter of the enterprise operation is **financial** compactness, which means the low cost of a highly effective manufacturing process. In this case it is necessary to use CMS, which should have the appropriate parameters:

- **functional** compactness means effective performance of the most difficult and labour-consuming operations through automated equipment. Other necessary actions are carried out manually (to reduce the pay-back values);
- **temporary** compactness provides high efficiency and mobility of the design and technological operations and that in turn provides essential reduction of the production cycle from order reception to its execution (reduction of the pay-back period);

- **spatial** compactness is achieved by the small dimensions of the basic process equipment and results in reduction of the required area for the production zone (reduction of expenses of buildings and structures or rent);
- **information** compactness results in a reduction in expense of design and technological preparation for manufacture by the application of "paperless" technology based on standard programs and technical maintenance (reduction of turnaround means with a rather low level of capital expenses).

To achieve these aspects, compact manufacturing organisation general methodology is based on seven main principles: I) conformity of the structure of CMS to its purpose; II) localisation of the functional invariant; III) recursive decomposition of CMS hierarchical structure; IV) functional sufficiency of the CMS components; V) optimal parity of expenses of the functional invariant and variable adapter; VI) evolutionary local change of the structure of CMS at the expense of the equaliser adaptive reorganisation; VII) reflection of stages of system development in its structural components.

The principle (I) in the concentrated form expresses that, first, the purpose (Z) is the main creation factor; secondly, the object in view can be achieved to some extent by creation and/or use of a set of the CMS structure {St}; thirdly, the achievement of the objective is carried out by the selected CMS structure by means of the execution of hierarchically organised functions (F):

$$Z \Rightarrow \{F\} \Rightarrow \{St\} \tag{1}$$

The principle (II) allows on the basis of principle (I) separate common essential (invariant) units of the multipurpose CMS purposes objectives, functions and structures sets:

$$\text{Inv}\ \{Z\} \Rightarrow \text{Inv}\ \{F\} \Rightarrow \text{Inv}\ \{St\} \tag{2}$$

The principle (III) provides the presence of invariant and adaptive modules at each level of hierarchy of the structure of the system:

$$St\ (CMS) = \bigcup_{i=1}^{N} \text{Inv}_i \cup \text{adp}_N \tag{3}$$

The principle (IV) regulates a degree of parametric implementation of any hierarchy level functions above the necessary minimum value for CMS purpose achievement, since any exceeding of this value results in an unjustified increase in expenses of CMS creation and maintenance:

$$L_f = [L_f] \Rightarrow L_E = L_{E\,opt} \tag{4}$$

The principle (V) determines the best variant of the allocation of resources at the implementation of the constant and variable parts of the CMS according to their functional importance:

$$\frac{L_3\,(\text{Inv})}{L_3\,(\text{adp})} = \frac{R\,F_{inv}}{R\,F_{adp}} \tag{5}$$

The principle (VI) of the evolutionary approach to the development and modernisation decisions for the CMS permits permanent structural adaptation of the CMS to varied external conditions:

$$St\ (CMS)_0 \Rightarrow St\ (CMS)_1 \Rightarrow \ldots \Rightarrow St\ (CMS)_T \tag{6}$$

The principle (VII) together with a principle (VI) determines CMS structure at each given moment of its functioning time:

$$f: [St\ (CMS)_0 \Rightarrow \ldots \Rightarrow St\ (CMS)_T] \rightarrow St\ (CMS)_T \tag{7}$$

The process of creation of CMS as complex technical systems consists of three main stages [3]: CMS macro-design; CMS structural and parametric synthesis; CMS adaptive structural adjustment (Figure 2).

The macro-designing stage includes marketing and CMS macro-technical shape creation. The task of market research is the definition of the nomenclature of production of CMS normal (profitable) operation during the design period. The search of potentially profitable production is carried out by finding "areas of activity" in the space of economic activity and forecasting the dynamics of their change.

As a result of primary analysis of the market on the basis of different information sources some set of the goods, which production probability will be highly profitable is established during the design period. The capacity of target segments of the market is predicted simultaneously.

The selected sorts of production are analyzed with the purpose of definition of a degree of their technological generality. The standard technological processes of their manufacture are compared (Figure 3). The importance of a technological generality is expedient for estimating, with the help of the relative given expenses, an operation:

$$K = C_{Mi} t_i / \sum (C_{Mi} t_i),$$

C_{Mi} - given minute expenses for operation, t_i - absolute duration of operation.

I. CMS MACROSTRUCTURAL SYNTHESIS

I.1. CMS structure formation

1. Search of areas of activity in the whole space of economic activity.
2. Analysis of character and prospects of that activity (fast or slow growth or recession).
3. Definition of a set of potentially favorable production (products and services).

I.2. CMS technical shape formation.

4. Search of typical technological processes of manufacture for the selected kinds of production.
5. Analysis of a degree of similarity of structure of typical technological processes of manufacturing of different kinds of production.
6. Formation of competing sets of production.
7. Choice of the best set of production.
8. CMS industrial program formation.

II. CMS STRUCTURAL SYNTHESIS

9. Planning organizational structure of generalized technological processes and CMS.
10. Allocation of CMS technical means functional invariant.
11. Optimization of technical parameters of the CMS process equipment invariant (base).
12. Analysis of dynamics of the adapter structure change in a complex of CMS technical means.
13. Optimization of functional and technical parameters of the CMS process equipment.

III. ADAPTIVE STRUCTURAL ADJUSTMENT

14. Market conjuncture operative monitoring.
15. Reconstruction of the adapter of CMS technical means.

Figure 2: The integrated algorithm of CMS structural synthesis

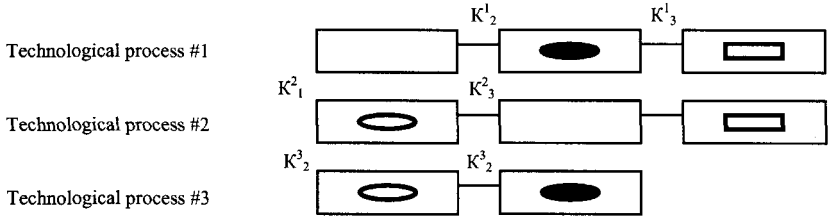

Figure 3: The invariant components of technological processes

The secondary analysis of the market will be carried out with the purpose of creation of the best set connected (by technological invariants) types of production. The CMS profile thus is formed. At the last stage of the macro design the CMS general specification is formed.

The structural synthesis is carried out on the basis of the earlier considered principles of CMS creation and the use of the results of the previous design stage. The structure of the CMS equipment complex has clearly expressed its modular character. During the process of choice of CMS equipment the problem of parametric synthesis is solved. The numerical values of parameters nominals are determined by functional-cost analysis of the whole system.

After CMS definition in operation the process of its design continues in form of refinement so that as the varying conditions of the external (market) environment make necessary adaptive structural adjustment of the industrial system this can be included. The procedures of the third design stage in general repeat the first two stages, however their results carry more local character, being limited by changes of structure and parameters of the adapter, not the technological invariant unit. During CMS operation information on the parity functional and cost parameters of the invariant and adaptive units is stored. It allows a more precise selection of the best parity between expenses and the implementation of CMS functional units with the help of principle (VII).

3. CMS CONCURRENT DESIGNING

Designing of such complex technical systems as CMS requires the simultaneous work of a large collective. The acceptance of agreed solutions usually increases common project operating time owing to the realization of various procedures on coordination of shared intellectual efforts and integration of individual solutions. In this situation the problem of the design process productivity rise without loss of quality of design is solved by the wide use of modern information technologies and computer network systems. The participants of design conferences working in dialogue using computers which have access in real time to anyone for necessary information and program resources and also the possibility of dialogue with colleagues both inside and outside of the design collective. For intensification of processes of thinking and information interchange it is possible to use associative units (basic psychological images). Such possibilities are made available by hypermedia technology which allows communication not only by word but also the possibility to store files of any type of data (figures, sounds). There is the possibility of simple and reliable connection with each other of data items irrespective of their format, that is especially important with creation and use of design databases. The participants of collective design are joined by a local network and have access to the global network. Many procedures such as search, collection and preliminary analysis of commercial information and formal forecasting at a market research stage, search of standard technological processes, primary grouping (classification) of production is simple to carry out with the help agent-based systems. The intellectual agent will form the active information filter connecting the global network with a local network of collective design. A similar methodological approach was applied in the CAD Research Centre at Vitebsk State Technological University. Nowadays the employees of the Centre develop a compact system of new products for light industry manufacturing. They already had success in creating CMS for Rapid Production and its subsystems such as Reverse Engineering and Rapid Tooling in Concurrent Design.

4. CMS REALISATION

A CMS based on laser machining for Rapid Production consists of automated equipment of the CAD, Rapid Prototyping, Rapid Tooling and Manufacturing types (Figure 4). A proving of the object of manufacture unification on the basis of the complex application of two groups of technological methods results in creation of an integral compact manufacturing system, which consists of adaptive and invariant modules. The adapter realises a "level-by-level synthesis" method. The technological invariant provides final production manufacture by "shell-cover" methods. Thus the basic practical task of the developers is the definition of the methods of designing and manufacturing of cheap expendable adapters [4].

The lean CMS for small-lot Rapid Production consists of a Reverse Engineering subsystem (Figure 5), which supplies a Circulation subsystem (for example sheet-stamping press) with necessary cheap adapters (dies). The structural adaptation of such an industrial system to change in a market is carried out by programmed adjustment of the Rapid Tooling subsystem on a CNC controlled laser set-up base (Figure 6) as an adaptive component of an in-line technological complex of the whole Rapid Production system.

Structure of the laser machining subsystem consists of:

- CO_2-laser (power consumption 800 W);
- The optical channel;
- Control system (personal computer), for direct conversion of graphics information (standard file of graphics exchange) in co-ordinate desktop control signals;
- Co-ordinate desktop.

The system has the following technological parameters:

- Processed materials: plastics, wood, textiles, natural and artificial leather;
- Overall dimensions of products — Up to 1700 x 1200 mm;
- Thickness of source material — Up to 20 mm;
- Technological accuracy — Up to 0.05 mm;
- Technological speed — Up to 24 m/min;
- Overall dimensions of installation — 3000 x 2000 mm.

Use of a universal laser, is easily adapted to order stream changes of a program-technical complex nature (on the basis of the personal computer), allows the manufacture of a wide range of industrial products (Table 1).

The application of the laser CMS for manufacturing of complex 2D, 2.5D and 3D objects for machine-building, light and other industries allows a sharp reduction (up to 5 ... 8 times) cost and design time and technological preparation for competitive product manufacture.

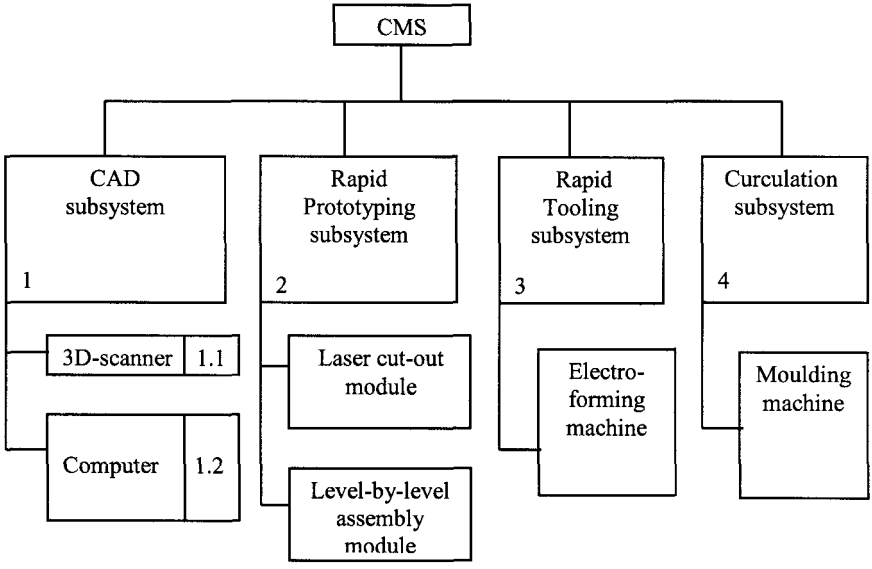

Figure 4: Structure of CMS for Rapid Production

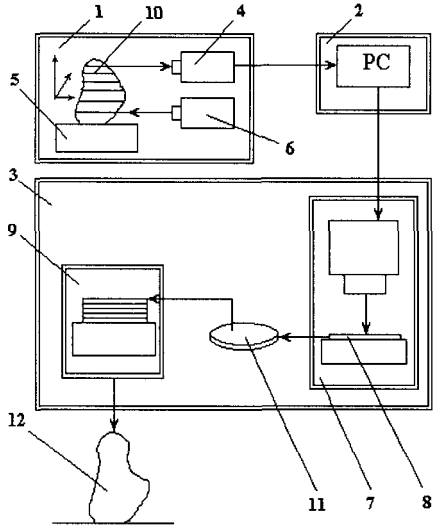

1 - the information input module; 2 - the information processing module; 3 - the industrial module; 4 - a video camera; 5 - a co-ordinate table; 6 - a projector; 7 - a laser cutting installation; 8 - cut material; 9 - an assembly unit; 10 – an initial (analogue) object; 11 - a cut-out layer; 12 - a completed object (die).

Figure 5: A compact reverse engineering subsystem configuration

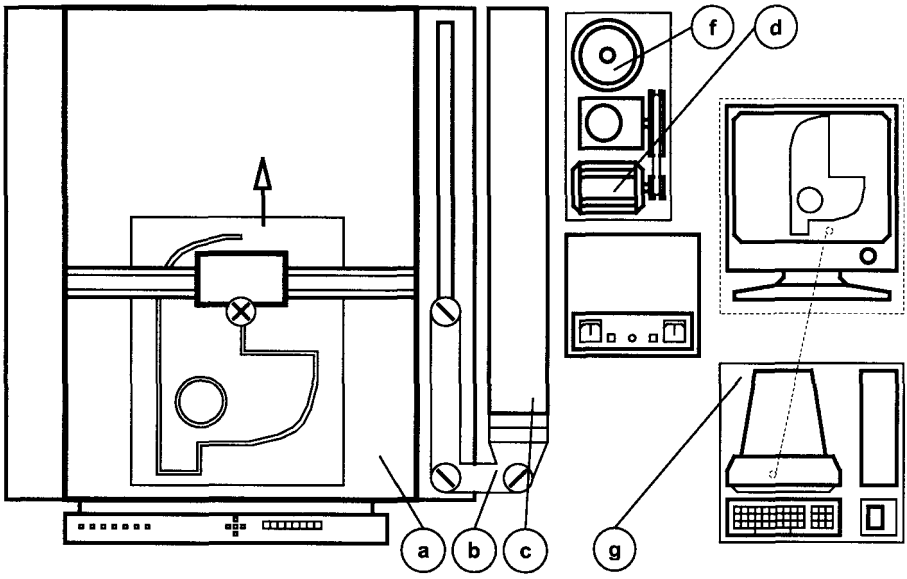

a) - a co-ordinate table, b) - an optical system, c) - CO_2-laser, d) - a cooling system, f) - an air-flow system, g) - a control system; the system of ventilation and clearing is not shown.

Figure 6: CO_2-laser cutting subsystem

The products type		The products sort	Industry or other sphere of activity
Plane		Patterns, templates	Tailoring, foot-wear, dry goods
		Incrustation	Furniture, art
		Layings	Repair firms, shop
Relief		Signboards,	Art, advertising
		Stamps	Graphic arts, dry goods
Volumetric	Modular	Special furniture	Furniture
		Exhibition stands	Advertising, design
	Shell	Components for sport vessel and airframe	Sport, tourism
	Continuous	Foundry models	Casting
		Matrixes, form	Products from plastic and ceramics production
		Stamps	Pilot production
		Models, card	Cartography, training appliance

Table 1: Laser CMS application area

5. CONCLUSION

The contradiction between consumers desire to receive original goods and manufacturers desire to make identical products results in market overflow by cheap but unattractive goods and expensive exclusive

production. In these conditions essential attempts to lower expenses of the manufacturing system have resulted in the "Compact Production" concept. The compact manufacturing system design process is based on allocation of a constructive invariant in a diverse production set and its transformation by the technological invariant of the laser based Rapid Manufacture subsystem.

References

1. Svirsky D., *Annals of DAAAM for 2000*, Vienna, 2000, pp. 455-456.
2. Svirsky D.N., *Proc. 8th IFAC Symp. on computer aided control systems design*, Salford, 2000.
3. Svirsky D., *Communications*, 2000, 1, pp. 51-56.
4. Svirsky D, *Proc. Int. conf. on advances in production engineering,* Warsaw, 2001, part 2, pp. 119-128.

This page intentionally left blank

Reducing the uncertainty of the prototyping decision

K A M STEELE, G J RYDER, W J ION, and **A I THOMSON**
Rapid Design and Manufacture Centre, University of Strathclyde, Glasgow, UK

ABSTRACT

As RP technologies have evolved, it has become clear that an RP system can no longer be used in isolation within any given situation, rather; each particular technology requires to be combined with either a secondary finishing technique, or be "chained" with a Rapid Tooling technology. This leads to uncertainty as to which technologies are compatible with each other. By reviewing existing RP selection systems, and by presenting three industrial case studies, this paper concludes that the success of a RP process chain selection decision is dependent on three factors; firstly any selection system must accurately represent the requirements specification of the prototype, that the knowledge base of a selection system contain two critical elements, and thirdly, commercial influences within a company have a bearing on how RP is utilised. This paper proposes a model on how a prototyping decision should be structured, and what lessons need to be learned in future selection systems.

KEYWORDS: Selection, Methodology, Knowledge, Prototyping, Chain

1. INTRODUCTION

It is a well known fact that organisations engaged in the area of engineering design can profit substantially from the benefits arising from the application of Rapid Prototyping (RP) technology. However, since the introduction of the early systems such as Stereolithography (1987), Fused Deposition Modelling (1990), and Selective Laser Sintering (1992), the number of different RP systems available to industry has increased almost tenfold in the last ten years. This has presented a new problem to the designer, namely which technology to use in a given situation. This problem is compounded when one considers the proliferation of different new materials, post-processing options and Rapid Tooling (RT) techniques that have emerged to complement RP. Since 1994, a number of studies have been carried out into the development of methodologies, decision support techniques and software tools for assisting the RP user in selecting the correct technology, or combination of technologies.

2. BACKGROUND

The notion of designing systems to assist in decision-making support within RP is not new, and the problem has been tackled in the past at a number of different levels. It can be seen that three basic approaches to the selection of RP / RT techniques have evolved over the past seven years. These can be classified as follows:

- RP Process Planning methodologies
- Simple RP selection Knowledge Based Expert Systems (KBES)'s
- Selection Methodologies
- Rapid Prototyping Process Chain Selectors

The first of these classifications is mainly concerned with the planning of build orientation, layer thickness and other set variables peculiar to each individual RP technology, therefore will not be covered here. However, early studies focused on the development of expert systems that made use of a rule base of individual RP system capabilities to evaluate the options available to the designer. The typical model rule base would be stored within a relational database application, and the user would input a set of criteria (e.g. model dimensions, wall thickness, model purpose, size envelope, required mechanical properties etc.) that the resulting model would require to meet. The system would then interrogate the rule base to suggest the most suitable technology (or technologies) for manufacturing the model, and perhaps, the most suitable material. Examples of such systems include the knowledge-based systems developed by *Narayanan et al, Muller, Bauer et al, Jones and Campbell,* and the web based systems developed by Helsinki University of Technology. [1] [2] [3] [4]

Other approaches include the RP Advisor system developed at Arizona State University by *Phillipson,* which used Quality Function Deployment to identify those requirements that were most important and relevant to the

model (in this case, speed, cost and quality). [5] Various mathematical relations based on multi-criteria optimisation were then developed to find the most suitable prototyping process for the model in question.

2.1 Process chain selection methodologies

Early studies into RP process selection looked at just Rapid Prototyping in isolation, neglecting the fact that parts produced by the vast majority of layered manufacture systems are seldom useable in their raw state without some form of post processing being required. This may take the form of simple post curing and finishing (in the case of SLA), through to wax or polymer infiltration (in the case of 3D Printing). A tertiary process may also be necessary for those wishing to form an injection moulding tool from the RP master. This has given rise to the term "Rapid Prototyping Process Chain" (RPPC). An example of the RPPC concept is shown below.

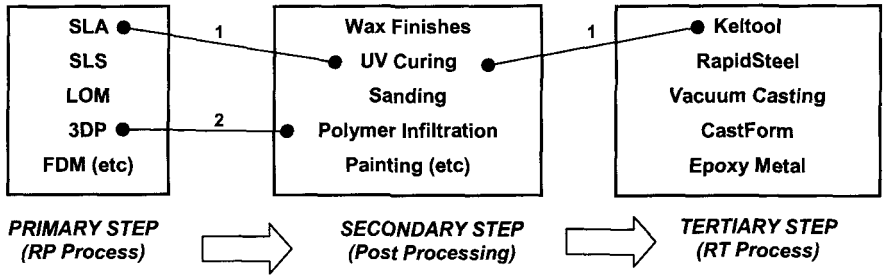

Figure 1: The Rapid Prototyping Process Chain (RPPC) Concept

Typically, an RPPC will involve anything up to three individual steps, depending on the desired physical characteristic of the prototype. For instance, a concept model may be manufactured in 3D printing and infiltrated using a polymer, thus only requiring a primary and secondary step, while a fully functional part may be fabricated using Stereolithography, followed up by post-curing and the Keltool Rapid Tooling process, therefore requiring a three step process chain. More recent studies have concentrated on developing selection methodologies and software tools that are geared towards the design and selection of an RPPC. Examples of these include the EU funded RAPTEC project, which developed a weighted rating system to take into account corporate opinion, and environmental, physical and functional factors associated with producing a prototype. [6] By combining these ratings with the known capabilities of each process, the designer can, in theory, assess the suitability of different process chains relative to each other. Another approach was typified by the PROTOOL system, which was developed at the University of Chemnitz. [7] [8] This is done through the means of a rule base/expert system approach as used in the systems described earlier. The user enters in general requirements of the model, and the rule base narrows the field down to a smaller, more manageable number of process chains. In a second step, using more detailed questioning in conjunction with a "weighted objectives" method, the key decision variables (identified as cost, time and quality as in the Phillipson system described above) are aggregated to give a breakdown of the suitability for the remaining process chains in relation to the purpose of the prototype in question.

The next stage in RPPC selection methodologies is the development of systems that can automatically configure process chains. By the end of the 1990's, two systems had emerged, the first having been developed by *Bernard, Deglin et al*, primarily a knowledge based system which used a combination of case-based reasoning and examining the compatible inputs-outputs of the primary, secondary and tertiary steps of a process chain in order to arrive at a solution (known as the "bottom-up" generation of processes. [9] [10] [11] The second was completed by *Dreher et al* as part of an integrated engineering decision support system known as iVIP, and again, was largely a rule-based system. [12]

2.2 Existing selection systems - summary

The general themes that have come out of analysis of the various selection systems is that the generally acceptable form for structuring knowledge has been to place the information about RP processes and materials

into a relational database. It should be noted however, that most of these systems have, to date, only been trialled using a small number of different possible RP processes and materials within their databases. The number of possible combinations could easily escalate to numbers in the order of 30,000; and this does perhaps throw the stability of a selection system into question.

The RAPTEC and PROTOOL systems have only been tested using a tiny number of process chains. The iVIP system would appear to be the most advanced RPPC selector yet developed, claiming to be capable of selection of any process chain – but considering that it appears to rely solely on a rule-based expert system to arrive at a solution, doubt is cast over its reliability when one considers the unexpected scenarios which may arise in a design problem, and examples of this will be detailed in the case studies. For this reason, a case-based reasoning approach would have to be an essential requirement in an automatic selection methodology. Another important factor to consider is that many selection systems, having already established that time, cost and quality are the three most important variable rely on subjective judgements on the likely costs of a process. Where an RP model is being made by a service bureau, it is very difficult to ascertain an exact breakdown of the costs involved without an intimate knowledge of the exact material, build style, machine model used etc. This is also linked to the point that while some of the aforementioned systems incorporate a direct link to the original CAD data, most rely on the user manually entering in the prototype requirements. As will be seen in the case studies, this approach can lead to key information being omitted from the model specification, resulting in waste.

3 CASE STUDIES

3.1 Case study 1: Instrumentation enclosures

This case study centres on a US-owned multinational manufacturer of specialist test and measuring equipment, and principally, its Scottish manufacturing base. It is particularly unique as it is the only manufacturing company in Scotland with its own in-house RP facility – a Z-Corp 3D printing machine. The machine was purchased in early 2000 to assist in the development of a particular product family that the company was intending to introduce.

Their use of RP is being spearheaded by a small group of engineers within the manufacturing function. After numerous consultations with various RP centres, and attendance at conferences, the company has developed the following process chain:

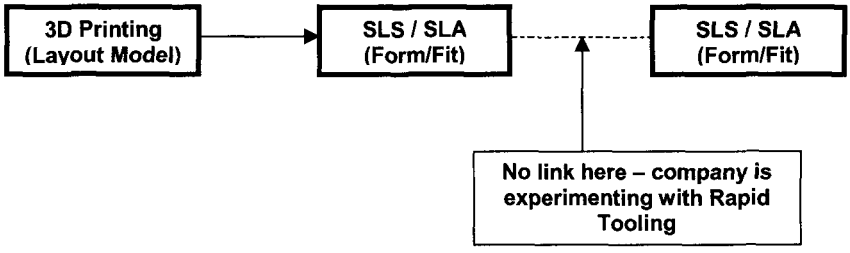

Figure 2: Rapid Prototyping Process Chain used within the instrumentation manufacturer

As can be seen, the company uses their own 3D Printing resource as a means of manufacturing models for both marketing and developing the product's overall architecture (i.e. the layout of external controls and interior circuit boards and other componentry. As a second step, the company will then use a stereolithography master to produce a vacuum casting mould. Prototype parts for the casing are then manufactured in polyurethane material using vacuum casting in order to assess the form and fit characteristics of the components. Increasingly, the company is also using SLS models for this purpose.

When questioned about the likely barriers towards RP adoption within the company, the manufacturing group concluded that accuracy and time were the key drivers in their prototyping decision. Cost was largely

insignificant, although one important observation was made in that the speed at which RP models were turned around by outside contractors exposed inefficiencies within the procurement systems in place within the company. Typically, there was a time lag of approximately one week between an order to an RP service bureau being placed and the actual delivery of the completed model, potentially erasing any time advantage in using RP in the first place. To remedy this problem, the engineers concerned regularly bypass the official procurement route, much to the disdain of the procurement section of the company. Other problems that arose in the company surrounded the acceptance of the 3D Printer as an in-house facility. For example, it was discovered that other design groups within the company are reluctant to use the machine, and appear to suffer from a "better the devil you know" syndrome, in going to technologies that they already have experience with, regardless of whether another technology may be more suitable.

3.2 Case study 2: Water control valve

This is a small company, based in the south side of Glasgow manufacturing both mainstream plastic plumbing products, from the familiar white plastic waste fittings to the specialised chrome plated shower and bath fittings for foreign markets. Typically, the specialised products are manufactured in the Far East, based on CAD data generated in-house. Traditionally, specialised metal fittings, which needed to be cast, would typically go through an expensive build-test-scrap-rework development cycle. A tool would be manufactured, in order to produce test prototypes. If the prototype did not perform to the required standards, then it was a case of altering the design and re-fabricating another tool. In an attempt to reduce the significant costs involved through developing a new product in this way, the company wished to utilise Rapid Prototyping within the RDM Centre in order to develop a control valve assembly for a new product they were intending to introduce. FDM was chosen as the preferred technology as the company wished to perform form and fit studies on the model in addition to water flowrate tests. A quick solution had to be found, and this took the form of immersing the completed FDM parts in a hot wax, which had the effect of sealing up the voids within the part, giving it waterproof properties. In manufacturing the prototype using this method, the company was able to experiment with different designs until the optimum solution was found. It also allowed several alternative versions of the control valve to be evaluated, meaning that the designers could experiment with different handle sizes, thread lengths and assembly configurations before the final commitment to production was made. The key difference within this company as far as RP adoption is concerned is that the decision to use RP came from the higher management of the company. Therefore there were no organisational barriers to overcome. This made for a relatively trouble-free implementation of RP technology within the company. Unfortunately, no data exists for the key requirements that the company sees as being the most influential in a RP decision, but preliminary deduction illustrated that cost is not a consideration here, and instead functionality is clearly the preference.

3.3 Case study 3: Mobile phone antenna frame

This company is a major Original Equipment Manufacturer (OEM) to the mobile phone industry, designing and manufacturing custom antennae, and in the summer of 2000, it was in a position where there was a requirement to tender for a new internal aerial design. The company came up with square shaped frame around which a coil was wrapped. For the original design, the company wanted to manufacture a prototype of the design for the purpose of the tender. The first process chain that the company attempted was to use 3D Printing to manufacture the prototype. Subsequent radio frequency tests were carried out on the prototype, and it was found that the dielectric strength of the 3DP material (gypsum) was adversely affecting the reception characteristics of the antenna. A second attempt was made by the company to prototype the antenna, and after using ABS plastic as the build material using FDM, the antenna worked successfully, and enabled the company to successfully tender for the contract.

3.4 Case studies: Conclusions

Several important themes can be drawn from analysis of the case studies, principally: that in most cases, cost is not a primary consideration within the prototyping decision. Instead, the most important requirements appear to be in the area of the overall functionality and technical characteristics of the resulting prototype. In a small questionnaire survey carried out among fifteen companies who had models built locally within the RDM Centre, it was found that the most important factor of using an RP model was not the direct costs associated with using the technology, but instead was the ability to visualise early in the design process. When asked about the uses of the models in question, it was found that three quarters of the respondents used the models for showing to

person's outwith the research and development team. This brings with it the conclusion that once again, functional characteristics of the model are of greater importance. Another point is that in Case Studies 2 & 3, it was shown that the prototyping decision was clouded by the appearance of special requirements such as dielectric strength and the ability to be waterproof. This has exposed two key weaknesses with existing RPPC selection systems, chiefly that:

- Form based interfaces with the selection system are inadequate in that they promote "tunnel vision" to the engineer, and force him not to look beyond the requirements that are on the form. Therefore situations such as the ones described above would have been easily missed.
- It would appear from the likelihood of so-called "special cases" (as those mentioned above), that the use of a CBR approach is an essential feature of any RPPC selection system.

Finally, the case studies have exposed the fact that commercial, and organisational factors have a large bearing on the outcome of the prototyping decision. Firstly, in comparing Case Studies 1 & 2, it can be concluded that the likelihood of RP adoption is highly dependent on which level of the company the initial impetus to use the technology comes from. In the first case, company wide adoption was hampered by the fact that the RP adopters were a small band of visionaries struggling against a bureaucratic framework for purchasing and procurement, while in the second case, RP was adopted instantly by the higher management of the company. Therefore, it could be argued that the uncertainty of the prototyping decision is increased by organisational factors, leading to the conclusion that an RPPC selection system cannot ignore the influence that they have.

4 GENERAL DISCUSSION

While it has already been shown through earlier literature studies, that the whole question of developing Rapid Prototyping selection systems has evolved in a natural manner – progressing from simple expert systems to the point where there are systems that can actively make the links between RP, RT and their associated materials – the Process Chain concept. The case studies have revealed weaknesses in existing approaches, principally the lack of ability to clearly identify and enter prototype requirements, and an ignorance towards the effect of organisational influences.

However, it is worth noting at this stage that very few RP system selectors have made the transition into industry, and part of this is down to the question of developing a reliable methodology to accurately select an RPPC depends on the formation of a suitable model and system architecture.

From the iViP and CAPP systems, it has already been proven that the technology to automatically configure RPPC's using a knowledge/rule-based approach already exists. And in the case of CAPP, and the PROTOOL systems, it can also be concluded that the practice of using case based reasoning (CBR) in conjunction with a rule base for narrowing down the range of alternatives is well established. As the case studies have demonstrated, a successful RPPC selector would have to be aware of the novel, combinations of RP system and post-processing method. A method based on the use of a database of case studies would appear to be the most efficient way of doing this, even though such a database would have to contain a substantial body of historical knowledge, and would have to be able to be readily updated. This is additional to the commonly held view among system developers that the rule base of process and material capabilities itself needs to be large and readily updateable.

More significant however, is the fact that functional requirements are largely the most important factors in determining the nature of a prototype model of a product. The cases have shown that existing methods of eliciting prototype requirements for an automatic decision support system in many situations, have no value, and what is required is a more reliable means of gleaning and stating prototype requirements before the intricacies of how a Process Chain is configured are even tackled. Clearly, one route is to bypass the human element, and provide a direct link to the CAD data – and indeed some systems already use this technique, but ultimately this will only provide a detailed insight into the overall topology of the part in question. Moreover, the cases have demonstrated that commercial and organisational factors have a bearing on how RPPC's are used efficiently, and if time and cost are only peripheral influences on the prototyping decision – then there still must be some way of taking these factors into account when making that decision.

Figure 3 shows a suggested means on how the prototyping decision could be structured.

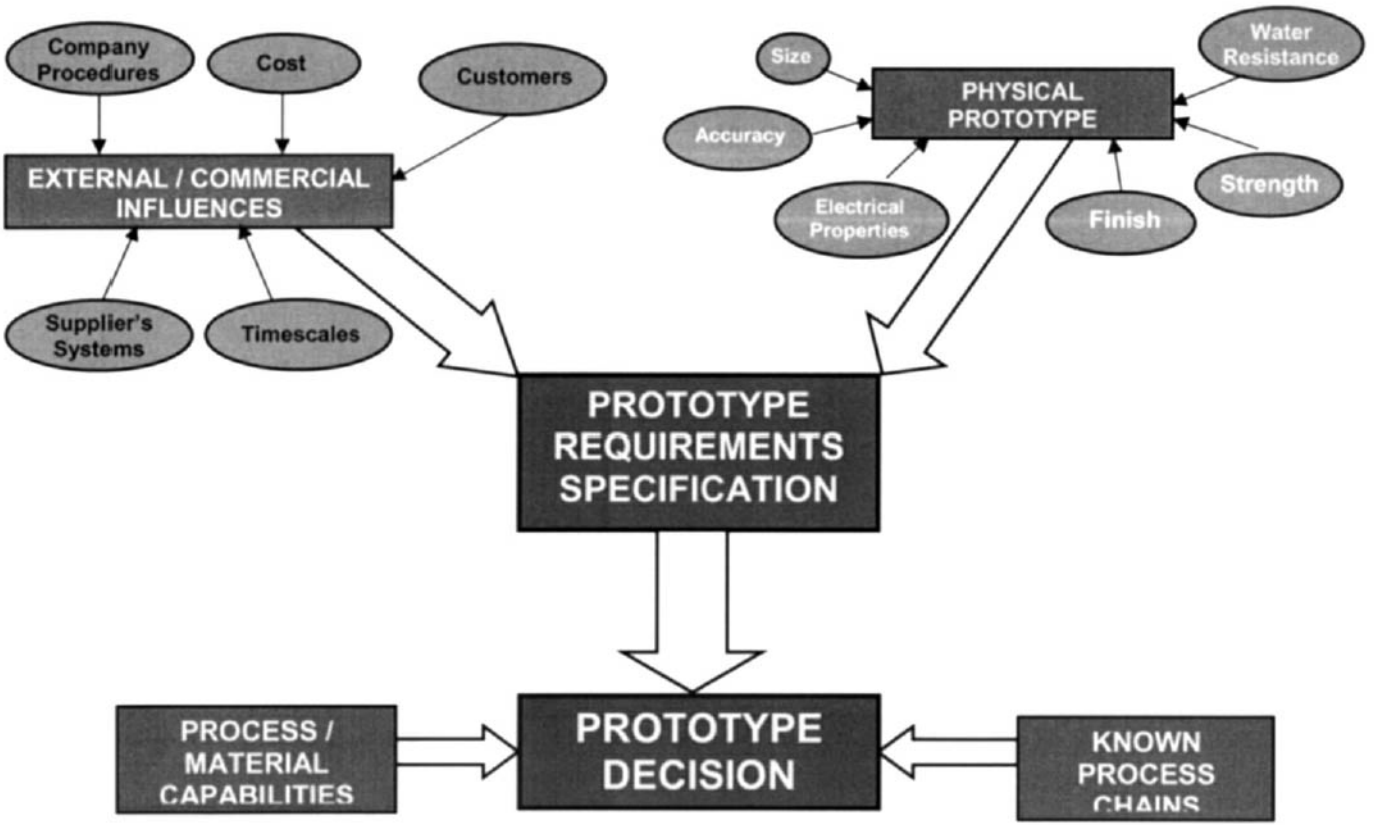

Figure 3: Model for the Modelling of the Prototyping Process Chain Decision

4.1 Description of the model

As can be seen, the two key inputs in the prototyping decision can be grouped together as "Physical Prototype Requirements" and "External/Commercial Influences". Referring back to the review of existing prototyping selection systems – it can be said the former of these two groupings is the equivalent of "Quality", while the latter encapsulates "Cost" and "Time". With regard to quality, here the assumption is made that quality is defined as how well the prototype adheres to the initial starting requirements, therefore the physical characteristics will ultimately define what would commonly be defined as quality.

What is missing is how these two broad based bands come together to form what has been defined as a "Prototype Requirements Definition". The key problem is how to formulate reliable means of taking largely subjective and qualitative data such as:

- The function and uses of the prototype
- The nature of the industry and the product it will be used within
- Company constraints that may affect the outcome prototyping decision
- The likely personnel who will see and/or use the model

Quantitative data such as required strength, accuracy and size envelope are directly compatible with existing selection systems due to their numeric nature. Processing this data is not a problem, because it is directly compatible with the existing knowledge on the capabilities of both RP and RT technologies and their materials, which is largely of a numeric nature. On the other hand qualitative information is harder to process, and this therefore would require a technique such as Quality Function Deployment to generate possible variables for prototype selection.

The final stage of the decision is to use this specification to generate a prototype. As was mentioned above, this requires a two-stage selection system, based on both existing knowledge of processes and materials, and detailed case studies where a process chain has been developed to fulfil a given set of requirements.

5 CONCLUSION AND RECOMMENDATIONS

It has been found, through the analysis of case studies that the functional characteristics of a prototype have a greater bearing on its final configuration rather than either its cost or its time-to-manufacture. It has also been found that existing RP process chain selection systems are flawed in the sense that the means that they elicit knowledge from the user in a way that can in some cases, fail to take into account of all physical requirements of the prototype. It has also been found that some means should be incorporated into these systems to recognise that the external commercial, and internal organisational constraints on a company has an influence on the way in which prototyping is carried out.

However, what can also be said, is that it would appear logical to select or configure an RPPC using a combination of both hard numerical data on process capability, and also on historical data relating to successful use of a novel or new RPPC, and the latest selection systems do indeed achieve this goal, at least in part.

However, an effective decision can only be taken however with a reliable means of combining known quantitative physical requirements, quantifying subjective data such as knowledge of case studies, industry sector organisational constraints and product function, and combining these in a way that formulates a Prototype Requirements Definition that can be understood by the latest generation of Process Chain selection systems. An adaptation of Quality Function Deployment is one possible method of achieving this.

References

1. Venkataraman Narayanan, Chua Chee Kai and Bernard Ang, "A Selection Expert System for Solid Freeform Manufactuirng", Proceedings of ICCIM '95, Second International Conference on Computer Integrated Manufactuing, pp 1416-1423, 11 - 14 July 1995, Singapore.
2. Muller, H, Bauer, & H-H Klingenberg, "Computer Based Rapid Prototyping System Selection and Support", published by Bremen Institute of Industrial Technology and Applied Work Science, 1996, http://www.biba.uni-bremen.de/groups/rp/rptsel_e.html

3. Jones, K.G., Campbell R. I., "Rapid Prototyping Decision Support System", Proceedings of the Solid Freeform Fabrication Symposium, pp 551-558, 11 – 13 August 1997, Austin, Texas
4. Muller, D, Joppe M, & Meier, I.R; "RP Workbench – Continuous Visual and Interactive Data Preparation for RP-Processes", Proceedings of the IASTED International Conference, Computer Graphics and Imaging, October 2-27, 1999 Palm Springs, California
5. Phillipson, D.K, Henderson, M.R; " Rapid Prototyping Machine Selection Programme", Proceedings of the 6th European Conference on Rapid Prototyping and Tooling, pp 291-303, July 1997, Nottingham, UK.
6. Muller, H, & Schimmel, A.; " The Decision Dilemma – Assessment of Rapid Prototyping Process Chains", Proceedings of the 8th European Conference on Rapid Prototyping and Tooling, July 1999, Nottingham, UK.
7. Durr, H, Kascha, U; "An Approach for Selection and Comparative Evaluation of Conventional and Rapid Tooling Process Chains", Proceedings of the 7th European Conference on Rapid Prototyping and Tooling, pp 93-107, July 1998, Aachen, Germany.
8. Kaschka, U, Auerbach, P., "Selection and Evaluation of Rapid Tooling process chains with Protool", Rapid Prototyping Journal, pp 60-65, Volume 6, Number 1, 2000. ISSN 1355-2456
9. Bernard A., & Deglin, A., "An Original Approach for the Generation of Rapid Product Development Processes", Proceedings of 9th European Conference on Rapid Prototyping & Manufacturing 17th-19th July 2000, Athens, Greece.
10. Bernard A., & Deglin, A: "Knowledge-Based System for the choice of Rapid Prototyping process", Proceedings of the 10th Solid Freeform Fabrication Symposium, pp 39-45, Austin, Texas, August 1999.
11. Bernard A., & Deglin, A: "A Knowledge-based enviroment for modelling and Computer-Aided Process Planning of Rapid Manufacturing processes", Proceedings of the SPIE Conference on Concurrent Engineering, pp 1/11-11/11, Lyon, France, July 2000
12. Dreher, S: "Software for the Interactive Configuration of RP Based Process Chains", Proceedings of Time Compression Technologies Conference, September 2001, Manchester.

Benchmarking the rapid design and manufacture process

G J RYDER, D K HARRISON, G GREEN, W J ION, and **B M WOOD**
The Rapid Design and Manufacture Centre, Glasgow, UK

ABSTRACT

As part of the research programme at the Rapid Design and Manufacture Centre a number of benchmarking studies have been conducted with the aim of informing students and local industry as to the capabilities of a range of rapid prototyping technologies. These benchmarking studies have focused on both 'Soft data' comprising of aesthetic qualities such as appearance, surface texture, robustness, cost and time to produce or 'Hard data' such as accuracy, flexurial, compressive modulus and surface roughness. Both are compared here with a view to creating a range of tools that allow comprehensive analysis of application requirements versus process capabilities.

KEY WORDS: Benchmarking, accuracy, Rapid Prototyping, comparison, manufacture.

1. INTRODUCTION

Since the late eighties a number of benchmarking studies have been published in an attempt to determine working accuracy and strength of the systems that can then be used by industry to determine process suitability for their application. However, in many cases including product design and sculpture, accuracy and strength are not as important as the softer characteristics of relative accuracy, surface texture, robustness, cost and time, while in applications such as aerospace, automotive and electronics it is critical that 'hard' quantitative data is used to establish the optimum process. The Ultimate aim in most of these studies is the creation of a database of process criteria that can be used to develop process selection tools. Deher [1], Bernard [2], Jones [3] and Muller [4] have all based part of their studies of process chain selection on this 'Hard' data. It should be noted at this stage that it is not the purpose of this paper to describe the individual rapid prototyping processes both Kruth [5] and Pham [6] have written excellent resources that can be used in parallel with this paper for this purpose.

Many of these benchmarking studies suffer from a number of problems that mean that the data is not as conclusive as it could have been. Typically a wide range of different benchmarking models are used and non-consistent methodologies are used. Where these studies overlap, i.e. same process, different machines, different machine set-up and non-consistent measurement techniques means that the data is not consistent. Finally non standard data analysis and presentation is used. This lack of coherent benchmarking practice leads to confusion over actual machine capabilities. An example of this apparent confusion can be seen from two separate benchmarking studies carried out by Loose and Nakagawa [7] and Farentinos [8]. In both cases the same process is used, but different models, methodologies, measurement techniques and data analysis techniques are used. So which one represents the best indication of the process accuracy? For benchmarking data to be of real global applicability it is essential that all of these issues are addressed. A standard for benchmarking Rapid Prototyping has been discussed many times following closely standards that are used for benchmarking other manufacturing processes, however, because there is no common material or material deposition process except that the models are built up layer-by-layer this would be difficult to implement. The Ultimate aim in most of these studies is the creation of a database of process criteria that can be used to develop process selection tools.

2. PREVIOUS BENCHMARKING STUDIES

A variety of measurement methodologies have been used across the wide range of papers previously published on the subject of the benchmarking of RP systems. While a large number of studies have been carried out there are 6 commonly cited studies of particular relevance to this work and these are detailed below. It should be noted that most of these studies look at quantitative hard data and in particular focus on process accuracy.

Loose and Nakagawa [7] looked at a wide range of processes for their study comprising of the 7 core RP processes of Stereolithography (SLA), Selective Laser Sintering (SLS), Laminated Object Manufacturing (LOM), Fused Deposition Modelling (FDM), Three Dimensional Printing (3DP), Multi Jet Modelling (MJM) and Droplet On Demand (DOD). Further detail may be sought from the original reference, however, the study looked at List price (In Japanese Yen), Manufacturing Cost (in Japanese Yen), Manufacturing Time, Material and Accuracy. The test part was made of simple geometric shapes including; flat planes, blocks, cylinders and holes. With feature sizes from 0.2 mm upwards. Altogether 29 measurements were taken of each part using a Co-ordinate Measuring Machine (CMM). A cumulative Error Distribution analysis was used to give a percentage of measurements falling within a given range of error, together with an absolute average error across x, y and z for each part. Farentinos and Khoshnevis [8] looked at a range of SLA, SLS, LOM and FDM processes as part of their study. The part was a flat plane with four half spheres, one in each quarter of the square base. They used a Mitutoyo B231 Co-ordinate Measuring Machine (CMM) with a Renishaw probe to capture the data and used a standard deviation analysis to give; average, standard deviation, min/max and profile measurements. Both Shellabear [9][10] and Reeves and Cobb [11] used the same test pieces and collected the same data. A simple test part is used with a series of flat planes of various angles that would be used to measure surface finish. These planes also make up a number of reference points that can be used to measure x, y and z dimensions. Shellabear's benchmark study was conducted as part of the activities of the Raptec consortium. The North American Stereolithography User Group part (Ippolito [12]) was built on SLA, Solid Ground Curing (SGC), FDM and LOM systems and the accuracy was reported. Finally Childs and Juster [13] designed a special benchmarking part containing a wide rage of features including; flat planes, curved surfaces and holes was built on the SLA, SLS, FDM and LOM systems. Only accuracy was reported.

3. BENCHMARKING STUDIES AT THE RDM CENTRE

As part of a feasibility study carried out at the RDM Centre [14] a case study was conducted that illustrated that there were a number of qualitative criteria that were just as crucial in evaluating RP technology as the more usual quantitative data such as accuracy, strength and surface finish. These qualitative criteria or 'Soft Data' such as appearance, texture, materials available, are rarely cited by authors instead making up that knowledge acquired by users of the technology and sometimes called 'know-how'. The Centre has constructed a criteria matrix that can be used to select RP processes or expanded to capture further knowledge as it is acquired by the Centre.

The benchmarking project aimed to identify a number of common criteria across the range of RP technologies available in the UK. The product chosen for this benchmarking study was the Rotilt concept buggy handle. This product was designed and developed by Glen Heavnor was part of the Glasgow 1999 collection and was awarded 'Millennium Product' status. The concept has now been extended into a range of other products including:

- Frying pan handles,
- Hairbrushes and
- Toothbrushes

During this study the various stages of the design process were investigated, key aspects of each of these stages was recorded and shown in Table 1.

- Hand Modelling
- 3D CAD
- Rapid Tooling
- Reverse Engineering
- Rapid Prototyping
- Traditional Manufacturing Processes (Computer Numerically Controlled Machining CNC)

3.1 Hand Modeling

In the Rotilt project the designer used an existing buggy handle and modelling compound to develop a more ergonomic design. This allowed the designer complete control over the shape of the handle geometry at this early stage in the design process.

3.2 Reverse Engineering

One of the key challenges in this project was the capture of the geometry developed by the designer and transfer it into the 3D CAD so that it could be further developed. Two reverse engineering processes were used during this process.

Photogrammetry: two digital cameras were used by the Turing Institute to capture the geometry that has a random pattern of dots projected onto it. Software then triangulates the position of these dots from the two images to reconstruct the 3D geometry.

Manual Data Capture: The part was also encased in a block of modelling compound that was then cut into 5 mm slices. The front and back of these slices are scanned using a 2D document scanner to create a series of cross-sectional profiles that are then joined together to form a copy of the 3D geometry.

3.3 3D CAD

The package used in this study was Form – Z this allowed the creation of the 3D geometry. However 3D CAD (whichever package is used) is the starting point or gateway into the digital section of the design process. The software also allows the 3D geometry to be refined and modified. Once this has been done it can be exported to a number of file formats that allow it to be transferred to either rapid prototyping or CNC machining.

3.4 Rapid Prototyping

The geometry was output from the 3D CAD package in the STL format, a surface triangulation file. This STL file was sent to the appropriate vendor or group:

- 3D Systems Ltd: Stereolithography and Thermojet Models
- DTM: Selective Laser Sintering Models
- Laser Lines: Fused Deposition Models
- LIP Tool: Laminated Object Modelling, Sanders Prototype and 3D Printing Models.

The parts were then built and sent back to the RDM so that they could be examined against each other.

3.5 Rapid Tooling

Once the more accurate parts have been made using either RP or CNC machining they can be used to create typically 25 copies using a process called Vacuum Casting. There are other forms of rapid tooling but this was the process studied here. In vacuum casting the accurate master model is encased in silicone rubber which once cured is cut in half to release the master. These two halves are then rejoined and a two part polyurethane resin poured into the cavity to form the model. These parts were then used to carry out initial testing and marketing of the new buggy handles.

3.6 Traditional Manufacturing Processes (CNC Machining)

Depending on size and complexity of geometries, CNC machining can still be considered a rapid prototyping process, in addition to this almost any material polymer or metal can be used. In general large or small, low complexity parts can be created using this process. In this benchmark study it was used to create the accurate masters used to vacuum cast the prototypes.

	Advantages	Disadvantages	Accuracy	Speed	Cost (£)
Hand Modelling	Good degree of control over geometry, low cost, high speed of iteration.	Poor accuracy, difficulty of transferring data to latter stages of the design process.	>1mm	Hours	10's
Reverse Engineering	Allows user to take advantage of the hand modelling process by reducing lead time	Very complex process, accuracy limited by cost, requires very expensive software to get full advantage of data, impossible to capture internal detail.	0.1 – 0.2 mm	Hours	100's to 1000's
3D CAD	A powerful way of creating very accurate 3D geometry	Capability limited by user familiarity with Software. Can be expensive	As modelled	Minutes, Hours	100's to 1000's
Rapid Prototyping	Fast method of physically realising 3D geometry, gives designer enhanced interaction with the prototyping process	Can be expensive for large parts, limited range of materials available, modest accuracy of most processes	0.08 – 0.5mm	Hours	100's to 1000's
Rapid Tooling	Relatively low cost way to make up to 25 copies, a wide range of materials available	High cost of the Room Temperature Vulcanising silicone rubber, relatively short life of silicone tool	As for master	Days	1000's
Traditional Technologies	Still fastest prototyping process for large or low complexity geometries, high accuracy, wide range of materials.	Can be slow for more complex geometries and difficult materials.	<0.01mm	Hours to Days	100's to 1000's

Table 1: the stages of the design process side by side

4. RESULTS OF THE PHYSICAL RP BENCHMARKING

Once delivered back to the RDM the parts were evaluated against a number of criteria that can be used to evaluate systems applicability for a range of applications. However, at this stage the benchmarking part chosen – The Rotilt buggy handle would only yield 'Soft Data':

- Relative accuracy: The relative accuracy of each of the machines is evaluated against each other, it is not always necessary to measure this directly for most applications it is enough to refer to the vendors literature.
- Robustness: This criteria evaluates how confident a user could be in using the part in an application that requires the application of any type of load. Can the part be dropped, or handled.
- Speed: This criteria is based on the speed of the process but also on the speed of delivery of the parts from each of the groups concerned. This is less important in a bureaux setting, most will quote a 2/3 day delivery on most parts regardless of the type of process used.
- Capital Costs: How much is the entry level machine. Important for groups thinking of purchasing technology.
- Running Costs: Critical for groups wanting to purchase the technology but can also give an understanding of how much a bureaux might charge for the part.
- Surface texture and surface texture of downward facing surfaces: This set of criteria evaluates how smooth the surface of the part is, again relative to each other, the down-facing texture is important to understand the effect of supports on parts. Many processes that use supports will leave evidence of this on the part.

- Material Range: How wide a range of materials is available, important in understanding how versatile a single technology can be, but also if the type of material used, is known then a reasoned judgement of the strength of the part can be made.
- Metal Pathways: What pathways are available to obtain metal parts? Some processes provide direct methods to obtain metal parts and therefore can be used in Rapid Tooling applications.
- Advantages and Disadvantages: an impartial look at the criteria that sales people do and do not tell purchasers when buying or using a system.

The characteristics of each of the models received will be described here in terms of the criteria outlined above, but also in terms of more general concepts such as appearance, feel and weight

4.1 Constructing the Criteria Matrix

It would take considerably longer than allowed in this paper to describe the full method for the creation of the criteria matrix, however, it is crucial to describe the core process. Therefore the first two criteria will be described here. It should be noted while reviewing the criteria matrix that the information reviewed here is qualitative, based on the experience at the RDM Centre and those with different experiences might come up with a different matrix.

4.1.1 Relative Accuracy

A reasonably thorough examination of available literature including web site information and other peoples case studies will provide a guide to the relative accuracy of the rapid prototyping processes, i.e. how they compare against each other. The most accurate system on the market at the current time is the Solidscape droplet on demand (DOD) system, therefore this is given the highest rating of 10. The 3D Systems Stereolithography (SLA) and the Objet Quadra (Objet) systems have comparable accuracies and so are both given a rating of 8. Objet has not been on the market long enough to be fully evaluated and as more information is made available it's placement may change. Selective Laser Sintering (DTM-SLS) formerly of DTM Corporation now of 3D Systems is next with a rating of 7. Fused Deposition Modelling (Stratasys-FDM), Laminated Object Modelling (Helisys-LOM) and Thermojet (MJM) all have comparable accuracies and are rated at 6. 3DP (ZCorp) is the least accurate system in this study and is rated at 4. Table 2 shows how these values compare against each other.

	SLA	SLS	FDM	LOM	3DP	MJM	Objet	DOD
Relative Accuracy	8	7	6	6	4	6	8	10

Table 2: relative accuracy rated via a 0-10 dimensionless scale

4.1.2 Robustness

In general robustness here means how confident the group was in handling the parts.
The strongest part received was from the SLS process and was built using the glass filled Duraform material it is rated at 10. The FDM part built using ABS was next and rated 8, but it should be noted that this strength only applies for features built in the XY plane. Features built in the XZ and YZ planes tend to delaminate under stress. LOM and 3DP have a similar strength and are given the same rating of 6. The strength of the 3DP part is highly dependant on the infiltrant used to strengthen the part and so it's rating could change. Objet and SLA are rated the same at 5 due to their use of a similar class of materials. The Solidscape Droplet on Demand and 3D Systems Thermojet parts are rated at 2, both are wax based and extremely fragile. Table 3 shows how these values compare against each other.

	SLA	SLS	FDM	LOM	3DP	MJM	Objet	DOD
Robustness	5	10	8	6	6	2	5	2

Table 3: robustness rated via a 0-10 dimensionless scale

4.2 The Benchmarking Criteria Matrix

When all the values for each of the individual systems are put together in a single matrix as shown in Table 4, the user has a tool that can be used to compare the machines against each other.

Systems / Criteria	SLA	SLS	FDM	LOM	3DP	MJM	Objet	DOD
Relative Accuracy	8	7	6	6	4	6	8	10
Robustness	5	10	8	6	6	2	7	2
Speed	6	6	5	5	9	8	10	2
Capital Costs	2	3	5	5	8	9	8	9
Running Costs	1	1	4	3	9	7	7	3
Surface Texture	10	4	6	5	5	10	10	10
Texture of downward facing surfaces	10	4	4	5	5	3	10	10
Material Range	5	10	5	5	7	1	3	1
Metal Pathways Available	Quickcast	Laser form Inv. cast	Inv. cast	Inv. Cast	Inv. Cast	Inv. Cast	Inv. Cast	Inv. Cast
Advantages	Excellent Accuracy. Improving range of materials. Good surface finish.	Large range of materials. Robust materials. Tooling options.	Good engineering materials. Soluble supports. Office based system.	Large system volume. Good for inv. Casting.	Large range of materials Simple process. Fast process. Low running costs.	Fast. Good upper surface finish. Good for inv. casting.	N/A	N/A
Disadvantages	Materials degrade. Needs supports. Expensive to run.	Poor surface finish. Expensive to run.	Slow. Requires supports.	Slow process. Paper based mats.	Powder messy.	Needs supports. Poor downward surface finish.	N/A	N/A

Table 4: the benchmarking criteria matrix showing processes against criteria rated via a dimensionless 0-10 scale

5. COMPARING 'HARD DATA'

The ultimate goal in the work conducted at the Centre is to develop a range of tools that can be used by Students and companies to evaluate the appropriateness of the different types of rapid prototyping and rapid tooling technologies to various applications. Both the 'Soft' qualitative data developed earlier and the 'Hard' quantitative data presented

here, will be used side by side to capture a wide range of useful knowledge. Before starting to collect the 'Hard' data a thorough study of current methods used in benchmarking rapid prototyping techniques and standards used in industry was conducted. Wherever possible the Centre will use existing standard parts or methods. In the measurement of accuracy the Centre uses a variant of the North American Stereolithography User Group test part and in the measurement of tensile strength BS 2782 [15] is used. The Data from the RDM Centre was collected over a number of student projects from Vincent Pretet [16][17] in collaboration with the Scottish Polymer Technology Network and Andrew O'Donnell [18] in collaboration with the University of Glasgow.

5.1 Process Accuracy

The accuracy results from the RDM Centre for Fused Deposition Modelling and 3D Printing are presented in Table 5 along with the results from the Shellabear [9][10] study. The prismatic accuracy shown for the processes, relates to 150 mm, where these values are not identical a range of values is displayed.

Process	Material	Accuracy - mm	Source
SLA	SL5170	0.2	**Shellabear**
SLS	Duraform	-0.36	
LOM	LOM paper	-0.4 to 0.2	
Thermojet	Wax	-1.11 to –0.125	
FDM	ABS	-0.235 to 0.04	**RDM**
3DP	Plaster untreated	-0.875 to 0.35	

Table 5: process accuracy compared

5.2 Ultimate Tensile Strength, Ultimate Strain and Young's Modulus

The Data from the RDM Centre for the tensile tests is compared against the values for tensile tests carried out by the RAPTIA group [19] and compared in Table 6. The Raptia group is a European thematic group studying the state of the art in Rapid Prototyping and disseminating the results within a consortium of companies across Europe. More information on RAPTIA including the full results of their benchmarking study can be found on their website [19]. This data is also compared against the Youngs Modulus for ABS and Nylon PA6 from the efunda materials database [20] giving a clear standard to compare against.

Process/Material	Ultimate Tensile Strength (MPa)	Ultimate Strain (%)	Young's Modulus (GPa)	Source
Injection Moulded ABS	-	-	1.03 to 2.4	**efunda**
Injection Moulded Nylon PA6	-	-	2.62 to 3.2	
SLA (SL5170)	75.4	3.6	4.4	**RAPTIA**
SLS (Duraform)	46.8	21.1	2.46	
LOM (SIBCO MRP5022)	36.4	4.4	4.04	
Thermojet (Wax)	2.4	0.6	0.47	
FDM (ABS)	21.4	5	1.81	**RDM**
3DP (ZP100 UREOL 6405)	9.32	0.22	4.03	

Table 6: tensile test results compared

6. CONCLUSIONS

The goal of the RDM Centre remains to build a comprehensive database of process data that can be used to help select RP technologies. It can be seen from the data presented here that this can be useful to anyone interested in

establishing the performance of the processes relative to one another. However, this work is ongoing and a large amount of data remains to be collected. Flexural strength, Compressive Strength, Thermal Conductivity, Maximum Operating Temperature, Surface Finish and Dielectric Strength among those criteria that companies have expressed an interest in identifying. As for the 'Soft' data, it remains necessary across industry to capture the 'knowledge' accumulated by the organisation. To make all this data relevant it is essential that established procedures are followed and where established procedures do not exist that either closely related procedures are adopted or new procedures are established in broad consultation across the RP industry.

References

[1] S. Deher, Software for the interactive configuration of RP based process chains, Proceedings of Time Compression Conference, Manchester, Sept 2001.

[2] A. Bernard, A. Deglin, A Knowledge-based environment for modelling and Computer aided process planning of rapid manufacturing processes, Proceedings of the SPIE Conference on Concurrent Engineering, p1/11 – 11/11, Lyon, France, July 2000.

[3] K. G. Jones, R. I. Campbell, Rapid Prototyping Decision Support System, Proceedings Fast Freeform Fabrication Symposium, University of Texas at Austin, Austin, pp551 – 558, 1997.

[4] H. Müller, J. Bauer, H. H. Klingenberg, Computer based Rapid Prototyping System Selection and Support, Time-Compression Technologies '96 Conference, Warwickshire, England 1996.

[5] J. P. Kruth, M. C. Leu, T. Nakagawa, Progress in Additive Manufacturing and Rapid Prototyping, CIRP Annals – Manufacturing Technology, Vol 47, No 2, 525-540, 1998.

[6] D. T. Pham, R. S. Gault, A Comparison of Rapid Prototyping Technologies, Int. J. of Machine Tools & Manufacture, 38, 1257-1287, 1998.

[7] K. Loose, T. Nakagawa, Benchmarking Various Methods of Layer-Manufacturing Systems in Rapid Prototyping, unknown source, 1998.

[8] S. Farentinos, B. Khoshnevis, A Study of Accuracy in Automated Fabrication, University of Southern California, www.pmli.com/accuracy_study.html, 1999.

[9] M. Shellabear, Model Manufacturing Processes – State of the Art in Rapid Prototyping, RAPTEC, Task 4.2, Report 1, 1998.

[10] M. Shellabear, Benchmarking Study of Accuracy and Surface Quality in RP Models, RAPTEC, Task 4.2, Report 2, 1999.

[11] P. E. Reeves, R. C. Cobb, Surface Deviation Modelling of LMT Processes – A Comparative Analysis, Proceedings 5th European Conference on Rapid Prototyping and Manufacturing, 1996.

[12] R. Ippolito, L. Lullano, A. Gatto, Benchmarking of Rapid Prototyping Techniques in terms of Dimensional Accuracy and Surface Finish, CIRP Annals – Manufacturing Technology, Vol 44, Pt1, pp157-160, 1995.

[13] T.H.C. Childs, N.P. Juster, Linear and Geometric Accuracies from Layered Manufacturing, Annals of the CIRP, vol. 43/1, pp163-166, 1994.

[14] G. J. Ryder, A. McGown, W. Ion, G. Green, D. K. Harrison, B. Wood, Rapid Prototyping Feasibility Report, Rapid Prototyping Group, Glasgow Caledonian University, ISBN 1901248763, 1999.

[15] British Standards Institute, BS 2782: Part 10: Method 1003:1977 EN 61, Determination of tensile properties of Glass Reinforced Plastics.

[16] V. Pretet, Accuracy and Surface Finish Quality in the ZCorp 3D Printer, Internal RDM Report, 2001.

[17] V. Pretet, Mechanical Properties of the ZCorp 3D Printer Materials, Internal RDM Report, 2001.

[18] A. O'Donnell, Testing the Capabilities and Accuracy of Rapid Prototyping Parts, University of Glasgow Final Year Project, 2000.

[19] Ing Olfur O Dorbjornsson, Tensile Strength Benchmarking Study, Raptia Workshop, CIRTES, www.raptia.org, September 2000.

[20] efunda, engineering fundamentals, www.efunda.com, Feb 2001.

The development of three-dimensional printing techniques for 'concept modellers' to competitive rapid prototyping systems

P M HACKNEY
Centre for Rapid Product Development, University of Northumbria at Newcastle, UK

ABSTRACT

The rubicon has been crossed and we have moved from traditional high capital, maintenance and material costs associated with traditional rapid prototyping techniques such as SLA, FDM and SLS processes to low capital, low maintenance and low material costs of the so called "concept modellers". This paper will focus on the new 3D printing techniques and their industrial and tooling applications, together with the possibilities of new materials which are now becoming justifiable to large and medium sized enterprises as well as large OEM companies. Concept modellers such as 3D System's ThermoJet and Z-Corp's 3D Printer will be examined, together with Objet's new 3D UV Reactive Resin Printer. New materials developments undertaken by researchers at Northumbria University into both the materials and accuracy of the Z-Corps process will also be presented.

KEYWORDS: Rapid Prototyping, Concept Rapid Prototyping, 3D Printers, Benchmarking

1. INTRODUCTION

Rapid Prototyping (RP) is a range of technologies, which describe a process capable of creating complex physical parts directly from 3D digital CAD data [1]. There are now several commercial processes available, all of which work on much the same principle, i.e. layer manufacture, whereby the 3D digital part is sliced into many very thin layers that are then formed subsequently on top of one another to form the finished component or assembly. The use of RP is becoming more widespread as 3D CAD as a design tool is being used by small to medium sized enterprises (SMEs) to design and manufacture new products [2]. The advantages of RP over traditional CAM based tools are both time and cost of manufacture, ensuring the designer can hold a part designed yesterday in his/her hand today.

At the moment the RP industry is split into two distinct areas:

- High cost, high precision systems – SLA, SLS, FDM, LOM,
- Low cost (<£50k) "concept modellers" – 3D "Ink Jet" Systems - 3DSystems ThermoJet, Objet's Inkjet System and Z-Corps 3D Printer.

The high cost RP machines are predominantly situated in bureau companies with a range of machines to enable them to serve all their customer needs. The low cost RP machines are predominantly being installed in design houses and large OEMs to enable design verification and to serve as a communication tool. This paper will review the current concept modelling processes and benchmark these processes. The paper will also investigate the application of the Z-Corps ZP400 3D Printer, and illustrate, via case studies, the use of the ZP400 RP process.

2. THE BENEFITS OF CONCEPT MODELLING TECHNIQUES

The principle of the "concept modellers" is that the parts are produced to a low accuracy of normally ±0.5 mm, low part strength <15 M*Pa,* with limited engineering part utilisation. The benefits include:

- Low system purchase and operating costs;
- Low part costs;
- Load and go capability.

However these "concept parts" have been successfully used in several projects as parts, sacrificial patterns or tools for production of working components. A good example is the Z-Corps 3D printer binder cartridge head cap shown in figure 1. This component is actually produced on the same machine that made itself. The ThermoJet uses a type of investment casting wax, and is now being used regularly in the production of aluminium and steel parts via the investment casting process without expensive new processes or process modifications at the foundry.

Figure 1: Z-Corps 3D Printer, Print head Cap

3. REVIEW OF CONCEPT MODELLING PROCESS

3.1 3D Systems ThermoJet system

The MJM ThermoJet system [3] uses a print head to spray droplets of molten wax build material (also used as support material). The print resolution is 300 x 400 x 600 dpi (x, y, z). The process operates by first slicing the 3D CAD data into layers, these layers are then printed onto the layer below with several passes of the head required to deposit the full width of the component.

Figure 2a: Part from ThermoJet Process

Figure 2b: ThermoJet Machine

A support framework is required for the underside of the components and any overhangs unconnected to lower regions of the model. The support removal is facilitated with the parts first being refrigerated to embrittle the support structure. This is one limiting factor of this process. Upper facing surfaces are capable of excellent detail, but underside surfaces are poor and the requirement for support removal means that wall thickness is limited.

- **Benefits**
  Excellent for investment casting waxes;
  Excellent upper surface definition;
  Easily joinable via melting;
  Choice of two materials – ThermoJet™ 2000, 88;

Able to smooth models with heat gun or hot knife;
Supported by 3D Systems (largest RP machine manufacturer).

- **Drawbacks**
  Support material removal;
  Brittle parts;
  Poor underside surface finish;
  Not suitable for thin walled parts.

3.2 Objet's inkjet system

The Objet system [4] was developed in Israel and uses similar resins to the SLA processes, i.e. it uses UV sensitive photopolymer. The process comprises the inkjet head traversing the build area, and where the part is solid, fine droplets of model material are deposited simultaneously with the support structure for future layers. The resin is deposited with a print resolution of 600 x 300 dpi (x, y). An UV lamp situated above the build platform cures the resin droplets. The head has a y deposition width of 60 mm, thereby several strips of resin are laid for wider parts. The build platform lowers by one layer thickness (20 microns) and the process repeated. The parts are cleaned and the support structure removed by a combination of hand and water jet washing.

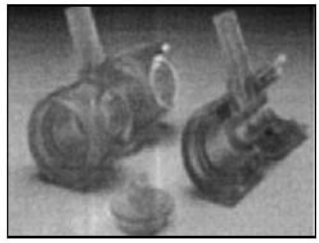

Figure 3a: Part from Objet Process

Figure 3b: Objet Machine

- **Benefits**
  Material strength;
  Speed/width of build strip;
  Similar to SLA resins;
  Finest layer resolution and print resolution;
  Form and fit testable;
  Vacuum castable;
  Two machine variants;
  Large research and development budget.

- **Drawbacks**
  Technology still under development – reliability, accuracy;
  New start-up company.

- **Machines:** Object Quadra Tempo, Object Quadra.

3.3 Z-Corps 3D printer

The 3D printer is available in three machines. The basic build process is the laying down a layer of powder (ceramic or starch based) 0.1 to 0.25 mm thick. The model is sliced and the solid sections printed via "Canon InkJet cartridge" in the y-axis, the carriage increments (similar to paper feed) in the x axis and another strip of binder is deposited. The parts are formed in the build chamber that drops by one layer thickness as more material is deposited and bound above it.

The machine is capable of building several layers per minute. As the powder supports the part no support structure is required therefore allowing complex parts to be built. The binder can be coloured with a dye allowing coloured parts to be generated, for example the results of a Finite Element Analysis. The surface finish on the underside is poorer than the topside due to seepage of the binder into the surrounding material.

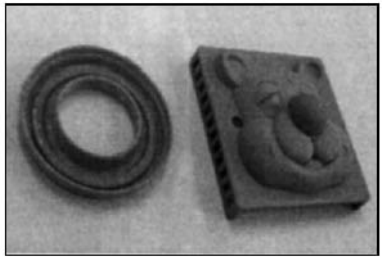

Figure 4a: Parts from 3D Printing Process

Figure 4b: Z-Corps ZP400 Machine

- **Benefits**
  Fastest build speed;
  No support structure;
  Complex parts, thin walled parts;
  Two materials - starch – rubberising, investment castable;
  - ceramic – detail, definition strength;
  New large build volume machine (largest of concept modellers);
  Colour capable;
  Easy clean;
  Alternative powders – metallic, conductive.

- **Drawbacks**
  Least accurate of concept modellers;
  Underside surface finish – poor;
  Poor strength;
  Limited fit and function usage.

- **Machines** ZP400, ZP406, ZP810.

3.4 Stratasys – FDM system

A new low cost fused deposition modeller (FDM) is due to be launched soon. However, to date little technical data is available to review/benchmark this machine.

4. BENCHMARKING OF CONCEPT MODELLERS

When relative criteria is used between 1 and 10 this is from user feedback and part inspection, (1 – lowest, 10 – highest).

	3D Systems ThermoJet MJM System	Z-Corps 3D Printer ZP400/ZP406/ZP810	Objet's InkJet Printer Quadra/Quadra Tempo
Build Size (mm)	250 x 190 x 200	250 x 200 x 200/ 500 x 600 x 400	270 x 300 x 200
Material	Thermoplastic wax	Starch, ceramic	Photopolymer
Resolution (x, y, z) dpi/mm	300 x 400 x 600/ 0.08 x 0.065 x 0.04	300 x 300 x 360/0.08 x 0.08 x 0.07	600 x 300 x 1270/ 0.04 x 0.08 x 0.02
Accuracy Relative (1-10)	5	4	7
Office Environment	Yes	Yes	Yes
No of build materials	Build material only	Power and Binder	Two – build & support photo-polymers
Support requirements	Yes	No	Yes
Date of Introduction	1998	1998/2000/2001	2000
Colour	Single neutral, grey black	Any single, colour upgrade/colour/colour	Amber (SLA colour)
Durability Relative (1-10)	Brittle – wax 2	Brittle – plaster 2, Infiltrated 6	Excellent 8
Support removal	Yes – Refrigerated	No	Yes – Waterjet
Speed (1-10)	4	8	7
Material Recyclable	No	Ceramic – Yes, Starch – Limited	No
Medical models usage	Yes	No	Yes
Investment casting	Yes	Starch only – limited application	No
Bureau usage (UK)	Yes	No – In house	Yes
File type	STL	STL	STL
Support/Equipment	Fridge, technician	De-powdering unit, autowaxer (supplied)	Water jet washer
Typical costs per part (min costs may apply)	£20	£5 ceramic, £10 starch	£30
Detail upper surface	Excellent	Good	Good
Detail lower surface	Poor – where supports removed	Average – Mottled underside	Good
Materials development expected	Improved strength thermoplastics	Metals, ceramics, carbons	Increased as per SLA process
Cost	£36k	£37k	£46k
Maintenance (per annum)	£5k	£3k	£6k
Start up Cost	£1.3k	£1.5k	£5k

Table 1: Benchmarking of Concept Modellers

5. ANALYSIS OF Z-CORPS 3D PRINTING PROCESS AND MATERIALS

A series of investigations at the Centre for Rapid Product Development, Northumbria University, were undertaken to characterise the Z-Corps 3D printing process.

5.1 Accuracy analysis

Fifteen test parts were built in three phases, in four quadrants of the bed. The build binder core and shell saturation and layer thickness was also varied. This comprised over 200 tests with both ceramic and starch based materials. The conclusions are as follows:

ZP11 – starch based

- Parts built consistently 0.7% to 2% smaller, an Anisotropic scaling factor of 1.0073, 1.0013 and 1.0025 in x, y, and z-axis.
- Build time directly proportional to binder and core saturation.
- Wax infiltration reduces part size by 2%.
- Raw parts absorb moisture and should be sealed to maintain accuracy.
- Build location, particularly with contaminated build material affects parts' geometric shape and accuracy.

ZP100 – ceramic based

- Binder print area spreads outwards from print area causing the cylinder inner diameter to become too small, whilst its outer diameter is too large, therefore no single scale factor can be used.
- Greatest error in z direction.
- Parts repeatable in x, y, but not z-axis.
- Wax infiltration has negligible effect on accuracy.
- Anisotropic scale factor of 0.998 in x and y-axis required for accurate parts dependent on cross-section area.
- Parts need to be left to harden in the machine for several hours to allow removal.

5.2 Material hardness

Due to build characteristics parts were tested on all sides as shown in figure 5. ZP11 Starch Based – The base was found to be the softest and the top hardest. The average hardness was 27 Vickers, with the highest 29 and lowest 25. ZP100 Ceramic Based – The results were found to be similar to ZP11 in that the top layer was harder. However the ceramic material is 180% harder overall.

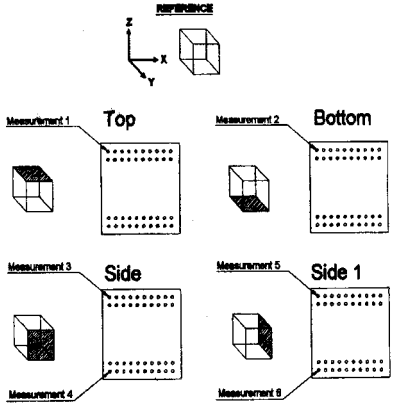

Figure 5: Hardness Measurement

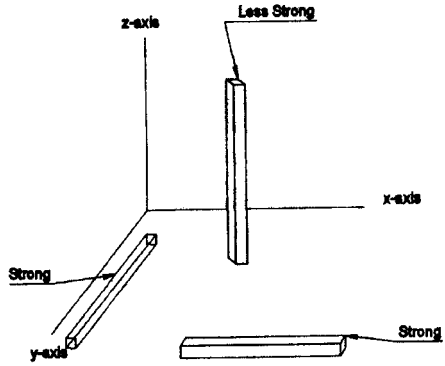

Figure 6: Build Orientation effect on part strength

5.3 Build strength analysis

A set of British Standard tensile test specimens were produced and Finite Element Analysis carried out to assess the theoretical stress versus actual failure mode. The orientation of the part on the build platform was investigated and the results are shown in Fig 6. This revealed that the highest strength is in either direction, in the x-y plane, and weakest is vertically across the build. The binder concentration was varied from the prescribed values and a variance of 15% can be obtained in part strength. The binder concentration was varied from the prescribed values and a variance of 15% can be obtained in part strength.

ZP11 – Starch Based 75N on an 8 x 4 mm section.
ZP100 – Ceramic Based 112N on an 8 x 4mm section.

This shows that the ZP100 is 150% stronger than the starch. It was also found that wax infiltration doubled the above values.

5.4 ZP402 material characteristics

X-Ray Diffraction (XRD) is a technique used to characterise materials. This technique takes advantage of coherent scattering of x-rays by polycrystalline materials to obtain structural information. This technique is used to characterise the ZP402 build materials.

ZP11 – starch based
Starch is the common name given to white granular powder that is odourless and tasteless. A complex carbohydrate ($C_6H_{10}O_5$) is abundant in cereal plants, also a significant amount of sucrose (sugar) ($C_{12}H_{22}O_{11}$) was found.
This material is water-soluble and the effect of heating above 180^0C results in the material becoming liquid.

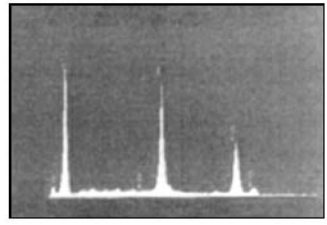

Figure 7: XRD Analysis ZP11 Starch Based Powder

ZP100 – ceramic based
XRD revealed calcium sulphate ($CaSO_4$ $2H_2O$), also called "Gypsum". It is very common in dried salt pans and sedimentary rocks such as limestone. The material is in semi-hydrate form $(CaSO_4)_2$ H_20 such as Plaster of Paris. This sets rapidly (10-20 minutes) by recrystallising with water. A significant amount of calcium Ca was also found.

5.5 Material structure

A Scanning Electron Microscope and Optical Microscope was used to reveal the structures of the build samples before and after wax infiltration when studied (figures 8, 9, 10, 11). The starch based build material clearly has an open "candy floss" fibrous structure which latter tests revealed had lower hardness and strength. The ceramic build material is closer grained and this is reflected in the better part finish and strength.

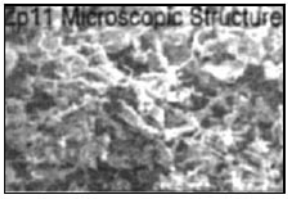

Figure 8: ZP11 Microscopic Structure

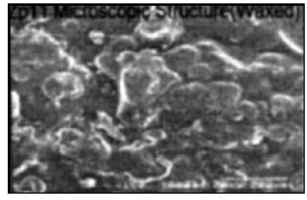

Figure 9: ZP11 Microscopic Structure (Waxed)

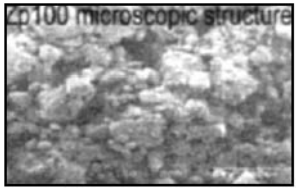

Figure 10: ZP100 Microscopic Structure

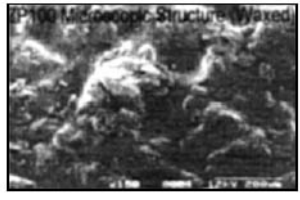

Figure 11: ZP100 Microscopic Structure (Waxed)

6. CASE STUDY

A local company approached the CRPD after encountering problems with a new product they were developing. The function of the product was to produce the recess for electrical wall sockets, in a plaster/breeze block/brick wall. The product fits onto industrial impact hammer drills (with the drill action turned off); the component consists of a square plate with symmetrically arranged teeth in the shape of daggers, debris is allowed to fall between the teeth and out of the rear of the tool. The hole is produced by first drilling a location hole for the socket, the hole cutter is then located by this hole with a tapered extension, the cutter is aligned to the wall and 30 seconds of impacts occur. A furrow is then produced in the masonry, the tool is rotated 90 degrees and a further 30 seconds of impacts occur. The processes of furrow making and dislodging the brittle masonry in this pattern, rapidly makes the hole of the required size and depth even in very hard engineering bricks.

The problem the company was experiencing was that the hard brittle tool steel (D2) were found to be cracking and fracturing after limited usage. The company had been through the lengthy and costly process of design modifications, tooling modifications, wax pattern production and investment casting using traditional techniques several times. This cycle took typically 13 weeks from failure to new design, CAD design, tooling, casting and production of working prototypes. The public and their OEM's were losing faith in their product and their capabilities. To solve the problem, the CRPD and The CADCAM Centre worked together to redesign the cutter to reduce weight and critical stress concentrations by 40%. The FEA analysis however could not fully simulate the high-speed impacts and resonance, therefore physical prototypes were required as shown in figures 12 to 14. Several sacrificial patterns were produced on the Z-Corps printer within the CRPD and successfully cast at a commercial investment casting foundry, which eliminated the tooling and wax production stages, therefore cutting 5 weeks off a 6 week process to get to the trial stage. The company now had D2 tool steel prototypes on test within a week of a new design being finalised and sent for RP production at 25% of the cost previously paid. These sacrificial patterns are now being made using the ThermoJet process at the Digital Factory, Bishop Auckland College, as this process is more tuned to investment casting than the Z-Corps process.

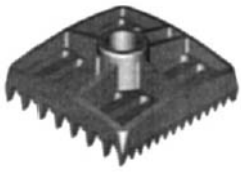

Figure 12: 3D model of design of square hole

Figure 13: FEA Analysis

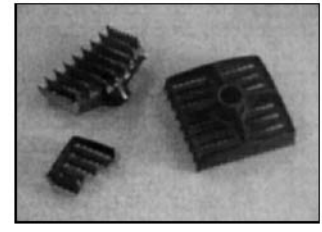

Figure 14: Original Casting and failed castings *(courtesy of Cleveland Engineering Ltd)*

7. CONCLUSIONS

The advent of mid range 3D CAD solutions capable of being used by Engineers as design tools, not just 3D modellers, has resulted in a requirement for rapid prototyping. Concept modellers as described in this paper can fulfil some of the design, test and evolution requirements found in the product development process. The choice of which system is dependent on the end use of the parts produced. The Objet process produces the most accurate and durable parts, the Z-Corps 3DP process the quickest and most complex parts, and the ThermoJet the most suitable for investment casting and excellent upper surface detail. The cost advantage of concept modellers over traditional RP processes allows companies to create models as the design progresses, allowing increased communication and participation of all stakeholders in the product development process.

Acknowledgements

The author would like to thank Government Office North East for providing the ERDF funding to support this project, together with the CRPD core team, Professor M Sarwar, Dr T J Bond, Mr D Bell and Mrs F Todd.

References

1. P M. Hackney & M. Sarwar, *Development of Time Compression Techniques to Assist SMEs with Product Competitiveness*, FAIM Conference 2001, Dublin.
2. P. M. Hackney & M. Sarwar, *Operating Characteristics of the Z-Corps 3D Printing Process*, NCMR Conference 2001, Cardiff University.
3. 3D Systems Website: www.3Dsystems.com (accessed 04/02/02)
4. Objet Technology Website: www.2Objet.com (accessed 06/02/02)
5. ZCorporation Ltd Website: www.Zcorporation.com (accessed 21/01/02)

This page intentionally left blank

Fabrication of functional metal parts using laser sintering – a case study

D E DIMLA and **H SINGH**
Rapid Prototyping and Manufacturing Group, De Monfort University, Uk
M DAY
Scientific and Laboratory Services, Pall Europe Limited, UK

ABSTRACT

Laser sintering is a Rapid Prototyping (RP) technique used for the direct manufacture of solid objects layer by layer, using CAD models. The aim is to determine an application area for porous metal parts obtained through Direct Metal Laser Sintering (DMLS) and test their suitability. The pore structure of DMLS parts was determined using experimental guidelines specified in a British Standard and was found to be potentially suitable for filter applications. Parts were manufactured, and tests were conducted using internationally recognised tests for hydraulic filters to determine its filtration performance. The tests showed the structure to have good strength and integrity, a narrow pore size distribution and a filtration rating of 14μm. However, the configuration chosen had a significantly higher pressure drop and lower contaminant-holding capacity than conventional filters. In this form it would be only suitable for low viscosity fluids or 'last chance' filter application. Further development would produce a more optimum configuration.

KEYWORDS: Direct metal laser sintering, porous metal parts, direct manufacture and filtration.

1. INTRODUCTION

RP processes are a group of emerging technologies that have revolutionised product development and manufacturing. These processes are capable of producing complex geometric components directly from three-dimensional computer generated models. All RP techniques build parts layer by layer with each layer containing the cross-section of the CAD file data. The applications of RP have been shown to greatly reduce the design to manufacturing cycle, resulting in reduced cost and increase competitiveness [1].

There are many commercially available RP systems such as Stereolithography, Laser Sintering, Laminated Object Manufacture, Fused Deposition Modelling, Solid Ground Curing and Three-Dimensional Printing. All RP systems have a limited range of material types from which prototypes can be manufactured. Of these systems, laser sintering is probably the most attractive because of the wide range of materials available for product manufacture, including several polymers, sand and metals [1].

The laser sintering process produces parts when a CO_2 laser scans the CAD data onto a bed of powder material. The interaction between the laser and the powder raises the temperate above 'glass' transition temperature for the polymer, and just below the melting temperature. As a result, the exposed particles deform and fuse with neighbouring particles [2]. The build platform is then lowered by the layer thickness and a new layer of powder is applied, levelled and the laser scans the next layer of CAD data. This process is repeated until the entire CAD slice data has been scanned onto the powder bed and the object has been completed. Figure 1 shows a typical configuration of the laser sintering process.

Laser sintering RP processes can be split into two categories, Selective Laser Sintering (SLS) that can be regarded as indirect and Direct Metal Laser Sintering (DMLS). Laser sintering powders generally are composed of metal particles coated with a thermoset polymer. In the SLS process, the laser is not used to fuse metal powder directly instead it is used to raise the temperature sufficiently to cause the polymer coating to soften and partially cross-seal then solidify bonding the particles together. DMLS powders are composed of low and high melting point metal particles; a CO_2 laser of about 200W is used to fuse the lower melting point powder together, without the use of a thermoplastic binder [1].

In the SLS build process; a roller spreads the thermoplastic powder over the surface of a build cylinder. The piston in the cylinder moves down one object layer thickness to accommodate the new layer of powder. The powder delivery system is similar in function to the build cylinder. Here, a piston moves upward incrementally

to supply a measured quantity of powder for each layer. The CO_2 laser beam then traces over the surface of the tightly compacted powder to melt and bond it to form a layer of the object. The fabrication chamber is maintained at a temperature just below the melting point of the powder so that heat from the laser need only elevate the temperature slightly to cause sintering, speeding up the process. The process is repeated until the entire object is fabricated. After the object is fully formed, the piston is raised to elevate it. Excess powder is simply brushed away and final manual finishing may be carried out. No supports are required with this method since overhangs and undercuts are supported by the solid powder bed [1].

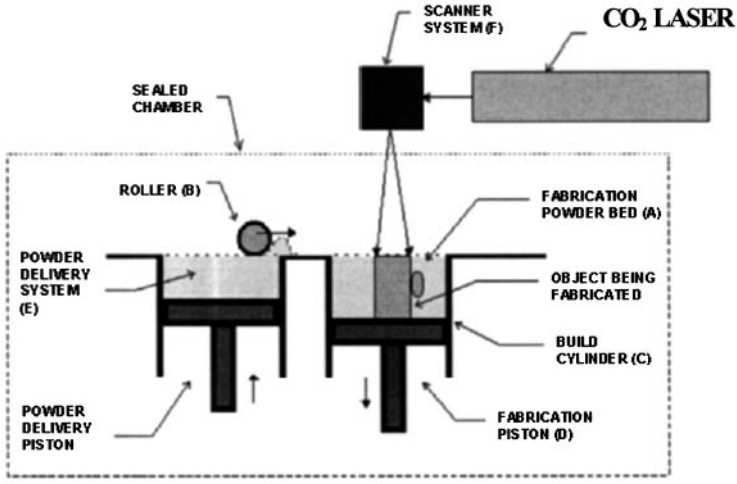

Figure 1: Configuration of the SLS process

The most common RP technique for the direct production of tools for die-casting, injection moulding and functional parts is DMLS. DMLS parts produced through this process are permeable but no infiltration is required. For SLS parts, post-processing sealing is undertaken by infilling with molten copper, bronze or epoxy resin [2] as most applications require fully dense parts for both durability/strength and long life. The DMLS parts however can be used in applications that require porous parts [3], the focus of this investigation.

Porous metal parts can be used for a wide range of applications and can generally be classified into three groups:

- Filtration applications: includes diffusion and control of gases and liquids.
- Mechanical application: self-lubricating bearings that can be used for light bearing applications i.e. small electric motors of spindle bearing for high speed machining.
- Other applications: porous parts can be used for the suppression of noise and sound damping (i.e. silencer barrels for firearms and catalytic converter components), the production of moulds for the vacuum forming process because their porosity allows air to be drawn out from the mould while provide structural integrity. The die casting industry can also use this process for producing mould veins for dies, as trapped air can escape via the porous metal inserts, resulting in improved part quality.

The aims and objects of this work were to investigate the use of the DMLS process for the manufacture of porous metal parts. Typical parts were manufactured on a DMLS machine and these were tested for suitability and functionality in one specific application area, that of the filtration of hydraulic liquids. The powder used in the sintering process consisted of a bronze/nickel mixture containing a small amount of copper-phosphide, marketed as 'DirectMetal' or 'DM' (currently available as the DM 50μm and DM 100μm). This low melting point component was used since it requires less laser energy and time to melt the metal powder.

Parts can be manufactured on the DMLS machine using a variety of different scanning strategies such as laser scanning speed, hatch spacing and border scanning. These factors affect the pore structure of the part and hence determine the likely application area [1]. It is therefore essential to set the correct build parameters to optimise

the performance of the product. The sintering and densification is greatly affected by the laser scanning speed and strategy, laser type, power and radius, mechanical layering of powder (layer thickness) and atmospheric control [4]. The scanning strategy is the most straightforward to modify and thereby adjust the density of the part. Parts can be produced using a variety of the skin and core scanning strategies. The skin principle involves scanning the border of the part and then hatching the internal part area while the core principal involves hatching the internal part area only without hatching the border. The hatching strategy can also be varied in the X or Y/X and Y directions on the same layer and alternating layers. A standard laser scanning speed of 500mm/s and hatch spacing 0.1mm were employed in this study.

2. TEST FILTER DESIGN AND MANUFACTURE

A test filter (Fig. 2) was designed to incorporate similar design features and with dimensions similar to commercially available hydraulic filters to aid testing (i.e. fitting to existing jigs and test equipment). It was built in the vertical direction with vertical wall to add uniformity to the pore structure and also to reduce the need to incorporate supports. The filter is approximately 60mm in length, and the internal and external radii of the cylinder are 30 and 40 mm respectively. However, much larger filters could be manufactured, as the build volume of the machine used is 250 x 250 x 150mm.

Figure 2: Test filter CAD model

The test filter was manufactured using the bronze DM 50μm powder. The core scanning strategy was utilised to add uniformity to the pore structure and density throughout the part. This would result in the part having uniform permeability thus improve the performance of the filter.

3. EXPERIMENTAL PROCEDURE AND DATA ANALYSIS

Initial test pieces (Figure 3) were built using various build strategies and parameters (laser scan speed, part orientation and part thickness) in the vertical direction. Tests were conducted to determine their pore structure using guidelines specified in BS 1752 [5].

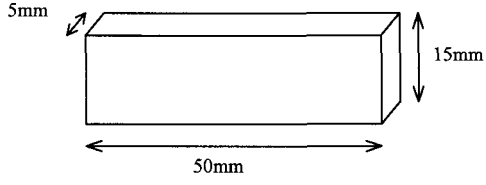

Figure 3: Test piece dimension

The apparatus used for the determination of the pore size index is shown in Figure 4. The experiment involved passing air through a test piece placed above a sealed chamber and covered with a thin layer of water. Air was allowed into the chamber using a control valve to gradually increase the pressure within the chamber and hence the differential pressure across the test piece. The pressure was slowly increased until the first air bubble broke away from the surface of the test piece. At this point, the pressure within the chamber was recorded using a manometer and the value used to calculate the diameter of the largest pore using the following formula:

$$\text{Pore size } (\mu m) = 30 \times \gamma / P$$

'γ' is the surface tension, in dynes per centimetre of the test liquid (water = 73).
'P' is the effective pressure, in millimetres of mercury.

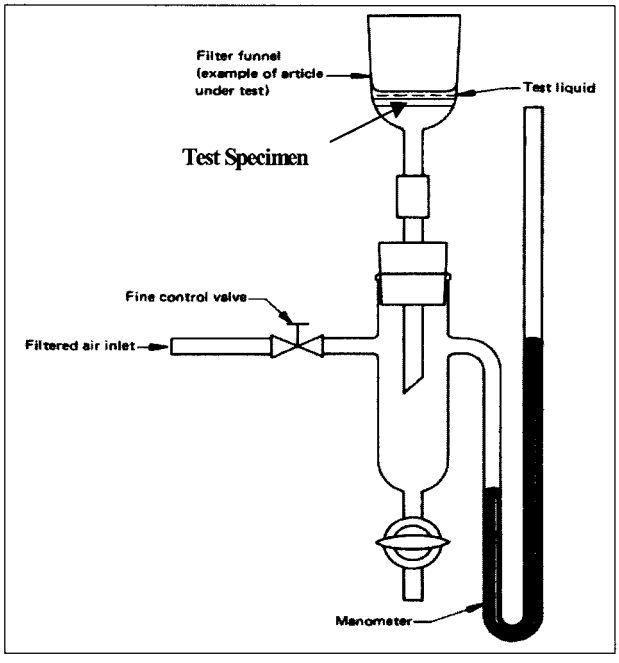

Figure 4: Apparatus for determination of pore size [5]

The manufactured filters (DMU 'A' and DMU 'B') were tested for their suitability for application of hydraulic filtration using the following ISO defined tests:

- ISO 2942:1994 [6] – This test is designed to evaluate the fabrication integrity of the filters, in this case the success of the adaptation to fit into a standard hydraulic housing. It is effectively a repeat of the BS 1752 test excepting that the test liquid was propan-2-ol. The procedure involved increasing the pressure inside the filter progressively to determine the first bubble pressure. Although not part of the ISO test, the pressure was further increased to measure higher bubble point values including the 'mass' or 'fizz' point. The fizz point is effectively a measure of the minimum pore size. Consideration of these two values gives a measure of the structure's permeability.
- ISO 3968:2001 [7] - A method for determining pressure drop/flow characteristics of hydraulic filters.
- ISO 16889:1999 [8] – Multi-pass filtration performance test. The test is conducted using an artificial contaminant and performance data was obtained at particle sizes of 3, 6, 8, 10 and 12$\mu m(c)$[1]. This test was used to determine the filtration rating of the filter and it also gives a measure of the dirt capacity of the filter. The test was performed up to a differential pressure of 10 bar.

[1] The subscript (c) denotes the use of automatic particle counters calibrated using ISO 11171

4. RESULTS AND DISCUSSION

4.1 Pore size analysis

Inspection of the part orientation versus pore size diameter (Figure 5) showed that the pore sizes of the parts produced are dependent on the direction of manufacture. The pore size remained relatively constant at about 2μm (bubble size) from 0° (perpendicular to wiper blade in the X and Y axis) to 55°, but increased thereafter to a maximum of at around 8μm.

The sudden increase in pore size after 55° was due to the thin unsupported test pieces deforming as the wiper blade met their sides, consequently the wiper blade was not levelling the top of the newly fused surface thoroughly. Parts from 70° – 90° failed to be manufactured due to the effects of the wiper blade. However this problem did not arise during the manufacture of the test filters as the filter walls support each other. These results demonstrate that functional filters with a relatively uniform pore structures can be built in the vertical direction and that the effects of the wiper blade on the pore size/structure are limited.

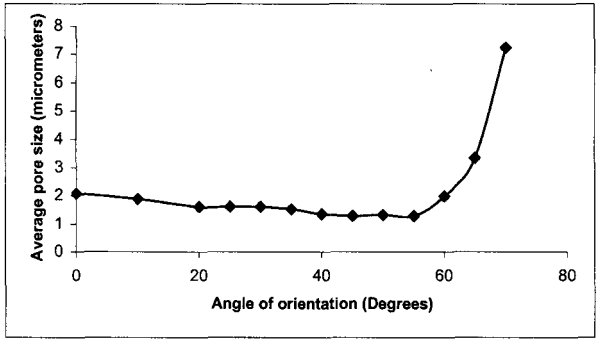

Figure 5: Part orientation versus pore size diameter

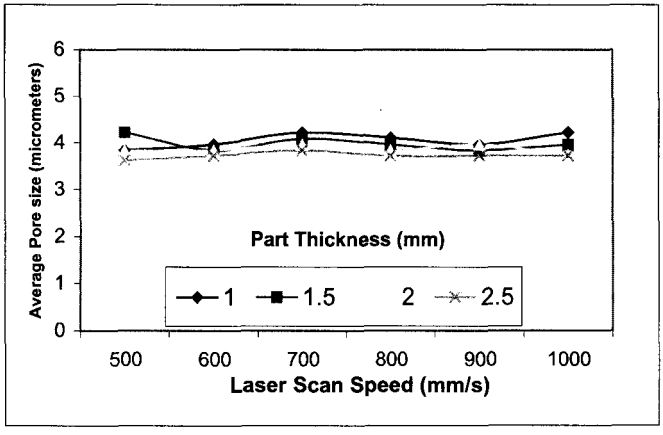

Figure 6: Graph of laser scan speed versus pore size

Examination of the laser scan speed versus the pore size (Figure 6) showed that altering the laser scan speed and part thickness had little affect on the pore size of the parts produced. However, the thinner parts generally had a smaller pore size, but this is not a true indication of the average pore size because the pressure required to pass air through them was less. These results show that to obtain a lower-pressure drop across the structure, the wall thickness must be kept to a minimum.

4.2 Differential pressure characteristics

The filter had a relatively high-pressure loss characteristic compared to a conventional element of similar rating and envelope size. This is due to the low flow area, as the element is not corrugated to the same extent, and also the thickness of the structure.

4.3 Filtration performance

The measure of the efficiency of the particle removal is the filtration or Beta ratio, and the higher the β value the more efficient the filter [8]. The ISO test gives the variation of Beta with particle size and this is a measure of the pore size distribution and the filter's response to a polydispersed contaminant as defined in the standard. The filtration capabilities of the filter are given in Figure 7 where it is compared to a similar test on a hydraulic filter of similar rating.

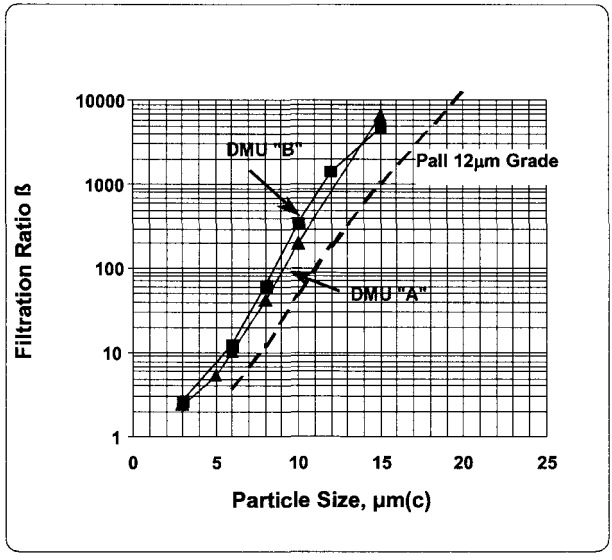

Figure 7: The variation in filtration ratio with particle size

From the gradient of the two filters, it can be seen that the pore size distribution and hence the removal capabilities of the sintered filter are comparable with the standard conventional hydraulic filter, suggesting that laser-sintered filters are suitable for use in fluid filtration. The similarity in the data of the two test samples showed that the reproducibility of the process was good. The data shown in Figure 7 is the average of all data collected to 10 bar differential pressure.

Scrutiny of the filtration ratio with element differential pressure (Figure 8) showed that as the particles accumulated on the surface of the filter, it became clogged and the filtration ratio increased. This is partly due to the pores becoming blocked by contaminant and partly because of the development of a porous 'cake' of

contaminant on the surface of the filter. The variation in performance seen in Figure 7 is considered to be more a function of the development of the surface 'cake' than of the differences in the structure.

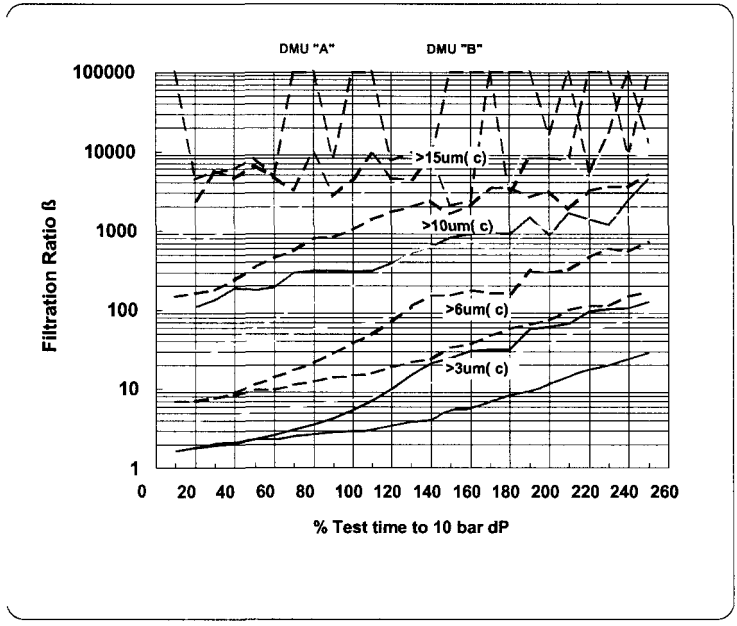

Figure 8: Filtration ratio versus element differential pressure

5. CONCLUSIONS

Test revealed that DLMS parts have a degree of porosity and uniform pore size/structure. The application area of filtration was identified as being suitable and a test filter was manufactured using DM 50μm bronze powder. Filtration tests revealed that the test filters performed successfully at removing contaminants from hydraulic fluid. The pore structure was uniform with a mean pore size of about 8μm. However these parts in their present configuration would not see general use in the hydraulics market as the pressure drop is too high and the dirt capacity is too low. Nevertheless filters manufactured by the DMLS process could be used for the direct protection of critical components where pressure drop and dirt capacity is not an issue but collapse strength is important, and with low viscosity fluids such as solvents, water and gases.

Although the results of this trial look promising, there are a few limitations to overcome before the concept is suitable for hydraulic filters. The two main areas are the high-pressure drop across the structure and the low dirt capacity, which will give rise to service life problems. However in its present form it is eminently suited to low viscosity applications (<5 cSt) and where moderate flow densities are concerned.

6. FURTHER WORK

The pressure drop across the sintered filter could be reduced by decreasing the wall thickness or by lowering the density by increasing the scan speed or hatch spacing of the laser or by using the DM 100μm powder. The reduced wall thickness or part density will result in increased permeability of the part, therefore, reducing the resistance to fluid flow and hence reduce the pressure drop across the structure. However, the parts produced will have reduced strength and problems may arise during their manufacture (i.e. thin sections may fracture due to loading during the recoating process).

Maximising the filtration surface area of the filters would increase the dirt capacity of sintered filters. The dirt capacity can also be increased by reducing the density of the parts resulting in an increase in the number of pores/internal volume hence increasing the volumetric/dirt capacity of these parts.

Acknowledgement

The advice and suggestions of Prof. David Wimpenny, head of the Rapid Prototyping and Manufacturing Group at De Montfort University in preparing this paper is gratefully acknowledged. Thanks also to Pall Europe Ltd for provision of their test facilities and expertise.

References

1. C. Kai and L. Fai, Rapid Prototyping: Principles and Applications in Manufacturing. John Wiley & Sons, 1997
2. M. Agarwala, D. Bourell, J. Beaman, H. Marcus and J. Barlow, Direct selective sintering of metals. Rapid Prototyping Journal, 1995, 1(1), 26-36
3. S. Das, J. Beaman, M. Wohlert and D. Bourell, Direct laser sintering of high performance metal components. Rapid Prototyping Journal, 1999, 4(3), 112-117
4. J. Williams and C. Deckard, Advances in modelling the effects of selected parameters on the SLS process. Rapid Prototyping Journal, 2000, 4(2), 90-100
5. BS 1752:1983 (ISO 4793:1980)- Specification for laboratory sintered or fritted filters including porosity grading
6. ISO 2942:1994-Hydraulic fluid power filters-Verifications of fabrication integrity and determination of first bubble point.
7. ISO 3968:2001-Hydraulic fluid power filters-Evaluation of differential pressure versus flow characteristics.
8. ISO 16889:1999-Hydraulic fluid power filters-Multi-Pass method for evaluating filtration performance of filter element.

Influence of the heat treatment cycles on the properties of selective laser sintered (SLS) Rapidsteel$^{2.0}$

D UZUNSOY and **I T H CHANG**
Department of Metallurgy and Materials, The University of Birmingham, UK

ABSTRACT

Increasing competition in global markets leads the research on developing cost effective manufacturing process techniques. Rapid prototyping (RP) provides invaluable aids for the netshape manufactures of parts with complicated geometries directly from Computer Aided Designs (CAD). Among all rapid prototyping (RP) processes, rapid tooling (RT) has been developed to manufacture accurate tooling parts at a reduced cost within shorter time scales. At present the rapid tooling technology (RT) has been achieved by a combination of Selective Laser Sintering (SLS) of stainless steel powder and infiltration of molten bronze. Such tooling material is known as Rapidsteel$^{2.0}$ and has been developed by DTM Corporation, USA. Typical applications of this kind of material are plastic injection moulding and short-run die casting moulds.

This study offers a comparative evaluation of the mechanical properties of Selective Laser Sintered (SLS) Rapidsteel$^{2.0}$ processed using 30%H_2-70%N_2 and argon atmospheres. The preliminary investigation of the microstructure has shown the presence of chromium rich precipitates in SLS / Rapidsteel$^{2.0}$ parts after partial sintering and infiltration processes. The effect of those precipitates on the mechanical properties of Rapidsteel$^{2.0}$ was determined using both tensile and fatigue crack propagation tests.

KEYWORDS: Selective laser sintering, infiltration, microstructure, and mechanical properties precipitate formation

1. INTRODUCTION

Rapid Prototyping (RP) is an advanced manufacturing technology that offers reduced design-manufacturing cycle time, cost of product and increased competitiveness in the market [1,2]. There are many commercial RP technologies available on the market, such as stereolithography (SLA), selective laser sintering (SLS), laminated object manufacturing (LOM), and fused deposition model (FDM).

All RP systems have advantages and limitations compared to each other. Selective laser sintering (SLS) is one of the most successful rapid tooling processes suitable for a wide range of material [3,4]. For the production of metal tooling, SLS is used to fuse resin coated 316L stainless steel powder to form a green body and this is followed by liquid phase infiltration of bronze for densification with minimal dimensional changes. The tooling material is known as Rapidsteel^{TM} 2.0 and was developed by DTM Corporation, USA. It consists of a composite microstructure of 60 vol.% of 316L stainless steel and 40-vol.% of bronze (Cu-10 at. % Sn alloy). Currently, typical applications of this material are metal inserts for plastic injection moulding and short-run die casting moulds [5]. The aim of this paper is to determine the effects of the sintering/infiltration atmosphere such as N_2: H_2 and Ar atmospheres on the mechanical properties of Rapidsteel^{TM} 2.0 material for rapid tooling applications.

2. EXPERIMENTAL PROCEDURE

The production of Rapidsteel^{TM} 2.0 includes the three main processing steps. These are:

A. SLS Processing:

Rapidsteel^{TM} 2.0 powder is made up of low carbon stainless steel particles (316L) with a mean diameter of 40μm. The particles are coated with a mixture of thermoplastics (e.g. wax and phenolic resin). Selective laser sintering of the as-supplied stainless steel powders was performed using the DTM Sinter Station 2500 in an N_2

atmosphere to avoid oxidation of metal powders. The following conditions were used to produce flat test bars with dimensions of 65×13×18 mm^3: a laser power of 35W; a fill scan spacing of 0.10 mm; a scan rate of 7.62 m/sec; a layer thickness of 0.08 mm; and a powder bed temperature of 130 ^{0}C.

B. **Furnace Processing:**

Green body production was followed by two different heat treatment cycles. The first cycle involved the heating of the part to 1120 ^{0}C at a rate of 120 ^{0}C/hr and holding it for 3 hours to remove the binder and partially sinter the powder. The second cycle involved the heating of the part to 1050 ^{0}C at 120 ^{0}C/hr in the presence of a bronze piece and holding it for 2 hours. This was followed by cooling to room temperature at a rate of 180^{0}C/hr. Two different sintering atmospheres were employed. They were 30% H_2 and 70% N_2 and Ar atmospheres.

Tensile testing was carried out by using circular threaded end tensile test specimens with a gauge length of 18 mm. The ultimate tensile strength (UTS), 0.2% offset yield strength and percent elongation were determined from stress-strain plots. All tensile testing was carried out using a Zwick-1484 computer controlled machine fitted with a load cell of 200 kN, operating at a cross-head speed of 1 mm/min. Fatigue crack growth resistance was conducted on a servohydraulic load frame in load control, with an R ratio (σ min/σ max) of 0.1 and a loading frequency of 100 Hz. The tensile test was performed to generate mechanical property data for comparison with conventional tooling materials. The fatigue crack growth resistance experiment was used to assess the fracture behaviour of RS materials so as to avoid any premature failure during service. Selected fracture surfaces were examined using a JEOLSEM 6300.

3. RESULTS AND DISCUSSION

3.1 Microstructure

During sintering, an interconnected network of stainless steel particles with a distribution of precipitates is formed. This is due to the reaction between the sintering atmosphere and the stainless steel matrix. The type of precipitates formed during the first heating cycle, varied with the different sintering atmosphere. The microstructures of the partially sintered 316L stainless steel parts processed using 30% H_2 and 70% N_2 and Ar atmospheres are shown in figures 1(a-b), respectively. Figure 1c shows the microstructure of an infiltrated sample, which was processed in 30% H_2 and 70% N_2 atmosphere. All three sintering atmospheres have resulted in the formation of chromium rich $M_{23}C_6$ carbides. However, additional Cr_2N was found in samples sintered under 30% H_2 and 70% N_2. The compositions of these phases are shown in table1.

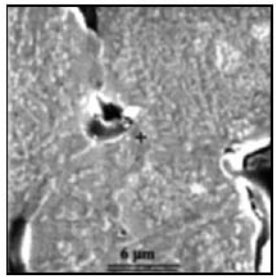

(a)

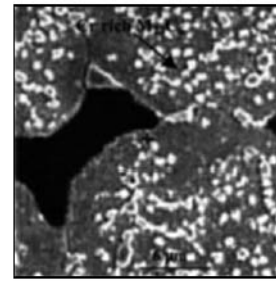

(b)

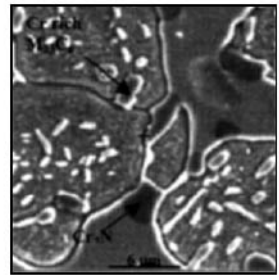

(c)

Figure1: SEM micrographs of samples after partial sintering under (a) 30%H_2-70%N_2, (b) Ar, and (c) after both sintering and infiltration under 30%H_2-70%N_2 atmospheres.

Parts	Atmosphere	Region	Fe	Cr	Mo	Ni	Si	Cu	Sn
			(wt.%)						
As-Supplied		316L SS powder	69.7	17.6	2.2	9.8	0.6	-	-
		Bronze Infiltrant	-	-	-	-	-	92.6	6.5
After Sintering	**30%H_2-70%N_2 Atm.**	SS Particulate	74.3	9.43	1.23	10.8	0.6	-	-
		Precipitate	18.6	64.1	6.9	1.7	-	-	-
	Argon Atm.	SS Particulate	69.6	13.8	2.0	10.5	0.5	-	-
		Precipitate	30.8	53.05	7.5	2.8	-	-	-
After Infiltration	**30%H_2-70%N_2 Atm.**	SS Particulate	69.3	8.02	1.04	10.1	0.6	7.1	-
		Infiltrant	2.04	0.3	-	1.8	-	84.6	11.08
		Fine Precipitate	24.02	54.8	5.5	2.3	-	2.8	-
		Coarse Precipitate	8.7	71.8	7.3	0.5	-	2.5	-

Table1: A summary of EDX results from as-supplied material and in partially sintered sample before and after infiltration

The photographs of the parts after Selective Laser Sintering (SLS) and subsequent heat treatment steps are shown in figure 2. Very little dimensional changes of parts are observed between various processing steps.

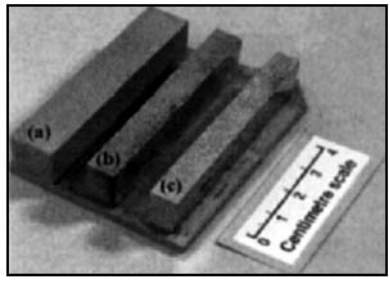

Figure 2: Photographs of (a) SLS, (b) partially sintered and (c) fully infiltrated parts. (b) and (c) samples were prepared for fatigue crack propagation studies

Detailed information about the microstructure of selective laser sintered (SLS) rapidsteel is given in our previous paper [6].

3.2 Mechanical Properties

The tensile stress-strain behaviour of the SLS 316L stainless steel after presintering under 30%H_2-70%N_2 atmosphere is shown in figure 3(a). Figure 3b shows the stress-strain plot of samples sintered/infiltrated using 30% H_2 and 70% N_2 and argon atmospheres, respectively. The fracture strength of partially sintered parts without infiltration was found to be 60-70 MPa as shown in figure 3a. The fracture strength of sintered/infiltrated samples using 30% H_2 and 70% N_2, Ar atmospheres were found to be 740 and 650 MPa, respectively. The increase in tensile strength of specimens sintered in a nitrogen-based atmosphere seems to be due to the presence of Cr_2N resulting from the interaction between powder and atmosphere [7]. The infiltration process improved fracture strength by a factor of ten due to the elimination of porosity. The sintering/infiltration using Ar has resulted in a noticeable increase in ductility due to the elimination of Cr_2N precipitates.

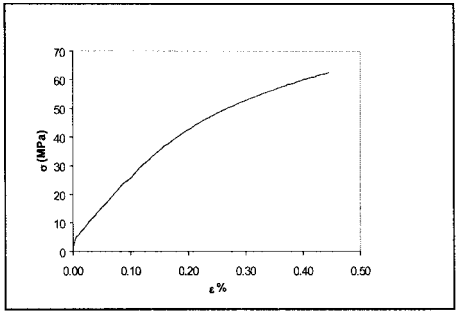

(a)

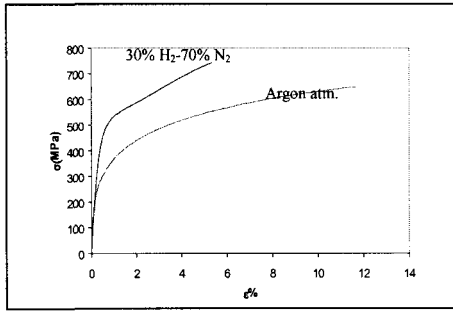

(b)

Figure 3: Stress-strain curves of specimens (a) before and (b) after infiltration in various atmospheres

Materials	Elastic modulus (GPa)	0.2% Offset Yield Strength (MPa)	Ultimate Tensile Strength (MPa)	Strain to failure (%)
Sintered/infiltrated in 30% H_2 - 70% N_2	127	464	747	4.5
Sintered/infiltrated in argon atm.	137.4	282	648	11.7

Table 2: Tensile Properties of selective laser sintered/infiltrated 316L stainless steel in 30% H_2 - 70% N_2 and argon atmospheres

The typical da/dN versus ΔK curve of samples before and after infiltration is shown in figure 4. From the slope of the plot the partially sintered sample shows faster crack propagation rates compared to the infiltrated sample as shown in figure 4. An inherent physical characteristic of partially sintered samples is the presence of pores. Due to the stress raising effects of pores, fatigue cracks tend to initiate from pores [8]. Pores reduce the load bearing cross sectional area and crack propagation occurs along the sintered particle necks. Figure 5a shows the separation of necks between particles. The atmosphere used in the sintering/infiltration processes influence the fracture behaviour as shown in figure 4. For example, the samples prepared using H_2: N_2 give a continuous increase in da/dN with ΔK. However, the sample prepared under Ar atmosphere gives a region of plateau in the da/dN vs ΔK plot. The reason for the difference in da/dN vs ΔK plots between H_2: N_2 and Ar sintered/infiltrated are being investigated.

In the infiltrated sample, open pores are filled with Cu-10at% Sn; this enhances the load carrying capacity and produces some toughening in the material. However, the closed pores remaining in the presintered sample cannot be infiltrated with bronze and they also remained after infiltration. Initiation of crack in the sintered/infiltrated sample is believed to occur at the interface between stainless steel particles and the bronze infiltrant. Crack propagation in the near threshold region occurred in regions of bronze infiltrant as shown in figure 5b. Figure 5b shows localised fatigue striations in a region of bronze infiltrant. Striations occur when plastic strains at the crack tip cause localised slip on planes of maximum shear, thereby producing step-like appearance of striations. In the final failure region, the fracture occurred in the stainless steel.

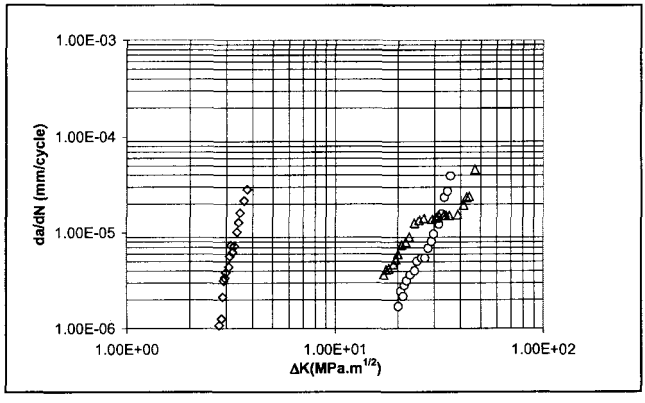

Figure 4: ΔK-da/dN curves of samples before and after infiltration

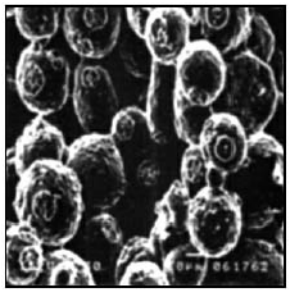

(a)

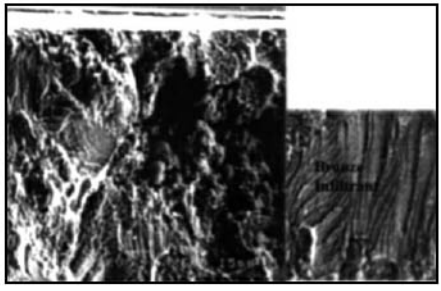

(b)

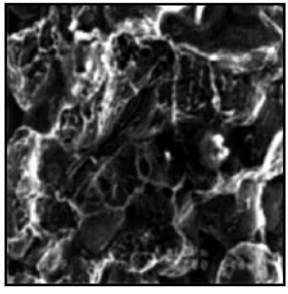

(c)

Figure5: Selected fractographs of (a) partially sintered and (b) infiltrated samples using 30% H_2-70% N_2 (c) sintered/ infiltrated samples using Argon atmosphere from near threshold region

4. CONCLUSIONS

The following conclusions can be made concerning the microstructure and mechanical behaviour of SLS Rapidsteel:

- The microstructure of Rapidsteel mainly consisted of an interconnected network of stainless steel surrounded by bronze infiltrant. Cr rich precipitates are observed in all samples prepared using different sintering/infiltration atmosphere. The type of precipitates varied with different sintering/infiltration atmospheres. The formation of these precipitates occurred as a result of the interaction between stainless steel, residual binder and sintering/infiltration atmosphere.

- The usage of an argon atmosphere has prevented the formation of Cr_2N precipitates. The tensile properties of samples prepared using an argon atmosphere showed a noticeable increase in ductility with a moderate decrease in fracture strength as a result of elimination of Cr_2N.

- Fatigue cracks propagate faster in presintered samples due to the porosity. Infiltration produced some toughening in the material due to pore filling by the infiltrant. Some closed pores remained in the presintered samples even after infiltration and they played an important role in fatigue crack initiation. Crack propagation occurred in the bronze infiltrant. The atmosphere has influenced the fracture behaviour of the Rapidsteel. The exact reason for this is still being investigated.

Acknowledgements

The authors would like to thank Profs. I.R. Harris and M.H. Loretto for the provision of facilities at the School of Metallurgy and Materials, and IRC at Birmingham University, respectively. In addition, Mrs Uzunsoy would like to thank the Turkish Government - Yildiz Technical University for their financial support.

References

1. I.Gibson and D.Shi, Rapid Prototyping Journal 1997,vol.3 no.4, pp.129-136
2. N.P. Juster , Assembly Automation 1994,vol.14 no.2, pp. 14-17
3. DT Pham, S. Dimov and F. Lacan, Proc Instn Mech Engrs 1999,vol. 213 Part B, pp.435-449
4. C.K. Chua, Rapid prototyping: principles and applications in manufacturing, 1997
5. DT Pham, S. Dimov and F. Lacan, Proc Instn Mech Engrs 2000,vol. 214 Part B, pp.107-116
6. I.T.Chang, D.Uzunsoy, P.Bowen, 2001 PM Tech Conference New Orleans, pp5-166 to 5-175
7. P.K.Samal, J.B. Terrel, 1997 PM Tech Conference Chicago, pp 14-55 to 14-65
8. R.M. German and R.A. Queeny ASM Handbook, vol. 19 1994

This page intentionally left blank

Ceramic microcomponents by rapid prototyping process chains

R KNITTER, W BAUER, D GÖHRING, and **P RISTHAUS**
Institute for Material Research III, Forschungszentrum Karlsruhe GmbH, Germany

ABSTRACT

For the fabrication of ceramic microcomponents a rapid prototyping process chain has been developed, combining the fast and inexpensive supply of master models by rapid prototyping techniques with a flexible and precise ceramic shaping technique. In this process chain the design is first generated as a three-dimensional CAD model. The master models are realised as polymer parts by different rapid prototyping techniques, and are then copied into silicone rubber moulds, which can directly be used as tools in low-pressure injection moulding. The final ceramic microcomponents are obtained after debinding and sintering. This process chain enables the fast, accurate and repeatable production of ceramic microcomponents from functional test components to pilot or small series. It is suited for shaping filigree patterning details in the submillimetre range but also enables the fabrication of components with outer dimensions of several centimetres. The quality of the ceramic parts is mostly affected by the quality of the master model.

KEYWORDS: rapid prototyping, ceramic microcomponents, stereolithography, injection moulding, microtechnology

1. INTRODUCTION

To speed up product development and to reduce the costs involved, nowadays rapid prototyping (RP) techniques are increasingly used. Due to the variety of RP techniques that are available and the diversity of processed materials, it is more and more possible to use RP models not only for mere design verification but also as functional test components. For ceramics, different solid freeform fabrication (SFF) techniques have been developed that offer the possibility to fabricate three dimensionally complex shaped parts. Most of these techniques, however, have drawbacks concerning the processibility of different ceramic materials and the attainable manufacturing precision. Methods such as multijet solidification (MJS) [1], selective laser sintering (SLS) [2], laminated object manufacturing (LOM) [3], and fused deposition of ceramics (FDC) [4] still exhibit a limited resolution of several tenth of millimetres, a restricted level of detailing, and mostly a rather high roughness, especially on vertical and inclined surfaces [5]. Since the development of stereolithography (SLA) for the fabrication of three-dimensional polymer objects by Hull [6], the resolution and precision of stereolithography techniques have been improved down to the micrometer range [7-9]. The development of photocurable ceramic-polymer resins [10-12] enables the use of stereolithography based technique for the fabrication of ceramic-polymer composites with higher resolution and precision than the above mentioned SFF techniques for ceramics. However, due to the use of ceramic filled polymer suspensions as resins the resolution is reduced compared to pure polymer resins. While this technique has already been proved to work successfully for the fabrication of macroscopic parts [12], the fabrication of microparts, however, is still a challenge [13-15]. In this case the process is complicated, as powders with small grain sizes have to be used. Thus either the viscosity of the resin will further be increased limiting the spreading of thin layers or the ceramic loadings have to be decreased, hence, often causing problems during binder burnout or sintering.

To circumvent the existing problems of SFF for ceramics and nevertheless benefit from RP techniques, a rapid prototyping process chain (RPPC) has been established, for the fabrication of ceramic microparts or micropatterned ceramics. This RPPC combines the advantages of rapid prototyping as an inexpensive and fast supply of polymer master models and the low-pressure injection moulding (LPIM) as a conventional shaping technique of ceramics. It enables the fabrication of parts of variable sizes made of multiple ceramic materials as functional models or pre-production lots with high moulding precision within a short time [16, 17]. The process chain will be illustrated by different ceramic components and a test pattern.

2. EXPERIMENTAL PROCEDURES

The rapid prototyping process chain presented here, sets out with the design of the components as three-dimensional CAD models. The master models are realised as polymer parts by RP techniques, and are then copied into silicone rubber moulds to be directly used as tools for the low-pressure injection moulding process. The final ceramic microcomponents are obtained after burnout of the organic additives and sintering (fig. 1).

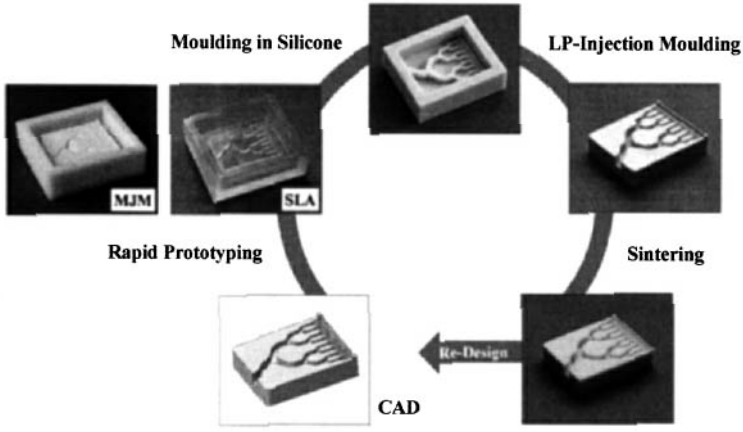

Figure 1: Process steps of the rapid prototyping process chain for the fabrication of ceramic microcomponents. (MJM: multi-jet-modeling, SLA: stereolithography)

2.1 Fabrication of master models and moulds

In the first step three-dimensional CAD models of the components were generated with the expected shrinkage of the ceramic material being taken into account. The CAD data were converted into the standard stereolithography file format "STL". Based on the sliced data, master models were subsequently realised by different rapid prototyping techniques like stereolithography based methods or printing techniques.

In stereolithography a liquid monomer resin is usually exposed by a scanning laser in a layer-wise manner and polymerised, according to the sliced CAD data. Following exposure of a layer, the cured polymer structure is lowered to a certain extent further into the liquid monomer and is then subjected to the next exposure. By repeating this process, three-dimensional parts are generated, which may be applied as master models for the process chain. In a first approximation, the achievable geometric resolution depends on the layer thickness, the beam diameter, and via beam intensity on the interaction volume of the monomer.

A commercial stereolithography facility (FS-REALIZER, Fockele & Schwarze, Germany) was used to produce epoxide master models. This facility has a positioning accuracy of 10 µm, and a solid-state laser with a spot diameter of 100 µm is applied to expose a liquid monomer on a construction platform in a scanning mode layer by layer. The construction platform was lowered in steps of 100 µm.

For higher resolution master models were made of acrylates using the Rapid Micro Product Development (RMPD) at microTEC (Germany) [7]. This modification of stereolithography, which is suited for microdimensioning, allows the process to reach a precision of about 5 µm and enables parallel fabrication of a number of components. Objects with a layer thickness of about 1 µm only may be generated. Besides selective irradiation, parts may also be produced by the RMPD mask technique. This is a combination of mask technology used in photolithography and RMPD, which allows large-area exposure of the monomer layer, and a considerable reduction of exposure times of 2.5-dimensional geometries. The used master models were fabricated in scanning mode with a layer thickness of 10 µm.

At 3D Systems (Germany) master models were fabricated on the new VIPER si2 system (3D Systems, USA) from epoxide (SL 5510) in the high resolution mode, i.e. parts were built in 50 µm-layers and a solid state laser with a beam diameter of 75 µm was applied.

If small-sized holes or narrow trenches are manufactured by stereolithography, often problems arise from partly cured resin in narrow gaps [18]. After removing the part from the resin bath these details can not be sufficiently cleaned from the adherent resin residues and the parts are hence replicated with poor accuracy. For the fabrication of such items a printing method like multi-jet modeling (MJM) should be preferred, where the parts are built by deposition of molten thermopolymers. Models were built on a ThermoJet at 3D Systems (Germany) with a drop size of 90 µm and a layer thickness of 40 µm.

To investigate the potential and limits of different RP processes to be used in the process chain, a test pattern with differently inclined or curved geometric patterns like pyramids and spirals was generated. Some of the pyramids were approximated by preselected steps of 100 or 200 µm in the CAD model (fig. 2). Master models with a side length of 10 mm were fabricated by different techniques. In addition, master models with a side length of 20 mm were built on a ThermoJet based on accordingly scaled CAD data.

Figure 2: 3D CAD model of the test pattern.

The master models were filled with liquid silicone rubber. For epoxide and thermopolymer master models an addition-polymerisation-curing silicone rubber was used (Elastosil M4670, Wacker), while for acrylate master models a condensation-polymerisation-curing silicone rubber (Elastosil M4545, Wacker) had to be applied [19]. To prevent air inclusions, the silicone was evacuated both prior to and after filling. Following the hardening of the silicone, the negative silicone moulds could be used directly as tools for low-pressure injection moulding.

2.2 Low-pressure injection moulding

It has already been proved that ceramic injection moulding has a high potential for the moulding of micropatterned parts made of a variety of materials [20, 21]. For the mass production of ceramic parts high-pressure injection moulding is the most promising process, but it is hardly appropriate for the fabrication of prototypes because of very high tooling costs. In low-pressure injection moulding, however, instead of high viscous thermopolymers, waxes and paraffins are used as binders [22-24]. Due to their low melting points the moulding can take place at temperatures of only 80-100°C and at pressures below 0.7 MPa [25]. As a consequence, polymer moulds or even soft moulds made of silicone rubber may be used as tools.

For the feedstock preparation ceramic powders like alumina (MR 52, Martinswerk, Germany, $d_{50} = 1{,}2$ µm) and zirconia (PYT 05-005, Unitec, UK, $d_{50} = 1{,}0$ µm) were dispersed in a paraffin-dispersant mixture and

homogenised for about 45 minutes. Feedstocks with ceramic loadings of up to 70 vol% were used for the moulding of different components as has been published elsewhere [26]. The maximum loading of the feedstock is limited by the viscosity, necessary to obtain a complete filling of the mould. From experiences gained so far a viscosity in the range of 3-9 Pa·s at a shear rate of 100 s^{-1} should be favoured. As ceramic powders with grain sizes in the submicron range will significantly increase the viscosity, a suitable feedstock will have a lower ceramic loading compared to those of coarser ceramic powders [27]. The ceramic moulding can take place at about 80°C in commercial injection moulding facilities (Peltsman, USA and Goceram I. V., Sweden) or by manual filling of the silicone mould in case of small feedstock amounts or few samples to be produced. In the latter case air inclusions were prevented by repeated evacuation of the still viscous feedstock inside the silicone mould. After cooling down to room temperature the green bodies were carefully demoulded. According to the experience gained so far, each silicone mould usually allows more than 100 ceramic components to be produced without any wear effects being detected.

In the next step the green bodies were submitted to a gradual thermal process up to 500°C for binder burnout and subsequent sintering up to 1700°C e. g. for alumina parts. The thermal treatment has to be carried out carefully to avoid distortion, cracking or warping of the parts. In general, heating rates and dwell times of both steps are also dependent on the size and wall thickness of the parts. The total duration of thermal treatment was in the range of 20-30 hours.

3. RESULTS AND DISCUSSION

The demoulding of the master models from the silicone moulds could easily be carried out, and due to the elasticity of silicone even slight undercuts could be demoulded. Only in case of master models with high surface roughness or high aspect ratios occasionally tiny, free-standing details of the models may be damaged [17]. As the silicone moulding exhibit a very high replication accuracy, every detail or fault, even the roughness of the master models is copied into the silicone mould [17, 19]. Therefore, in case of rough master models the demoulding of ceramic green bodies from silicone moulds is likewise aggravated. While aspect ratios of more than 10 could be fabricated from high quality LIGA master models (LIGA: German acronym for X-ray deep lithography, electrodeposition, and polymer moulding) or models fabricated by mechanical microfabrication [28], aspect ratios of more than 5 are difficult to demould when RP master models are used that always have an inherent surface roughness [18, 19]. Moreover, because of the less suitable properties like the lower hardness of the condensation-polymerisation-curing silicone rubber, in some cases the demoulding of green bodies from the moulds is more difficult than from addition-polymerisation-cured silicone moulds.

After sintering 95-97 % and 93-94 % of the theoretical density were typically achieved in alumina and zirconia parts, respectively. Depending on the ceramic amount of the feedstock the linear shrinkage of parts in the millimetre to centimetre range amounts to respectively 11-13 % and 14-16 % during sintering. As a whole, the replication steps of the rapid prototyping process chain exhibit a very high precision and accuracy in the micrometer range. When optimised feedstocks with high ceramic loadings are used, a high repeatability of the dimensions of structural details can be achieved with a standard deviation of 0.2 % only [17].

Due to the fast and easy feedstock preparation, ceramic components for different applications have been fabricated from a variety of materials such as Al_2O_3, ZrO_2, PZT, $BaTiO_3$, hydroxyapatite, and an electrically conductive Al_2O_3/TiN ceramic by means of this process (fig. 3). The RPPC has already been successfully applied to the development of new ceramic components like PZT transducers for fingerprint scanning devices [27] or alumina microreactor systems for the use in microreaction technology [29]. In both cases the fabrication of functional test components was indispensable for performance tests and the fast redesign of components with properties of the final product was an important advantage of the RPPC. Figure 4 displays details of some modular and exchangeable components that were fabricated for the microreactor system. Due to the layerwise fabrication of the master models by stereolithography (F&S) the 100-µm layers are visible at vertical walls, and each inclined area have to be approximated by steps. These surface characteristics are copied throughout both replication steps of the process chain into the ceramic parts. The detailed view of a static mixer component in figure 4a is moulded with high accuracy, however, revealing a typical roughness at vertical walls. In figure 4b the approximation of inclined surfaces of details of a catalyst carrier plate is evident. It should be pointed out, that only the surface characteristics are replicated in the ceramic part. As the ceramic shaping is done by injection moulding, this apparent layer structure can not cause delamination or damage of the components during thermal treatment.

Figure 3: Variety of microcomponents of different ceramic materials made by the RPPC.

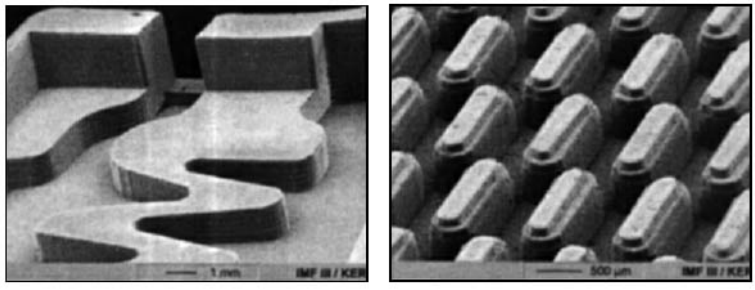

Figure 4: Detailed views of sintered alumina components, moulded from stereolithography master models.

To compare different RP techniques and to investigate the influence of the master model on the quality of the moulding process, differently fabricated master models of the test pattern were replicated in alumina and zirconia.

The acrylate master model fabricated by RMPD with a layer thickness of 10 µm exhibit a high precision. Inclined or curved surfaces of the model are approximated with high accuracy, sharp edges and very smooth steps. Due do the fact that condensation-polymerisation-curing silicone rubber was used, the demoulding of the green bodies, however, was aggravated, and some tiny cones or points of pyramids of the green body were sometimes damaged. The figures 5a and 5b display detailed views of a pyramid and an ellipsoid section moulded in alumina and zirconia, respectively. The slightly rough ceramic surface is a precise replication of the surface characteristics of the master model that seems to be built without the usually applied step of curing the contours of each layer.

The VIPER master model built with a layer thickness of 50 µm displays very smooth surfaces apart from the unavoidable stair-stepping effect at inclined planes and approximates the CAD model with high accuracy. Only few residues were detected in narrow gaps. The replication into ceramic were performed without difficulties.

While inclined surfaces of the alumina part clearly reveal the layerwise fabrication of the master model (fig. 6a), astonishingly, the 50-µm layers are barely visible at vertical walls of the master model or of the ceramic replication of the 200-µm stepped square pyramid (fig. 6b).

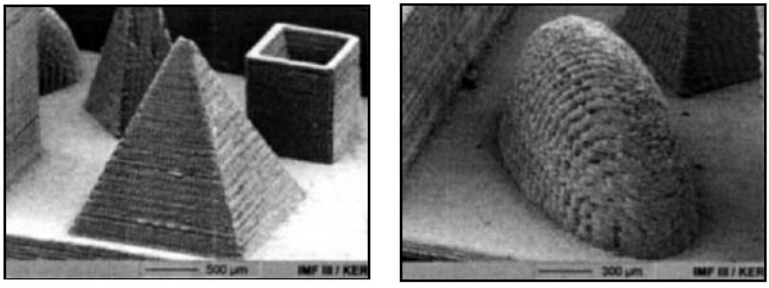

Figure 5: Details of (a) alumina and (b) zirconia components, moulded from an RMPD master model.

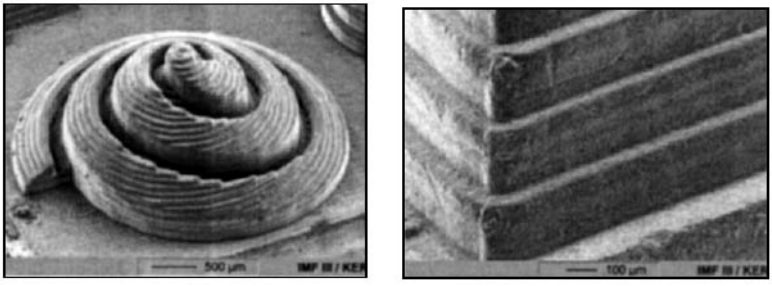

Figure 6: Detailed views of (a) alumina and (b) zirconia components, moulded from a VIPER master model.

In MJM master models of the test pattern with a side length of 20 mm the details of the CAD model are quite well reproduced, considering the lower resolution of this process. The master models with a side length of 10 mm, however, are of poorer quality and demonstrate the limits of this technique. Details like edges are rounded and stepped pyramids nearly have the same appearance as non-stepped ones. Nevertheless, the replication into ceramics could be performed with high moulding precision in both cases. In figures 7a and 7b a stepped pyramid of a zirconia moulding of the larger model is compared with an alumina part moulded from the smaller master model. The surface of the ceramic parts is strongly affected by the characteristics of the MJM process, revealing the droplet shape of the thermopolymer model (fig. 8). When MJM models are used, the roughness of the ceramic surface is dominated by the low resolution in x-y-plane instead by the layered structure of the model.

Because of the excellent moulding capability throughout the replication steps of the RPPC, the quality of the master models is of decisive significance for the reproducibility and the quality of the ceramic components. The resolution and surface quality of the ceramic parts are mainly limited by the resolution of the master models. Compared to this influence the grain size of the ceramic can be neglected in almost all cases. Therefore the RP technique and the resolution should be selected in accordance to the demands of the ceramic component to be fabricated. It should be considered, however, that an improvement of resolution by a factor of 2 will increase the manufacturing time of the master model in stereolithography roughly by a factor of 8. Nevertheless, stereolithography should be preferred when high surface quality and high resolution is required. If the surface roughness is no crucial point and the details to be fabricated are not smaller than about 250 µm, very good results can be obtained by less expensive printing methods like MJM.

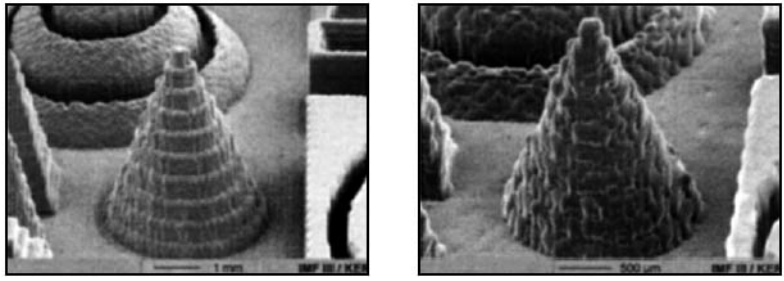

Figure 7: A stepped pyramid of (a) a zirconia and (b) an alumina part, moulded from MJM models of different sizes.

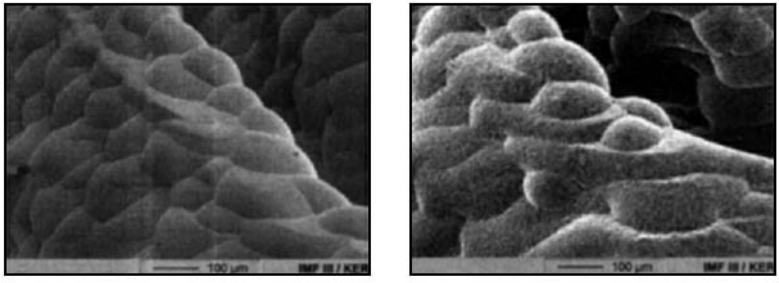

Figure 8: Surface characteristics of (a) MJM master models and (b) the alumina replication.

4. CONCLUSIONS

Ceramic microparts made of a great variety of materials can be fabricated by the rapid prototyping process chain with high moulding precision within a short time. The process chain is suited for the production of functional test components as well as for pre-production lots. Due to the intermediate replication step into silicone rubber, numerous differently fabricated master models can be used, and the demoulding of the green bodies is significantly simplified. The use of RP master models allows for a cost-efficient redesign and an accelerated development of new components. However, the quality of the master model turned out to have a decisive influence on the quality of the ceramic part. The surface characteristics of the master model not only dominate the surface of the ceramic component but also the demoulding behaviour of the green body in case of high surface roughness. The RP technique has to be carefully selected to meet the requirements of the ceramic components to be fabricated.

Acknowledgement

The fabrication of the master models by E. Hansjosten, Forschungszentrum Karlsruhe, F. Cremer and T. Herbert, 3D Systems, Darmstadt, and R. Götzen, microTEC, Duisburg, is gratefully acknowledged. Valuable contributions and significant assistance were provided by Dr. E. Anurjew, B. Dörzapf, E. Emde, and W. Laub.

References

1. M. Greulich, M. Greul and T. Pintat, *Rapid Prototyping J.* 1995, 1 [1] pp. 20-24.
2. K. Subramanuan, N. Vail, J. Barlow and H. Marcus, *Rapid Prototyping J.* 1995, 1 [2] pp. 24-35.
3. D. A. Klosterman et al., *Am. Ceram Soc. Bull.* 1998, 77 [10] pp. 69-74.

4. A. Bandyopadhyay et al., *J. Am. Ceram. Soc.* 1997, 80 [6] pp. 1366-1372.
5. J. G. Heinrich, *cfi / Ber. DKG*, 1999, 76 [5] pp. 29-35.
6. C. Hull, U.S. Patent 4,575,330, 1986.
7. A. Reinhardt and R. Götzen, Proceedings, TCT'99, Nottingham, UK, October 1999, pp. 123.
8. A. Bertsch, P. Bernhard, C. Vogt and P. Renaud, *Rapid Prototyping J.* 2000, 6 [4] pp. 259-266.
9. V. K. Varadan, X. Jiang and V. V. Varadan, *Microsterolithography and other Fabrication Techniques for 3D MEMS* (Chichester: John Wiley & Sons, 2001).
10. M. L. Griffith and J. W. Halloran, *J. Am. Ceram. Soc.* 1996, 79 [10] pp. 2601-2608.
11. C. Hinczewski, S. Corbel and T. Chartier, *J. Eur. Cer. Soc.* 1998, 18, pp. 583-590.
12. F. Doreau, C. Chaput and T. Chartier, *Adv. Eng. Mater.* 2000, 2 [8] pp. 493-496.
13. X. Zhang, X. N. Jiang and C. Sun, *Sensors and Actuators* 1999, 77, pp. 149-156.
14. C. Provin, S. Monneret, H. Le Gall and H. Rigneault, Book of abstracts, IMRET 5, Strasbourg, France, May 2001, pp. 133-135.
15. O. Dufaud and S. Corbel, Proceedings, Euro RP 2001, Paris, France, June 2001.
16. R. Knitter, W. Bauer, B. Linner-Krcmar and E. Hansjosten, in: *Ceramics - Processing, Reliability, Tribology and Wear*, EUROMAT - Vol 12 (Weinheim: Wiley-VCH, 2000) pp. 75-80.
17. R. Knitter, W. Bauer, D. Göhring and J. Hausselt, *Adv. Eng. Mater.* 2001, 3 [1-2] pp. 49-54.
18. R. Knitter, W. Bauer, D. Göhring and P. Risthaus, Proceedings, Euro RP 2001, Paris, France, June 2001.
19. R. Knitter, W. Bauer and D. Göhring, to be published in *J. Mech. Eng. Sci.*
20. V. Piotter, T. Benzler, R. Ruprecht and J. Haußelt, in: *Advances in Powder Metallurgy & Particulate Materials*, Volume 2, Part 5 (Princeton: Metal Powder Industries Federation, 1998) pp. 161-169.
21. V. Piotter, W. Bauer, T. Benzler and A. Emde, *Microsystem Technol.* 2001, 7 [3] pp. 99-102.
22. I. Peltsman and M. Peltsman, *Ceram. Eng. Sci. Proc.* 1981, 2 [9-10] pp. 1006-1010.
23. B. C. Mutsuddy and R. G. Ford, *Ceramic Injection Molding,* Materials Technology Series, (London, Chapman & Hall, 1995).
24. R. Lenk, *cfi / Ber. DKG*, 1995, 72 [10] pp. 636-642.
25. J. A. Mangels, *Am. Ceram. Soc. Bull.* 1994, 73 [5] pp. 37-41.
26. P. Risthaus, D. Göhring and R. Knitter, in: *Key Engineering Materials* Vol. 206-213, Euro Ceramics VII, Part 1 (Switzerland: Trans Tech Publications, 2002) pp. 337-340.
27. W. Bauer and R. Knitter, to be published in *J. Mater. Sci.* 2002.
28. W. Bauer, R. Knitter, G. Bartelt, D. Göhring and E. Hansjosten, Book of Abstracts, HARMST 01, Baden-Baden, Germany, June 2001, pp. 145-146.
29. R. Knitter, D. Göhring, P. Risthaus, and J. Haußelt, *Microsystem Technol.* 2001, 7 [3] pp. 85-90.

Experimental investigation of the direct metal laser re-melting of dissimilar metals

S POGSON, P FOX, and **W O'NEILL**
MSERC, The Department of Engineering, The University of Liverpool, UK

ABSTRACT

The Direct Metal Laser Re-melting of powder beds containing H13 tool steel powder and copper powder in different concentrations has been investigated. A range of metallographic techniques has been used to identify the effects of the major process variables (laser power, laser scan speed, beam overlap, composition) on the microstructures formed. It was found that the alloys in this system could be processed successfully over a wide range of parameters, but that the composition of the powder bed has a significant effect on sample morphology. This paper will discuss the problems involved when creating a layered structure of more than one metal using this Rapid Prototyping process.

1. INTRODUCTION

Direct Metal Laser Re-melting (DMLR) is a rapid prototyping/manufacturing process, based on Selective Laser Sintering (SLS), which can produce structural net shape metallic components. Selective laser sintering uses a laser to sinter together powders so as to produce a green component that is then further processed to produce the final item. It is a well-developed process that can produce parts from metal, ceramic or thermoplastic powders. There are, however, some limitations to the technique in that it requires the use of special powders containing 'binding' agents and does not produce fully dense components without a further infiltration stage. In comparison DMLR is a fairly new process that has up to now only had limited use. However, Morgan et al showed the viability of the process, when they produced almost 100% dense components in 316L stainless steel [1]. The major difference between SLS and DMLR is that whereas SLS utilises a low power (<50W) CO_2 laser to heat a metal powder to below its melting point, DMLR uses a high power (90W) Nd:YAG laser to directly melt the metal powder.

DMLR is in some ways similar to Laser Surface Alloying (LSA), in that a powder is melted onto a surface so as to build up the surface and, in the process, the microstructure or composition may be modified. However, the two processes have some significant differences, which make DMLR more suited to the production of accurate components. With LSA the powder is blown into the laser beam by a carrier gas were it is melted. The laser also melts the substrate so that the molten powder and the substrate alloy together. The beam diameters and laser power used in LSA are significantly greater than those used during DMLR and so the microstructures that can be formed are often much coarser. For example, Zeng et al selectively laser alloyed high nickel ductile iron with copper to modify its corrosion resistance [2]. They produced a layer over 200μm thick that had thorough mixing of the copper with the ductile iron. With DMLR the aim is use a laser with a much lower power and a smaller beam size so as to produce more complex structures with controlled mixing of the different components.

With DMLR the powder is pre-placed as a thin layer and the laser is then scanned across the surface melting the powder, thus structures are built up on a layer-by-layer basis. Although this process allows the building of complex structures they have always been formed from a single composition powder. This paper reports some initial work on the use of DMLR with mixed powders that have significantly different melting points and limited solubility in the solid state. Although all published work on DMLR has used 316L Stainless Steel, a more useful material from an industrial viewpoint would be a tool steel possibly with copper cooling channels. Therefore, this work will consider the interaction of H13 tool steel and pure copper, an understanding of this system being important if components with graded structures are to be produced.

Previous research has shown that variables such as temperature, heating rate and cooling rate affect the diffusion of one metal into another. Ping Shen et al showed that copper diffusion into iron was very temperature sensitive with copper penetrating rapidly up grain boundaries and between iron particles when the temperature exceeded 1083°C, the melting point of copper [3]. The presence of copper on the grain boundaries of the steel will have a

significant effect on the properties of the components produced, especially at higher temperatures and, therefore, should be minimised.

As the DMLR processing of H13 and copper will involve heating the metal to over 1450°C (the melting point of the bulk compositions considered), the interdiffusion of copper and H13 will have a significant effect on the microstructures observed. Also, the processes that occur during the rapid heating and cooling of mixed powders are significantly more complex than those observed with the processing of a single powder type. On heating the different powders will behave as two completely different systems each undergoing the phase transformations predicted by the relevant equilibrium diagram. Only when one of the powders melts will there be any significant mixing between the materials. The mixing will be fairly rapid in the convection currents within the melt pool, assuming that there is no significant surface oxidation of the powders, which may act as a barrier. On cooling, regions where no mixing has occurred will freeze according to the phase diagrams for the individual systems but in regions where mixing has occurred a more complex microstructure will be observed.

H13 is a chromium-molybdenum hot working steel, which can be used under both hot and cold work conditions. It is resistant to thermal fatigue and has a high toughness when used conventionally. To obtain optimum properties it requires a complex annealing treatment. In this report the properties of the DMLR processed H13 will not be considered but only its interactions with copper during processing.

2. EXPERIMENTAL PROCEDURE

This research considered the effects of build process parameters on samples produced by the Direct Laser Re-Melting of dry mixed powders of copper and H13 tool steel. The H13 powder was provided by Osprey Powders Ltd (nominal composition is given in Table 1) and a powder particle size distribution of 80% < 5 μm, i.e. 80% of the powder particle size is less than 5μm. The Cu powder was supplied by the same company and was OFHC 99.99% Cu with a particle size distribution of 80% < 22 μm, i.e. 80% of the typical powder is less than 22μm in size, which provides a mean size of 12μm.

Element	**Fe**	**C**	**Cr**	**V**	**Mo**	**Si**	**Mn**	**Ni**
Nominal Composition (wt %)	Bal	0.4	5.2	1.0	1.5	1.0	0.4	0.3

Table 1: Composition of H13 Tool Steel

The powders were mixed by adding a measured quantity of each powder (wt%) to a mixing vessel and then stirring vigorously for approximately ten minutes. The mixture of powders was poured into an aluminium tray of internal dimensions 70mm x 50mm x 7 mm high and compacted to produce a pre-placed powder bed. This procedure was repeated three times so as to produce three beds with different ratios of copper to tool steel (Table 2).

Composition A	75wt% (80% < 22μm) Cu and 25wt% (80% < 5μm) H13;
Composition B	50wt% (80% < 22μm) Cu and 50wt% (80% < 5μm) H13;
Composition C	25wt% (80% < 22μm) Cu and 75wt% (80% < 5μm) H13.

Table 2: Consistency of the three compositions used

The laser was programmed to produce a 5 x 5 array of coupons (1cm x 1cm) (Fig 1) each coupon having different laser parameters. The parameters that were changed during these particular experiments were laser scanning speed (varying from 150mm/s to 250mm/s) and laser power (varying from 45.8W to 68.6W). The laser spot size used was approximately 100μm diameter and subsequent scan line used a 25% beam overlap. All laser processing was carried out under nitrogen, the system being pulled under vacuum and back-filled three times

before laser processing was started. Thus each sample consisted of one layer, which was thinner than the powder bed depth so as to avoid interaction with the substrate.

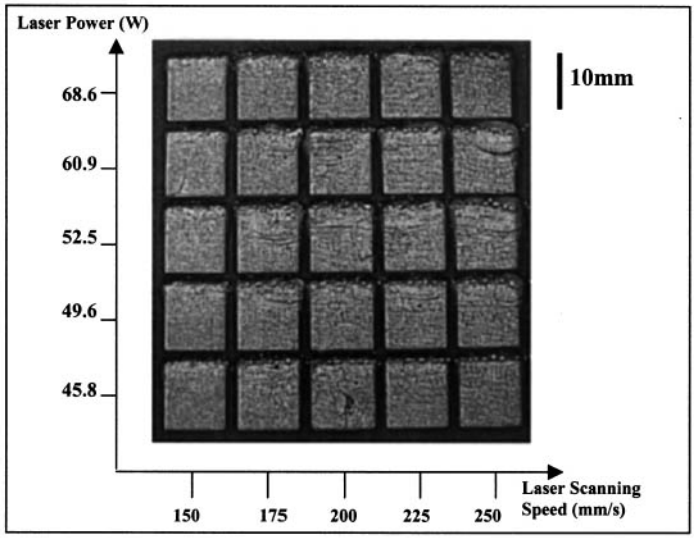

Figure 1: First Array showing the relationship between laser power and laser scan speed.

After scanning each powder bed, the coupons were carefully removed and gently cleaned to remove any excess powder. From the 75 coupons produced, six were selected, two samples from each composition, one set with a laser scanning speed of 175mm/s and laser power of 49W and the second with a laser scanning speed of 250mm/s and a laser power of 52.5W. Although a number of laser parameters can be altered they can be combined in to a single term known as the 'Andrew Number' [4].

$$A_n = \frac{P}{v \times d}$$

Where: P = Laser Power (W), v = Laser Scan Speed (m/s), d = Scan Spacing (m)

The cleaned coupons were analysed using a range of techniques (SEM/EDS, optical microscopy and micro-hardness) both of the surface and in cross-section. All surface examination was completed before the samples were sectioned and mounted using a cold mounting resin. Standard metallographic techniques were used to prepare the samples and they were etched using either 5% nital or aqueous ferric chloride to reveal the microstructures formed.

The use of cold mounting resin, rather than hot mounting, reduced the chances of damaging the samples during mounting but meant that the samples were non-conductive. They were, therefore, sputter coated with a thin layer of gold before SEM analysis. Both backscattered electron and secondary electron images were produced, while EDS was used to identify the elements present. A thin window EDS detector was used allowing the detection of lighter elements. Micro-hardness analysis was carried out across the specimens to produce hardness profiles to confirm the results produced by the EDS analysis.

3. RESULTS

Six samples of three compositions and two processing parameter sets where chosen from the 5x5 arrays, for full examination. However, optical examination showed that all the samples had one feature in common, the top surface was always copper coloured, while the bottom was similar in colour to the powder bed.

SEM analysis of the surfaces of the six specimens can be seen in Fig. 2. The micrographs show that two types of surface morphology were produced, the 50%Cu, 50%H13 and 75%Cu, 25%H13 samples showing 'balling', while the 25%Cu, 75%H13 samples where fairly flat. With the samples that showed balling there was no obvious alignment of any surface features with the movement of the laser beam, but with the flatter samples there were lines on the surfaces that were parallel to the laser scan directions. The difference in behaviour with the different powder mixtures was unaffected by the processing parameters and as all the experiments were carried out on the same day under the same conditions the differences observed must be due to the alloy compositions.

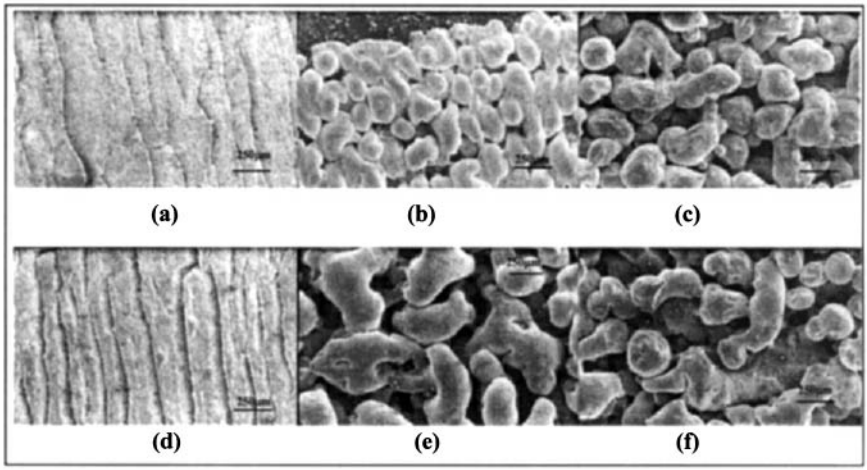

Figure 2: SEM Micrographs showing the surfaces of the six selected coupons with a) 25% Cu, 75% H13; b) 50% Cu, 50% H13; c) 75% Cu, 25% H13 composition produced with a 250mm/s laser scanning speed and 52.5W laser power. And d) 25% Cu, 75% H13; e) 50% Cu, 50% H13; f) 75% Cu, 25% H13 composition produced with a 175mm/s laser scanning speed and 49.6W laser power.

After surface analysis the samples were mounted, polished and etched to reveal their microstructure. Figure 3 shows the microstructures observed with different compositions and processing parameters, again it can be seen that the 50%Cu-50%H13 and 75%Cu-25%H13 samples are similar, while the 25%Cu-75%H13 samples behaved very differently. The samples richer in copper (50%Cu-50%H13 and 75%Cu-25%H13), where the molten metal balled up, showed two distinct regions, one iron-rich and the other copper-rich. The iron-rich regions are present as round precipitates with a range of sizes (Fig. 3c). However, each globule of metal tended to contain one or two large iron-rich regions and many smaller ones (Fig. 3e). Within each iron-rich region could be seen a fine needle structure and sometimes copper-rich precipitates (Fig. 4). The microstructure of the copper-rich regions was less distinct but was similar to a cast structure. With the samples that were flatter (25%Cu-75%Fe) the microstructure was finer and less distinct. It was also observed that these samples contained voids, which were not observed with the samples with the other compositions. However, there appears to be a mixing of the different phases. The ratios of the Fe, Cu and Cr kα peaks (from the EDS analysis) were plotted for different points across the coupons (Fig. 5). The upper surfaces were copper-rich, which is in agreement with the optical observations. Micro-hardness tests were also carried out and the data plotted against distance from the upper surface (Fig 6). Importantly, Fig, 6a shows that the microstructure of the 25%Cu75%H13 sample was fairly uniform but that the sample was harder nearer the lower surface. In comparison the other samples showed great variation in hardness due to the coarser microstructure, the indenter

sampling the different iron- and copper-rich phases. Analysis of the iron-rich regions using microhardness (Table 3) showed that there was a large variation in hardness and confirms that although these regions are iron-rich they will also contain copper rich phases.

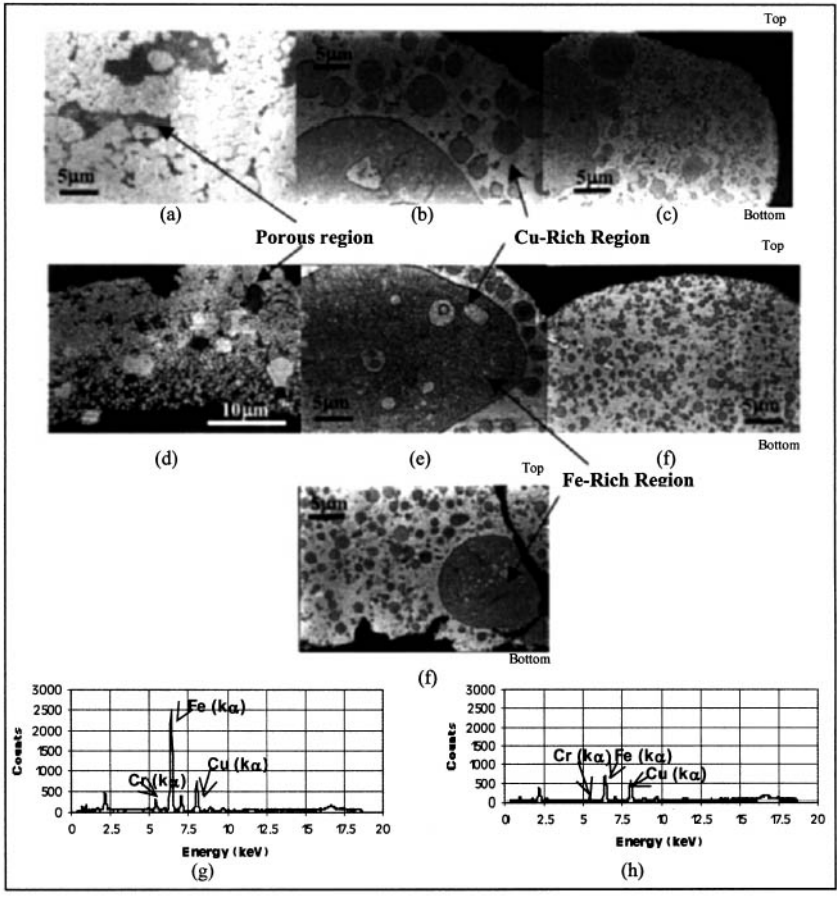

Figure 3: SEM Micrographs showing sections of the coupons produced with a) 25% Cu, 75% H13; b) 50% Cu, 50% H13; c) 75% Cu, 25% H13 composition produced with a 250mm/s laser scanning speed and 52.5W laser power and d) 25%Cu, 75% H13; e) 50% Cu, 50% H13; f) 75% Cu, 25% H13; g) 75% Cu, 25% H13 (alternative view) with a laser scanning speed and 49.6W laser power. EDS spectra highlighting g) Fe-rich region (0.12mm from upper surface); h) Cu rich region at upper surface, for specimens produced with a 50%Cu, 50% H13 composition, laser scanning speed of 175mm/s and a laser power of 49.6W.

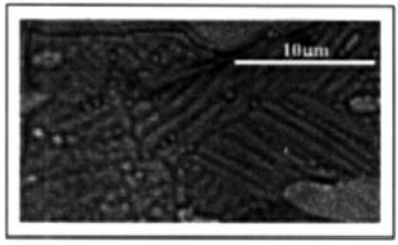

Figure 4: Optical microscope showing Fe-rich region on coupon produced with a 75% Fe, 25% Cu composition produced with a laser scanning speed of 250mm/s and a laser power of 52.5W.

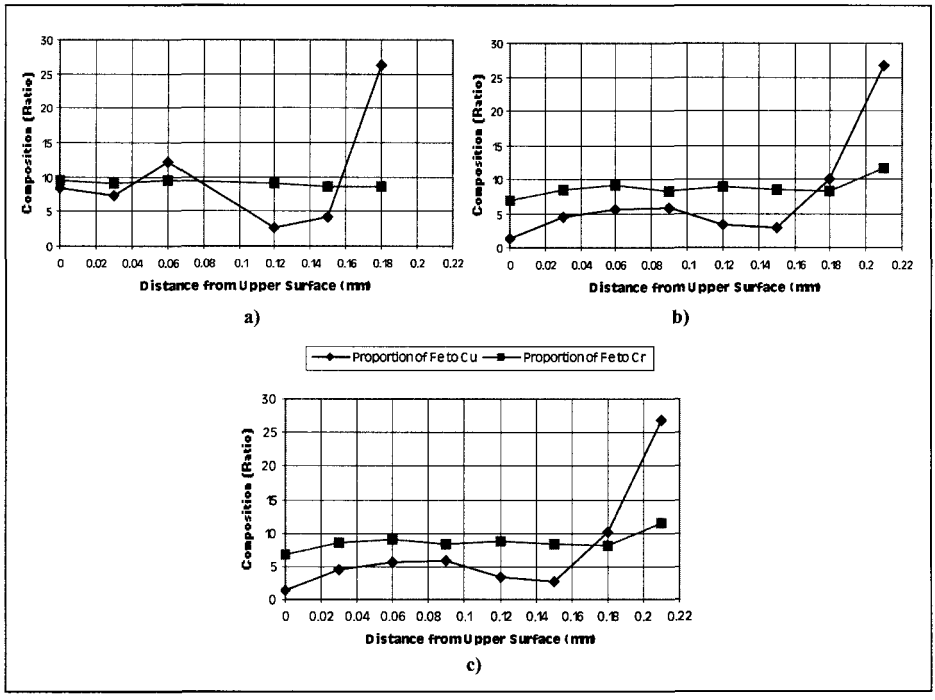

Figure 5: Plot of varying composition of Fe to Cu with distance from the upper surface derived from the EDS spectra with a) 25% Cu, 75% H13; b) 50% Cu, 50% H13; c) 75% Cu, 25% H13 composition for the three coupons produced with a laser scanning speed of 175mm/s and a laser power of 49.6W.

Coupon	VICKERS HARDNESS No.	
	Fe-Rich Region (Range)	Cu-Rich Region
25% Cu, 75% H13. v = 250mm/s, P = 52.5W	243.4 - 383.1	70.7
50% Cu, 50% H13. v = 250mm/s, P = 52.5W	316.6 - 383.1	101.7
75% Cu, 25% H13. v = 250mm/s, P = 52.5W	285.2 - 401.1	105.1
25% Cu, 75% H13. v = 175mm/s, P = 49.6W	236.5 - 424.5	54.7
50% Cu, 50% H13. v = 175mm/s, P = 49.6W	379.7 - 401.1	99.4
75% Cu, 25% H13. v = 175mm/s, P = 49.6W	338.6 - 428.6	84.7

Table 3: Table showing results of micro-hardness measurements (Vickers Hardness No.) across discrete Fe-rich and Cu-rich regions of the six selected coupons.

4. DISCUSSION

The samples examined were produced using two sets of scanning parameters, one with a laser scanning speed of 250mm/s, a scan spacing of 0.075mm, 25% overlap with a 100μm beam diameter and 52.5W laser power, giving an Andrew Number of 2.8J/mm^2. The other samples where produced with a laser scanning speed of 175mm/s, a scan spacing of 0.075mm and a laser power of 49.6W and had an Andrew Number of 3.8J/m^2. Thus, the different samples sets were produced with a significant difference in 'energy density'; however, there is little difference between the two sets of results. This implies that there is a large 'process-window' where the powder beds can be melted.

The research presented in this paper considers the laser melting of discrete powders of copper and H13 tool steel as a precursor to developing graded structures by this technique. The microstructures formed must be understood by considering the relevant phase diagrams, so that suitable build strategies can be developed to allow graded structures to be produced.

To understand fully the processes that are occurring a phase diagram for Fe-Cr-V-Mo-Si-C-Cu should be used, but unfortunately is not available. Instead in the analysis presented here the Fe-Cu-C, [5], and the Fe-Cu [6] diagrams will be used to describe the interaction between H13 and Cu. From the Fe-Cu phase diagram and for the compositions used, it would be expected that the alloys would start to melt at 1094°C and would be fully molten and fully miscible between 1400-1450°C. However the Cu-Fe-C diagram shows that the presence of carbon has a significant effect on the phases formed and leads to a miscibility gap, producing two immiscible liquids at some compositions. This miscibility gap is due to the low solubility of carbon in copper and will be increased by the presence of other elements such as silicon [7]. Thus when some of the alloys melt they are likely to form two liquids, one rich in copper and the other rich in iron.

At the start of these experiments the materials are present as discrete powders and each powder will behave independently on heating until one of the components melts. Only at this point will alloying start, as the liquid wets and then reacts with any solid material. The process is made more complex by the interaction of the laser beam with the powders. Firstly the Cu and H13 powders are different sizes and, therefore, have different surface to volume ratios. As the laser energy is absorbed only through the surface, a larger particle will take longer, than a smaller one, to reach a given temperature. A second complication is that the powders are of different metals and, therefore, absorb different amounts of radiation. The third effect is that the powders melt at different temperatures.

Another factor affecting the interaction of the powders is the presence of moisture, organics, adsorbed gases, and oxide/nitride films on the powder surface. These contaminants will affect the wetting of the powders on

melting and may also degrade mechanical properties [8]. The presence of an oxide on the powder surface will not only reduce wetting by altering the contact angle, [9] but will also increase the apparent viscosity and reduce flowability, as the oxide will be solid at the temperatures considered The use of an inert atmosphere in these experiments will reduce the oxidation of the melt but not affect other materials on the powder surfaces.

If the effects of size and absorption are small then the first region to melt will be the copper particles (1083°C), with the copper forming a melt pool as the temperature rises. If the solid H13 has time to react with the molten copper then it will dissolve to some extent. With laser heating the heating rates are very rapid and so interactions between the molten copper and the solid H13 are likely to be very limited and most of the H13 will melt at 1500-1530°C. For both the 50%Cu, 50%H13 and 75%Cu, 25%H13 samples, there are copper- and iron-rich regions and these are most likely formed by the two immiscible liquids. The copper-rich region makes up the matrix with iron-rich particles within it. Some of the particles are the same size as the original powder and probably melted and refroze without interacting with other particles. Within each region there was normally one or two larger iron-rich regions, which may have formed by Oswald Ripening or by the agglomeration of particles due to incomplete mixing. In these alloys the iron-rich regions are widely spaced and the copper-rich liquid will be able to flow easily allowing the material to 'ball'.

With the 25%Cu, 75%H13 samples the material remained reasonably flat and showed no tendency to ball up. The lines observed on the surface are likely to be due to 'powder robbing'; material being pulled into the melt pool as the laser passes nearby. This difference in behaviour between the 25%Cu, 75%Fe samples and those produced with the other compositions must be due to the way in which the alloy melts. The copper in the 25%Cu, 75%Fe will start to melt at the same temperature as before but there is only a limited amount of liquid formed and only a small amount of the H13 can dissolve in it. Thus, most of the H13 will melt when the temperature exceeds 1500-1530°C. Thus for most of the heating cycle the system will behave like a sintering process with one liquid phase. As with sintering the molten copper will wet and flow round the H13 particles, but when melting of the H13 occurs it will keep the H13 particles apart, stopping agglomeration of the molten particles. Thus for most of the heating and cooling cycle the 25%Cu, 75%H13 powder bed will be more viscous that the other compositions and less able to flow.

There is evidence of full melting in that iron is present in the copper-rich phase and copper in the iron-rich phase. The iron-rich liquid will freeze by the formation of austenite with copper in solid solution. As the temperature drops more austenite will form and the remaining iron-rich liquid will become richer in copper. The austenite will then transform to ferrite with the copper precipitating out at grain boundaries.

The laser beam used here was continuous wave and so the powder bed was exposed to the heat source for a longer time than if pulsing was used. Also the sample is subjected to multiple heating and cooling, as subsequent scans are processed, probably leading to further nucleation of copper-rich precipitates in this case within the iron-rich grains.

5. CONCLUSIONS

The structures formed during the laser re-melting of H13 and copper are due to the interaction of two immiscible liquids with iron- and copper-rich regions forming. It has been shown that the production of functionally graded materials requires not only the careful control of the heating and cooling of the sample but also an understanding of the interactions of the powders that form the graded structure within the component. The production of flat rather than balled materials was controlled, in this case, not by the process parameters but by the interaction of two immiscible liquids and that the microstructures produced were a consequence of their formation.

Acknowledgements

The Authors would like to thank the EPSRC for their financial support of this work and Osprey Metals.

References

[1] Morgan, R., C. J. Sutcliffe, et al. (2001). "Density Analysis of Direct Metal Laser Re-Melted 316L Stainless Steel Cubic Primitives." Rapid Prototyping Journal.

[2] Zeng, D. W., C. S. Xie, et al. (2001). "Investigation of Laser Surface Alloying of Copper on High Nickel Austenitic Ductile Iron." Materials Science & Engineer **A000**: 1 - 9.

[3] Shen, P., J. Hu, et al. (1999). "A Study on Laser Sintering of Fe-Cu Powder Compacts." Metallurgical and Materials Transactions **30A**: 2229-2235.

[4] Williams, J. D. and C. R. Deckard (1998). "Advances in Modelling the Effects of Selected Parameters on the SLS Process." Rapid Prototyping Journal **4**(2): 90 - 100.

[5] (1997). Alloy Phase Diagrams. ASM Handbook. Ohio, ASM International. **3:** pp 27, 28.

[6] (1958). Constitution of Binary Alloys. M. Hansen. New York, McGraw Hill**:** pp580-582.

[7] Smith, C. S. (1934). Journal of the Institute of Metals **54**: p251.

[8] Das, S. (2001). "On Some Physical Aspects of Process Control in Direct Selective Laser Sintering of Metals - Part 1." Solid Freeform Fabrication Symposium Proceedings, 2001: pp85-93.

[9] Asthana, R. and N. Sobczak (2000). "Wettability, Spreading and Interfacial Phenomena in High-Temperature Coatings." JOM-e **52**(1): pp1-20.

This page intentionally left blank

Rapid manufacturing of complex shapes by electrochemical machining

R TEMUR
Centre for Rapid Design and Manufacture, Buckinghamshire Chilterns University College, UK

ABSTRACT

This paper presents an integrated approach of electrochemical machining (ECM) by combination of three elements: a special tool electrode design, a graphic-analytic simulation of the process and an ECM machine based on adaptive control system. The workpieces machined are measured and analysed to evaluate the geometrical a dimensional accuracy improvements.

1. ELECTROCHEMICAL MACHINING

The electrochemical erosion processing method is an anodic dissolution process where the work piece is the anode and the tool electrode is the cathode for an electrochemical cell. A low voltage (7-25V) is applied between these two electrodes and the electrodes are positioned at a small distance from each other (0.025 – 0.5 mm). The electrolyte, usually a solution of NaCl or $NaNO_3$, is forced to flow at high speed between the two electrodes (30-60 m/s) in order to remove the residual material from the working area.

Electrochemical erosion processing was developed mainly to produce high complexity shapes and to manufacture alloys with high melting points and mechanical hardness (like those based on Ti, Fe/Co/Ni/Cr) from the aerospace industry. This type of steel is difficult to manufacture by conventional procedures because of low productivity and a short tool life. The characteristics of electrochemical erosion processing areas follow: it is a process carried out exclusively by chemical reactions; the mechanical characteristics of the material will not affect the processing; the temperature within the working area should not exceed the temperature limit of the electrolyte, the shape and the dimensions of a work piece are dependent on the shape and dimensions of the tool electrode as well as the size of the gap between this and the work piece.

In recent years, electrochemical erosion processing has been used more and more for obtaining a large variety of components such as: turbine blades aircraft, surgery implants, special cages for bearings, molds and dies, and so on. The reason for choosing this process is the ability to make more complex details and complicated shape contours, without distortions, scratches and internal stress. There are approximate 17 distinct methods for electrochemical erosion and here we can include electrochemical grinding, electrochemical burring (trimming), and electrochemical drilling for special shapes. It is difficult to estimate the number of electrochemical units in use at this moment in industry because aerospace or other specialists companies generally use these machines outside the public domain.

In conclusion the main advantages of electrochemical erosion processing are: a easy way to manufacture hard materials; this method will not produce residual stress in the work piece, the possibility of obtaining multiple of parts without distortion, a relatively good speed of processing, a good surface finish (0.1 up to 10 μm).

As well as advantages there are unfortunately drawbacks such as poor geometrical tolerances and a limitation in the estimation of final shape for the work piece. Also designing tools for producing high complexity shapes for this type of process is still a problem and a huge challenge. The designing process for tool-electrodes is still in its empirical stage and a scientific rationale has not yet been reached [1-4].

2. ECM - INTEGRATED APPROACH

The main objectives of this work were to improve the shape of work pieces machined by ECM, to increase the dimensional accuracy and to obtain a more stable and controllable process. For achieving these objectives an original approach of electrochemical machining was developed and tested.

This proposed approach represent a COMPLETE SOLUTION for electrochemical machining because involves a combination of process simulation, tool electrode design and automate control system for execution of desired work piece as is resulted from figure 1.

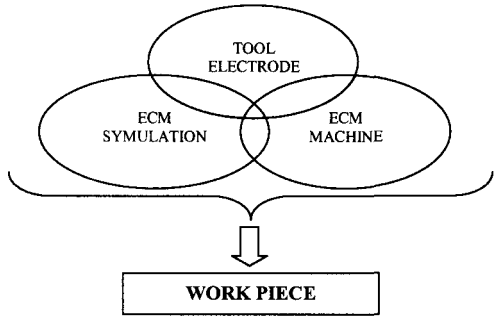

Figure 1: Obtaining the work piece in ECM machining

It is a SIMPLE SOLUTION because it is making the correct simplification for reduction of complicated mathematical models that characterise this process, without affecting the electrochemical phenomena. This allows writing the simulation program, which is reproducing machining conditions having as a result, the predicted shape of work piece. The applied approach is a RAPID SOLUTION due to special technique presented for tool electrode construction using rapid prototyping technique. Also, the automates control system is easy to implement and provide an efficient control and command

3. THE SIMULATION PROGRAM

Electrochemical machining is a complex process. Because it is difficult to derive a mathematical model by analytical methods, a combined graphic and analytic method was used for work piece determination.

The AutoCAD graphic editor was used for graphic component and AutoLisp program language for analytical solution. The simulation procedure was written based on mathematical model of an ideal electrochemical machining [5]. The simplification assumption characteristics to an ideal model were eliminated later by a tool electrode correction procedure and by measuring process perturbations within adaptive control system embedded into ECM machine. The perturbations from process as electrolyte temperature, pressure and tool electrode displacement are measured with appropriate sensors. The tool electrode correction is based on differences between simulated and desired work piece shape. This tool is used with the adaptive electrochemical machine proposed to obtain the real work piece.

4. THE TOOL-ELECTRODE

By using a Rapid prototyping master mould and electroforming copper onto this surface a tool electrode was obtained with a shape identical with the shape obtained from the simulation of electrochemical machining. Also a conventional CNC milling method was applied to execute a second tool electrode based on the same shape. Both this two electrodes are presented in figure 2 and 3.

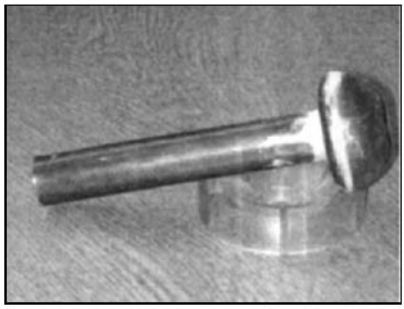

Figure 2: RP and electroforming Tool

Figure 3: CNC tool electrode

Time required to construct the tool electrode by CNC milling is bigger than time needed for RP tool electrode (when the same level of surface finish and accuracy is imposed). Also for complicated shapes of tool electrodes is much easy and cheaper to obtain this shape by the method of electroforming in RP mould model. Thus, the corrected tool electrode obtained by electroforming in RP mould parts was used in a real electrochemical machining process with the objective to verify the integrity of this electrode after processing and the accuracy of work piece obtained.

5. ECM MACHINE PROPOSAL

The computer used as a central control unit in the realised automatic controlled system is addressed to survey, command, diagnose and forecast the functioning of the electrochemical erosion installation.

Different to the traditional equipment this system includes a modular structure named process coupler (PC) that realises the information transmission from the controlled process to the computer and from the computer to the performing elements in the controlled process. The connection between the computer and process is realised as is shown in the figure number 4.

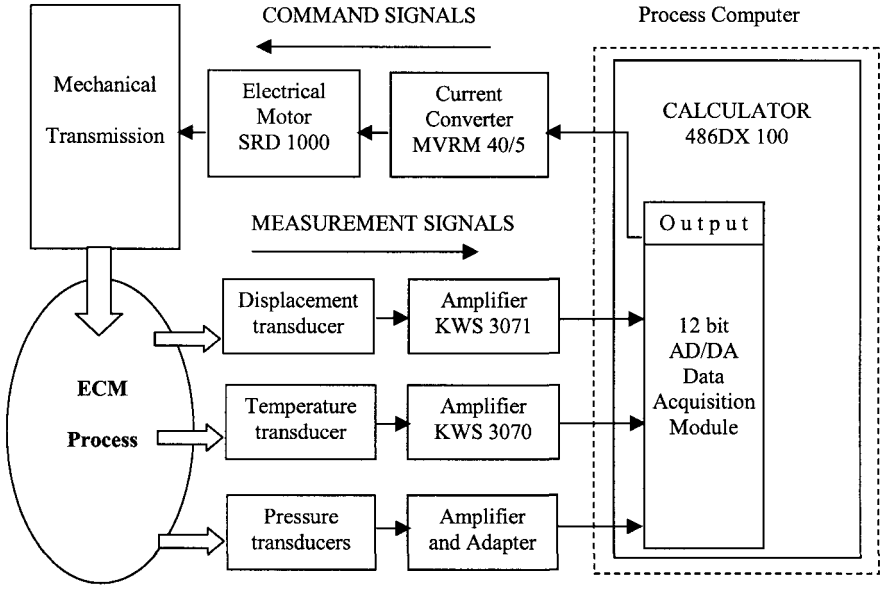

Figure 4: Process computer integration in ECM control system

The construction solution for assembly of all transducers on the moving tool-electrode slide is presented in figure 5. A fixed bed frame allows moving the tool-electrode slide up and down intermediate by a vertical rolling guide.

The electrolyte is flowing into process using a central hole where input pressure and temperature are measured. After going through inter-electrode gap the electrolyte is collected in a vat and redirected outside using eccentric holes where again the pressure is measured. Electrical signals from all these transducers are transmitted to the data acquisition board input channels in order to be processed later.

For higher dimensional accuracy during the machining process a small interstice should be maintained, but since the current across the interstice is inversely proportional with gap size, Joule effect heating will increase abruptly when a small interstice is employed producing electrolyte heating. This perturbation is measured via electrolyte temperature sensor and tool anodic dissolution rate, V_n is evaluated as a function of electrolyte temperature, T_e and frontal gap, S_{90}.

$$V_n = f(T_e, S_{90}) \tag{1}$$

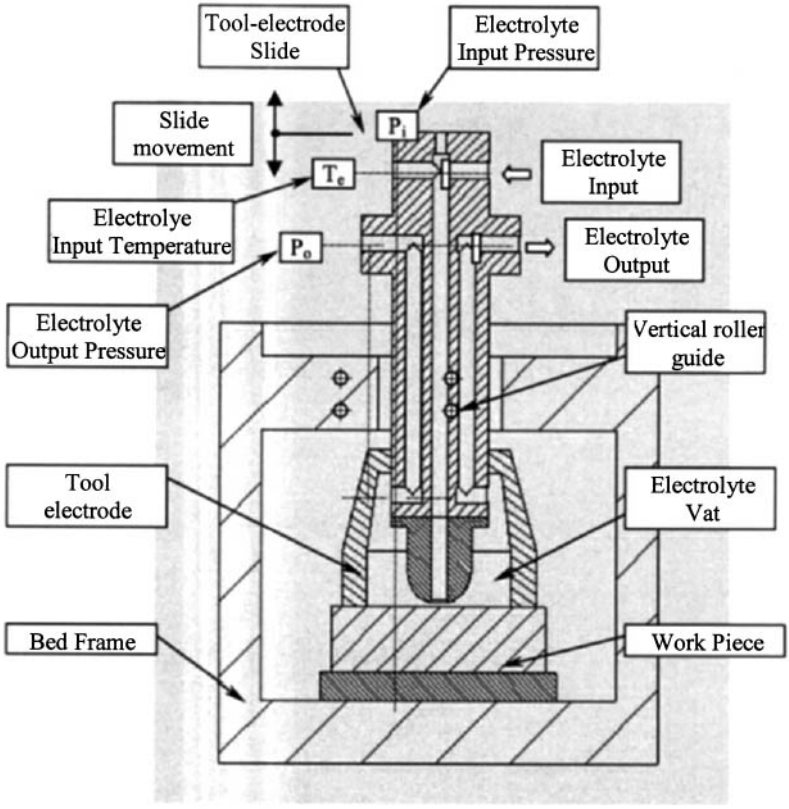

Figure 5: Assembly sensors configuration on moving tool electrode slide

A link between electrolyte pressure, which is measured continuously by pressure sensor, and the inter-electrode gap was mathematically demonstrated[4] and used to control the electrochemical process.

$$S_{90} = f(p_{in}, p_{out}) \tag{2}$$

In this way it is possible to know at any single moment of the machining process what value the inter-electrode gap is and keep it equal with the optimum value by changing the feed rate of tool-electrode.

The ECM adaptive system should be regarded as an automatic control system devised to adapt the machining process under course to the actual conditions in order to attain a specific objective. The objective envisaged by the implemented adaptive control is to maintain a constant interstice value throughout the duration of the machining.

$$S_{optim} = \text{Constant} \tag{3}$$

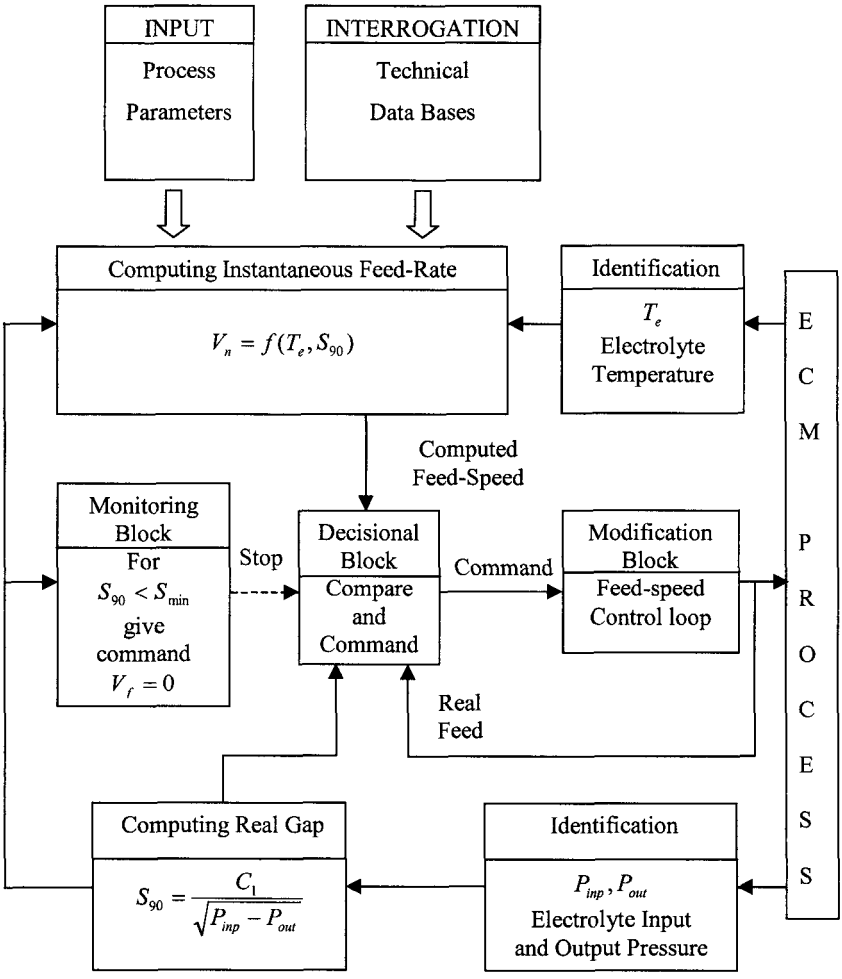

Figure 6: Adaptive control algorithm diagram

The adaptive control algorithm means, in this case, system behaviour modification by changing tool electrode feed speed. This feed speed change is executed to allow the following equality to be fulfilled: Tool electrode feed rate equal to anode material dissolution rate.

$$V_f = V_n \tag{4}$$

This relationship is a representation of the adaptive control objective, because by maintaining equality between the two speeds, the machining gap will be kept implicitly constant throughout the machining. Depending on electrolyte temperature during the process, as the identification block gives it, the adaptive control algorithm permanently computes the feed speed corresponding to the instantaneous condition from the process compares it to the actual speed and decides if a change in system behavior is necessary.

In figure 6 a complete diagram is given of the adaptive control algorithm. Apart from the feed speed control for finding the instantaneous optimum, there are problems connected with the restrictions of the technological system, which enable the definition of the variation domain for the control quantities.

The most important restriction is to avoid reducing working interstice below a given minimum value, which, if not maintained, would lead to short-circuit between the two electrodes. This is achieved by continuous monitoring of the interstice. If however the interstice varies and shrinks below a minimum safety value, then a zero speed command will be issued, subsequently stopping the machining process to avoid work-piece surface damage by electric discharges. This deviation from the optimum interstice is possible since the application of the presented adaptive control algorithm ensures constant interstice only with respect to temperature increase, a parameter considered to be the most important in the process. However, a complete definition of the restriction domain will require an upper limitation. The upper limitation of the speed control is achieved through the feed speed control loop whose structure will be presented in the following section.

6. THE RESULTS OF ECM MACHINING

Using the corrected tool electrode presented above and the ECM machine proposed a work piece was machined (figure 7) in order to evaluate the viability of the proposed approach.

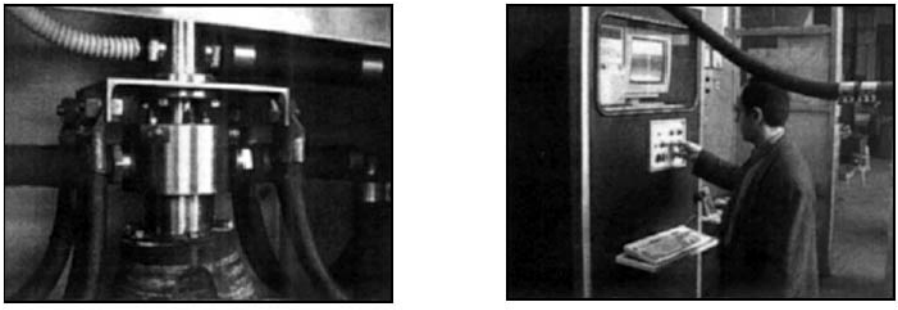

Figure 7: ECM machining of work pieces

The work pieces resulting from the machining with a corrected tool electrode is shown in figure 8 below.

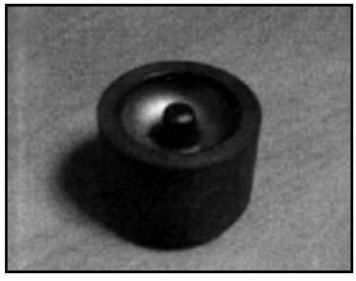

Figure 8: Work piece for corrected tool

Using a CMM machine, the work pieces from figure 8 was measured and a cross section contour was extracted and captured based on a collection of points. This contour was used in conjunction with the contour produced by simulation and with the ideal semispherical-shape to carry out the analyses.

First analysis executed makes a comparison between the work piece shape obtained with the uncorrected tool and the work piece shape machined with designed tool electrode on proposed ECM automated system. Overlapping images of the two contours is presented in figure 9 and is embedding the improvement obtained as a result of new tool design utilisation and the improvements obtained by using the ECM automated system.

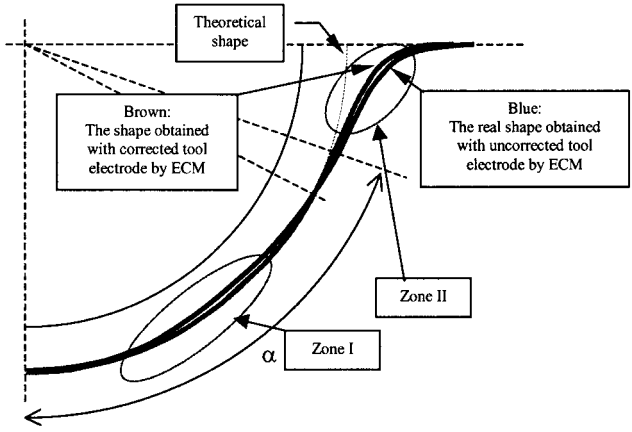
Theoretical shape
Brown: The shape obtained with corrected tool electrode by ECM
Blue: The real shape obtained with uncorrected tool electrode by ECM
Zone II
Zone I
α

Figure 9: Real improvement of work piece shape obtained by ECM

At the end of this study the second analysis is taken: the accuracy of final shape obtained by electrochemical machining following the proposed approach. Accuracy is defined as difference between the theoretical shape (figure 9) and the real shape machined. This is the final quotation regarding what the simulation is offering and what the machining is implementing.

The conclusion is that the simulation is predicting an improvement in shape of machined part for zone II and zone II (figure 9) and an accuracy of 0.025-0.5 mm is obtained for angles α less than 80°.

REFERENCES:

1. Freeer, H.E., Martin, H.P., "A pressure sensitive Adaptive Control System for ECM". ISEM 6 CIRP.
2. Larsson, N.C., "Adaptive Control of ECM based on Flow Measurement". ISEM 6 CIRP.
3. Astroshchenko, V.V., "Automatic System for Adjusting the Electrode Gap". Soviet Engineering Research, Vol. 2, No. 4, pp. 99-100, 1988.
4. Ivan M, ECM systems and technology, Transilvania University, Romania, 1995.
5. R. Temur, T. Coole, C. Bocking, Simulation of the Electrochemical Machining Process, Solid Freeform Fabrication Proceedings 2001,Texas US, pp 486-496.

Tool electrode design for electrochemical machining

R TEMUR and **C BOCKING**
Centre for Rapid Design and Manufacture, Buckinghamshire Chilterns University College, UK

ABSTRACT

The tool electrodes design method presented in this paper consist in correction of an initial tool electrode shape obtained as an offset of desired shape, based on differences between predicted and real work piece shape. For validation of this method two tool electrodes were constructed using different techniques and used in a real electrochemical machining (ECM) to obtain the work piece. Finally the geometrical and dimensional accuracy of work piece is evaluated and improvements highlighted.

1. TOOL-ELECTRODE DESIGN PROCESS

The electrochemical erosion processing method is an anodic dissolution process where the work piece is the anode and the tool electrode is the cathode for an electrochemical cell. A low voltage (7-25V) is applied between these two electrodes and the electrodes are positioned at a small distance from each other (0.025 – 0.5 mm). The electrolyte, usually a solution of NaCl or NaNO3, is forced to flow at high speed between the two electrodes (30-60 m/s) in order to remove the residual material from the working area.

Concepts and the methodology regarding the design of tool-electrodes for electrochemical erosion processing are different than those for conventional machines. For the particular case of an electrochemical erosion process a tool should meet the following requirements: to allow a uniform flow of electrolyte into the work gap; to allow a good electrical isolation in some required areas in order to avoid stray current flows; to present a surface with a good finish (without small scratches) and without errors; to resist internal electrolyte pressure from inside without vibrations; to be fabricated from a material with good electrical and thermal properties; to be easy to manufacture; to have good resistance to corrosion and to be plentiful.

Copper, bronze, steel, and titanium (90% purity) are only a few of the materials used in making tools for electrochemical erosion processing. The design process for such a tool generally consists in calculation of the tool-shape. This tool-shape used in appropriate working conditions will produce the desired work piece shape and the final size of the work piece. An analytical solution for this problem is complicated by a large number of parameters that interact with each other and by a direct interdependence of these parameters. The tool shape required to obtain a final part having a precisely defined profile can be calculated by applying a number of mathematical models. These existing models simplify the real situation and can lead to inexact results especially when complicated shapes are involved. Due to the poor precision of analytical solutions, the approximate profile (shape) of electrochemical tools is obtained in reality using standard calculation techniques (or CAD) where some corrections are added, based on practical considerations regarding complexity of profile. To date a general method for an analytical design of tools used in electrochemical processing has not been established and a practical design method for these tools by trial and error techniques is expensive and time consuming.

The following analytical methods for designing ECM tool electrodes were reported in the literature [1-6]: cosines θ method, graphic method, finite differences method (equilibrium gap method), boundary element method, complex variables method, correction factor method, finite element method (one-dimensional and two-dimensional).

Over the past few years, several electrochemical simulation packages have appeared [7], the most important are: SIMULA, CONDESIM, DIGISIM, EASI, GPS-CV, ESP, ELSIM3 TRANSIENT, POLAR, etc. All these are generally based on a finite difference method and are only capable of simulating mass transport in a maximum of one spatial dimension and provide.

2. TOOL ELECTRODE DESIGN TECHNIQUE

Proposed method consists of obtaining the shape of the tool electrode initially as an offset from the work-piece shape with a distance equal with gap size. This initial shape of the tool electrode is used in the simulation of the electrochemical process allowing the determination of a predicted shape for work piece. The final shape of the tool electrode is obtained by automated correction of the initial shape based on the measured differences between the predicted work-piece shape and desired shape. This sequence is presented in figure 1 and can be repeated until the required accuracy is achieved.

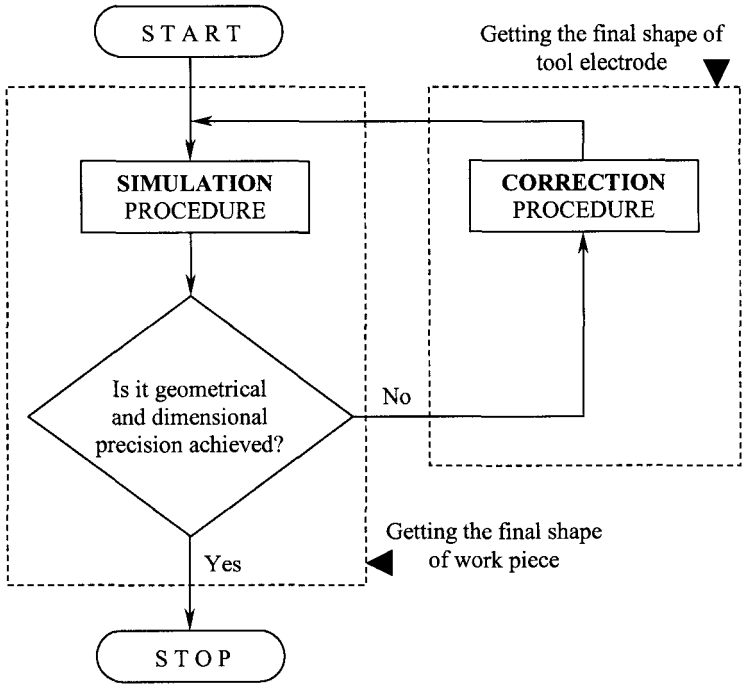

Figure 1: Block diagram of connection between electrochemical simulation procedure and tool electrode correction procedure

3. THE SIMULATION PROCEDURE

The principle used for the determination of the shape of the processed piece is presented in figure 2 where each calculation step is given together with a graphical description (for a particular case of spherical tool electrodes). The input dimensions and parameters assumed at the beginning of simulation are available for the entire process. The contour defined by the anode surface, cathode surface and limitation side surface represent the starting point for calculations in the procedure.

For this geometrical configuration the intensity of electric field on the anode surface will be calculated. Based on this intensity and with the contribution of electrolyte conductivity, current density and electrochemical machinability coefficient the volume of material removal is determined at each point considered on the anode contour. In the next step, the amount of the metal removal can be calculated for a specific time interval, in the direction normal to the anode surface and at each node considered. All N individual points obtained after the metal removal calculation will describe the next anode contour.

Once the new position and shape of the anode contour is available then the mathematical description of inter-electrode area for next simulation step is possible.

4. THE CORRECTION PROCEDURE

The tool electrode correction routine was written using the programming language AutoLISP for full compatibility and integration with the previously developed simulation procedure. This routine is structured in three main parts, as is presented in figure 5:

- Identification of the contour-type graphical elements resulted after simulation procedure execution;
- Calculation of contour correction in each node from the electrode previously considered;
- Drawing the new tool-electrode contour based on calculated corrections.

This routine has been written to assure a high level of generalisation that allows this to be used for any shape of tool-electrode. The correction principle is presented below and illustrated in the correction scheme for the spherical electrode from figure 3. The shape of the tool-electrode obtained following this principle is shown in figure 4.

The initial part of this routine (identification of contours) deals with three contour elements for a later correction. These three are the tool electrode contour, the work-piece contour obtained after simulation, and the desired work-piece contour to be obtained by electrochemical erosion. The last two contour elements represent the input data for the second part of the routine where corrections to each node will be calculated.

In the second part of the correction routine, two calculus subroutines will be repeatedly executed through all nodes on the tool contour. The first subroutine determines the error between the desired and obtained work-piece contour in each node. This error is calculated in the normal direction on the tool-electrode contour at each considered node. The second subroutine uses this calculated error to make a tool contour correction in the current node. This correction is made also in the normal direction on the tool electrode but through inside of this. The third part of the correction routine is started after going through all nodes and carrying out all the calculation. This part will determine a graphical representation of the new tool-electrode contour.

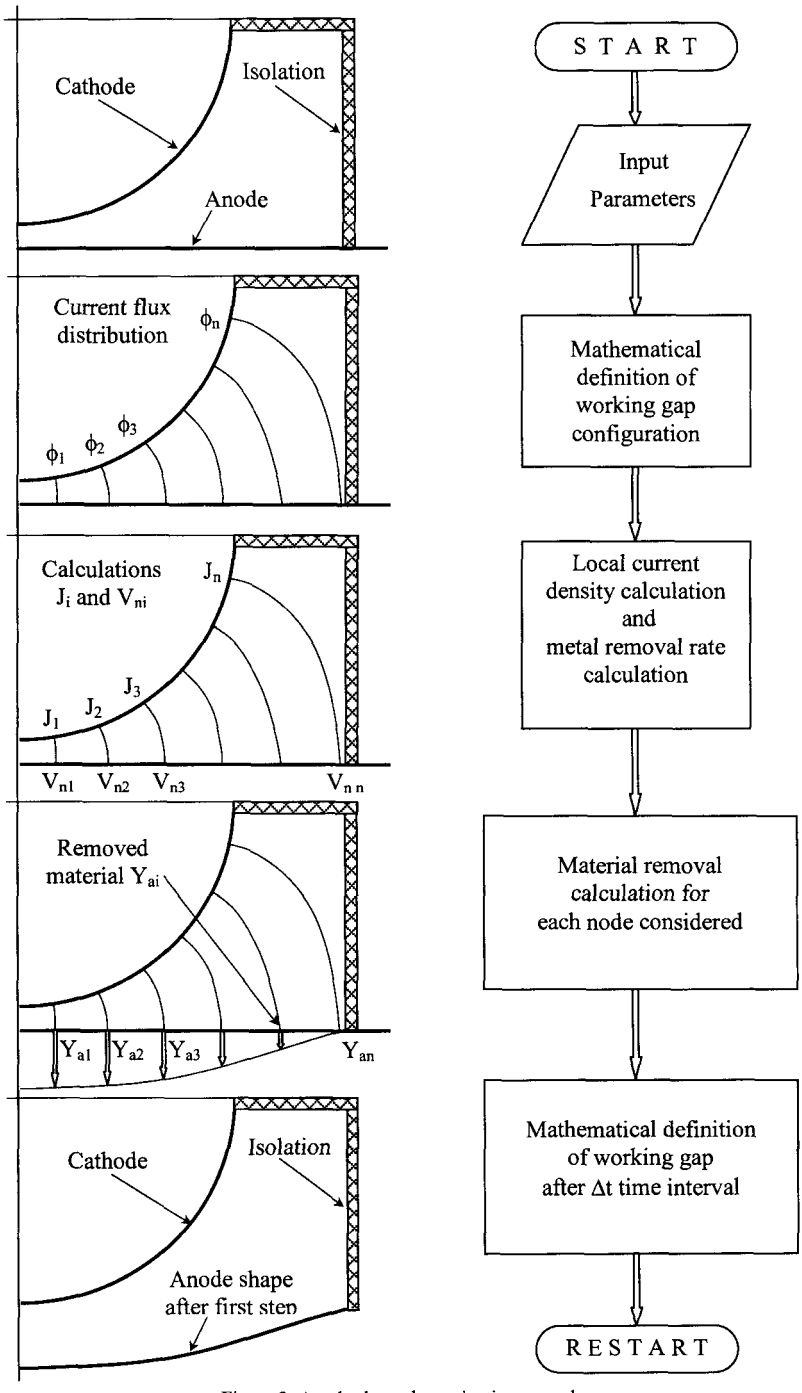

Figure 2: Anode shape determination procedure

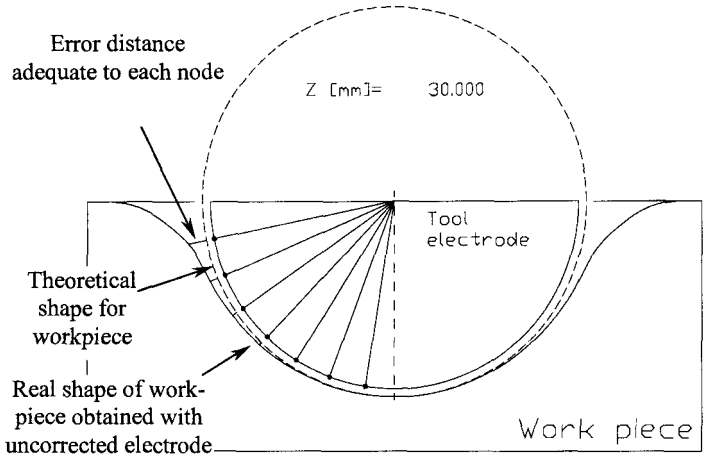

Figure 3: Graphical determination of anode shape errors

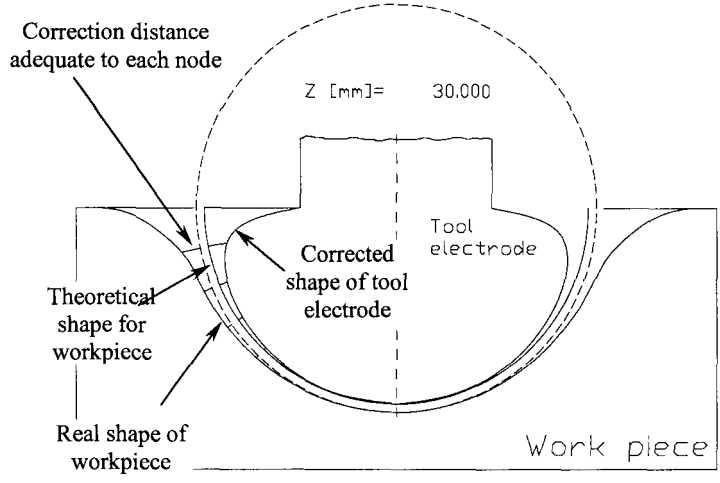

Figure 4: Tool electrode shape correction

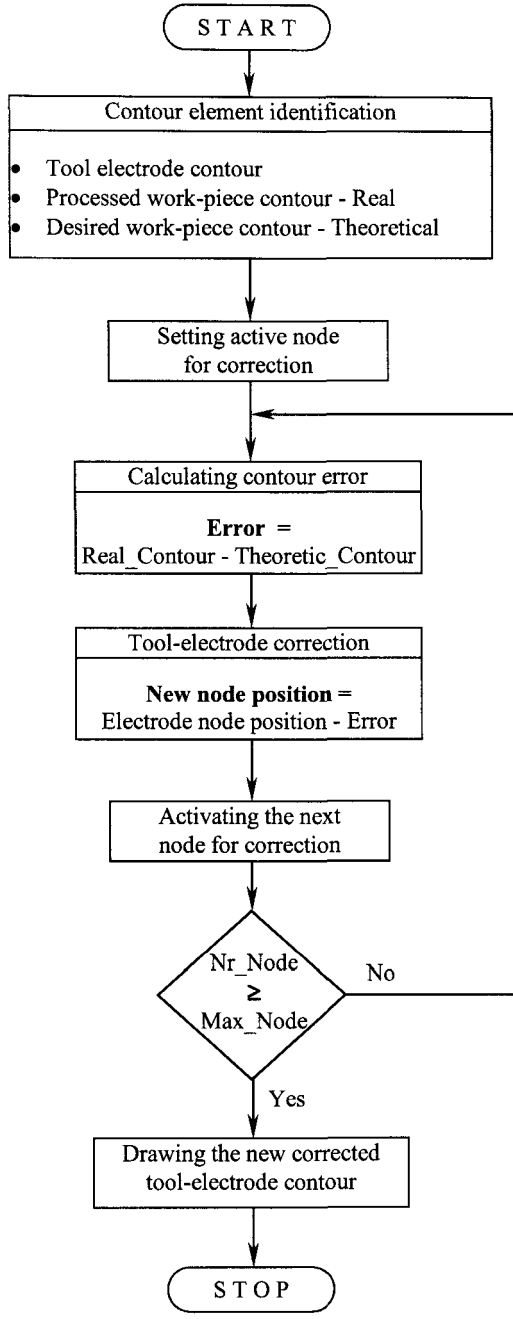

Figure 5: Logical scheme of tool electrode correction procedure

The new contour is initially assimilated with a succession of lines based on previously calculated points representing the new nodes of tool. New nodes were obtained by applying an error correction to the old nodes. It is clear that for a better accuracy of the new corrected tool-electrode contour, a higher number of nodes will be needed. After that the succession of lines obtained is transformed to a smooth contour by interpolation calculus. This is the new shape for tool-electrode and now it is possible to use this contour again in simulation. This dual process of actions: the simulation and tool-correction can be repeated until the geometrical precision and dimensional accuracy requested is obtained. The last tool-electrode corrected contour is saved and used to build a real tool-electrode for real electrochemical erosion processing which will follow this theoretical simulation.

5. TOOL ELECTRODE CONSTRUCTION

By using a Rapid prototyping master mould and electroforming copper onto this surface a tool electrode was obtained with a shape identical with the shape resulted from design (figure 6). Also a conventional CNC milling method was applied to execute a second tool electrode with the same shape resulted from design stage (figure 7).

Both two tool electrodes were used on a ECM machine to validate the tool electrode construction and more important to verify the geometrical and dimensional accuracy of work-piece.

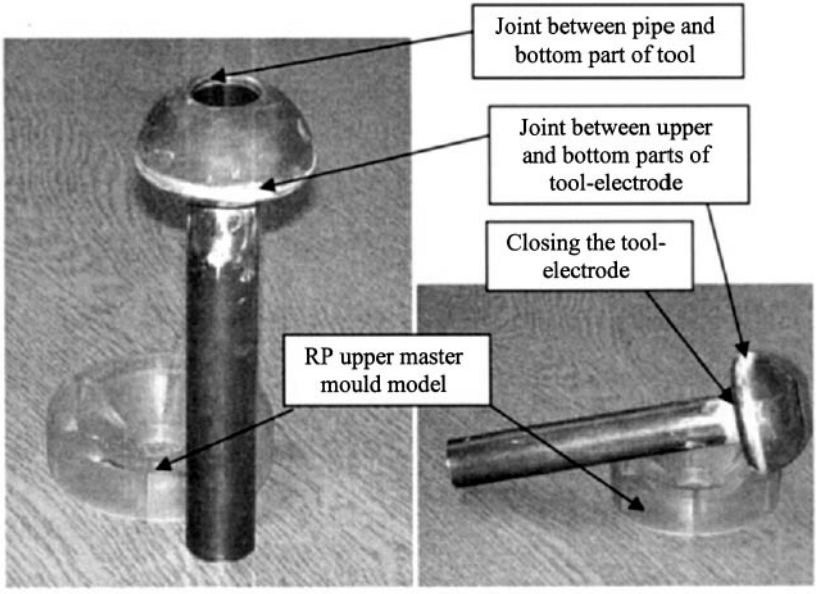
Joint between pipe and bottom part of tool
Joint between upper and bottom parts of tool-electrode
Closing the tool-electrode
RP upper master mould model

Figure 6: Tool electrode constructed by electroforming copper on a RP master mould model

Figure 7: Tool electrode constructed by CNC milling

6. RESULTS AND CONCLUSION

In figure 8 is presented the work piece shape obtained by electrochemical machining simulation with the new tool electrode designed. By using this tool the work piece accuracy is 0.05 mm for an angle up to 80° comparative with maximum 30° if an uncorrected tool electrode is used. Also if the general tolerance characteristic for this process and 3D shapes is 0.1-0.3 mm by applying this design for tool electrode the accuracy is increased up to 0.05mm.

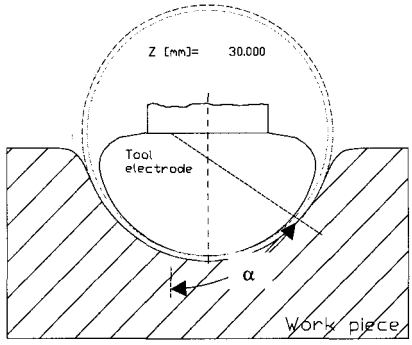

Figure 8: Result of machining with corrected tool electrode

References

[1] Konig, W., and Humbs, H.H., "Mathematical Model for the Calculation of the Contour of the Anode in Electrochemical Machining". Annals of the CIRP, 26/1, 1977, p.83-86.
[2] Tipton, H., "The Calculation of Tool Shapes for Electrochemical Machining". Fundamentals of ECM. The Electrochemical Society, Princeton, 1971, p. 87-102.
[3] Raju, K.R., Jain, V.K., Lal, G.K., "Cathode Design in ECM: Two Dimensional Analysis". ASME Symposium on Research and Technological Advances in Non-traditional Machining. Vol. PED-34, 1988, p. 89-104.
[4] Seimiya, K., "An Approximate Method for Predicting Gap Profiles in Electrochemical Machining". Proceedings of the 5th International Conference on Production Engineering, 1984 p.389-394.
[5] Hewidy, M.S., Rajurkar, K.P. "Computer-Aided Tool Design in ECM". Proc. of the Third Int'l. Conference on Computer-Aided Production Engineering, 1988, p. 371-380.
[6] Jain, V.K., Rajurkar, K.P. "An integrated Approach for Tool Design in ECM", Submitted for review to the Precision Engineering, May 1990.
[7] John Alden PhD. 1998 Oxford University – Compton Group.

Authors' Index

B

Bauer, W 131–138
Bennett, N G 39–46
Bocking, C 63–70, 157–164

C

Chang, I T H 123–130
Chatterjee, A 9–16
Cheshire, D G 55–62
Coole, T J 55–62, 63–70
Corney, J R 1–8
Cruz, F 63–70

D

Davies, J B C 1–8
Day, M 115–122
Dhande, S G 9–16
Dimla, D E 115–122

F

Fox, P 139–148

G

Göhring, D 131–138
Green, G 97–104

H

Hackney, P M 105–114
Harrison, D K 97–104
Hedges, M 17–24
Herbert, N S 71–78

I

Ion, W J 89–96, 97–104

K

Kiecher, D 17–24
Knitter, R 131–138

L

Liang, J 25–30
Lim, T 1–8
Loretto, M H 25–30, 31–38

M

Matos da Rocha, E 47–54
Mei, J 25–30
Mulyadi, I H 39–46

O

O'Neill, W 139–148
Oliveiera Baptista, R M 47–54
Onuh, S O 39–46

P

Pires, A R 55–62
Pogson, S 139–148

R

Rennie, A E W ..... *ix*
Risthaus, P 131–138
Ritchie, J M 1–8
Ryder, G J 89–96, 97–104

S

Sharman, R 31–38
Simões, J F A 47–54, 55–62, 63–70
Singh, H 115–122
Steele, K A M 89–96
Svirsky, D N 79–88

T

Temur, R 149–156, 157–164
Thomson, A I 89–96

U

Uzunsoy, D 123–130

V

Voice, W 31–38

W

Wood, B M 97–104
Wu, S 31–38
Wu, X 25–30